EXPLORATORY STUDIES OF FLAME AND EXPLOSION QUENCHING

Prepared for

UNITED STATES DEPARTMENT OF THE INTERIOR
BUREAU OF MINES

by

MIDWEST RESEARCH INSTITUTE
425 VOLKER BOULEVARD
KANSAS CITY, MISSOURI 64110

Bureau of Mines Open File Report 112-77

FINAL REPORT

June 30, 1972 - December 31, 1975

on

USBM Contract No. HO122127

June 25, 1976

DISCLAIMER NOTICE

The views and conclusions contained in this document are those of the authors and should not be interpreted as necessarily representing the official policies or recommendations of the Interior Department's Bureau of Mines or of the U. S. Government.

BIBLIOGRAPHIC DATA SHEET	1. Report No. BuMines OFR 112-77	2.	3. Recipient's Accession No.
4. Title and Subtitle Exploratory Studies of Flame and Explosion Quenching			5. Report Date June 25, 1976 6. Performing Organization Code
7. Author(s) Thomas A. Milne and Jacob E. Beachey			8. Performing Organization Rept. No.
9. Performing Organization Name and Address Midwest Research Institute 425 Volker Boulevard Kansas City, MO 64110			10. Project/Task/Work Unit No. 11. Contract/~~Grant~~ No. H0122127
12. Sponsoring Agency Name and Address Office of Assistant Director--Mining Bureau of Mines U.S. Department of the Interior Washington, DC 20241			13. Type of Report & Period Covered Contract research 14. Sponsoring Agency Code

15. Supplementary Notes
Approved for release by Director, Bureau of Mines, June 28, 1977.

16. Abstracts Using flame stabilization and direct sampling techniques developed under this contract, the combustion and inhibition processes in coal dust-air flames was studied. Premixed, laminar, flat flames of 10 to 20μ Pittsburgh seam coal, stabilized on a 6.3-cm burner, were probed for both gaseous and particulate species. The emphasis was on high spatial resolution sampling of the ignition and primary reaction zone. Results are presented involving five kinds of profiles through rich coal-air flames as follows: (1) direct, molecular beam mass spectrometry of O_2, N_2, CO_2, H_2O, nitrogen, and sulfur-containing species; (2) gas chromatography of collected samples for O_2, N_2, CO, CO_2, H_2, CH_4, and C_2 hydrocarbons; (3) proximate analysis of coal and char samples collected in bulk; (4) scanning electron microscopic analysis of directly impacted coal and char particles; and (5) fine-wire thermocouple temperature measurements. Also included are observations on the quenching behavior or Pittsburgh seam coal-air flames and of the gaseous potassium- and phosphorus-containing species evaporating from dry-powder inhibitors in the reaction zone of CH_4 air flames. Suggestions for future research are made.

17. Key Words and Document Analysis 17a. Descriptors

Explosions	Coal combustion
Quenching	Coal mining
Flame speeds	Mass spectrometry
Flames	Combustion pollutants
Flame inhibitors	Safety
Thermodynamics	Burners
Coal dust	Particulates
Flame sampling	

17b. Identifiers/Open-Ended Terms

17c. COSATI Field/Group 08I, 17C, 19A

18. Distribution Statement	19. Security Class (This Report)	
Release unlimited by NTIS.	UNCLASSIFIED	
	20. Security Class (This Page) UNCLASSIFIED	22. Price A12-A01

FORM NTIS-35(10-70)
US COMM-D C 40329-P71

EXPLORATORY STUDIES OF FLAME AND EXPLOSION QUENCHING

by

Thomas A. Milne
Jacob E. Beachey

Prepared for

UNITED STATES DEPARTMENT OF THE INTERIOR
BUREAU OF MINES

by

MIDWEST RESEARCH INSTITUTE
425 VOLKER BOULEVARD
KANSAS CITY, MISSOURI 64110

Bureau of Mines Open File Report 112-77

SUMMARY TECHNICAL PROGRESS REPORT
June 30, 1972 - December 31, 1975

on

USBM Contract No. H0122127

June 25, 1976

FOREWORD

This report was prepared by Midwest Research Institute, Kansas City, Missouri, under USBM Contract Number H0122127. The contract was initiated under the Coal Mine Health and Safety Program. It was administered under the technical direction of PM&SRC, with Mr. Joseph Grumer acting as the Technical Project Officer. Mr. A. G. Young was the contract administrator for the Bureau of Mines.

This report is a summary of the work recently completed as part of this contract during the period June 30, 1972 to December 31, 1975. This report was submitted by the authors on March 12, 1976.

The principal investigator has been Dr. Thomas A. Milne, with Mr. Jacob E. Beachey carrying out the major portion of the experimental work and directing the final phase of quenching studies. Involved in the program over the years have been Dr. Frank T. Greene, Ms. Carol Green, Mr. Joe Bossert, Mr. Sidney Hamilton, Mr. Doug Weatherman, Mr. Gene O'Donnell, and Mr. Thurman Oliver.

Professor Walter Kaskan, Department of Chemistry, State University of New York at Binghamton, served as consultant until his recent untimely death. Mr. Gordon Gross, Head of the Materials Sciences Section during most of the program, was technical manager.

Approved for:

MIDWEST RESEARCH INSTITUTE

Michael C. Noland

Michael C. Noland, Director
Engineering Sciences Division

June 25, 1976

TABLE OF CONTENTS

TABLE OF CONTENTS (Continued)

TABLE OF CONTENTS (Continued)

List of Figures

List of Figures (Continued)

List of Figures (Continued)

List of Figures (Continued)

List of Figures (Continued)

List of Figures (Continued)

List of Figures (Continued)

List of Figures (Continued)

List of Figures (Continued)

List of Figures (Continued)

List of Figures (Concluded)

List of Tables

List of Tables (Concluded)

I. EXECUTIVE SUMMARY

A. Goal of the Research

As part of the broad program to improve the safety of underground coal mines, the Pittsburgh Mining and Safety Research Center sponsored several detailed studies on the inhibition of coal dust-air explosions. The present study was one of these. The goal of the research was to advance the development of improved coal-dust explosion inhibiting agents by determining, on a laboratory scale, the basic chemical processes involved in the inhibition of coal-dust flames by dry-powder agents.

B. Our Approach

Neither the basic molecular processes involved in coal combustion, nor the molecular mode of action of dry-powder agents, are known with certainty. Our approach, therefore, involved the direct determination, by sampling techniques, of species behavior in small, aerodynamically simple flames. To further aid in separating behavior of coal and dry-powder inhibitors, the latter were studied in CH_4-air flames.

Project work was divided into six tasks as follows:

Task I - Stabilizing Coal Dust-Air Flames on Small Burners.

Task II - Sampling and Characterization of Flame-Inhibiting Particles.

Task III - Direct Sampling of Gaseous Species from Coal Dust-Air Flames.

Task IV - Direct Sampling of Coal and Ash Particles from Coal Dust-Air Flames.

Task V - Direct Sampling of Potassium, and Phosphorus-Containing Species from CH_4-Air Flames Inhibited with Dry-Powder Agents.

Task VI - Quenching Behavior of Coal Dust-Air Flames.

Key experimental developments involved stabilizing flat, laminar, free-burning coal-air flames; interfacing such flames with a direct, real-time, molecular beam, mass spectrometric sampling systems; the sampling of particulates from coal-air flames; and the sampling of particulates and gaseous, condensible species from dry-powder inhibitors injected in CH_4-air flames.

C. Results of These Tasks

Task I - We were successful in stabilizing a variety of coal-air flames, both conical and flat, on burners 1 to 12 cm in diameter. No augmentation, pilot flame, or furnace walls were required, so that we achieved a nearly-ideal, coal-air flame for sampling diagnosis. Only rich flames were stabilized and studied, though it is believed that with appropriate geometrical changes, stoichiometric or lean flames can be stabilized and sampled.

Task II - The direct sampling and preservation of dry-powder inhibitor particles from the reaction zone of CH_4-air flames was less successful. The principal problem was caused by the extremely hygroscopic nature of particles from powders like Purple-K, Monnex, or potassium oxalate, when collected from the reaction zone. Evidence as to the extent of physical breakup of dry-powder agents early enough in these flames to have an influence on inhibitor effectiveness, was inconclusive.

Task III - We were successful in sampling a variety of gaseous species directly from the primary ignition and reaction zone of coal-air flames, with high spatial resolution. Species profiles for CO, CO_2, H_2O, O_2, H_2, CH_4, C_2-hydrocarbons, NO, NO_2, HCN, H_2S, SO, and SO_2 were measured in rich coal-air flames.

Task IV - We were successful in sampling coal and char particles, with high spatial resolution, from coal-air flames. Subsequent analysis by scanning electron microscopy and proximate composition determination helped fill in the overall picture of coal combustion in the primary reaction zone.

Task V - Gaseous potassium and phosphorus-containing species were observed to be evaporating from dry-powder agents early in the CH_4-air flame reaction zone. The species K, KOH, P, and PO were tentatively identified as the major products of evaporation.

Task VI - It was demonstrated convincingly that minimum quenching diameters for 10 to 20 μ Pittsburgh Seam coal are as small as 1 cm, by observing flashback and propagation of a coal-air flame for 5 to 10 diameters down cold Pyrex tubes.

D. Significance of the Results

The demonstration that coal dust-air flames may be stabilized on small burners and sampled with high spatial and time resolution, opens the way for the application of this technique to a variety of explosion, coal combustion, and conversion processes.

The lack of extensive pyrolysis in advance of ignition, and the rapidity of oxygen consumption of volatile matter, are key observations against which to test theories and models of slow-moving coal-dust explosions and pulverized coal combustion.

The observed effectiveness of dry-powder agents in inhibiting these slow burning coal-air flames argues for a "chemical" effect which may not have time to operate in fast, well-developed coal explosions of large scale. The observation of significant evaporation of dry-powder to provide possible gas-phase inhibition species, could be consistent with the reported failure of these agents to inhibit in very fast explosions, due to evaporation limitations.

The very small quenching diameters observed for Pittsburgh Seam coal indicate that explosion hazards could exist under a broader range of geometrical circumstances than previously thought. It is also believed, based on an experience in the present program, that poor dispersal and lack of uniformity of coal dust suspensions, particularly in larger tubes and ducts, may have invalidated some past work on quenching, propagation limits, burning velocities, and attempts to stabilize pre-mixed flames on burners.

The early and rapid appearance of significant quantities of HCN and NO should be significant in assessing proposed mechanisms of bound-nitrogen conversion to NO_x in combustion processes.

E. Need for Continuing Work

It is recommended that safety-related studies of coal dust-air mixture behavior be continued. These should include systematic observation of quenching diameters for a variety of coals and particle sizes and the extension of the direct molecular beam, mass spectrometric sampling techniques to the monitoring of propagating flames as a function of tube diameter and propagation speed.

A whole variety of studies relevant to coal combustion for power production are made possible by the ability to stabilize flat flames and to sample them with high spatial resolution for gases, ions, and particulates.

II. SUMMARY OF EXPERIMENTAL RESULTS

A. Introduction

The aim of this research has been to provide a more detailed understanding of the mechanisms by which dry-powder agents suppress coal dust- air explosions. Such increased understanding should augment the present almost entirely empirical approach to agent improvement and explosion suppression device development. These studies[1] were sponsored by the Pittsburgh Mining and Safety Research Center of the U.S. Bureau of Mines, as part of a broad program to improve the safety of underground coal mining. Simultaneously, roughly parallel programs of basic research were initiated at Brigham Young University[2] and the University of Illinois.[3]

To make significant advances in the understanding of the inhibition of coal dust-CH_4-air explosions, information on molecular processes was thought to be necessary in two areas. First, much remains to be learned about the basic processes in the combustion of pure coal dust-air mixtures. In particular, the early ignition and rapid devolatilization stages, which are presumably the most important point of attack by inhibiting agents, are very poorly understood. To permit study of these stages, and the effect of inhibitors thereon, we sought to achieve small, stable flames of coal dust-air mixtures, which could be interfaced with molecular beam sampling systems for both gaseous and particulate species. Second, it was desired to observe both the physical breakup and vaporization and vapor species when dry-powder agents passed through flame fronts. Because of the known difficulties of stabilizing small coal dust-air flames, and the problems of sampling small amounts of inhibitor particles from a coal dust flame, the tasks were simplified by separating the coal dust burner studies from the inhibitor particle sampling studies.

The work was divided into six tasks titled as follows:

Task I - Stabilizing Coal Dust-Air Flames on Small Burners.

Task II - Sampling and Characterization of Flame-Inhibiting Particles.

Task III - Direct Sampling of Gaseous Species from Coal Dust-Air Flames.

Task IV - Direct Sampling of Coal and Ash Particles from Coal Dust-Air Flames.

Task V - Direct Sampling of Potassium and Phosphorus-Containing Species from CH_4-Air Flames Inhibited with Dry-Powder Agents.

Task VI - Quenching Behavior of Coal Dust-Air Flames.

Details of progress on these tasks has been reported in two annual progress reports,[4,5] 11 quarterly reports,[6] and reprints of two papers presented at Western States Combustion Institute meetings.[7,8]

This final report draws extensively on verbatum material from these progress reports in order to show the significant aspects of equipment and technique development and to present, in a collected format, the data required. It is intended to publish these results in a journal format, with more documented and critical interpretation, in the very near future.

This section contains a summary of the research undertaken, typical results obtained, and their interpretation and significance. The details of methods and results are included as appendices.

B. Stabilization of Coal Dust-Air Flames

1. Previous attempts to stabilize pure coal dust-air flames on laboratory burners: Studies aimed at understanding the burning characteristics of pulverized coal extend back many years. These studies range from observations of the behavior of individual coal particles in furnaces and gaseous flame products to attempt to burn coal dust-air mixtures on laboratory scale burners without any augmentation. Appendix A lists some of the major attempts to maintain and characterize the burning of pure coal dust-air mixtures on small burners.

A review of the papers in Appendix A indicated that stabilization of an unconfined laminar unaugmented coal dust-air flame had not been achieved at the time our studies were initiated. Therefore, one of the chief goals of the research was to try, through the use of rather large flat-flame burners, to stabilize such a flame so that it could be studied in detail by mass spectrometry and particulate sampling-probe methods (and perhaps by optical spectroscopy as well).

2. Stabilizing coal dust-air flames on small burners: For the subsequent purposes of sampling both gaseous species and particulates from inhibited coal dust-CH_4-air flames, it was desirable to have a small one-dimensional laminar upward-pointing flat-flame burner capable of stabilizing pure coal dust-air flames. It was desirable that such a burner achieve

steady, reproducible burning for an hour or more to facilitate measurement of temperature, composition and particulate profile. The three anticipated problems were: (a) to provide a pulverized coal feed system that would deliver powder at a rate which is constant to a few percent over a period of hours; (b) to devise a burner which would fully entrain and mix the CH_4-air and coal dust, and yet deliver a laminar, uniform flow at the burner mouth; and (c) to stabilize a laboratory size flame with no excess oxygen, with no sheath flames and with minimum (hopefully zero) addition of CH_4.

The key analytic device to be used to obtain species profiles through the flame was a direct, molecular-beam, mass spectrometer. This device could only be used with an upward burning flame without extensive reconstruction. Hence, a constraint on the studies performed throughout this 3-year program was that powders be delivered against gravity in an upright burner system.

We were successful in stabilizing both upward and downward burning flames of coal dust-air, with no CH_4 addition, no stabilizing flame, and no external heat source. The coal used and the coal delivery system are described in Appendix B. The burners tested, the problems encountered, and the best design of burner system are described in Appendix C.

The most successful upright burner was a short cylindrical burner, 6.3 cm in diameter, with a honeycomb smoothing and anchoring grid. This burner was used for almost all of the sampling experiments reported below.

It was observed that the flame anchored quite closely to the uncooled, honeycomb grid, heating it appreciably. This heating of the grid increased the flame stability and flatness. To better understand the grid heating and its interaction with flame stability, thermocouple temperature measurements were made on, within and above the grid. Details of the temperature profiles in the grid are presented in Appendix D.

C. Species and Temperature Profiles Through Coal-Air Flames

1. Conditions of burning and probing: Early in the program we adopted a standard burner configuration and test coal in order to proceed with enough systematic direct sampling to characterize the probing problems and general behavior of coal dust-air flames. The burner was a 6.3-cm diameter, upright cylinder, fed from a conical section where the air and coal entered in a very turbulent flow, and terminating in one or more layers of honeycomb which smoothed the flow. A photograph of the burner,

honeycomb and inlet is shown in Figure 1. A photograph of a typical flame appears in Figure 2. An enlarged hole was created in the central area of the honeycomb, resulting in a slightly raised, conical portion of the otherwise flat coal-air flame. This permitted the probe to sample from the unburned gas region without penetrating below the surface of the honeycomb.

The coal used in all experiments was Pittsburgh Seam, which had been air classified into narrow size fractions. All results reported below involved a 10 to 20 μ size fraction. The fluidized-bed coal dust feeder described earlier[4] was used with coal concentrations monitored by timed collections from the burner mouth and weighing before and after experimental probing. Cold gas velocities were maintained at 10 cm/sec for all experiments, with the flames anchoring by nonadiabatic interaction with the uncooled honeycomb grid.

Sampling and probing conditions were slightly different for each analytical mode and are briefly described in the following sections. In all cases, the primary sampling orifice presented to the flame front was a spun copper, 90-degree cone, 1/2-in. high, soldered to a large, water-cooled flat plate and containing a 30-mil diameter hole in its apex.

2. Molecular beam mass spectrometry of gaseous species: The two-stage expansion, molecular beam, direct mass spectrometric sampling system described earlier[4] was used, with two modifications. First, to partially overcome the orifice plugging problem when sampling the early, sticky region of coal-air flames, the self-cleaning feature shown in Figure 3 was added. Such a device permitted sampling times of 5 to 10 min, typically, with a 30-mil orifice. The pressure drop across the first orifice was greater than a factor of 10 so that sonic flow prevailed. The subsequent expansion was via free-jet to molecular flow and collimated, modulated molecular beam. Second, an Extranuclear quadrupole was mounted on top of the Bendix TOF ion source, intercepting the same beam as traversed the Bendix and providing about two orders of magnitude greater detection sensitivity for flame species. (Details of direct sampling system tests are given in Appendix E.)

Tests of probe-flame interaction, using one atmosphere, CH_4-air flames, indicated that the 30-mil sonic orifice was broadening the reaction zone profiles. This fact, coupled with the variability of the coal-air flame due to imperfect dispersion of coal dust and the waffled nature of the "flat" flame due to the honeycomb grid, tends to reduce the actual spatial resolution of sampling.

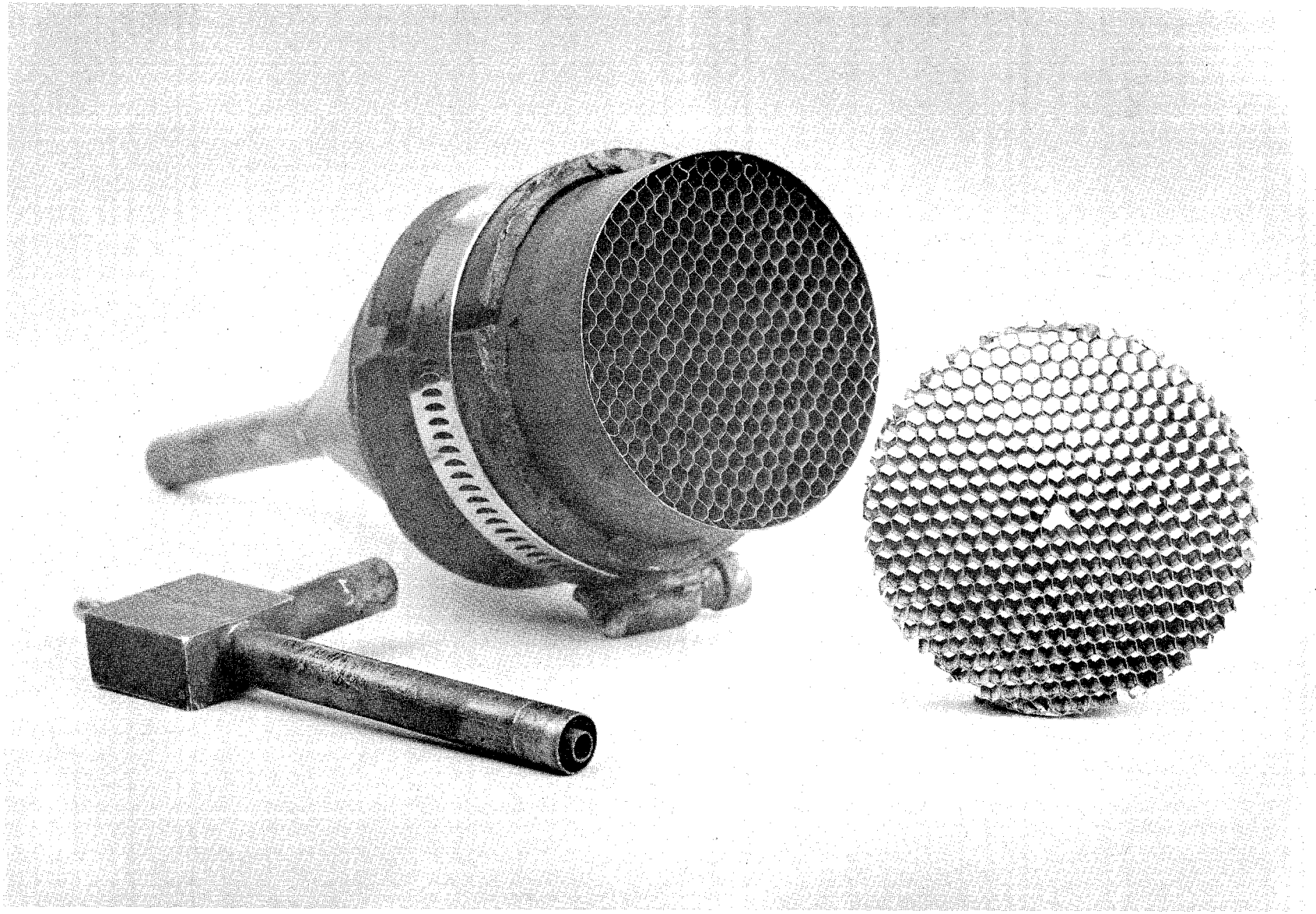

Figure 1 - Photograph of Burner, Honeycomb and Coal-Air Inlet for the System Used in Flame Sampling Studies

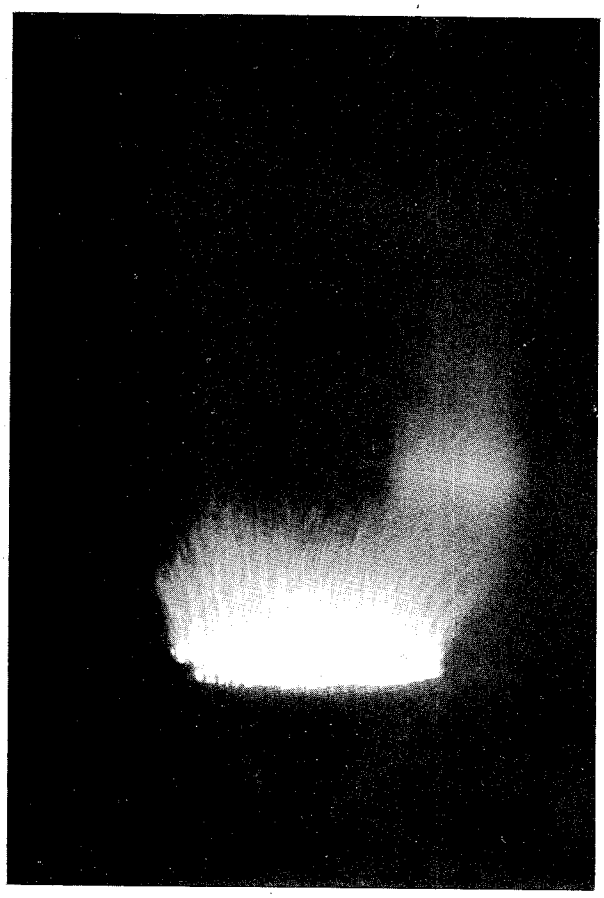

Figure 2 - Photograph of Rich, Coal Dust-Air Flame Burning on an uncooled, 6.3-cm Diameter, Burner with a Honeycomb Matrix. Coal dust is 10 to 20 μ at a loading of about 268 mg/liter.

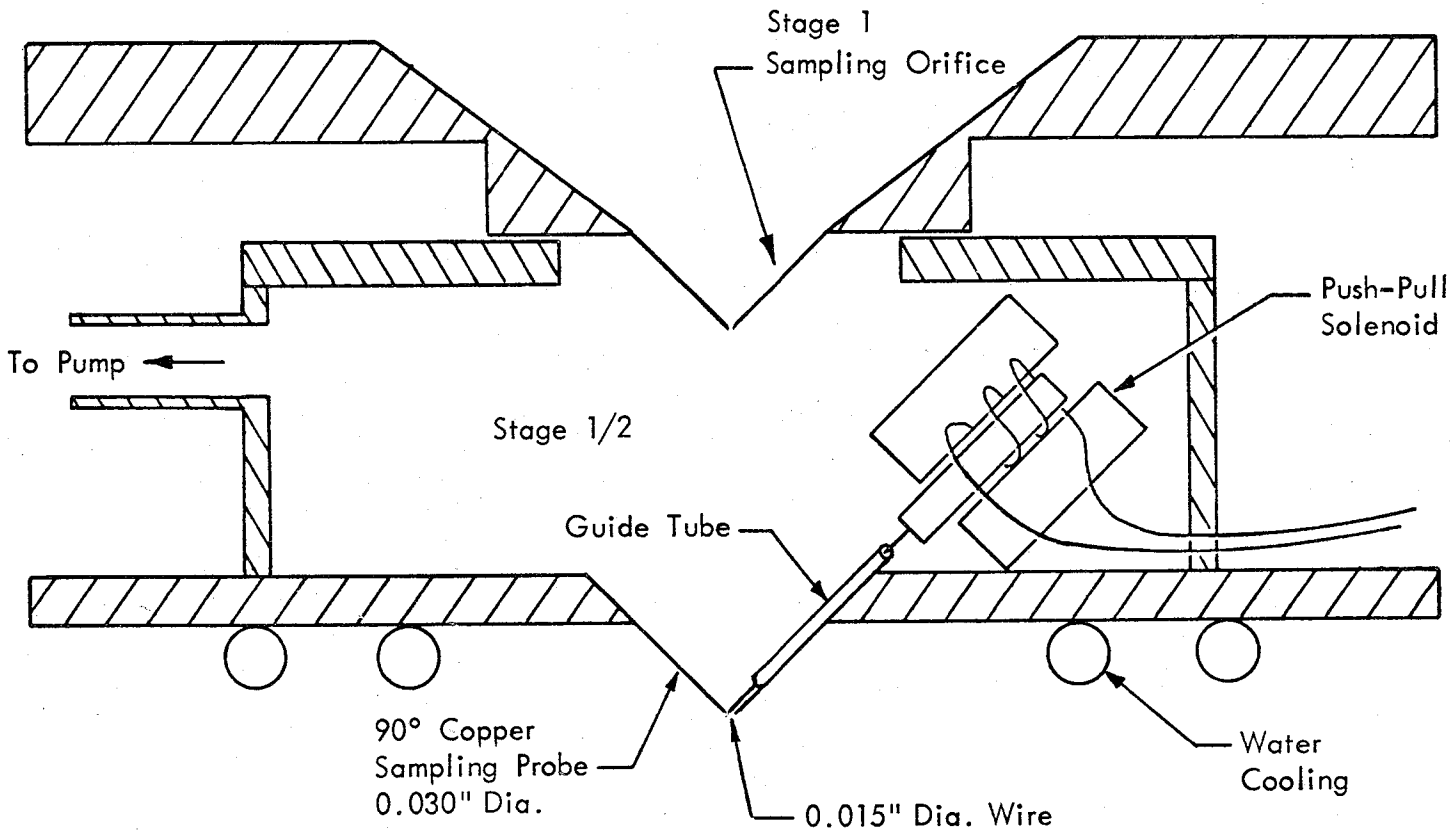

Figure 3 - Schematic of Mechanical Device Used to Keep the 30-mil Copper Orifice Unplugged During Sampling of Coal-Air Flames

Typical results of flame probing for stable species are shown in Figures 4 through 6 and for nitrogen- and sulfur-containing pollutant species in Figures 7 through 9. (Additional results are given in Appendix F.)

The stable-species ratios have been corrected for sensitivity using the burnt-gas region of lean methane-air flames as the calibrating gas. The pollutant species are presented as uncorrected ion ratios, with the presumed precursors indicated in Table 1.

3. Gas chromatography of gaseous species: Samples collected in glass, 250-ml bottles were analyzed by conventional gas chromatography. Since the bottles were intially evacuated and then filled to one atmosphere pressure, the flow conditions at the orifice ranged from sonic to isokinetic and slower. The net result should be to move the effective sampling distance slightly downstream of the sonic flow sampled mass spectrometry results. Figures 10 through 12 show typical results obtained. (Appendix F contains additional results.)

4. Proximate analysis of bulk samples: The same copper, conical probes were used to collect bulk samples of coal and char on fritted-disk filters. About 1/2 g was collected at each position in the flame, with a pressure drop of about a factor of two across the orifice. The effective sampling distances for this probing should be intermediate between those with the mass spectrometry and gas chromatography. The Pittsburgh Mining and Safety Research Center[9] performed the proximate analyses, the typical results of which are presented in Table 2 and Figures 13 through 15. (See Appendix G for details and additional results.)

5. Scanning electron microscopy of individual particles: Individual coal and char particles were collected by impaction on sticky, aluminized tape on small electron microscope mounting stubs. Collection was by nearly isokinetic sampling through the 30-mil copper probes and is believed to have favored the large, unfragmented coal and char particles. A large number of particles were collected and photographed with typical features displayed in Figure 16. The effective sampling distances relative to the burner grid, would be expected to be shifted downstream from those probe results involving sonic and partially sonic conditions (see Appendix G).

6. Thermocouple temperature profiles: Approximate temperature profiles were obtained by inserting fine Pt-Pt-10% Rh thermocouples into the coal-air flames. One-mil wires with about a 3-mil diameter bead were used. No corrections have been attempted, though it was noted that char and soot buildup seriously affected readings. A typical profile is shown in Figure 17 (see Appendix H).

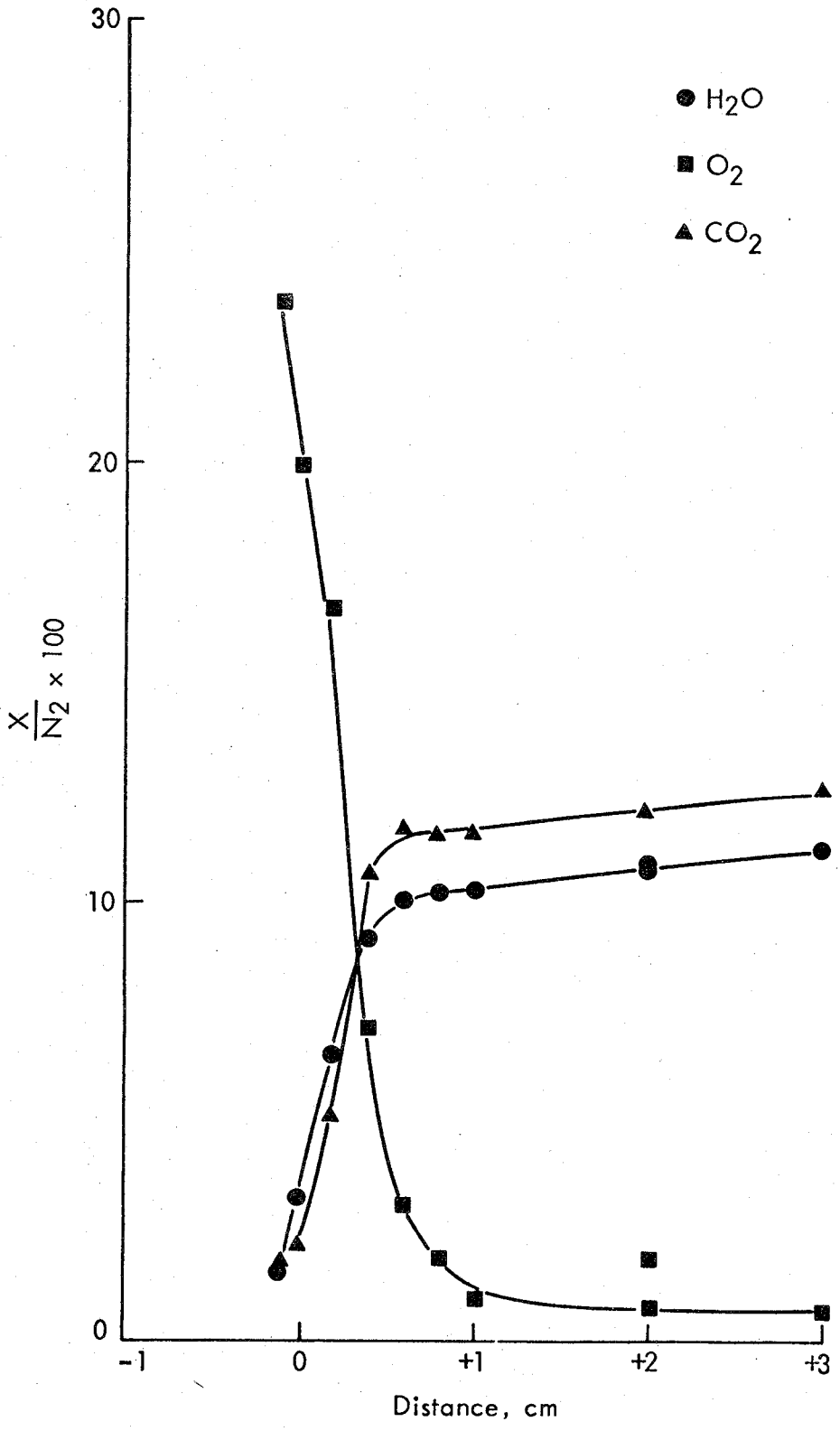

Figure 4 - Calibrated Mass Spectrometer Profiles Through a 10 to 20 μ Coal-Air Flame on a 6.3-cm Diameter Burner. Coal varied from 277 mg/liter to 207 mg/liter.

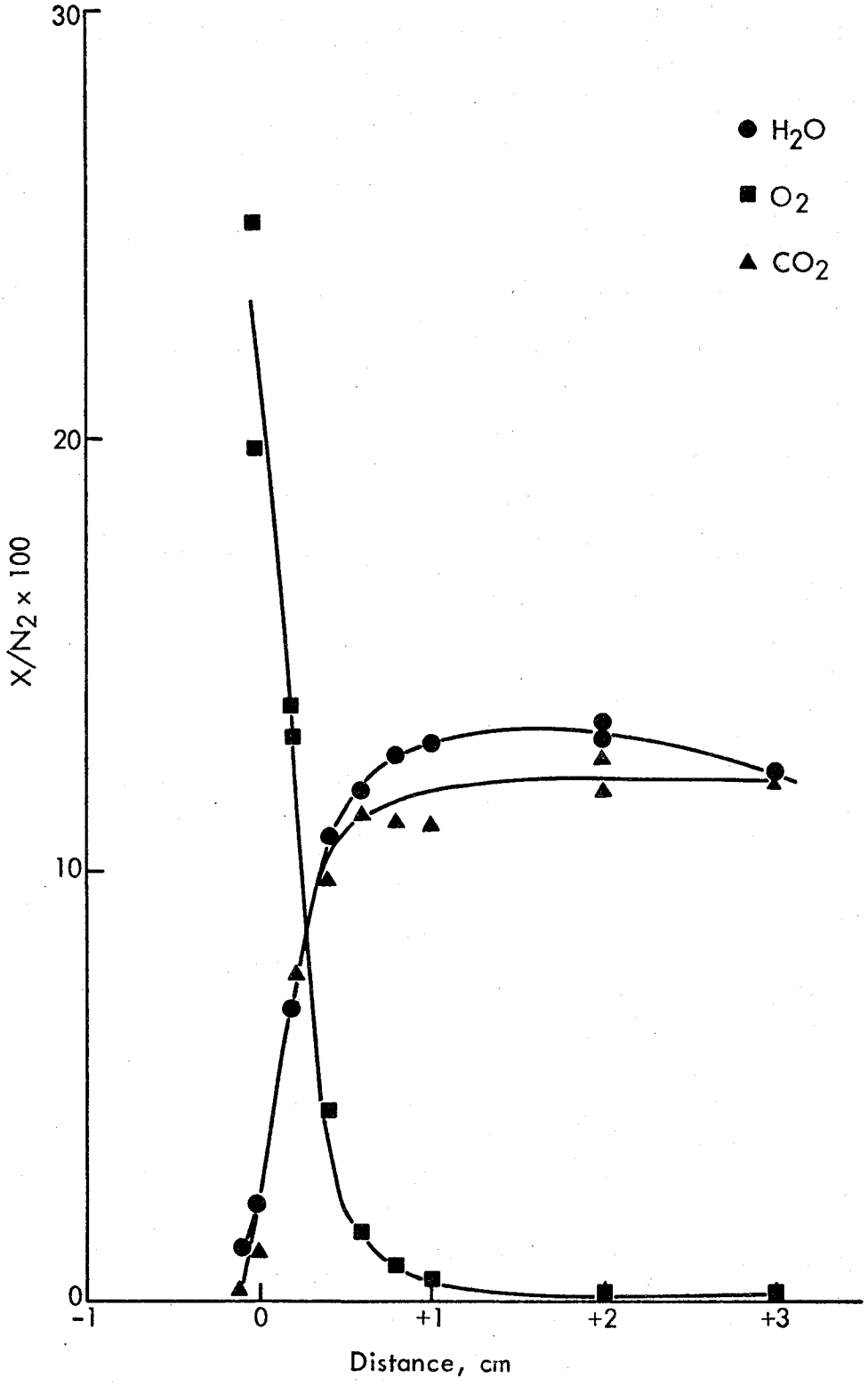

Figure 5 - Calibrated Mass Spectrometer Profiles Through a 10 to 20 μ Coal-Air Flame on a 6.3-cm Diameter Burner With a Copper-Plated Honeycomb Grid. 291 mg/liter.

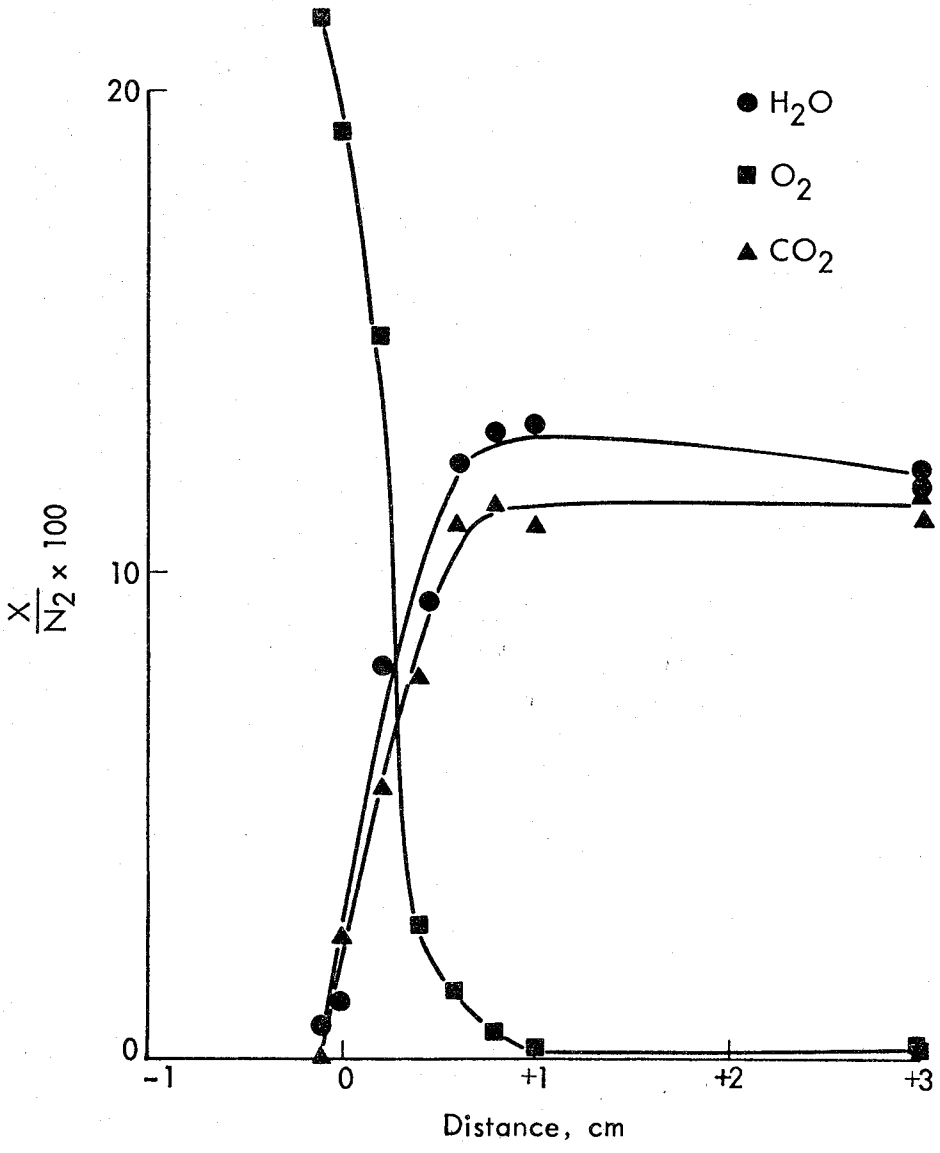

Figure 6 - Calibrated Mass Spectrometer Profiles Through an Unsieved Coal-Air Flame on a 6.3-cm Diameter Burner. 257 mg/liter.

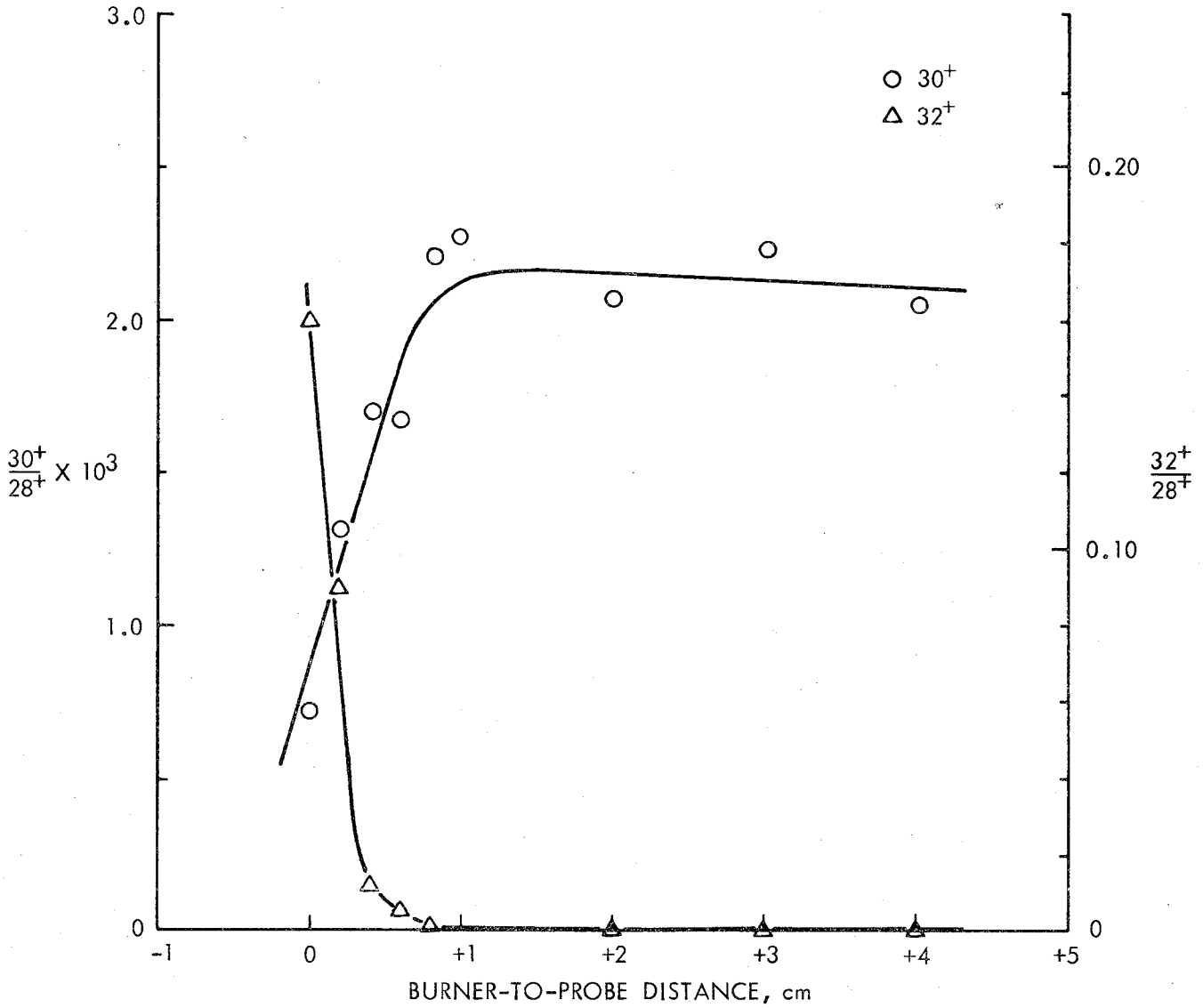

Figure 7 - Profile of NO and O_2 Through a 208 mg/liter Coal-Air Flame

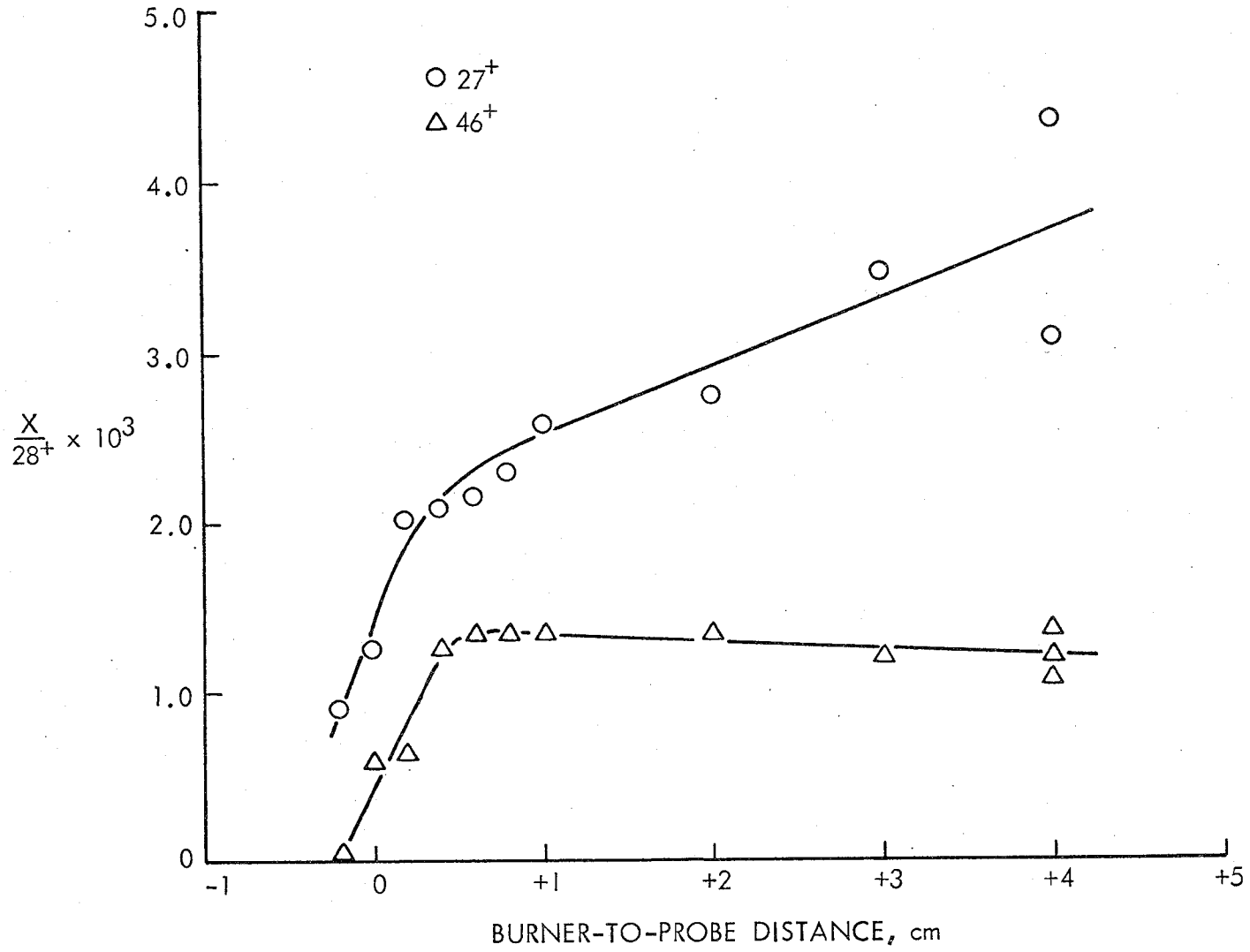

Figure 8 - Profile of 27^+ and 46^+ Through a 145 mg/liter Coal-Air Flame

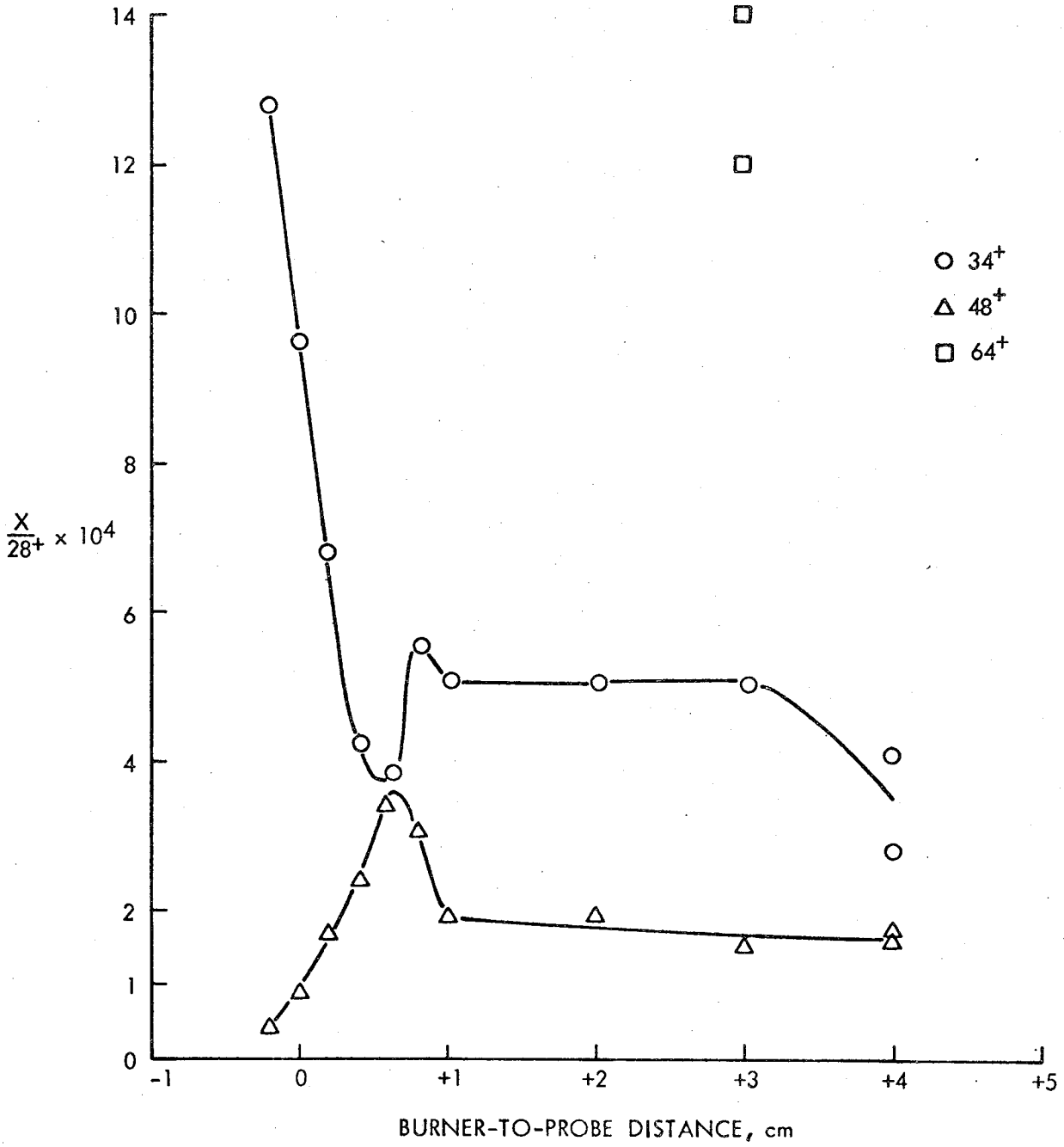

Figure 9 - Profiles of Sulfur Species in a 149 mg/liter Coal-Air Flame. The 34^+ peak is dominated by a O_2 isotope contribution early in the flame.

TABLE 1

POSITIVE IONS, AND PRESUMED PRECURSORS, FOR POLLUTANT SPECIES MEASURED IN COAL-AIR FLAMES

Positive Ion Observed	Presumed Precursor	Data Given In
27	HCN	Figure 8
30	NO	Figure 7
46	NO_2	Figure 8
34	H_2S	Figure 9
48	SO	Figure 9
64	SO_2	Figure 9

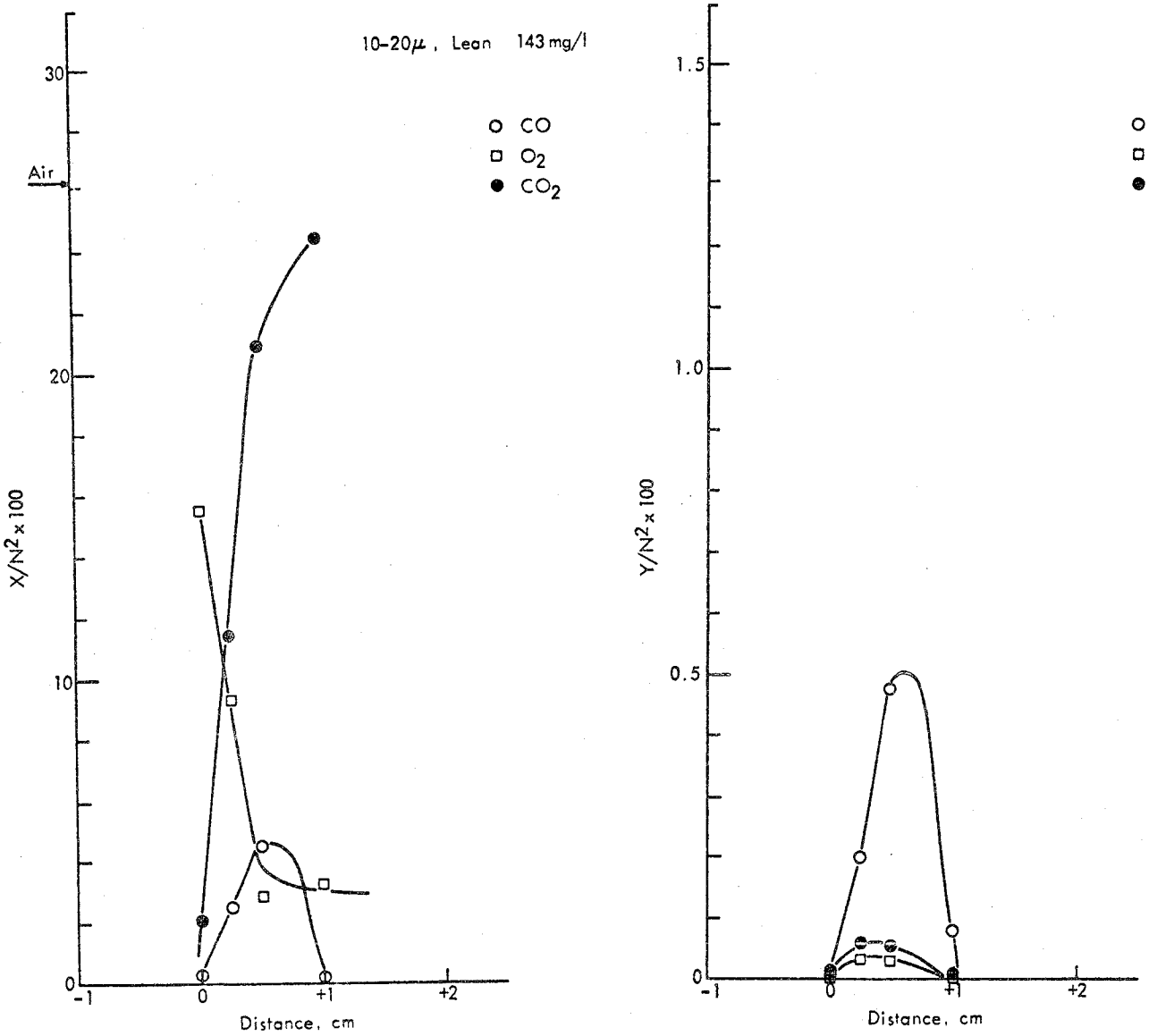

Figure 10 - Results of Gas Chromatographic Analysis of Samples Collected From a Relatively Lean, 10 to 20 μ, Coal-Air Flame.

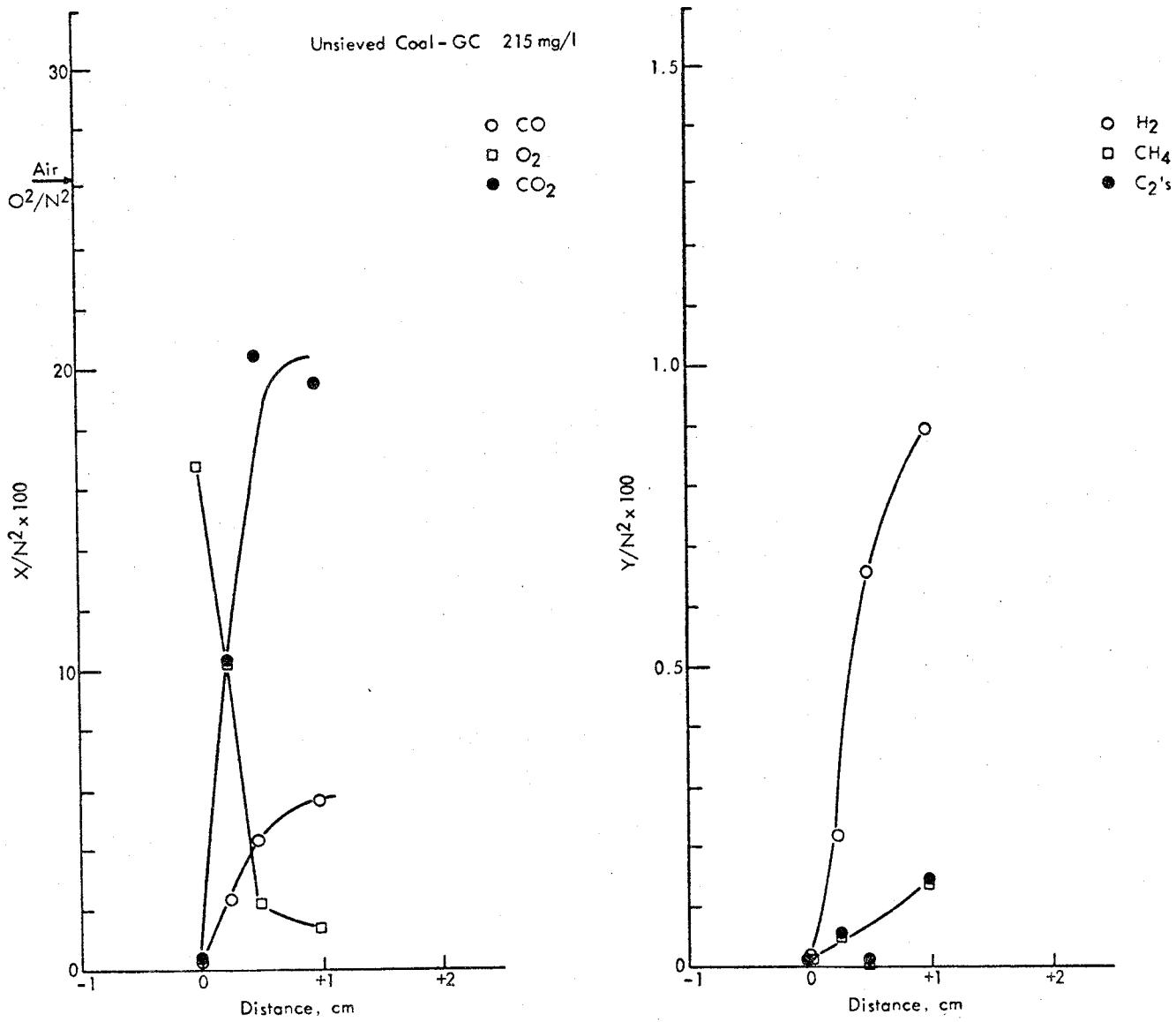

Figure 11 - Results of Gas Chromatographic Analysis of Samples Collected From a Medium, Unsieved, Coal-Air Flame.

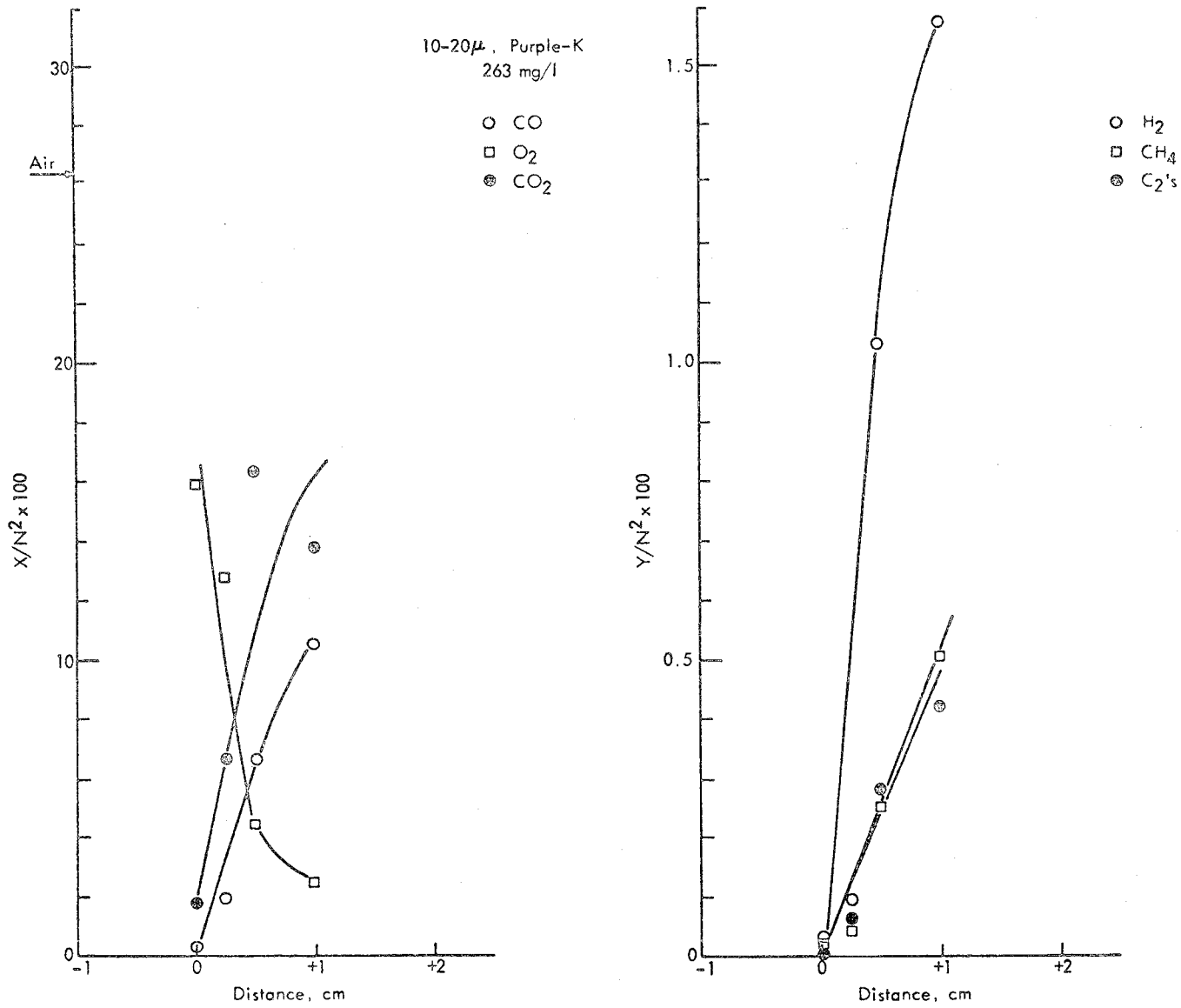

Figure 12 - Results of Gas Chromatographic Analysis of Samples Collected From a Rich, 10 to 20 μ, Coal-Air Flame to Which Purple-K Dry-Powder Inhibitor Had Been Added.

TABLE 2

PROXIMATE ANALYSES OF COAL AND CHAR SAMPLES EXTRACTED FROM THE EARLY REACTION ZONE OF PULVERIZED COAL-AIR FLAMES

Sampling Distance, cm	Sample No.	Coal (mg/liter)	% Moisture	% Ash	% Volatiles	% Fixed Carbon	% Remaining: $\frac{\%\ VM}{\%\ Ash} \div \frac{\%\ VM\ o}{\%\ Ash\ o} \times 100$	% Remaining: $\frac{\%\ FC}{\%\ Ash} \div \frac{\%\ FC\ o}{\%\ Ash\ o} \times 100$	Remarks
1	1	213	3.8	20.8	6.6	68.8	5.89	41.5	Unsieved coal
1/2	2	213	3.6	8.5	4.6	83.3	10.0	123	
1/4	3	213	3.6	9.3	13.2	73.9	26.3	99.8	
0	4	213	2.0	8.4	28.0	61.6	61.8	92.2	
0	5	141	2.2	-	28.0	-	~ 61.8	-	10 to 20 μ coal
1/4	6	141	2.4	8.7	24.2	64.7	51.6	93.4	
1/2	7	141	4.8	8.1	8.4	78.7	19.2	122	
1	8	141	5.1	21.1	7.6	66.2	6.69	39.3	
0	9	231	1.5	13.2	32.9	52.4	46.2	49.9	10 to 20 μ coal
1/4	10	231	2.8	17.4	19.4	60.4	20.7	43.7	
1/2	11	231	3.6	11.0	9.5	75.9	16.0	86.7	
1	12	231	3.7	19.0	6.9	70.4	6.75	46.6	
0	13	260	1.5	8.9	35.3	54.3	73.7	76.7	10 to 20 μ coal
1/4	14	260	3.2	15.1	20.6	61.1	25.3	50.8	
1/2	15	260	4.5	12.1	7.1	76.3	10.9	79.2	
1	16	260	4.3	8.5	4.4	82.8	9.60	122.4	
0	17	199	1.6	13.4	31.0	54.0	43.0	50.6	Purple-K added at 6 mg/liter, 10 to 20 μ coal
1/4	18	263	2.8	11.3	21.8	64.1	35.8	71.2	
1/2	19	263	2.6	13.3	14.4	69.7	20.1	65.9	
1	20	263	2.9	13.8	12.0	71.3	16.1	64.8	
0	17A	199	1.6	10.6	32.6	55.2	57.0	65.4	Materials scraped from samples wall after each of Runs 17 to 20
1/4	18A	263	2.5	13.5	25.3	58.7	34.7	54.6	
1/2	19A	263	3.2	15.4	13.0	68.4	15.6	55.7	
1	20A	263	5.3	17.2	8.8	68.7	9.49	50.3	
	21	-	1.0	6.9	37.2	54.9	100.00	100.00	Raw coal

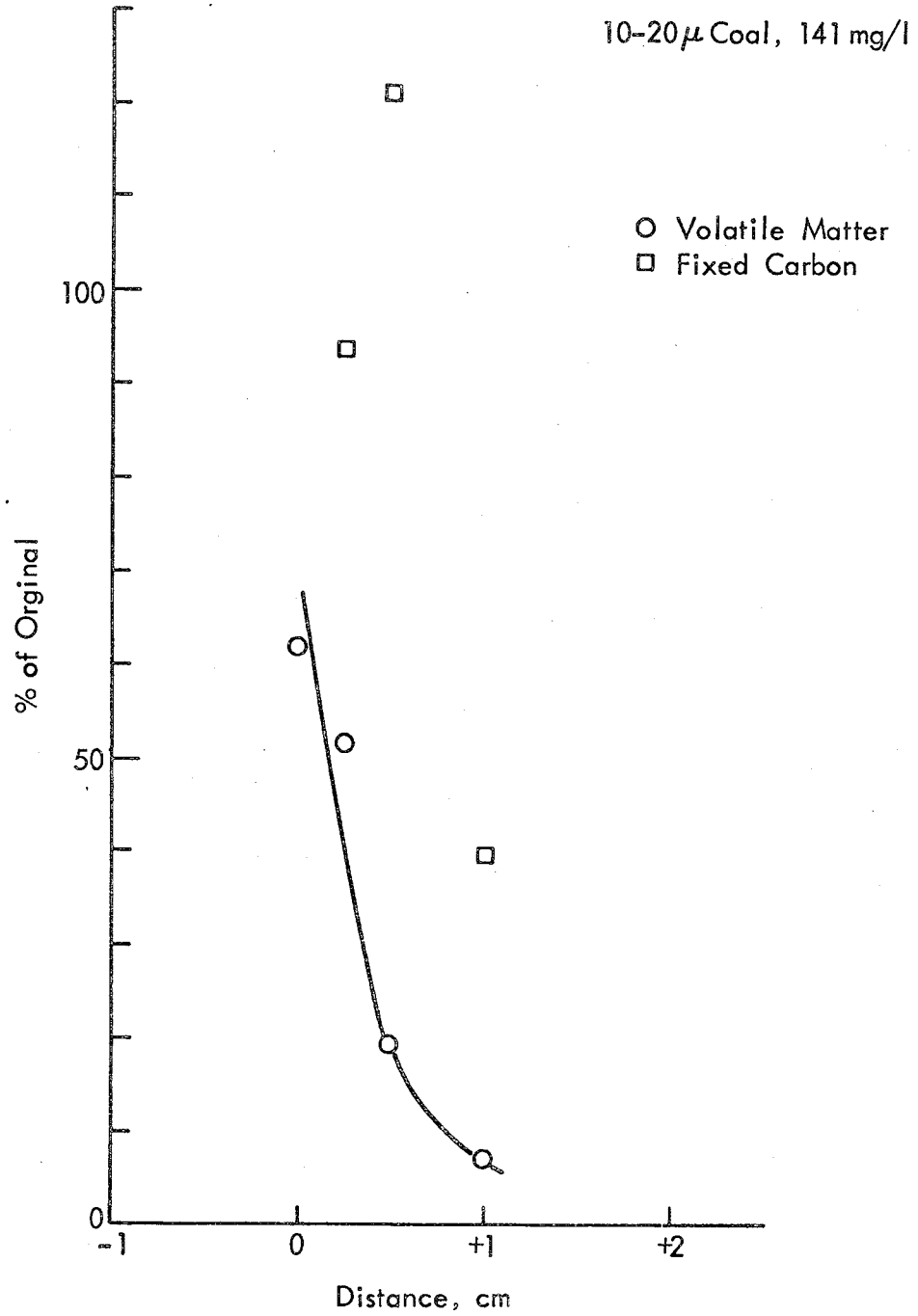

Figure 13 - Proximate Analysis Results for Particulates Sampled From the Early Region of a 10 to 20 μ Coal-Air Flame. 141 mg/liter.

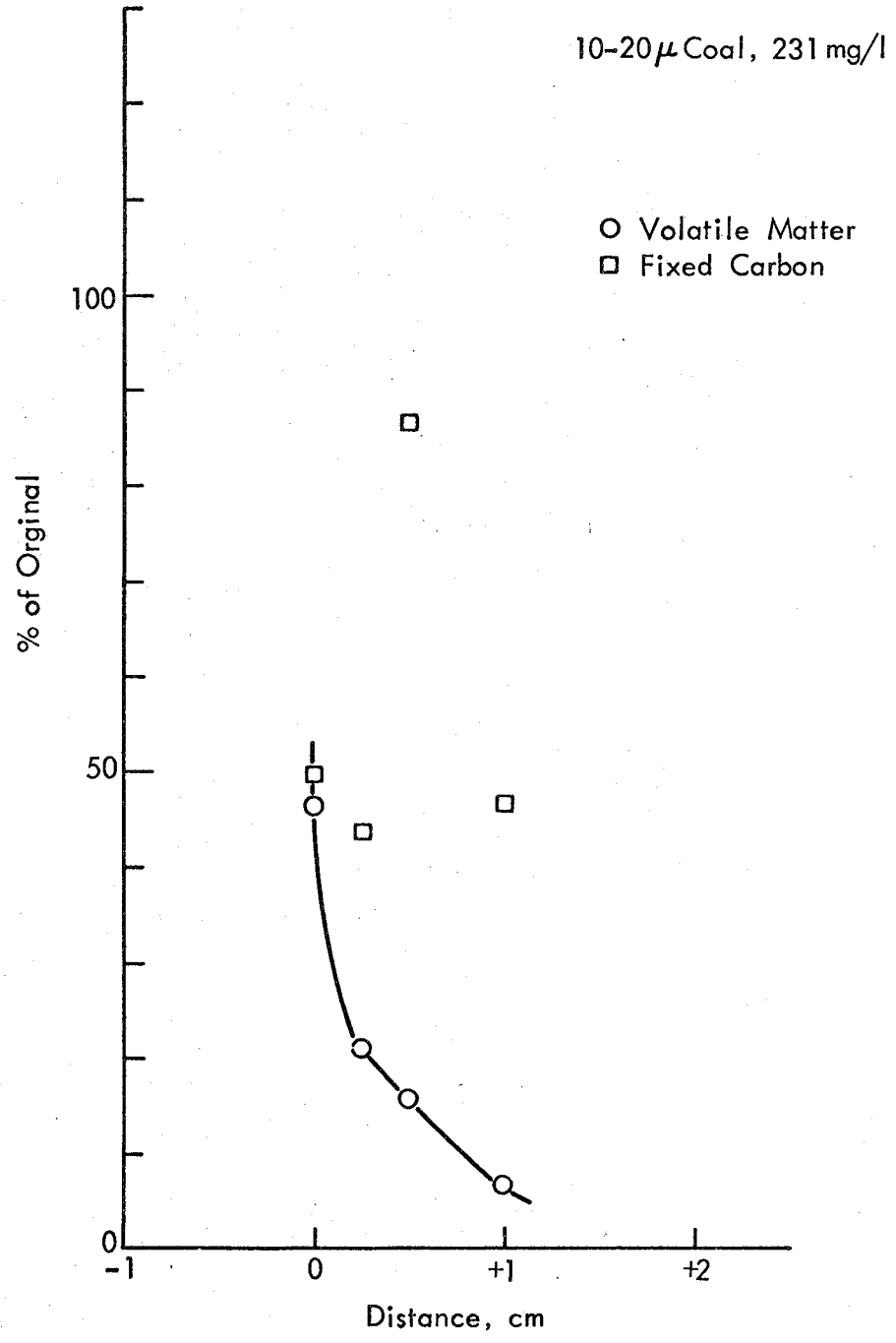

Figure 14 - Proximate Analysis Results Particulates Sampled From the Early Region of a 10 to 20 μ Coal-Air Flame. 231 mg/liter.

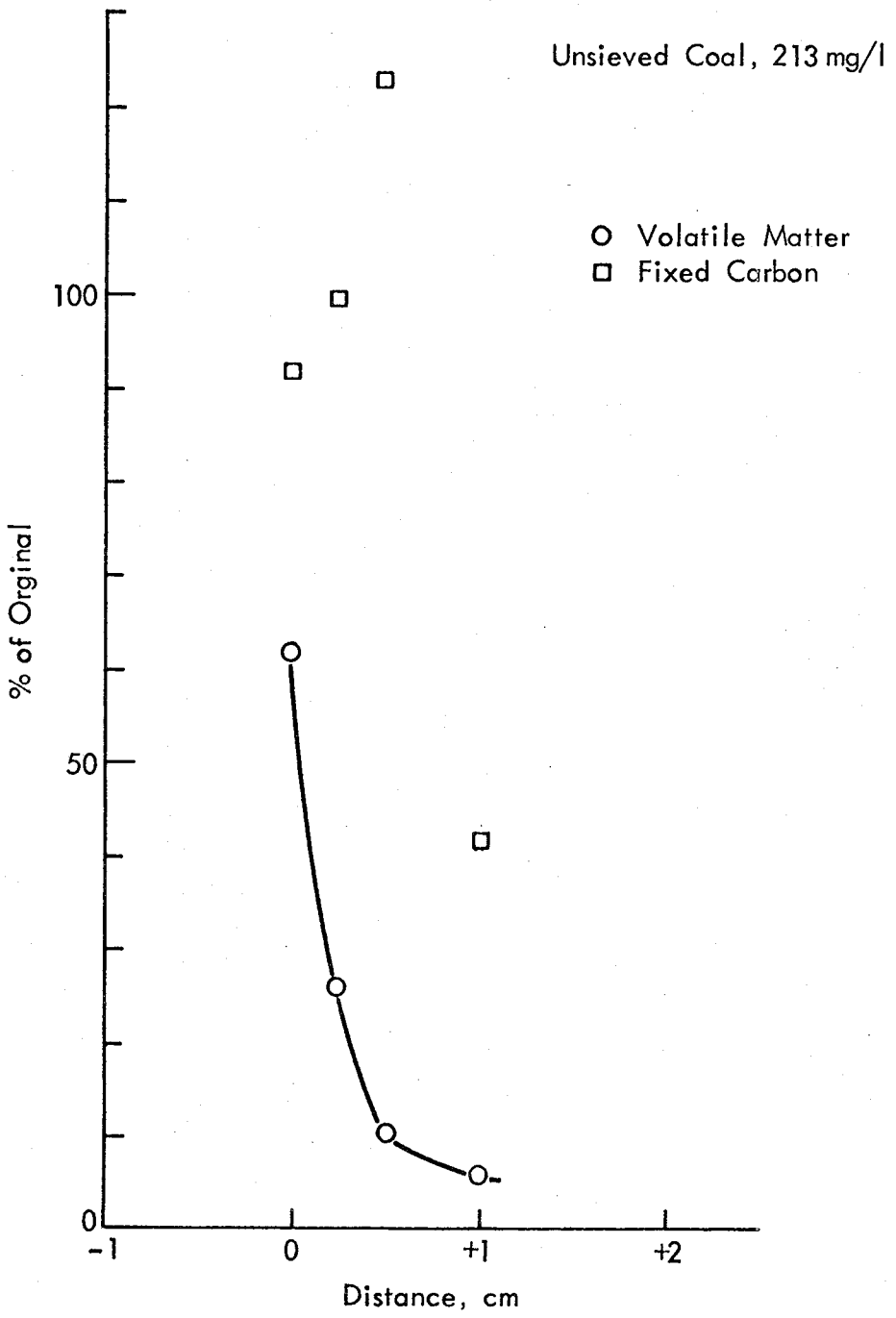

Figure 15 - Proximate Analysis Results for Particulates Sampled From the Early Region of an Unsieved Coal-Air Flame. 213 mg/liter.

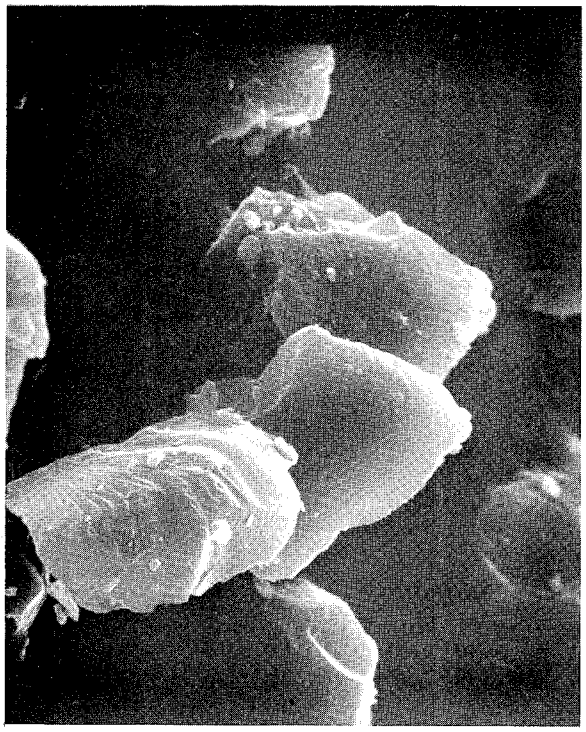

RAW COAL

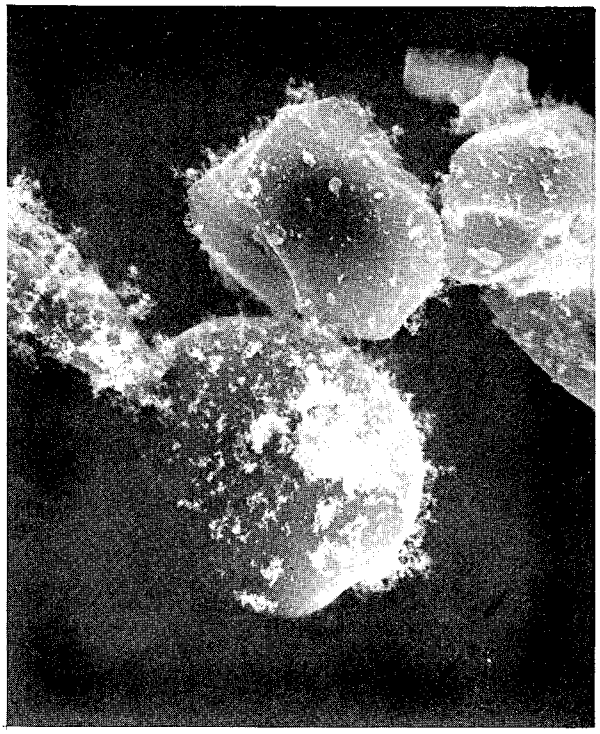

0 cm

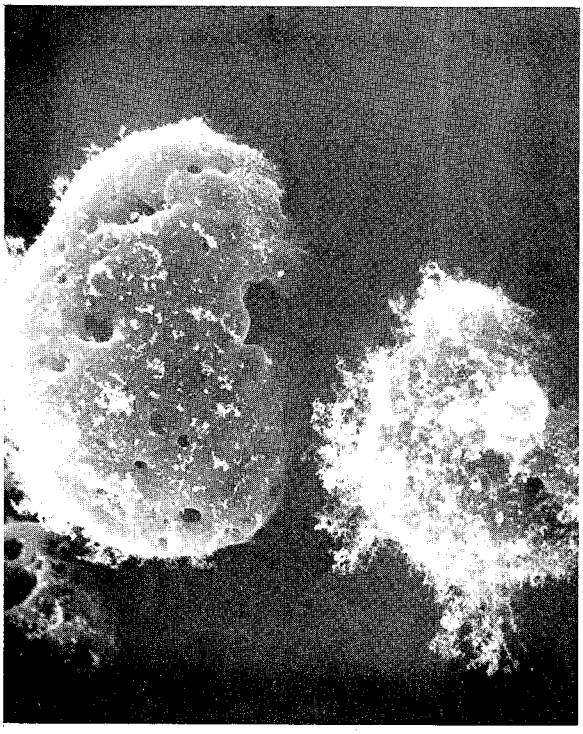

0.5 cm

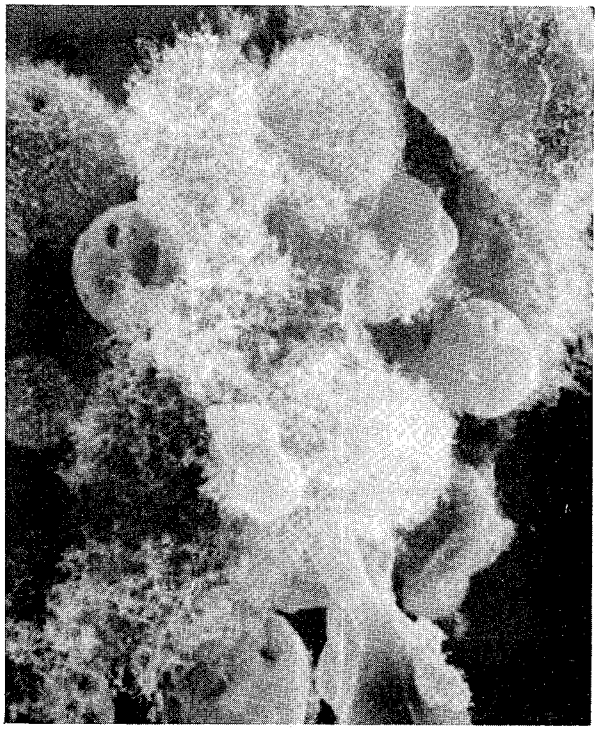

4.0 cm

10 μ

Figure 16 - Scanning Electron Microscope Photographs of Typical Particles Sampled from a 10 to 20 μ Coal-Air Flame. Coal concentration was 176 mg/liter.

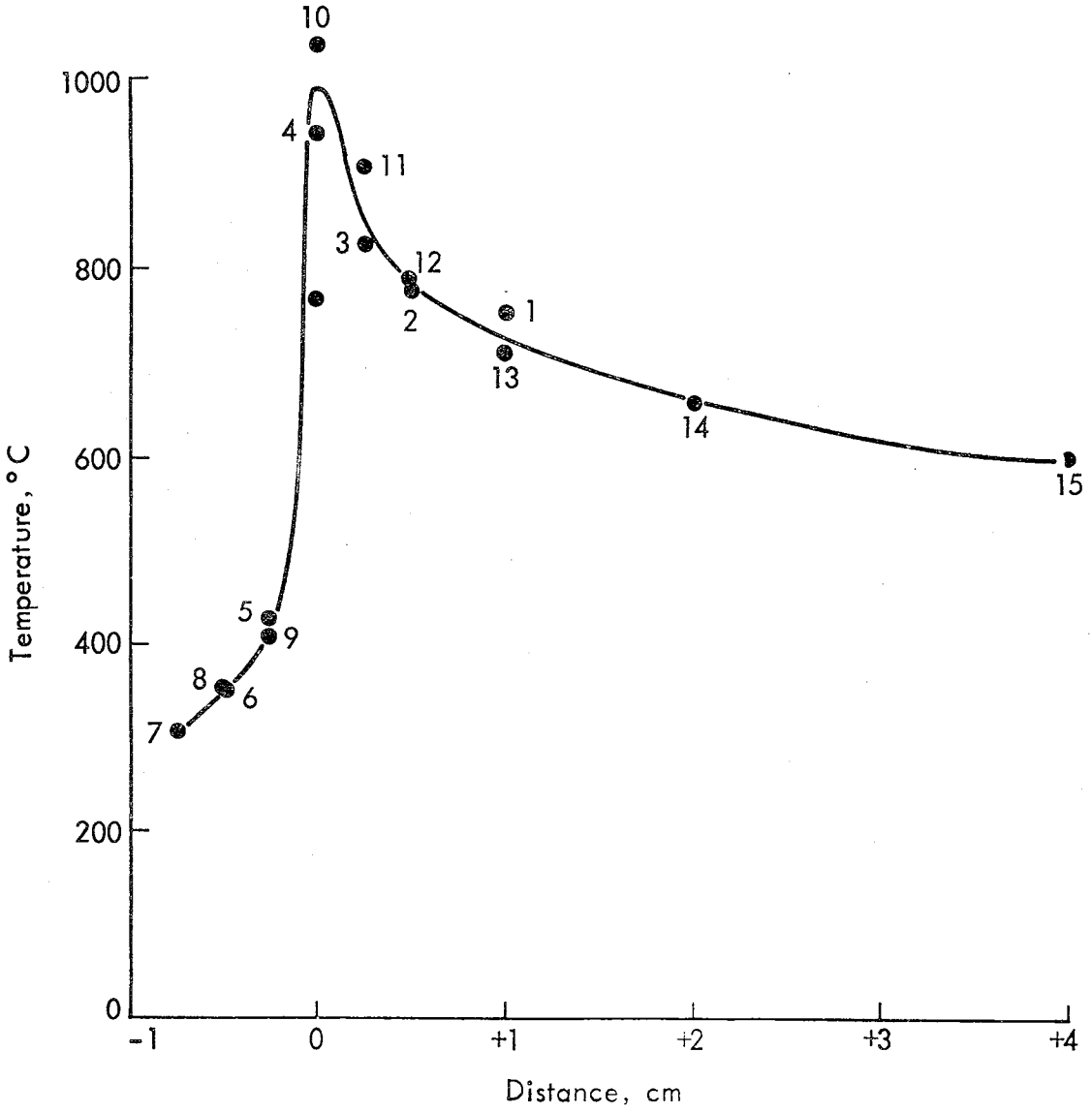

Figure 17 - Strip Chart Data for Coal-Air Flame. Coal concentration varied from 220 to 189 mg/liter.

diameter tubes. The logical extension of our flame work is to sample, in real time, explosion waves in tubes of 5 to 25 cm diameter. Peak switching in the 1 millisecond range, or entire mass spectral scans in the 10 millisecond range, should permit detailed characterization of the chemical processes in a fast-moving explosion as it passes selected direct sampling ports.

Systematic study of the quenching behavior of a variety of coal dust-air mixtures would also be fruitful in understanding explosion behavior and assessing relative explosibility of dusts under well-controlled conditions.

Further studies should be undertaken of the evaporation behavior of dry-powder agents in both hydrocarbon-air flames and ultimately in coal-air flames. Detailed profiles of species in inhibited flames, including the important free radicals involved in propagation, might at last resolve the question as to the primary mode of action of dry chemicals in inhibition. The behavior of these powders as the combustion wave speed increases would be especially interesting in the mine explosion context.

The techniques applied to coal dust-air mixtures appear equally suitable for application to other dusts, whether organic, metallic, or fossil in origin.

D. Recommendations for Related Energy Studies

While not of direct interest to the sponsors of the present work, the energy related studies listed below are also made possible by the results of this research. The combination of stabilized, flat coal-air flames and direct mass spectrometry appears well suited to the elucidation of many processes of importance to the understanding and improvement of coal combustion and conversion processes. We are currently applying such techniques, in work for ERDA, to the identification of gaseous sodium- and sulfur-containing species that may participate in fireside corrosion processes.

Other areas of application include the detailed analysis of conversion of fuel-N_2 to NO_x and fuel sulfur to SO_x, including the ability to measure gaseous species such as HCN, HNO_3, Na_2SO_4 and H_2SO_4. Under the realistic combustion conditions these small flames provide, one could follow the partition of nitrogen and sulfur between volatile matter and char-burning stages, and the effect of temperature, stoichiometry, and additives on conversion to NO_x and SO_x.

The isokinetic sampling of particulates throughout such coal-air flames should permit, for the first time, a detailed study of the conversion of coal mineral matter to fly ash and slag. As with gaseous pollutants, one could determine the effects of coal type, particle size, temperature, stoichiometry, and additives on fly ash formation, with implication for ash fouling, electrostatic precipitator collection and trace-element segregation processes.

Under unusual coal combustion conditions, such as those proposed for open-cycle, coal-fired MHD combustion, the direct, molecular beam sampling technique should be unexcelled in providing information on the behavior of gaseous species, ions and particulates. Condensible species resulting from seed additives and mineral matter evaporation, under the very high temperatures encountered in these combustors, can perhaps be measured in no other way.

Direct sampling of coal systems under atmospheres simulating coal gasification or flash hydrogenation conditions, is another promising application. The sampling technique developed so far should be applicable to high-pressure systems, though with greater difficulty.

REFERENCES

1. Milne, T. A., and J. E. Beachey, Midwest Research Institute, USBM Contract No. H0122127.

2. Smoot, L. D., and M. D. Horton, Brigham Young University, USBM Contract No. H0122052.

3. Strehlow, R. A., L. D. Savage, S. C. Sorenson, and H. Knier, University of Illinois, USBM Contract NO. H0122122.

4. Milne, T. A., J. E. Beachey, and F. T. Greene, "Exploratory Studies of Flame and Explosion Quenching," First Annual Technical Progress Report, June 30, 1970 - June 30, 1973, U.S. Bureau of Mines Contract No. H0122127.

5. Milne, T. A., and J. E. Beachey, "Exploratory Studies of Flame and Explosion Quenching," Second Annual Technical Progress Report, June 30, 1973 - June 30, 1974, U.S. Bureau of Mines Contract No. H0122127.

6. Milne, T. A., J. E. Beachey, and F. T. Greene, "Exploratory Studies of Flame and Explosion Quenching," First Quarterly Technical Progress Report, June 30 - September 30, 1972, through Eleventh Quarterly Technical Progress Report, October 1 - December 31, 1975.

7. Milne, T. A., F. T. Greene, and J. E. Beachey, "Pulverized Coal Combustion Studies on Flat-Flame Burners," paper preprinted and presented at the Western States Section/The Combustion Institute, 1974 Spring Meeting, May 6-7, at Pullman, Washington.

8. Milne, T. A., and J. E. Beachey, "Laboratory Studies of the Combustion, Inhibition, and Quenching of Coal Dust-Air Mixtures," paper preprinted and presented at the Western States Section/The Combustion Institute, 1976 Spring Meeting, April 19-20, Salt Lake City, Utah.

9. Grumer, J., private communication, Pittsburgh Mining and Safety Research Center.

10. Singer, J. M., A. E. Bruszak, and J. Grumer, "Equivalences of Coal Dust and Methane at Lower Quenching Limits of Flames and Their Mixtures," Bureau of Mines Report of Investigations RI-6761 (1966).

11. Powell, F., "The Effect of Inert Dust on the Combustion Limits of Lycopodium Spores Dispersed in Air," Combustion and Flame, 6, 75 (1962).

12. Litchfield, E. L., private communication, Pittsburgh Mining and Safety Research Center.

13. Howard, J. B., and R. H. Essenhigh, "Mechanism of Solid-Particle Combustion with Simultaneous Gas-Phase Volatiles Combustion," Eleventh Symposium (International) on Combustion, the Combustion Institute, p. 399 (1967).

14. Iya, K. S., S. Wollowitz, and W. E. Kaskan, "The Mechanism of Flame Inhibition by Sodium Salts," Fifteenth Symposium (International) on Combustion, the Combustion Institute, p. 329 (1975).

APPENDIX A

A LISTING OF EXPERIMENTAL ATTEMPTS TO STABILIZE SMALL, COAL DUST-AIR FLAMES

1924-1927: Newall and Sinnatt[1] examined individual coal particles as they entered a hot furnace. Before ignition the particles swelled, forming thin, hollow spherical bubbles. Furnace temperatures of 800°C were required for steady ignition, a value higher than observed for ignition in a steady-burning pulverized coal flame.

1934: Fuhrmann and Koettgen[2] were one of the first to try to achieve stabilization of flames of coal dust, but they could not do so without the addition of methane.

1942: Orning[3] reported volatiles burning around individual coke particles with the coke itself burning later.

1955: Ghosh and Orning,[4] using a furnace to achieve burning, saw a gradual transition from isolated particle ignition and burning to what they interpreted as collective ignition in a flame front as the pulverized coal density increased.

1956: Ghosh, Basu and Roy[5] burned coal dust flames in two highly augmented situations. A flame could be stabilized on a 0.5-cm diameter tube placed in a furnace held at 800 to 950°C. Open burning was achieved on a 1.1-cm diameter tube but only with synthetic air containing 60% O_2. Flame speeds were estimated from gas velocities at the burner mouth. These authors postulated that radiation played a prominent role in flame propagation.

1956: Hattori[6] burned coal dust-air by stabilizing with a central gaseous flame. He used a 0.4-cm diameter core flame of C_2 H_2-air in a 2.72-cm diameter surrounding coal-air mixture to achieve an inverted conical flame. Outer cone angles were interpreted to yield flame speeds of 20 to 50 cm/sec for coal dust-air.

1956: Cassel, Liebman and Mock[7] burned carbon dust in pure O_2 on a "Mache"[8] nozzle. The larger the flame, the higher the burning velocity. This effect was attributed to the role of radiation heat transfer in flame propagation.

1958: Burgoyne and Long[9] burned coal dust-air on a downward pointing, 1.6-cm diameter burner, with gas extraction to counteract buoyancy. They could only achieve stable burning in air with an annual surrounding flame of coal gas-air, however. From inner-cone areas and total coal-gas flow they deduced flame speeds as a function of concentration and particle size. A sample of their results is reproduced in Figure 1 to illustrate the generally observed variation with size and concentration and to indicate two stoichiometric endpoints. (The coal used had 36% volatiles by the standard test.) Burgoyne and Long report an initial narrow zone of intense luminosity followed by a protracted residue burning zone.

1961: Long,[10] reporting on studies started in 1952, attempted to burn 11 μ average diameter coal with 34% volatile content. He reported great difficulty in stabilizing coal dust suspensions between 100 mg/liter and about 0.4 g/cc (fluidized bed densities). His approach was to maintain turbulence as long as possible before converting to laminar flow just ahead of the flame. Even so, Long reports he "could only produce stable flames in the presence of some maintained source of ignition." He measured flame speeds from conical flame fronts with 1.6-cm diameter burners either placed in a furnace at 1000°C or with an annular stabilizing flame. Remarkably, these two methods gave compatible flame speed results, showing behavior similar to that presented in Figure 1. Long postulated that a 1.6-cm diameter flame of coal dust in air was inherently unstable due to limited radiative heat transfer. He estimated that initial bright zone to be about 2 mm thick and to involve about 7 msec residence time for particles passing through. Long viewed the combustion of volatiles as controlling the burning rate, with the release of volatiles governed by heat transfer, rather than by the kinetics of pyrolysis.

1964: Marshall, Palmer and Seery[11] sought to extend the studies of Burgoyne and Long to smaller particle sizes. Working with 2.6 and 3.1 μ mass-mean diameter coal, of 34% volatility, they still could achieve stable laminar flames only with a hot stabilizing-ring flame holder and with 28% O_2 in the "air." A 2-cm diameter burner tube was used, with a cold N_2 sheath gas flowing annularly. Flames with pure air could only be achieved momentarily by pulsing the O_2 flow. Their results could be rationalized, in a particle size scaling law, with Burgoyne and Long's. Observing an initial bright zone of some 2 mm thickness, they note that this is much thicker than is characteristic for gaseous premixed flames and therefore conclude that volatiles are not rapidly released and then burned, nor does gaseous diffusion of the volatiles into the surrounding air control burning. They make the significant postulate that with the burning controlled by the rate of release of volatiles, small addition of inhibitors would not be expected to slow the rate of burning. They claim, but report no data, that addition of CCl_4 to coal dust-air flames caused no change in flame speed until the flame went out. It is concluded that the "dynamic" ignition temperature may be as low as 600°K (in a propagating flame), that thermal conduction is the main mode of heat transfer in their small flame, and that the rate of propagation varies with $1/(\text{diameter})^2$.

1965: Howard and Essenhigh[12,13] have made perhaps the most detailed study of laminar coal dust-air combustion using an enclosed (hot walls) plug-flow reactor. This study contains many relevant measurements and an extensive analysis of the role of heterogeneous versus homogeneous burning of volatiles in the initial ignition and reaction zone.

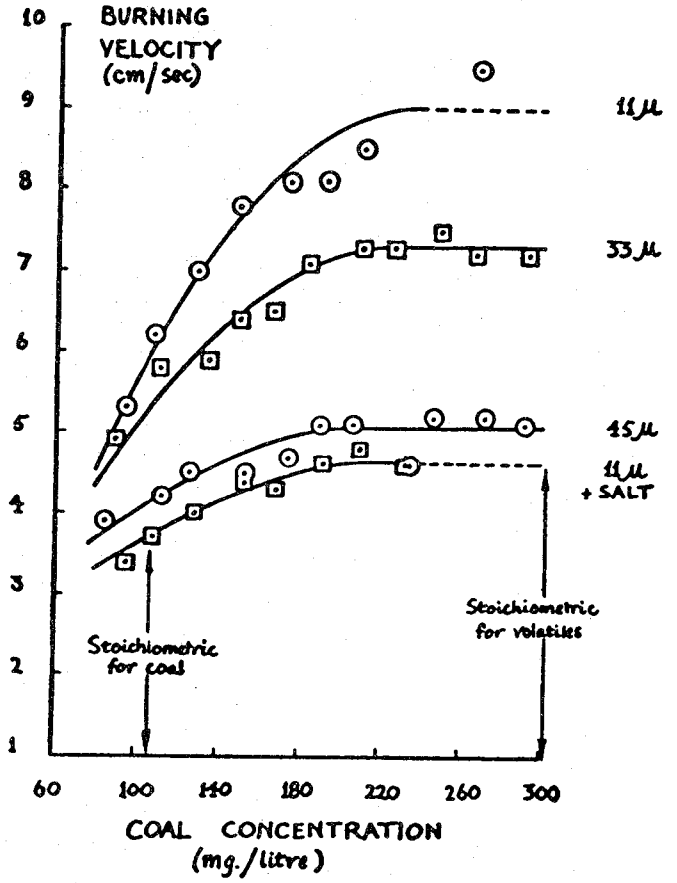

Figure 1 - Literature Results of Burgoyne and Long for Burning Velocities of Stabilized Coal Dust-Air Mixtures

Two recent presentations by Essenhigh[14,15] contain highly relevant comments about problems remaining in coal combustion science.

The study of the evolution of volatiles under the very rapid pyrolysis condition (10^4 to 10^6°C/sec) found in coal dust-air flames is also very germane to the problem of inhibition of these flames. A number of recent studies of rapid devolatilization have been carried out using various heating[16-29] schemes, but the conditions of actual coal dust-air flames are hard to simulate. A point of particular contention is the fact that both the nature and amounts of volatiles released from a given coal depend on rate of heating as well as final temperature achieved.[30]

Progress on the contemporaneous programs at Brigham Young[31-33] and the University of Illinois[34-38] has been reported in a series of annual reports and papers, not all of which are publicly available at this writing. In the presentation of research results below, only very limited reference will be made to these studies, with detailed comparisons and comments being reserved for later open publications.

APPENDIX B

EXPERIMENTAL COALS AND POWDER DELIVERY SYSTEMS

A. Experimental Coals Used

Two batches of finely ground Pittsburgh seam coal, supplied to us in 55-gal. drums by the Bureau of Mines, were used for the reported experiments. The first drum supplied was used for approximately the first 2-1/2 years of apparatus development and testing, and for some of the early flame species profile measurements. This batch had an anomolously high mineral matter content so that a second batch was procured and used for the final series of flame probing and sampling experiments.

Table 1 presents the proximate and ultimate analyses for these two coals as determined by the Bureau. Because our initial sieve results caused concern that there might have been size segregation of the coal during shipment to Kansas City, the Bureau[39] carried out size and composition analyses of samples from both the top and bottom of the barrel. The results indicated no "unmixing" of the coal. The ash content of 11 to 12% was higher than expected for Pittsburgh Seam and was apparently the result of a little too much rock being included in this particular batch prior to grinding. Analyses were also carried out on the air classified samples, showing little segregation by such treatment.

Figures 2 and 3 show size analyses of the coal as received, and for the 10 to 20 μ size fractions that were used in most of our flame tests. Air classification was performed by the Majac Company.[40]

B. Coal Dust Feeder

A great variety of powder feeding devices have been described, employing a range of mechanical principles. These include auger feeds such as have been used for short periods of time at the Bureau[41] and at MRI[42] and an elaborate, large system, used quite successfully by Howard and Essenhigh to feed their inverted, rectangular, one dimensional, enclosed furnace chamber. A system recently described in the literature,[43] employing a fluidized bed, is reported to give stable delivery of pulverized coal for hours, is inexpensive to build and can deliver the quantities of coal needed for a 12.6-cm diameter burner. We chose this scheme for use with both coal dust and inhibitor powders.

For large delivery rates a feeder similar to Feeder C of Ref. 43 was adopted. A scale schematic of the simplified design we used is shown in Figure 4. The glass storage section is 10 cm Pyrex pipe of 30 cm length. Dry air from a cylinder enters at the bottom and passes through a sintered-metal porous disk. This fluidizing air passes up through the column of coal dust with a portion flowing out through the exit tube (protruding into the center of the copper cross) and the rest exiting through a filter and a flow meter at the top of the apparatus.

TABLE 1

PROXIMATE AND ULTIMATE ANALYSES OF PITTSBURGH SEAM COAL DUST PROVIDED BY THE BUREAU OF MINES

	Batch 1				After Air Classification by Majac					Batch 2		
Proximate Analysis	Sampled From Burner	Bureau Before Shipment	Bottom of Barrel as Received	Top of Barrel	< 10 μ	10-20 μ	From Fluid Bed Feeder	20-30 μ	> 30 μ	Sampled From Burner	Bureau Before Shipment	Bureau Before Shipment
Moisture	0.6	1.1	1.6	1.7	1.8	1.9	1.9	1.8	1.8	1.0	2.0	1.8
Volatile Matter	34.4	35.2	32.8	33.3	31.9	32.4	31.7	33.4	33.7	37.2	35.6	35.4
Fixed Carbon	54.5	53.2	53.7	52.8	52.8	53.8	54.5	55.2	53.5	54.9	55.9	56.5
Ash	11.2	10.5	11.9	12.2	13.5	11.9	11.9	9.6	11.0	6.9	6.5	6.3
Ultimate Analysis												
Hydrogen		5.0	4.9	4.9	4.8	4.9	4.9	5.0	4.9		5.3	5.2
Carbon		73.9	72.1	72.0	70.5	72.1	72.1	74.0	72.1		76.7	77.1
Nitrogen		1.5	1.4	1.5	1.3	1.4	1.4	1.4	1.4		1.7	1.5
Oxygen		7.8	8.4	8.1	8.9	8.7	8.7	8.6	8.4		8.6	8.8
Sulfur		1.3	1.3	1.3	1.0	1.0	1.0	1.4	2.2		1.2	1.1
Ash		10.5	11.9	12.2	13.5	11.9	11.9	9.6	11.0		6.5	6.3

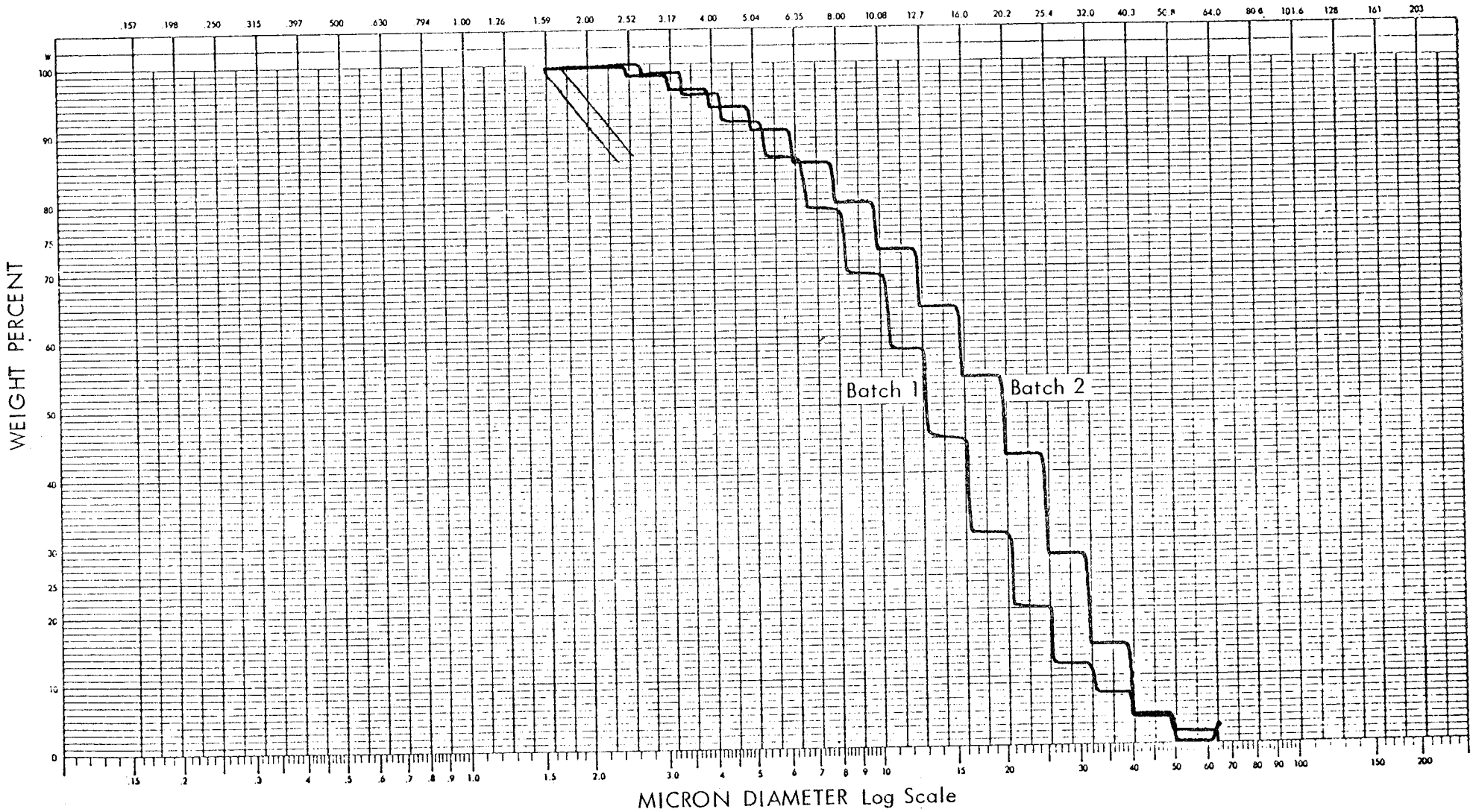

Figure 2 - Size Distribution, by Coulter Counter Analysis, of Batches 1 and 2 Pittsburgh Seam Coal Prior to Air Classification

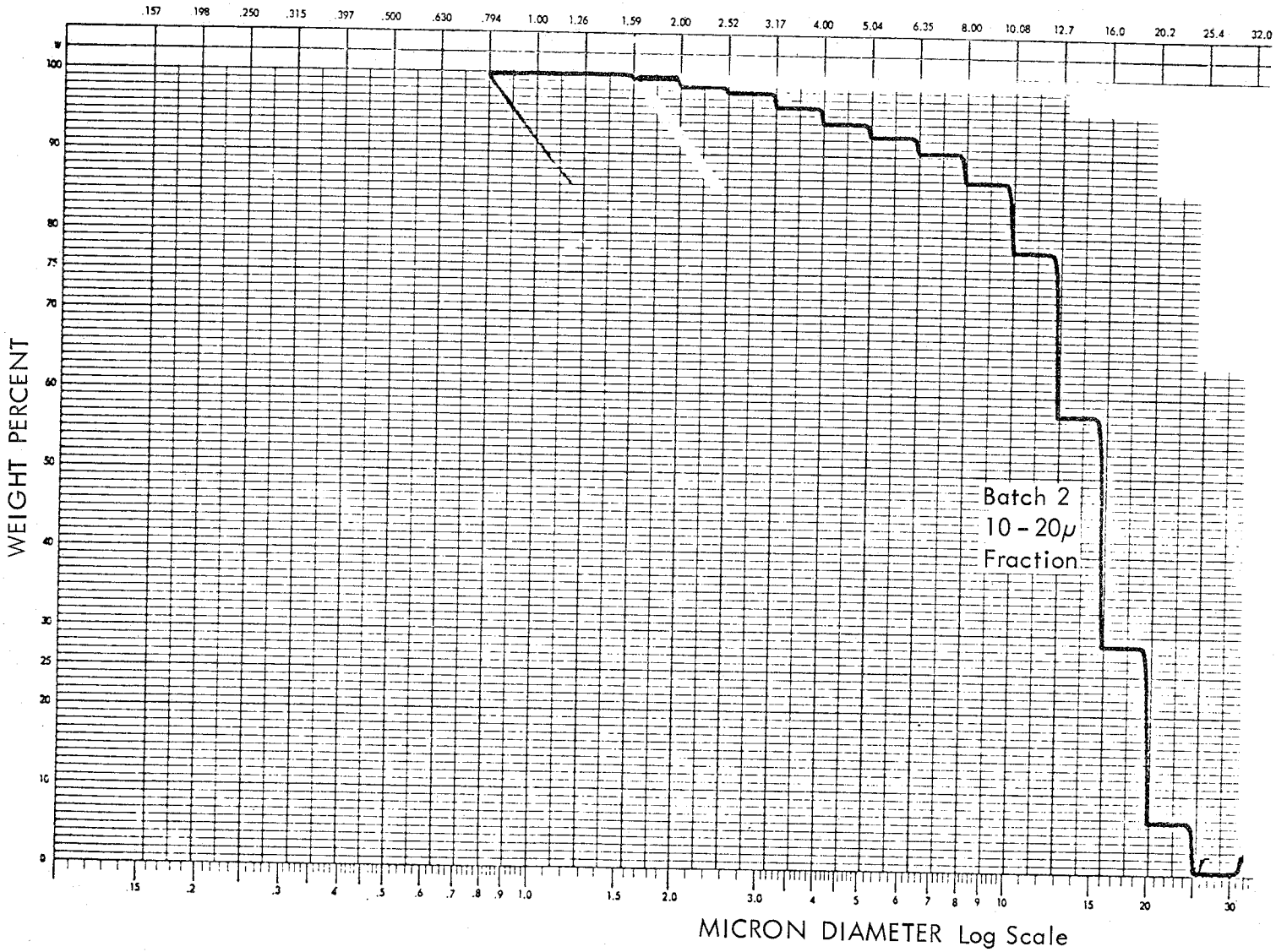

Figure 3 - Coulter Counter Analysis of 10 to 20 μ Fraction of Air Classified Batch 2, Pittsburgh Seam Coal

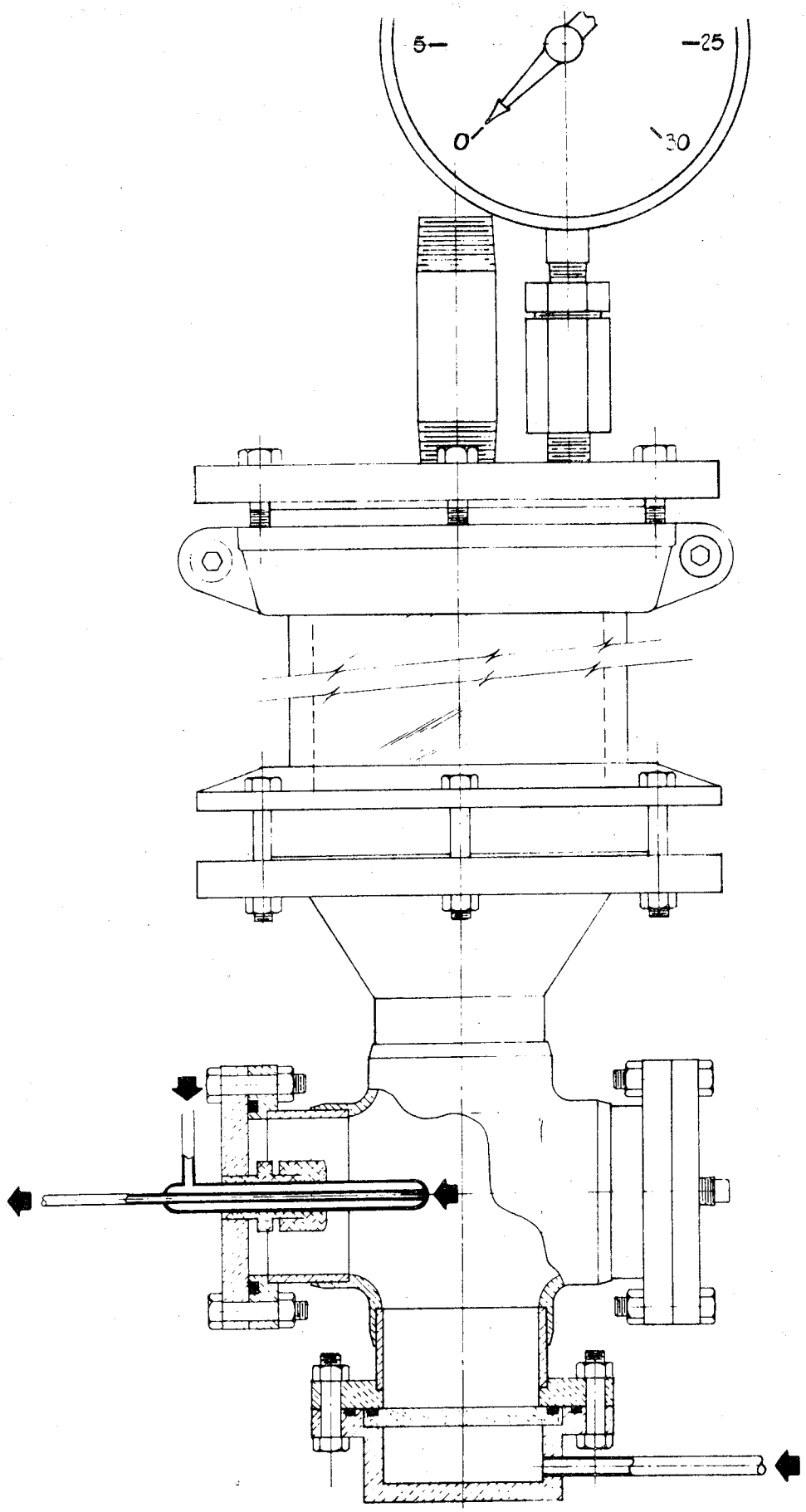

Figure 4 - Schematic of the Fluidized-Bed Pulverized-Coal Feeding Device, Reservoir and Coal-Feed Delivery Tube to the Burner

The exit tube is a stainless steel capillary of inside diameter 1 to 1.5 mm. An additional flow of gas, to aid transport of the coal-air along the tube and into the burner, is provided near the entrance of the off-take tube. Typically, the coal dust-air passes through about 30 to 40 cm of the capillary and similar size plastic tubing before entering either the burner or the gases feeding the burner.

During the course of using the feeder, the following changes were made to improve performance. A more impervious fluidizer-flow disk (porous bronze) was used to achieve a pressure drop of about 5 psi across the disk. A simple two-blade bed stirrer was introduced through the top of the fluidizer reservoir. The blades stirred the bed just above the off-take tube at about 100 rpm, resulting in steadier delivery and enhanced fluidization. Under proper operation the top surface of the coal rises about 3 to 5 cm when fluidization is achieved. The fluidizing and transport gas is dry air from a pressurized cylinder. To minimize plugging of the off-take tube, the coal dust is sieved to eliminate particles greater than 100 μ (there are few). Finally, a solenoid-vibrator was bolted to the off-take tube flange.

Typical results obtained with this system are shown in Figure 5 using a 1.0-mm diameter off-take tube. (A 1.5-mm tube resulted in too high a flow of coal at conveniently controlled fluidizer pressures.) Plotted in Figure 5 is the amount of coal dust delivered per minute (expressed as mg/liter for an anticipated burner flow of 80 liters/min) versus the gauge pressure in the fluidizer reservoir. Although for a given loading of coal dust and a given storage height in the reservoir, fairly reproducible results can be obtained, the same curve has not been obtained from day-to-day. It has remained necessary to perform fairly frequent collections of coal to calibrate the delivery rate. It is not known whether any size fractionation occurs during the feeding operations, but little is expected since coal dust is extracted directly from the fluidized material.

During the course of the program a number of tests were performed aimed at more quantitative control of the coal-air flames. First, the delivery of the coal from the fluidized-bed feeder was improved by two principal means. A regimen of periodic cleaning of the off-take capillary, by reaming with a stiff wire, reduced plugging to a negligible problem. Second, the steadiness of delivery was significantly improved by using a Cartesian diver type of pressure controller[44] to maintain a very constant pressure in the fluidized-bed chamber. Other changes which would be expected to improve operation involved extending the off-take capillary to the center of the fluidized bed and lowering the fluidizing air velocity as suggested by semi-empirical guidelines[45] for 10- to 20-μ powders.

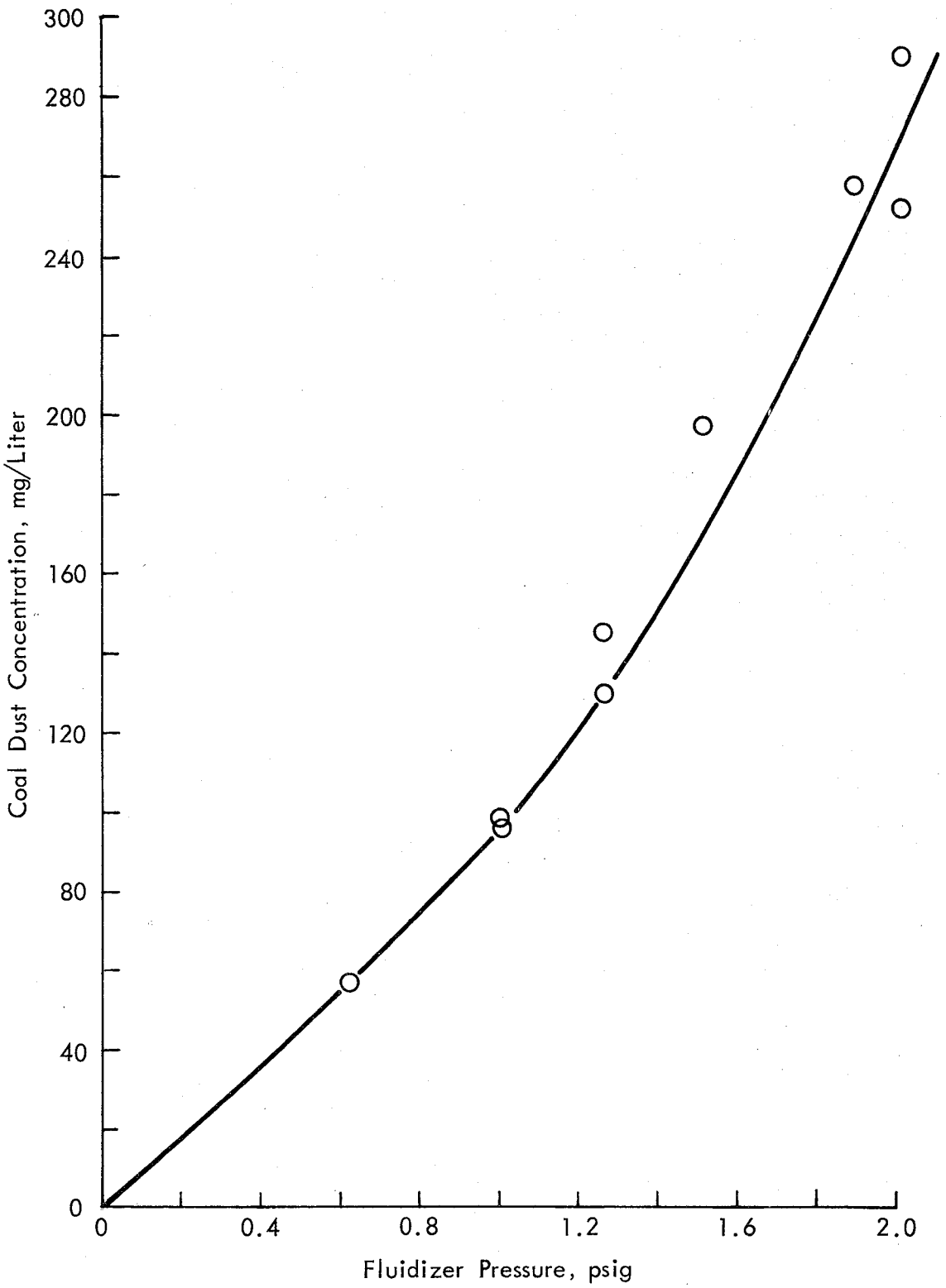

Figure 5 - Dependence of Coal Feeder Delivery Rate on Pressure in the Fluidizer Chamber. (Concentration applied to a mixture of the delivered coal in 80 liters/min of air.)

Two procedures for monitoring coal delivery rate were tested. First, a laser beam[46] was passed across the top of, and quite close to, the burner matrix. Transmitted light was detected by a commercial photoelectric detector.[47] It was found that at coal loadings in the range of 200 to 300 mg/liter, for unsieved Pittsburgh seam coal with a median particle diameter of about 10 to 20 μ, absorption was too great for convenient use of this technique to monitor feeder behavior. When the flame was ignited, transmission increased sufficiently to produce a measurable signal. However, the transmission depended strongly on flame position and fluctuations, leading us to abandon this technique as a means of dynamically monitoring coal delivery during burning. We did not try modulating the laser beam and using phase-sensitive detection, nor measuring scattered rather than transmitted light, though this might improve the usefulness of the laser monitoring technique.

As a workable expedient for monitoring coal delivery with time, we implemented a funnel collection scheme. A 65-mm diameter funnel with 15-cm filter paper, separated from the funnel by a screen to facilitate air flow, was connected to a 3 liter/sec mechanical pump. When the funnel was placed fairly closely over the burner matrix (with the flame out of course) the powder could be filtered and collected for easy weighing. Typically, 20-sec collections were sufficient.

The inhibitor power feeders are discussed in later sections describing powder evaporation and physical breakup tests.

APPENDIX C

FLAT-FLAME BURNER DEVELOPMENT

To facilitate interfacing the burner with either particle sampling probes or molecular-beam mass spectrometer sampling systems, a vertical burner with upward flow was desirable. Whether powder loadings of interest could be adequately entrained and swept through a vertical burner was one of the chief experimental questions.

Based on studies of the quenching behavior of coal dust-CH_4-air mixtures,[48] it appeared reasonable to try to stabilize flames on a 12.6-cm diameter flat burner. Figure 6 shows the schematic layout of the entire coal handling, burner and exhaust gas handling system for a burner of this size. This simple system, which was used for screening for workable burner configurations, was quite effective in keeping the coal dust confined to the hood, which was periodically vacuum cleaned.

Quite a number of combinations of coal-air mixing and inlet geometry burner geometry and flat-flame matrix designs were tested with mostly negative results. Most of the testing was done with the as-received coal (with only the $> 100\ \mu$ particles sieved out) using upright burners and requiring entrainment and delivery of the coal dust against gravity. The following considerations and tradeoffs were involved in seeking a feasible burner system.

1. The coal dust had to be kept continually swept out of the apex of the lower conical inlet portin of the burner. If accumulation once occurred, the entrainment progressively deteriorated and blowholes formed in the collected dust. Best results were obtained when the coal/air entered concentrically at the apex of a conical section at the bottom of the burner.

2. It was necessary to vibrate the burner continuously to obtain smooth coal delivery. Tests with a physically detached burner grid showed that it was the grid that required vibration, presumably to keep dust from collecting on the fine mesh openings. An industrial bell activator was used to vibrate the burner and grid as a unit.

3. The combination of burner geometry and grid thickness and openings involved the most serious tradeoff. Burners too short and grids too open did not adequately smooth the flow which was quite turbulent at the point of initial mixing. This resulted in erratically lifted flames and in individual conical flames from too coarse a matrix. Finer grids produced smoother flow and more fully merged flames but their performance was limited by hang-up of coal dust on the grid. On the other hand, burners which were too long, or which restricted flow through the grid, caused settling out of the coal-air suspension and thus prevented the desired powder loadings from being delivered against gravity.

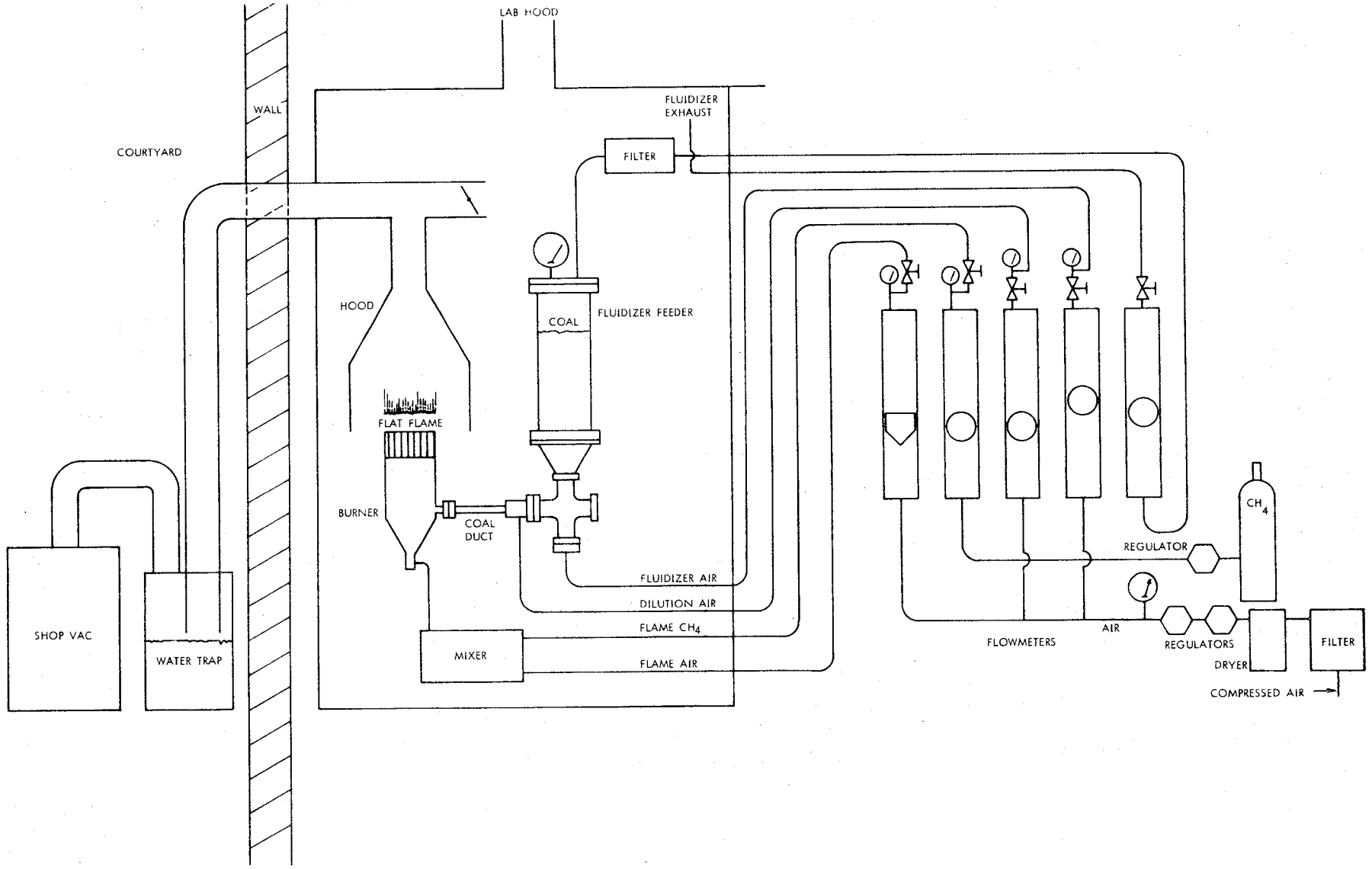

Figure 6 - Schematic of the Burner, Exhaust, Fluidizer and Flow Control Systems

Of the many empirically chosen variations in burner design that were initially tested, four showed promising performance characteristics.

A. Vertical, Conical, 12.6-cm Burner

With the 12.6-cm diameter burners, only upward flow configurations were tested because of the buoyancy problem with flames this large. The first achievement of a free-burning, unaugmented coal dust-air flame was with the conical burner shown in Figure 7. One of the finer matrices that could be used without collecting coal dust is shown in Figure 8 together with an early test version of the concentric coal-air inlet. The burner top is made from 2.2-cm wide corrugated copper shim stock (0.005 cm thick), rolled up with alternate layers of flat stock into the flat porous structure shown in Figure 8. The channels thus created were 2.2 cm long with a triangular cross section about 0.32 cm on a side. A corrugation with about 0.08 cm spacing proved too fine to transmit the coal.

Using an improved concentric, coal-air inlet, which allowed easy variation of the point of coal entry in the air stream and kept the two tubes aligned, it was possible to entrain sufficient coal in a slow enough air stream at the 12.6-cm burner exit plane to achieve stable, though unsteady, burning of pure coal dust-air. The coal dust-air could be ignited directly with a Bunsen burner flame, with no need for CH_4 addition, preheating or sheath flames. A screen, held about 1.3 cm above the matrix during ignition by the Bunsen burner, helped establish the flame. After burning was fully developed, the screen could be removed, leaving a freely burning coal-air mixture, although the presence of the screen led to a flatter, more stable flame.

A black and white print of a color photograph of such a flame is shown in Figure 9. The approximate fuel and air flows for the flame were: air = 59 liters/min, coal dust = 10.5 g/min ($\sim$ 177 mg/liter). (Unsieved coal, batch I, was used in all of the 12.6-cm tests.) The flows were not sufficiently uniform or low enough to give a steady one dimensional flame. Puffs of coal dust frequently occurred, through either the 2.2-cm thick open matrix or a simple screen. The total air flow needed to entrain coal appeared to be too large to permit stabilization of a completely flat flame, and the flame was constantly lifting off at one point or another near the edges. The instantaneous view of the flame by eye revealed a dark zone next to the burner matrix, then a very intense bright zone a few millimeters wide, followed by glowing streaks for many centimeters. The appearance of the flame zones was strikingly similar to the appearance of isolated coal particles burning in a lean CH_4-air flame. Attempts to improve on the behavior of the 30-cm long conical burner failed when using the as-received coal dust (with only $> 100\ \mu$ particles sieved out). A second series of experiments was then undertaken with a smaller (6.3-cm diameter) burner to give more flexibility in coal loading, burner configuration and length per diameter ratio.

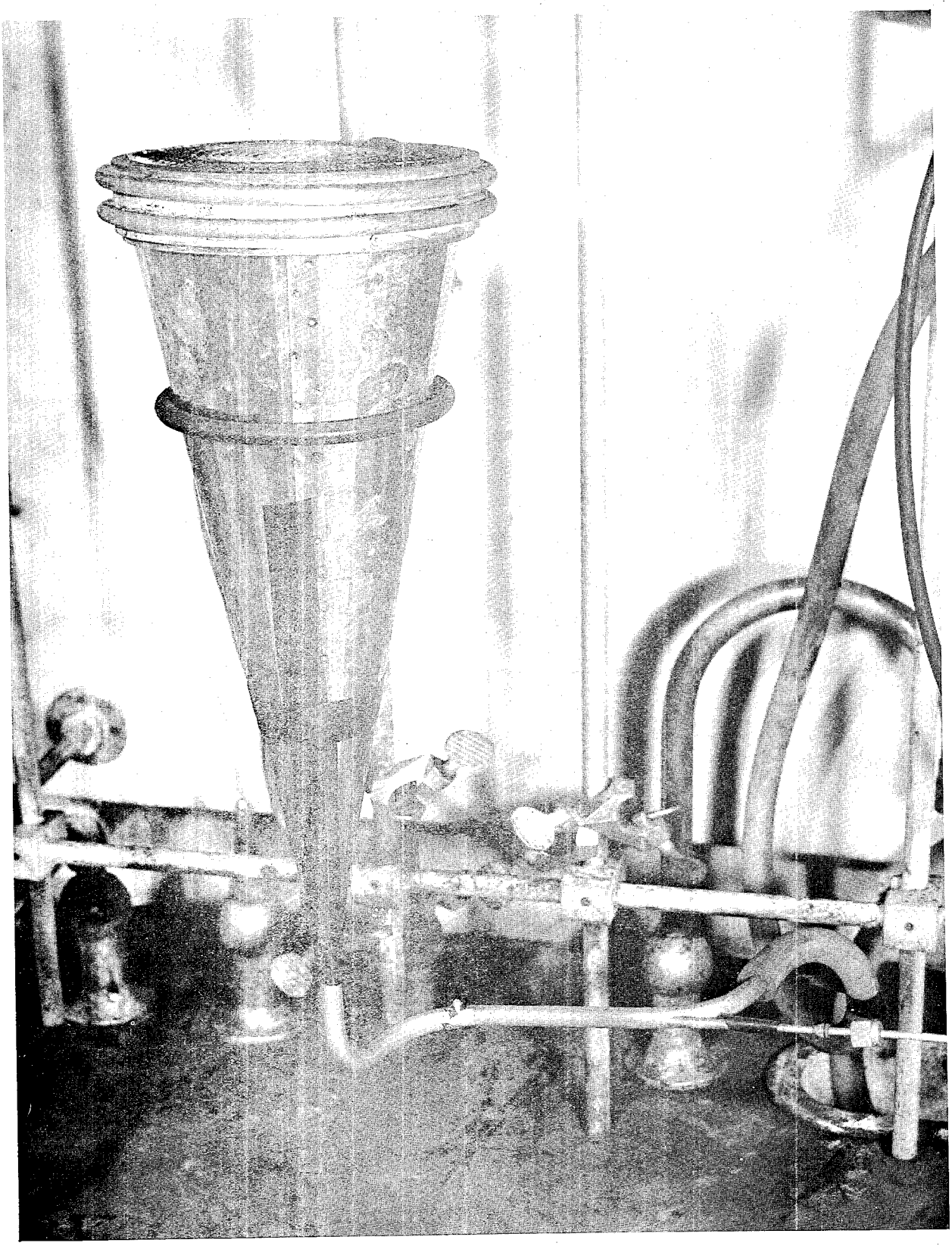

Figure 7 - Photograph of the Most Successful Burner-Inlet Configuration yet Tested

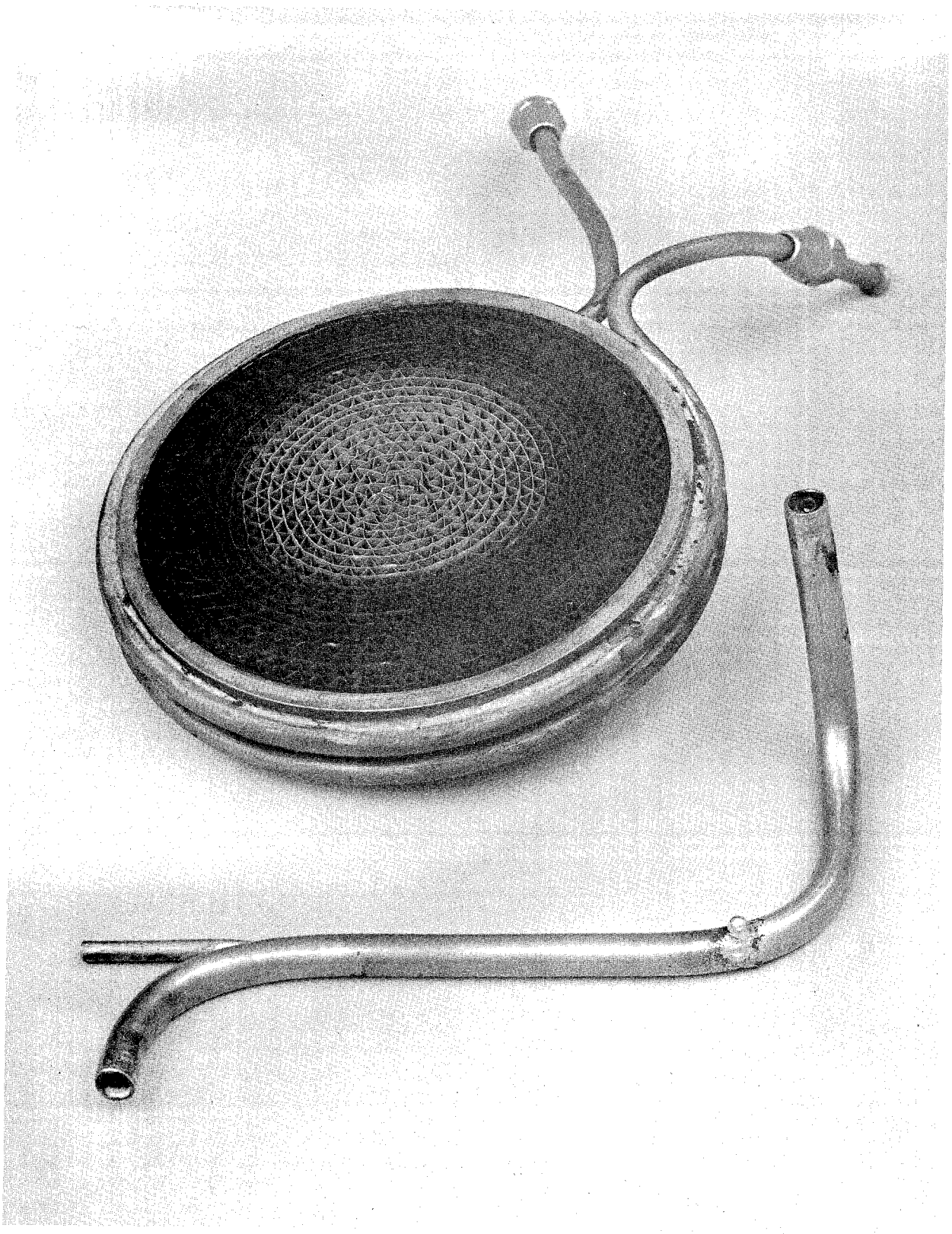

Figure 8 - Photograph of the Concentric-Tube Coal Dust-Air Inlet to the Burner and the Corrugated Matrix

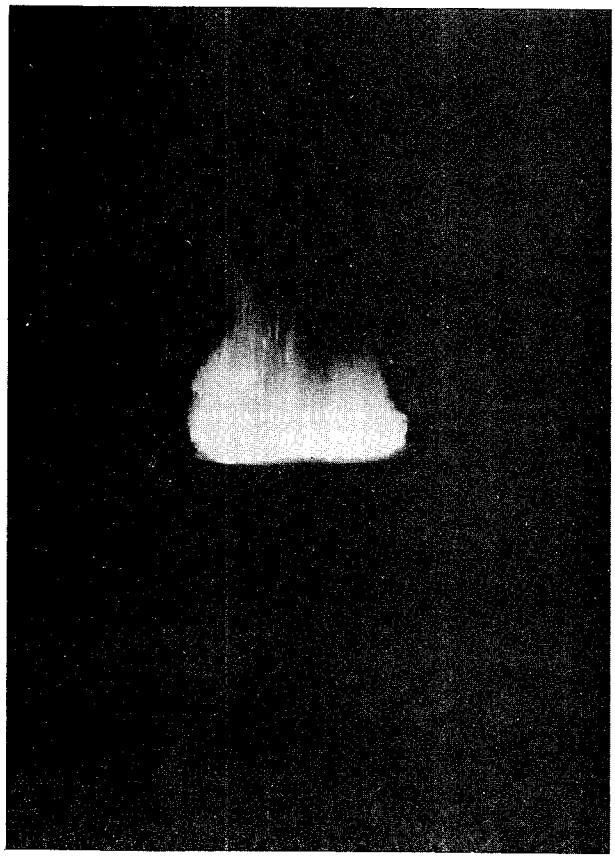

Figure 9 - Photograph of a Pure Coal Dust-Air Flat-Flame Burning on a 12.6-cm Diameter Burner

B. Vertical, Cylindrical, 6.3-cm Burner

The first burner of this class which was tested was made from a cylinder 36 cm long with cm long with a 7-cm long funnel inlet at the bottom. The same concentric coal dust-air inlet geometry was used as for the 12.6-cm burner. In both cases the coal dust entered the air stream about 1.3 cm upstream from the end of the air tube. We could not obtain steady burning on this burner, but by simply cutting down the length of the cylinder to 18 cm, and using two coarse screens as a burner matrix, stable burning was achieved.

Because of the long cylindrical section of tubing a conical type flame front was obtained, as shown in Figure 10. The approximate air and fuel flows for the flame in Figure 10 were: air $\cong$ 38 liters/min, coal dust $\cong$ 9 g/min ($\approx$ 233 mg/liter). The coal delivery was again somewhat uneven, and the flows of air necessary to entrain sufficient coal against gravity were too high, so that a fluctuating lifted flame resulted. The conical flame continually detached from the burner at one side or another, floated up and then reanchored to the burner rim. The instantaneous strcture of the flame zone was the same as that already noted for the 12.6-cm burner with, of course, a very obvious dark, preflame zone under the conical flame front. There appeared to be no basic quenching limitation on stabilizing flames as small as 6.3 cm in diameter on an unconfined burner. An upright, conical burner, 25 cm long x 6.3 cm diameter, was also tested. The flow profile was flatter, but the flame was only marginally stable. In quenching studies, described in a later section, conical flames of much greater stability were achieved on tubes of 1- to 3-cm diameter.

With both the large and small diameter burners, we were severely constrained between the low flow velocity needed for the slow burning coal dust and the high velocity needed to keep the coal dust entrained. An idea of the entrainment problem can be gained by making a simple Stokes law calculation for the free fall velocity of spherical coal dust particles in air. Such a calculation for a 50 μ diameter particle predicts a necessary flow velocity of about 10 cm/sec for entrainment, a value which is apparently comparable to the flame speeds being observed for coal dust-air. It can be appreciated from this calculation that even with fine coal, containing only about 5% by weight greater than 50 μ, enough coal might settle or drop out near the walls to cause the puffing and uneven delivery observed with the upright burner configuration.

The two obvious and direct approaches to alleviating the entrainment problem are: (a) to invert the burner so that coal is being fed by gravity; and (b) to use a finer coal with the upright burner. The second approach has been followed in the sampling studies to be described later.

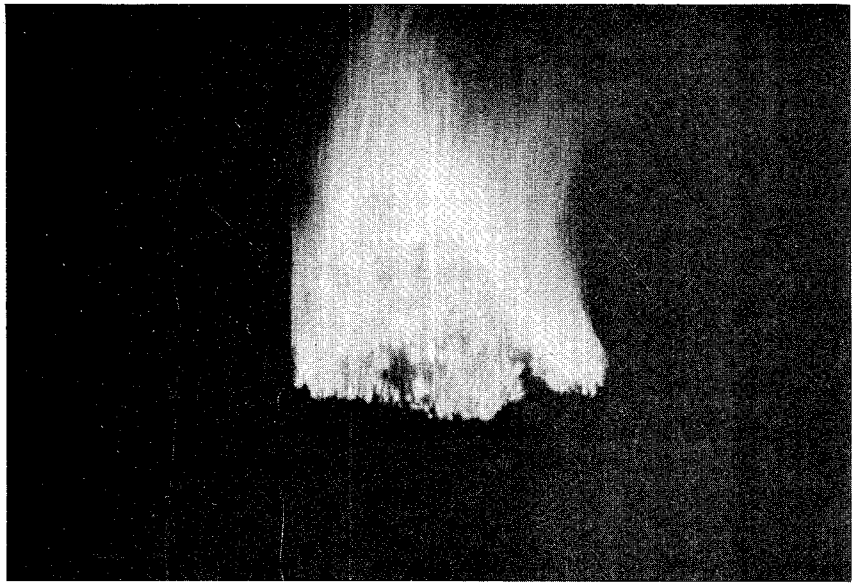

Figure 10 - Photograph of a Free-Burning Conical, Coal Dust-Air Flame on a 6.3-cm Diameter Burner

C. Vertical, Conical, 6.3-cm Burner

Experiments were carried out with a 25-cm long, 6.3-cm diameter, conical burner in an inverted position. The same coal-air inlet geometry was used as before, although ultimately, if an inverted burner were to be used, the coal-air might be first directed upward to the apex of a closed-end cone. Figure 11 shows a scale drawing of the inverted burner and the improved coal-air mixing geometry. With this burner, using a clapper-type vibrator to shake the whole burner cone, and a simple water-cooled screen soldered to the 6.3-cm opening of the sheet metal cone, quite successful burning was achieved. Figure 12 is a photograph of the upward burning flame.

One of the problems with the inverted flame is obvious from the photographs. If no forced draft is provided, the flame turns upward and the secondary reaction zone would be difficult to observe or probe. Use of a sheath gas of N_2 or argon and provisions for a suction exhaust, a few inches below the burner, allowed a reasonably one-dimensional, but unconfined, flame zone to be established with unobstructed viewing. The mass spectrometric probing of such a flame is a more difficult matter. Whereas the mass spectrometer does not care whether the sampled beam enters from above or below, the existing differentially pumped beam system would have to be replumbed and the presently used massive flame probes would interfere with the extraction of burnt gases necessary to overcome buoyancy.

The inverted 6.3-cm burner flame could be stabilized over fairly wide limits, even with no sheathing or forced draft. With total air flows of about 21 liters/min, burning was steady at total coal flows of from 5 to 10 g/min. At a coal flow of about 5 g/min, burning was achieved at total air flows ranging from 8 liters/min to 30 liters/min. The rich limit flames were very smoky while the lean flames were bright and clean. Figure 12 shows the 30 liters/min, 5 g/min flame.

The flow rates cited above are approximate only and by no means indicate achievable limits for steady burning. A series of approximate burning velocity and stability limits could be measured with the inverted burner for a whole series of coals and for various size cuts. A mixture of CH_4 would present no problem and additions of dry powders or gaseous agents should also be straightforward. The use of conical flames might be a particularly suitable way to make comparative burning velocity measurements with minimum interference by the grid or screens.

Tests were performed with the 6.3-cm conical burner in an upright position using various sieved and air-classifed size fractions of coal dust (Figure 11 burner). With coal sieved to contain $< 37\ \mu$ particles, we were not able to obtain stable burning in an upright position. It still required too high a total air flow, in this configuration, to maintain the coal dust in suspension.

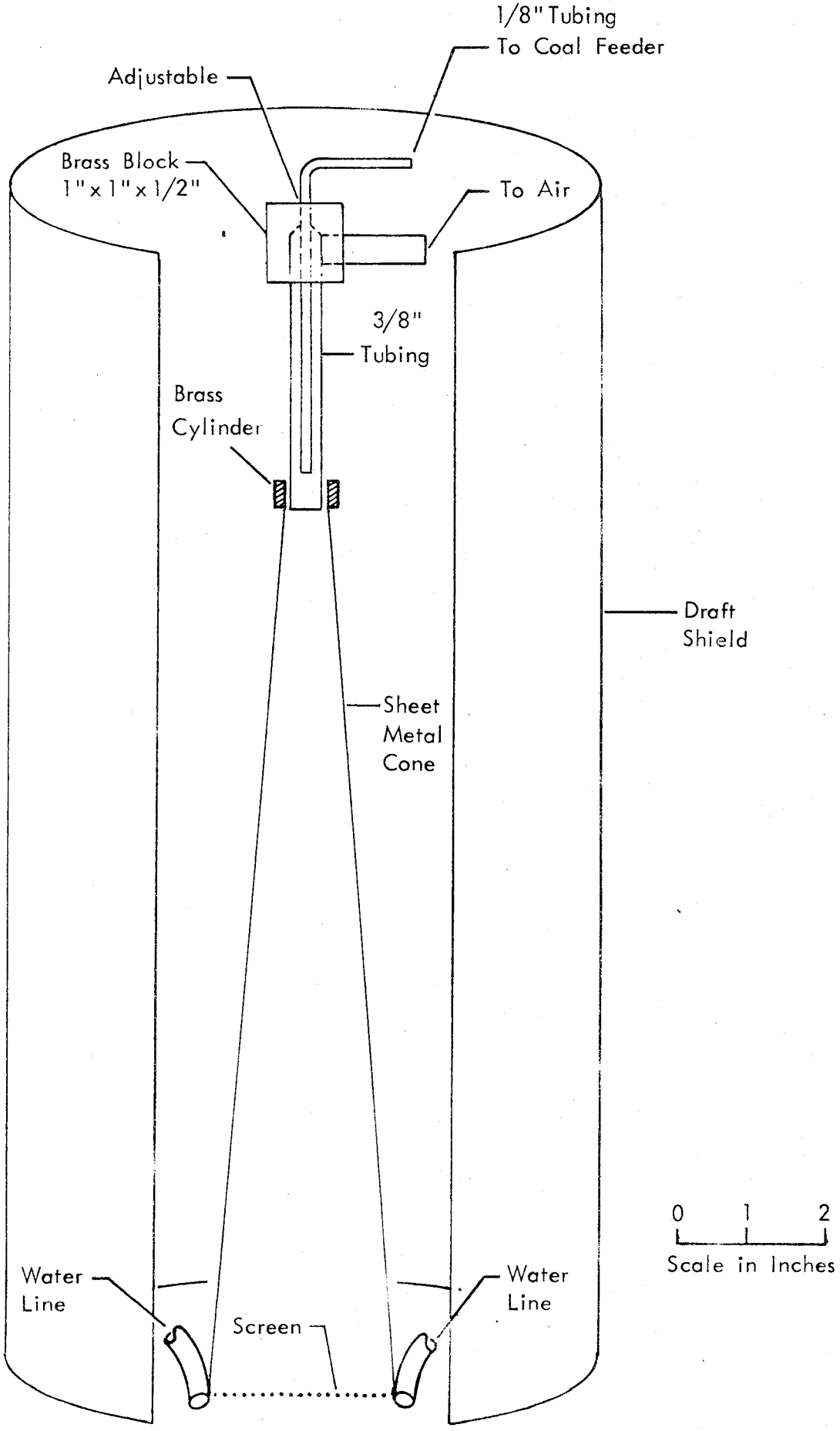

Figure 11 - Scale Sketch of the 6.3-cm Diameter Burner Used in the Inverted Position. The same coal-air mixing inlet was used for all burners.

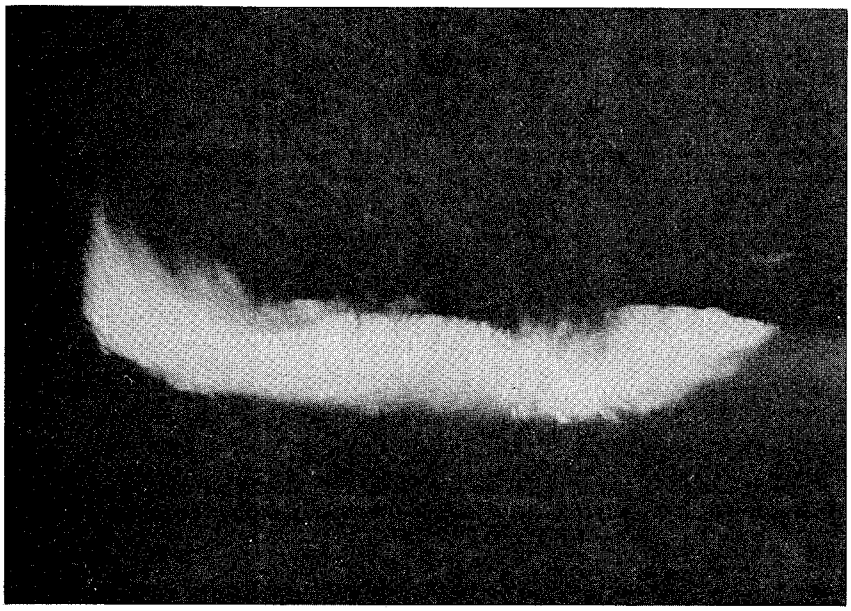

Figure 12 - Photograph of a Free-Burning, Flat, Coal Dust-Air Flame on an Inverted 6.3-cm Diameter Burner

We next tried burning a 10- to 20-μ size fraction, classified by the Majac Company. Both this and the previous coal fraction appeared to behave normally in the fluidized bed feeder. It was possible to burn the 10- to 20-μ coal with the conical burner in an upright position, but the flame was not steady and the air flow limits were rather narrow. Entrainment of the coal dust was still a problem, thus limiting burning conditions to high air flows. The use of a corrugated burner matrix in place of the screen did not help.

The final test with the conical burner configuration was made with the air-classified 0- to 10-μ coal dust fraction. This size fraction did not behave as well in the fluidized bed feeder. Powder delivery from the off-take tube was more erratic, and fluidizer pressures were more unsteady, than with larger coal fractions. We were unable to achieve stable burning, either upward or downward, using the conical burner and this fine coal. There was evidence that the fine coal was sticking to the transport tube walls and that it was agglomerating as it was delivered and dispersed in the burner. What appeared to be large agglomerates were seen issuing from the burner before ignition was attempted.

Since the 10- to 20-μ coal seemed to behave best in the upright conical burner, we used it in a final series of development tests using an upright, 6.3-cm burner.

C. Vertical, Conical-Cylindrical, 6.3-cm Burner

Using the 10- to 20-μ coal dust, the 6.3-cm cylindrical burner was tested using a 1.3-cm thick corrugated matrix. With the cylindrical section 18 cm long, only a marginally stable conical flame was achieved at high coal and air flows. Maintaining the coal suspension was still a problem, and hence the cylindrical section was cut down to 7.6 cm, leaving the burner configuration as shown schematically in Figure 13. A photograph of this burner appears in Figure 14.

The improvement in performance of this burner was dramatic. Apparently we have achieved a good compromise between turbulent transport and last-minute smoothing of the flow by the matrix. A flat Meeker burner-type flame was produced which could be burned for many minutes without noticeable plugging of the matrix. Each hole in the matrix gave a distinct small conical flame yielding a merged but waffle-like bright initial reaction zone.

This burner configuration appeared quite suitable for direct probe, molecular beam, mass spectrometric sampling. The flame attached quite well to the matrix, and, in fact, heated the grid to some extent, as is discussed in the next section.

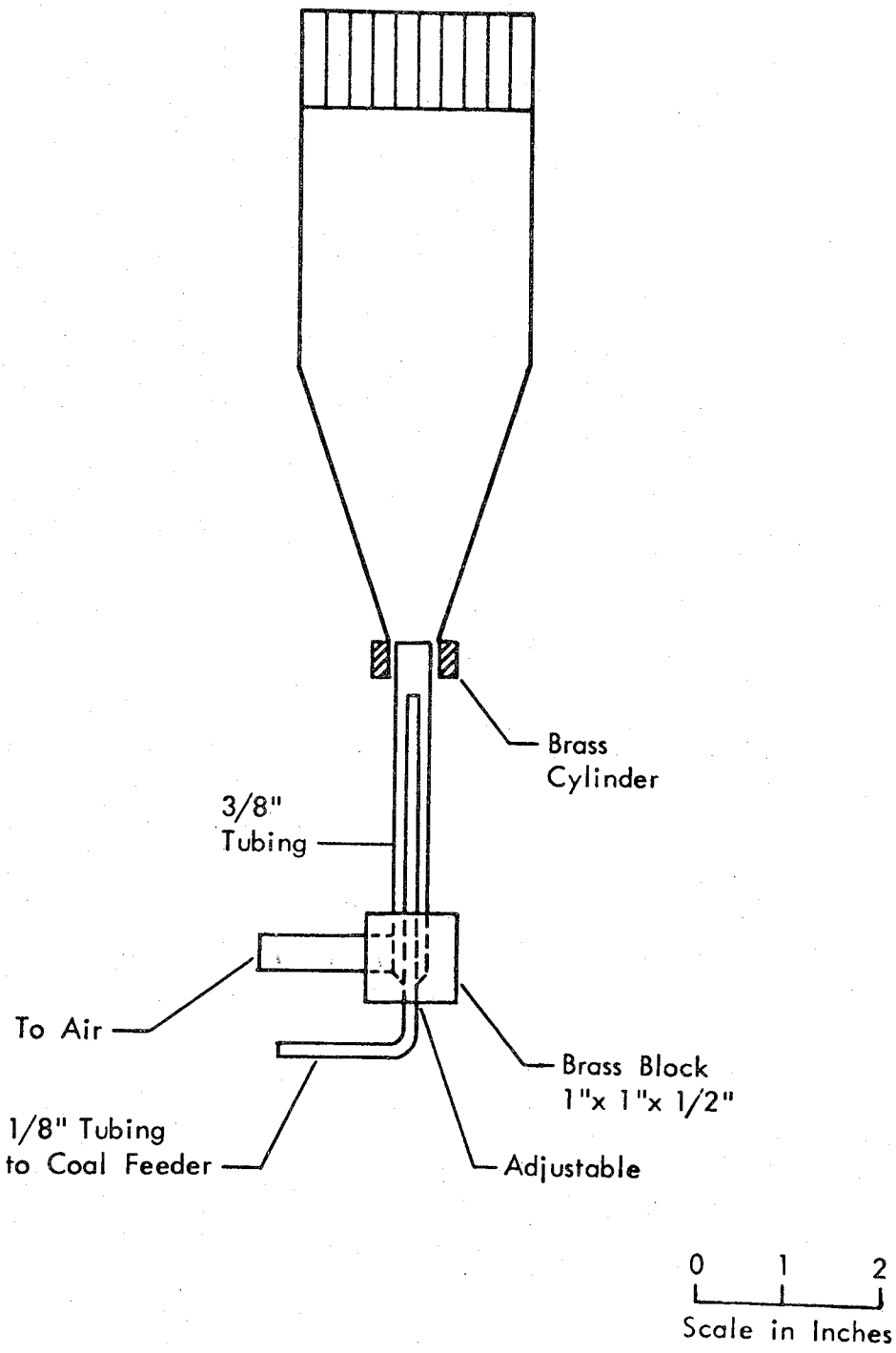

Figure 13 - Scale Drawing of the 6.3-cm Diameter Burner That Produced the Best Flat-Flame Burning of Coal Dust-Air

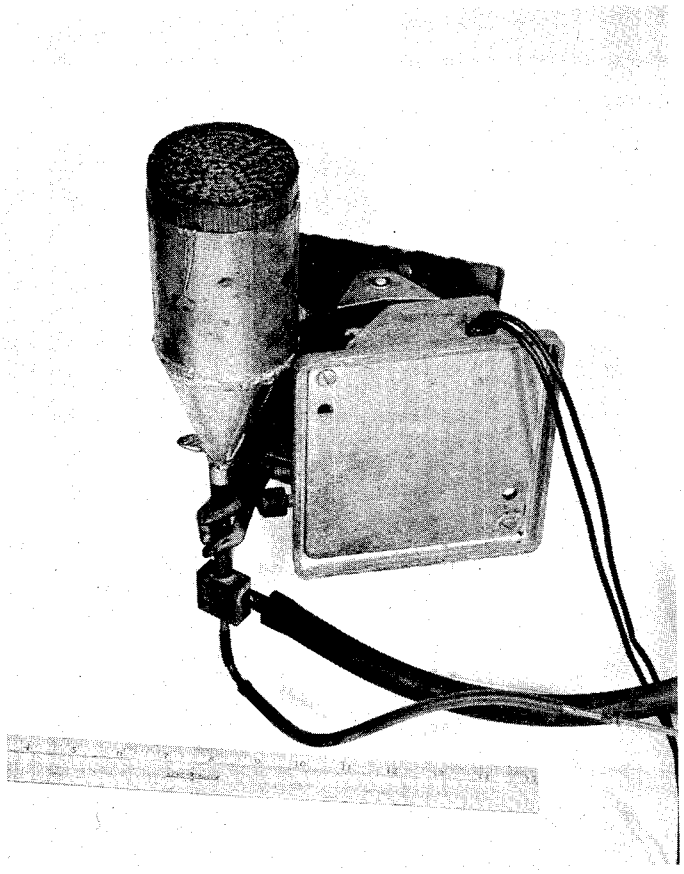

Figure 14 - Photograph of the Burner Shown in Figure 12

The flame remains attached over a wide range of air and coal flows. A photograph of the flame is shown in Figure 15, in which a 2.5-cm thick corrugated matrix with 0.32-cm openings was used. A brief color movie sequence was taken to show the general appearance, the ease of ignition and the stability of the flame. Typical operating conditions for flames used in sampling studies are shown in Table 2.

This basic 6.3-cm diameter burner was used for all direct sampling studies throughout the remainder of the program. The only changes made were to improve the vibration of the burner by means of a a more rugged mount and to try different smoothing matrices. In place of of the homemade corrugated foil matrix, we used a commercially fabricated honeycomb material. The new matrix is 5/16 in. thick and consists of a spot welded, hexagonal honeycomb. The cells are 0.07 in. on a side and 0.125 in. at narrowest dimension and are formed from a 0.003 in. thick high temperature nickel alloy. Burning tests with this matrix indicated that the flow smoothing is as good as or better than that obtained with the corrugated matrix of 1/2 in. thickness. A further advantage is the perfect regularity of the hexagonal openings in all but the perimeter of the burner mouth. A photograph of a typical flame is shown in Figure 16 showing the regular array of partially merged small conical flames.

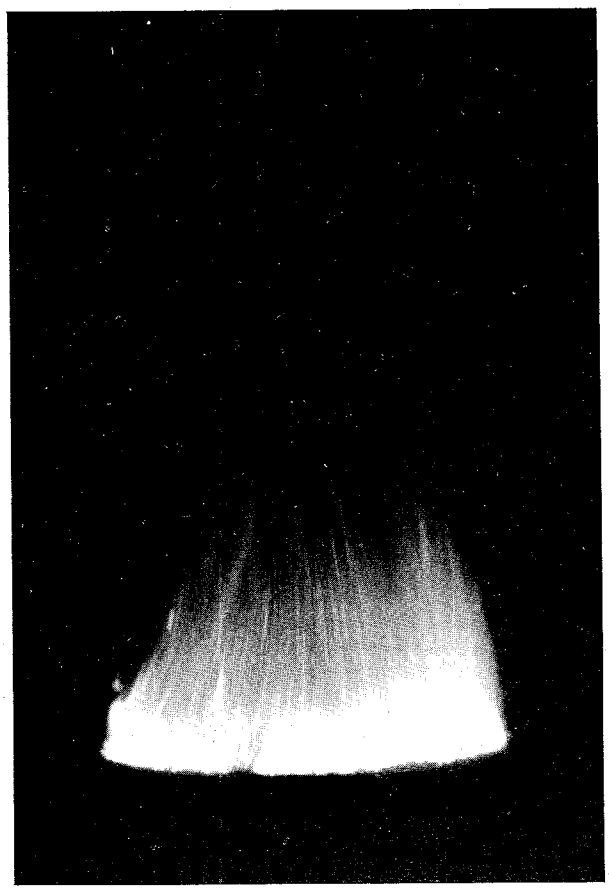

Figure 15 - Photograph of Best Flat, Coal Dust-Air Flame on a 6.3-cm Diameter Matrix Burner

TABLE 2

TYPICAL AIR AND PULVERIZED COAL FLOWS FOR STEADY BURNING ON A 6.3-CM DIAMETER BURNER

Primary Air	14.0 liters/min
Fluidizer Air	1.1 liters/min
Dilution Air	2.0 liters/min
	17.1 liters/min
Exhaust Air	-0.7 liters/min
	16.4 liters/min
Coal Dust (10-20 μ) Delivery Rate	4.4 g/min
Concentration of Coal Dust Cloud	270 mg/liter

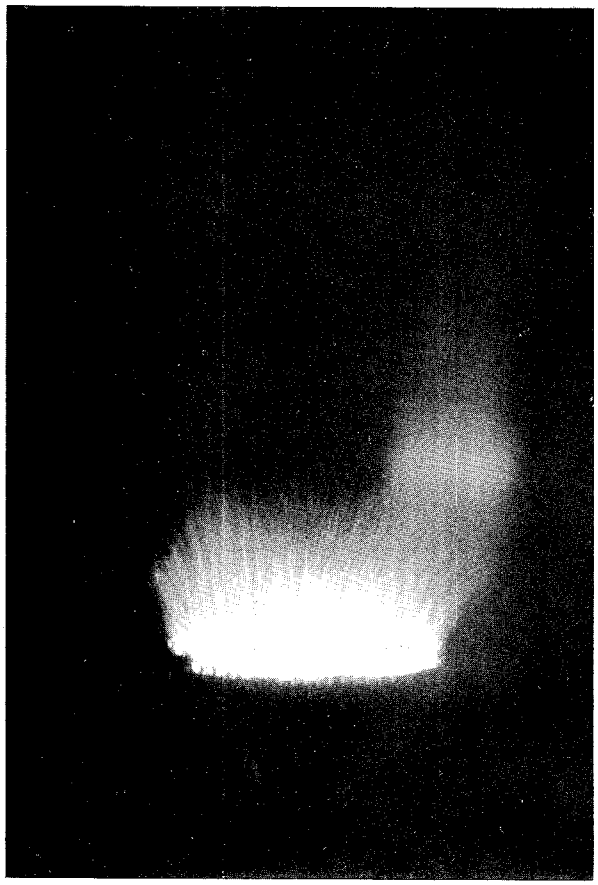

Figure 16 - Photograph of Rich, Coal Dust-Air Flame Burning on an Uncooled, 6.3-cm Diameter Burner with a Honeycomb Matrix. Coal dust is 10 to 20 μ at a loading of about 270 mg/liter.

APPENDIX D

TEMPERATURE MEASUREMENTS WITH COAL-AIR FLAMES

A. Heating Within the Stabilizing Grids

The 6.3-cm burner just described, when not water-cooled, heats up significantly soon after the flame is establihed. The center and top of the matrix heat the most, and this heating appears to help the flame anchor to the burner, although the flame does stabilize in the center immediately after ignition before significant warm-up can occur. To establish approximately the extent of heating of the matrix, and the preheating of the incoming unburnt gases, thermocouple measurements were made as follows. Four 28-gauge Chromel-Alumel thermocouples were spot welded onto the burner grid at separate locations. The thermocouple outputs, after passing through a thermocouple selector switch, were fed into a microvoltmeter, and then to a strip-chart recorder, providing a continuous record of temperature versus time. Figure 17 shows a typical record of the four temperatures. The locations of the thermocouples were as follows:

T_1 - Top of burner grid, near center.

T_2 - Lower edge of upper section of grid, near center.
Note: Burner grid consisted of four sections of nickel-alloy honeycomb, 5/16 in. thick each.

T_3 - Top of upper section, near edge of burner.

T_4 - Bottom of lower section, near center of burner.

All the thermocouple lead wires were brought in from below the matrix (inside the burner) to avoid passing through the hot coal-air flame gases. Figure 17 demonstrates that the burner grid is heated considerably.

Thermocouple measurements were also made in the flame gases (beads not attached to the grid), both inside the burner matrix and at the bright reaction zone. Figure 18 shows a typical record of temperature versus time.

T_1 - Top of burner grid, near the ton center. Attached.

T_2 - Lower edge of upper section of grid near center. Unattached.

T_3 - Top of burner grid, near center. Unattached.

T_4 - Bottom of lower section of grid, near center. Unattached.

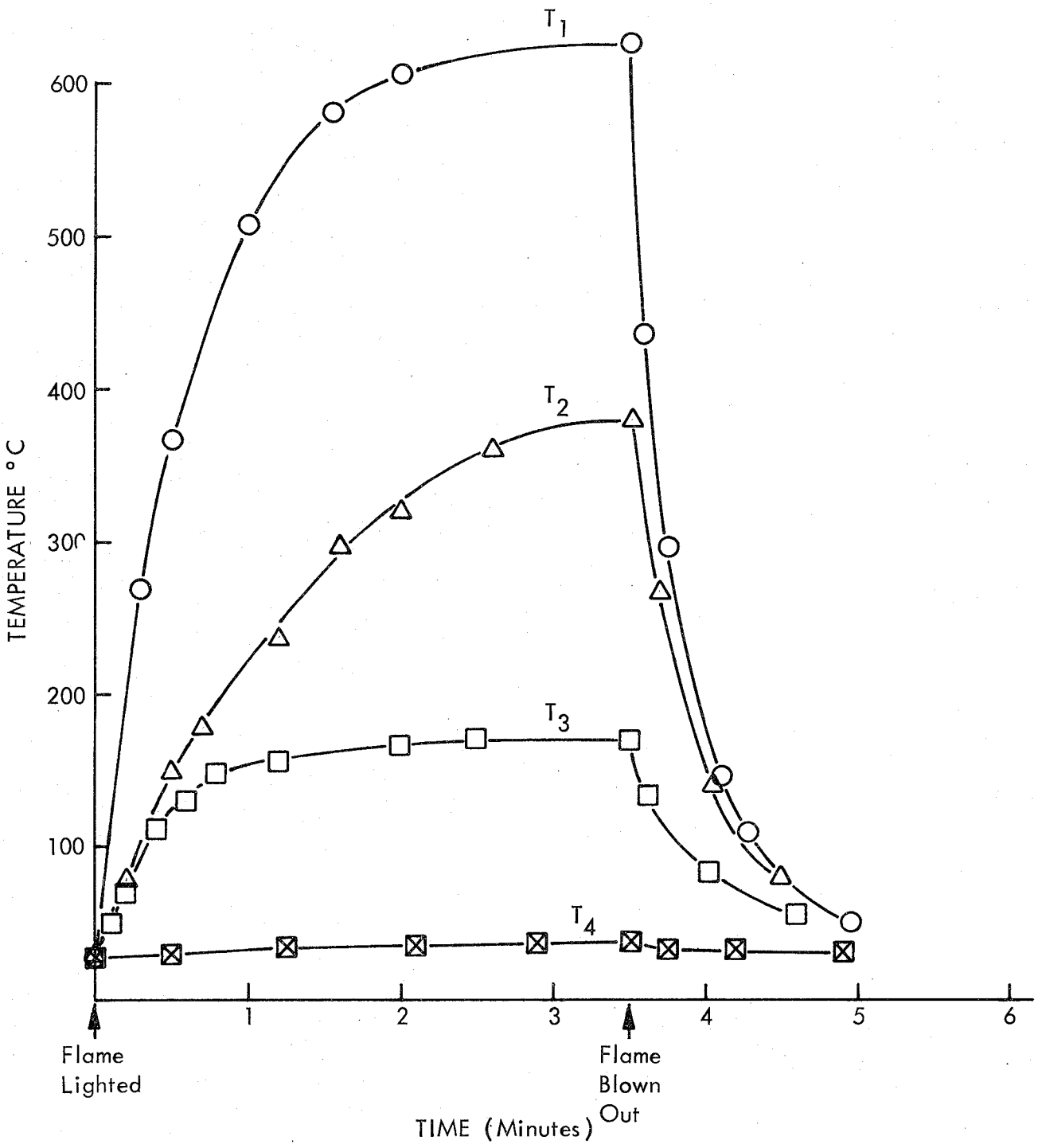

Figure 17 - Temperature History of the Honeycomb Grid on the 6.3-cm Coal Dust-Air Burner as a Flame is Established and Blown Out (flow left on). The temperatures T_1 - T_4 were measured by thermocouples attached as described in the text.

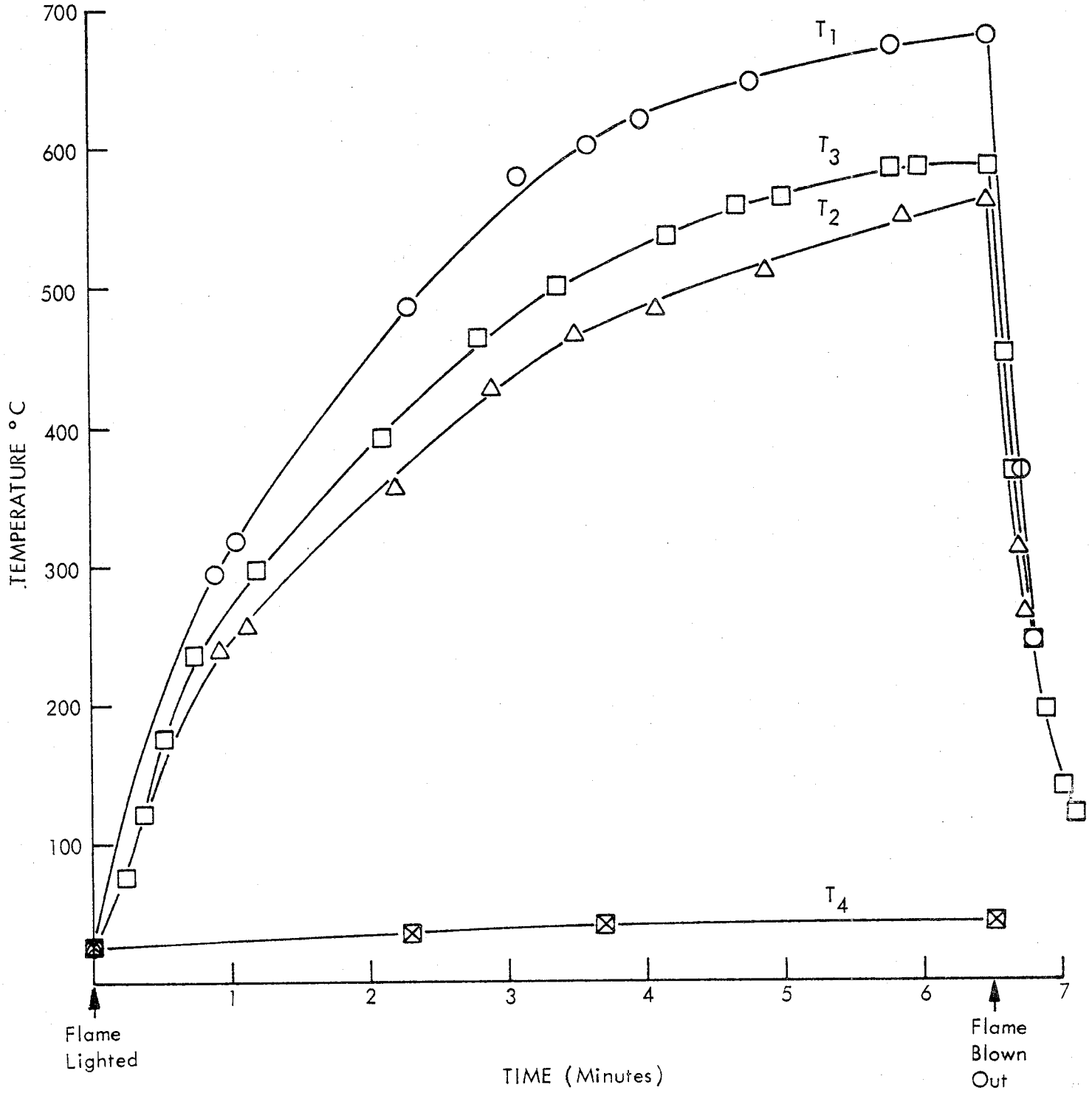

Figure 18 - Temperature History of Gases Entering and Passing Through the Honeycomb Grid on the 6.3-cm Coal Dust-Air Burner as a Flame is Established (flow left on). The temperatures T_2 - T_4 are measured by thermocouples placed in the gas stream at positions in the matrix described in the text.

Thermocouples Nos. 2, 3, and 4 were not in contact with the grid. All thermocouples were again 28-gauge Chromel-Alumel and entered the burner from below the matrix. The slow rise in gas temperature indicates that the grid and gas are thermally coupled. The rapid drop in temperature when the flame was blown out is partly due to the continued passage of room-temperature unburned gases, providing a cooling flow. To assess the effect of direct radiation from the flame on the thermocouple bead, a "hat" constructed from 0.003-in. stainless steel shim stock was placed over the honeycomb opening above the thermocouple measuring T_3. No significant temperature difference was seen. A comparison of T_1 in Figures 17 and 18 demonstrates the variation of grid heatup from run to run, depending on the degree of attachment of the flame. Since the air flow was carefully controlled and continuously monitored with flow meters, it is presumed that the variation is due to varying coal feed rates.

In the first attempt to get an estimate of the coal flame gas temperature, a 0.001-in. diameter Pt, Pt-10% Rh thermocouple was brought in from above the flame. The thermocouple bead, made in a CH_4-O_2 flame, was about four to five times the wire diameter. The 1/2-in. lengths of 0.001-in. diameter wire were fastened to 0.010-in. Pt, Pt-10% Rh extension wires. Using this thermocouple, the highest temperature recorded (uncorrected) was about 1000°C, considerably below the expected flame temperature. As shown in Figure 19, that temperature was observed just above the burner matrix. There is considerable scatter in the data, presumably due to the instability of the flame and rapid buildup of material on the thermocouple head. No temperature corrections were attempted for radiation or conduction, or for the coating found on the thermocouple. After making the measurements shown in Figure 19, there was a hard, glassy coating about 0.025 in. in diameter on the bead. Surprisingly, when a larger diameter (28-gauge) Chromel-Alumel thermocouple was introduced from above (through the hot gases), temperatures close to 1000°C were again obtained, indicating that conduction or radiation may not be a major source of error. Because of the likelihood that the coal flame varied from test to test, and because of possible thermocouple wire heat conduction errors, it is probably not valid to compare temperatures measured in Figures 18 and 19. In none of these preliminary runs was the coal concentration monitored, but the well-anchored flames probably were in the 200- to 250-mg/liter range.

B. Detached Flames and Water-Cooled Burners

With the above observation of quite high burner grid temperatures, and with preliminary sampling results showing (see below) a considerable loss in volatile matter and oxygen just above the grid one is led to speculation about the role of coal-air preheating, in the channels of the honeycomb matrix, in flame stabilization.

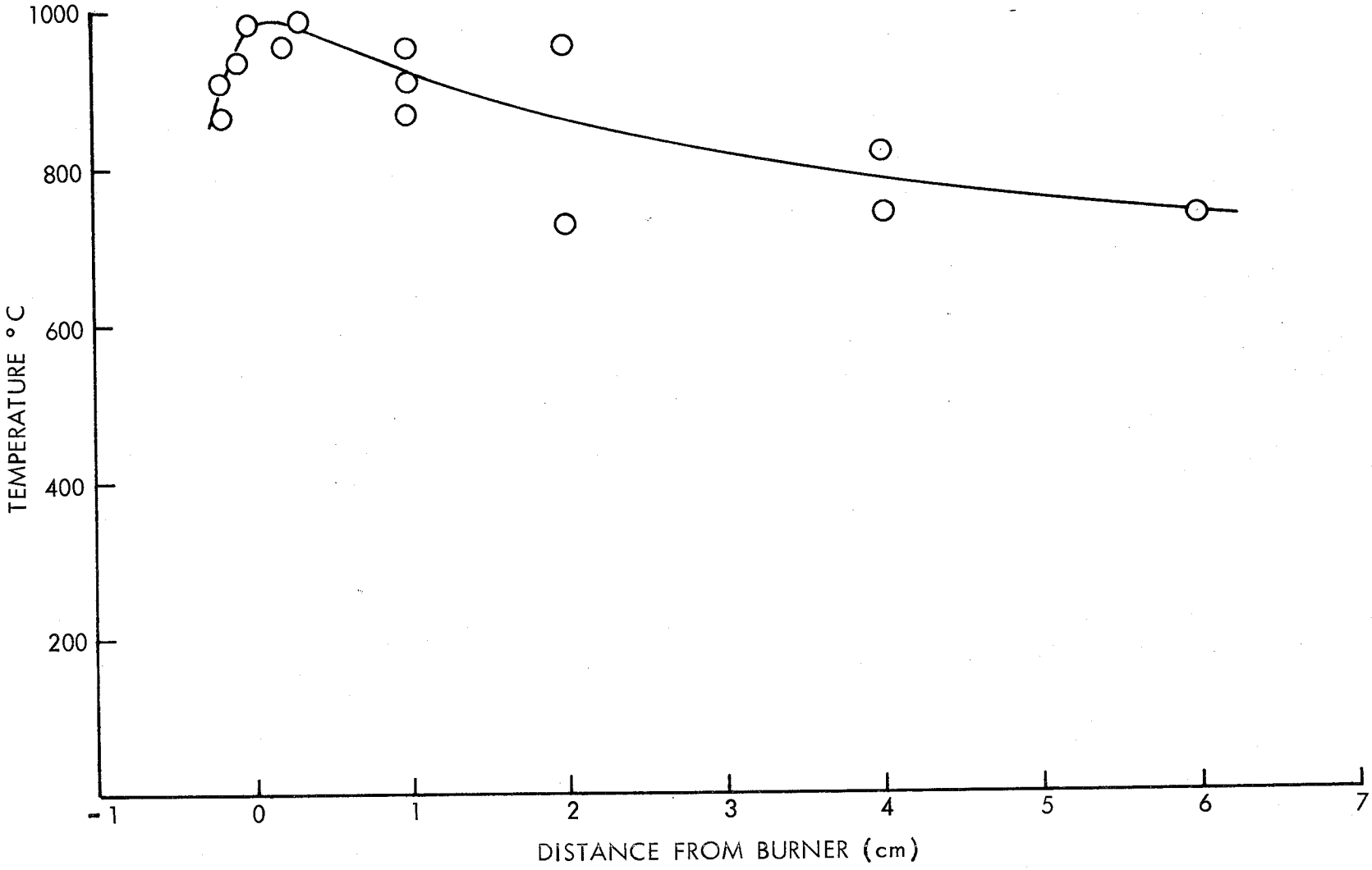

Figure 19 - Coal Dust-Air Flame Gas Temperatures (uncorrected) as Measured by Inserting a 0.001-in. Diameter Thermocouple Vertically Into the Flame from Above

It would be desirable to have a stable flame, lifted from a burner that does not preheat the gases in an indirect way. Thus several tests were carried out to assess the coupled effects of burner matrix temperature on flame behavior and flame conditions on burner matrix heating.

Three approaches to mitigating the possibility of preheating the incoming gases by conduction from the burner matrix, and to permitting more ready access to the earliest stages of devolatilization and ignition, were considered. One approach was to enlarge the central hole in the honeycomb matrix to create higher central flow velocities and form a central, lifted, conical flame. A second approach was to water-cool the honeycomb grid, preventing preheating by the grid and perhaps lifting the flame-front farther from the matrix. A third approach was to stabilize an inverted flame by placing a small blunt surface above the burner grid and attempting to attach the flame to this surface, allowing it to heat if necessary.

The third approach was tested first, but with completely negative results. Small, flat, brass disk surfaces of 1/4 in., 1/2 in., and 1 in. diameter were placed from 1/8 in. to 1 in. above the 10-cm diameter honeycomb burner. Attempts were made to attach a flame to these surfaces, heated and cold, at flow velocities higher than and equal to those used to stabilize the flat coal-air rich flame. Unfortunately, at least with the limited configurations tried, an inverted flame did not even approach being attached to the central flame holder.

With the standard burner configuration, the grid temperature reached depends on the composition of the flame and the smoothness of burning. The latter effect was dramatically demonstrated by placing smoothing screens or honeycombs 1/2 to 1 in. above the burner surface. Such smoothers produced a much flatter flame, better anchored to the outer perimeter of the burner. (These flames are always anchored best in the center.) They also increase grid temperature typically from 530° to 790°C.

In the second approach, three types of cooled burners were tested initially, none with very satisfactory results. First, a single-turn 1/8 in. copper cooling coil was soldered around the perimeter of the 5/8 in. thick honeycomb grid and flush with its upper surface. Thermocouples were spot welded to the top and bottom of the honeycomb grid section, near the center. Because of the poor conductivity of the honeycomb, only limited cooling was achieved. With the water off, central upper grid temperature reached 510°C and fell only to 475°C with the cooling water on. The presence of a 3/32 in. thick honeycomb flow smoother, 1/2 in. above the grid, raised the temperature of the grid to about 675°C with water off versus 600°C with water on. Similar grid heating behavior was observed with CH_4-air burning on the same burner at about the same total air velocity.

In an effort to cool the burner matrix without distorting the laminar flow through the 6.3-cm burner, a 1/2 in. thick section of the 3 mil thick, nickle-alloy honeycomb was copper plated. A wet chemical plating technique was used which appeared to result in a uniform, coherent copper deposit of about 3 mils over the entire honeycomb matrix. A single turn of 1/8 in. diameter copper cooling coil was soldered to the perimeter of the matrix. The entire assembly could be interchanged with the uncooled matrix used with the 6.3-cm burner.

With water cooling, the center of the copper-plated honeycomb remained at essentially room temperature and it was found to be impossible to stabilize even a rich coal-air flame. Only by shutting off the cooling water and allowing the grid to heat up to about 70°C or more, could a flame be attached to this burner. With no water cooling, the upper surface at the center of the grid reaches about 270°C and a well-stabilized, flat flame could be maintained. In a later section, mass spectrometer determined species profiles are shown for copper-plated and unplated honeycomb burner grids, showing little difference in species profiles.

Even with the cooler, copper-plated burner grid, stable flames were not lifted enough from the matrix surface to permit probing completely into the unburned gases. Hence, the expedient of forming an enlarged central hole, by cutting away one intersecting trio of cell walls, was used. Such a burner exhibits a raised central cone, discernible to the eye but difficult to photograph, through which probing into the unburned gases can be accomplished. No attempt was made to optimize this central hole size. Species profiles with and without the central hole are shown in later sections.

Second, a loop of the 1/8 in. cooling line was placed around the central 1 in. of the grid, recessed flush with the grid top surface. Perhaps due to physical obstruction to flow, flames were harder to light and stabilize on this burner, even with the cooling water off. With no cooling water and no smoothing screen, grid temperature reached 390°C, and fell to 170°C with cooling water on. With the smoothing screen at 1/2 to 1 in., the temperature increased to 250°C. With cooling water on, the flames were floppy and much less stable, though still consistently anchored in the center.

Third, to try to attain unperturbed flow but good, uniform cooling, a burner matrix was made by drilling closely spaced 1/8 in. diameter holes in a 1/2 in. thick copper disk, which had a perimeter cooling coil. In spite of the closely drilled holes, the flame surface was clearly broken up into unmerged, separate conical flames, presumably due to the large inherent dead area in such a drilled matrix. The flame could only be lit after the grid reached a temperature of about 100°C. With no water cooling and a honeycomb smoother at 1/2 in., grid temperature was about 180°C. When cooling water was turned on, the temperature fell at once and the flame could not be stabilized.

These results were quite puzzling. Repeated tests indicate that the flame, on the ordinary honeycomb matrix, can be lit and stabilized in a second or two, before either the gas or matrix have shown any appreciable heating. There seemed to be two possible interpretations. Either the grid temperatures measured are not representative of the actual grid surface closest to the flame or the cooled-grid tests were all dominated by aerodynamic effects.

APPENDIX E

DIRECT, MOLECULAR BEAM MASS SPECTROMETRY AND GAS CHROMATOGRAPHY OF GASEOUS SPECIES FROM COAL-AIR FLAMES

The 6.3-cm diameter burner and coal-feed system were transferred to a small hood built under the molecular beam sampling system inlet of the Bendix mass spectrometer. A schematic diagram of the hood (61 cm x 61 cm x 122 cm high) sampling system and Bendix ion source region is shown in Figure 20. The hood exhaust was moved to the bottom of the hood and under the burner in order to minimize cross drafts between the flame and sampling orifice.

The flame sampling orifices customarily used by us for 1-atmosphere gaseous flames have diameters of 0.005 to 0.010 in. With a skimmer diameter of 0.020 in., the sampling system shown in Figure 20 can operate as a free-jet sampling system, with pressures in each stage low enough to achieve adiabatic sampling and tolerable degrees of molecular beam scattering. A traditional test in our laboratory, of such adiabatic sampling is the Ar^+/Ar_2^+ ratio when sampling room temperature argon at 1 to 5 atmospheres through a 0.004-in. diameter orifice.

With gaseous 1-atmosphere flames we have usually employed rather short (1/8 in. high), 90-degree, spun Pt-Rh orifice cones, with the sampling hole drilled into the somewhat rounded apex. These cones are soft-soldered to the water-cooled orifice plate shown in Figure 20. Such orifices, short as they are, have been generally satisfactory in probing small, fast-burning, premixed flames burning on torch-tips.[49]

To assess quickly the new kinds of problems presented by the coal dust-air flame, the standard 0.010-in. diameter orifice was used to sample the coal dust-air flame. Whereas the unignited coal dust-air cloud did not plug the orifice over the course of several minutes of sampling, as soon as the flame was established, the orifice was plugged in a few seconds. Although the orifice could be re-opened by exposure to a CH_4-O_2 torch-type flame, the plugging time was too short to permit meaningful sampling data to be obtained with the Bendix mass spectrometer and its rather slow-response data acquisition system.

A. Optimizing the Sampling System for Larger Orifices

We next undertook a series of experiments to see if the sampling system configuration of Figure 20 could be operated with larger diameter sampling orifices and smaller skimmer openings. The basic sampling system configurations tried are listed in Table 3. The results can be summarized as follows: The sampling orifice diameter must be 0.020 in. or larger to prevent plugging with partially burned or heated coal particles. With a 0.030 in. diameter orifice and either a 0.020 in. or 0.010 in. diameter skimmer, Stage 2 pressures are too high to achieve workable skimmer-beam intensities. With a 0.020 in. diameter orifice and a 0.010 in. diameter skimmer, and with the diffusion pump off in Stage 2, a useful, but limited

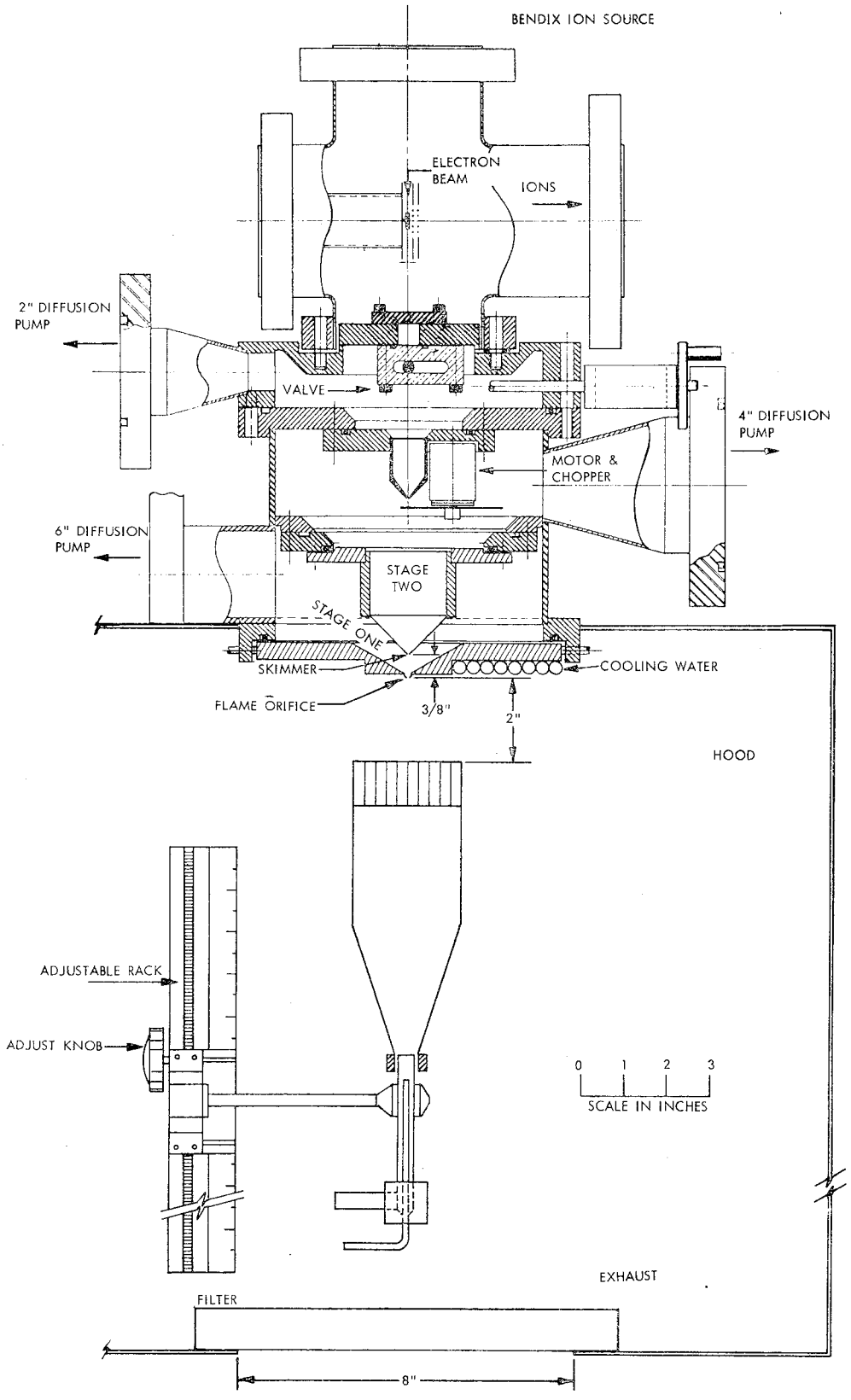

Figure 20 - Schematic Diagram of Hood, Sampling System and Ion Source of the Bendix Mass Spectrometer

TABLE 3

FLAME SAMPLING SYSTEM CONFIGURATIONS TESTED FOR SUITABILITY WITH 1-ATMOSPHERE COAL DUST-AIR FLAMES

Sampled Gas	Orifice Diameter (in.)	Skimmer Diameter (in.)	Stage One Pressure	Beam Intensity (arbitrary units)	Remarks on Performance
1 atm. argon	0.010	0.020	$\gg$ 10 μ	8,600 (40^+)*	Stage-1 diffusion pump on. Skimmer Beam.
Burnt gas of Bunsen flame (1 atm.)	0.010	0.020	> 10 μ	2,700 (44^+)	Lower density of hot gases lessens overload of stage-1.
1 atm. air	0.030	0.020	1,800 μ	No beam	Mechanical pump only on stage-1. Pressure in stage-2 too high to get even an effusive beam from the skimmer.
1 atm. air	0.030	0.010	1,800 μ	2,000 (28^+)	Mechanical pump only on stage-1. Only a very weak beam from skimmer.
1 atm. air	0.020	0.010	900 μ	12,500 (28^+)	Mechanical pump only on stage-1. Skimmer beam.
96 torr air	0.020	0.010	4.8 μ	660,000 (28^+)	Diffusion pump on in stage-1. Free-jet beam.
Burnt gas of Bunsen flame (1 atm.)	0.020	0.010	400 μ	50,000 (28^+)	Mechanical pump only in stage-1. Skimmer beam.
Coal-air flame (1 atm.)	0.020	0.010	300 μ	90,000 (28^+)	No plugging of orifice after 26 min of sampling well up in the hot burning region.

* Numbers in parentheses identify the ion measured in each case.

intensity skimmer-beam is obtained for cold, 1-atmosphere gases. Such a combination allows one to measure such stable coal dust-air flame species as CO_2, N_2, H_2O, and O_2 but two difficulties are anticipated. First, beam intensities and beam-to-background ratios are low enough that serious problems will occur with free radicals and with species of low concentration. Second, the beam intensity changes markedly in going from a cold to a hot gas source, due to the high gas loads to Stage 1. (This will always be the case to some extent and dictates that species ratios be followed in flame probing.)

One entry in Table 3 points to a way for improving sampling performance with basically the existing sampling configuration. If pressures in front of the Stage 1 orifice are kept to about 100 torr or less (for a 0.020 in. diameter orifice), then the Stage 1 diffusion pump can be operated and good free-jet-molecular beam expansion conditions can be achieved in the rest of the system, yielding large beam intensities and good signal/noise ratios.

B. Two-Stage Expansion Sampling System

To achieve these greater beam intensities, fast response time, and freedom from wall contact, a preliminary mechanically pumped stage of sampling was added. This new arrangement is shown in Figure 21. A drawn-Vycor sampling orifice (with 20 to 30 mil diameter orifice) extracts gas from the flame into a region of about 1/10 atmosphere pressure (controlled during sampling by a throttling valve on the mechanical pump). The expanded gas bathes a water-cooled skimmer-orifice, which is a 1/4 in. high, 90-degree, spun, stainless steel cone. Gas passing through the 20 mil skimmer-orifice expands as a free-jet and passes through the normal skimmer and thence to the ion source of the Bendix mass spectrometer.

The sampling arrangement in Figure 21 was tested in a number of ways prior to coupling it with the pulverized coal-air flame.

1. Tests with argon: Tests with Ar and Ar 2 were carried out to optimize orifice-skimmer distance (in Stage 1) and to gain insight into the two-stage gas expansion process in the Figure 21 sampling scheme. With a flat, thin, 20 mil diameter movable skimmer orifice, stagnant argon at 1/10 atmosphere in Stage 1/2 gave an $80^+/4 \times 40^+$ ratio (a measure of Ar_2/Ar proportions) of about 1.1×10^{-4} (compared to about 1.7×10^{-3} obtained with a 4 mil orifice and 1-atmosphere argon pressure). Use of the 90-degree conical skimmer orifice (1/4 in. high) shown in Figure 21 gave similar results for 1/10th atmosphere argon in Stage 1/2. Tests of the $80^+/4 \times 40^+$ ratio and beam intensity at 1/20 to 1/10 atmosphere indicated that the skimmer orifice to skimmer distance should be shortened from 5/8 in. to 3/8 in. This change was made by means of removable spacers at the skimmer flange.

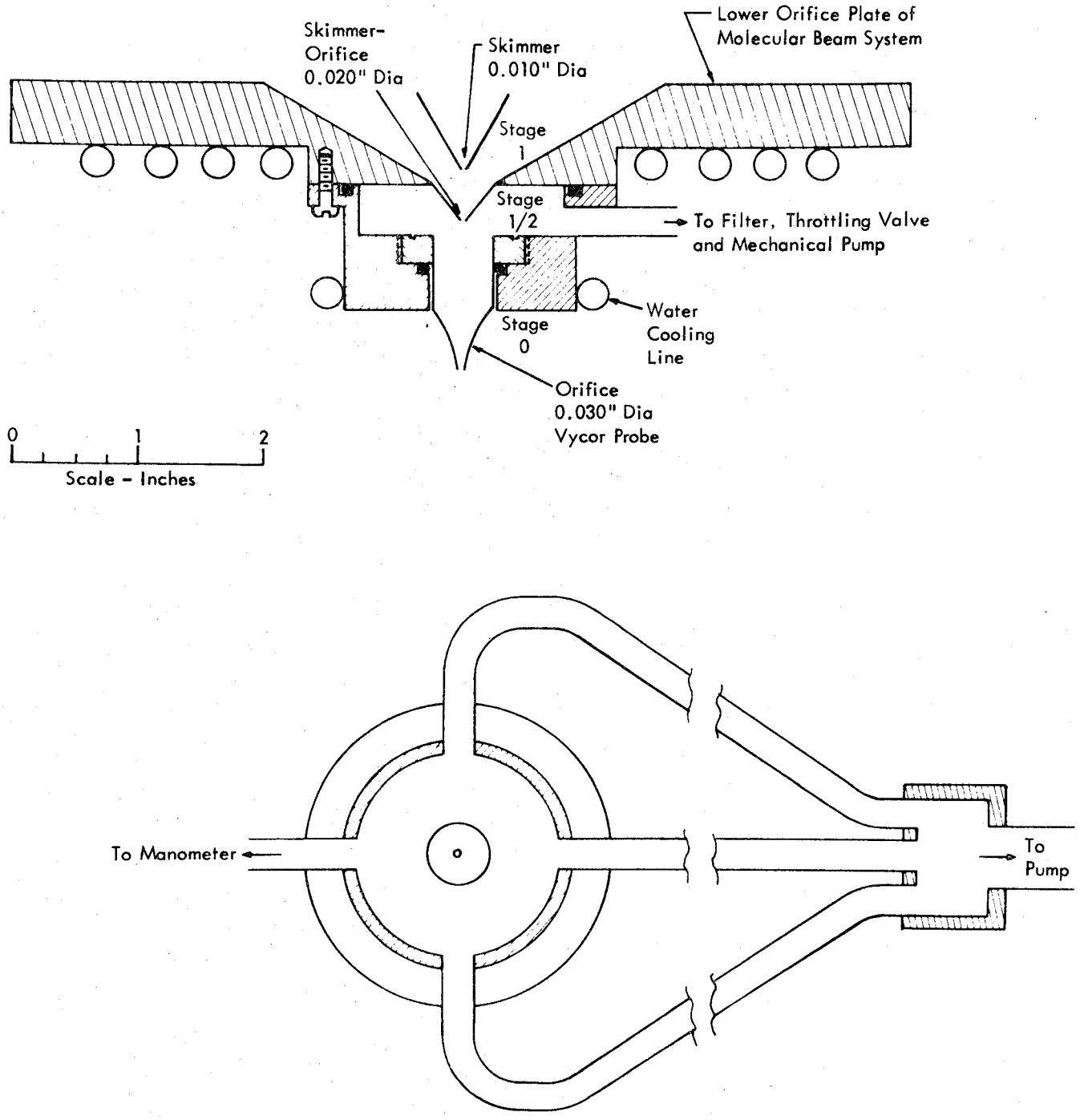

Figure 21 - Scale Drawing of New, Two-Stage Expansion, Direct Sampling System to be Used for Future Coal-Air Sampling

The sampling geometry shown in Figure 21, with the Vycor probe having a 30-mil orifice, gave the results shown in Table 4 for 1-atmosphere argon and 1-atmosphere air. The resulting 80^+ intensity with argon shows clearly that the gas is randomized before further expansion through the skimmer orifice.

2. Tests with flames: With the permanent gas tests of the Vycor probe and two-stage expansion indicating a significant increase in beam intensity, more realistic tests were carried out with a flame at 1-atmosphere pressure. In the first test, a stoichiometric CH_4-O_2-Ar (1/2/8) flame on a 1/2-in. diameter Pyrex tube burner was employed, but the flame temperature was high enough to cause a slow closing of the orifice over a period of minutes. The orifice was opened with a hot wire to approximately its original contour and diameter, and a cooler flame chosen. A CH_4-O_2-Ar flame of composition 1/1.6/8.0 was chosen on the basis of computed adiabatic flame compositions. This flame did not cause softening of the probe.

Results of direct sampling of this flame are presented in Figure 22 and Table 5. The results are shown to indicate the general behavior of the sampled species through the flame and to provide rough calibrations of system sensitivity for interpreting the first results with a coal-air flame. More careful calibrating experiments with CH_4-air flames are presented below, with discussion of sampling perturbations.

C. Coal-Air Flame Sampling Strategies

In quantitatively sampling gaseous species from coal-air flames, certain analytical complexities had to be faced. The chief problem is in distinguishing CO from N_2 since our Bendix mass spectrometer has insufficient resolution to separate CO^+ and N_2^+. Three approaches were considered: (a) use Ar-O_2 mixtures in place of air; (b) measure a set of parent and fragment peaks (such as 12^+ from CO), so that by calibration an algebraic deduction of both CO^+ and N_2^+ can be made; and (c) use batch sampling into evacuated bulbs and either Orsat or gas chromatographic analysis for N_2 and CO (and other species as well).

The disadvantages of the first approach are the expense of the large quantities of synthetic air needed, even for the 6.3-cm diameter burner, and the possible second-order effects on flame properties of replacing N_2 with argon. The second approach works in principle, but in practice requires highly precise measurements on minor fragment ions, careful calibration of the sampling system with known gases, and assurance that interfering parents, such as C_2H_4, are not present (or are accounted for by secondary corrections). The third approach has the disadvantage of foregoing the fast on-line response of the direct sampling, and in any event would have to be complemnted by direct sampling for species such as H2O and OH.

TABLE 4

SAMPLING SYSTEM PRESSURES AND PHASE-LOCKED BEAM INTENSITIES FOR TWO-STAGE EXPANSION CONFIGURATION

(For 1-atm, room temperature gases, sampled with the arrangement shown in Figure 34. Orifice diameter, 30 mils; skimmer orifice diameter, 20 mils; skimmer diameter, 10 mils.)

	Pressures in Torr					Beam Intensities (Arbitrary Units)			
Gas	P_0	$P_{1/2}$	P_1	P_2	P_3	28^+	40^+	80^+	$80^+/4^* \times 40^+$
Argon	760	76	5×10^{-3}	3×10^{-5}	1×10^{-5}		500,000	250	1.2×10^{-4}
Air	760	92	4.8×10^{-3}			240,000	--	--	

* The 80^+ signal is corrected by a factor of 4 to account for a presumed mass separation enhancement in the beam of a factor of 2 and an ionization cross section a factor of 2 greater than for 40^+.

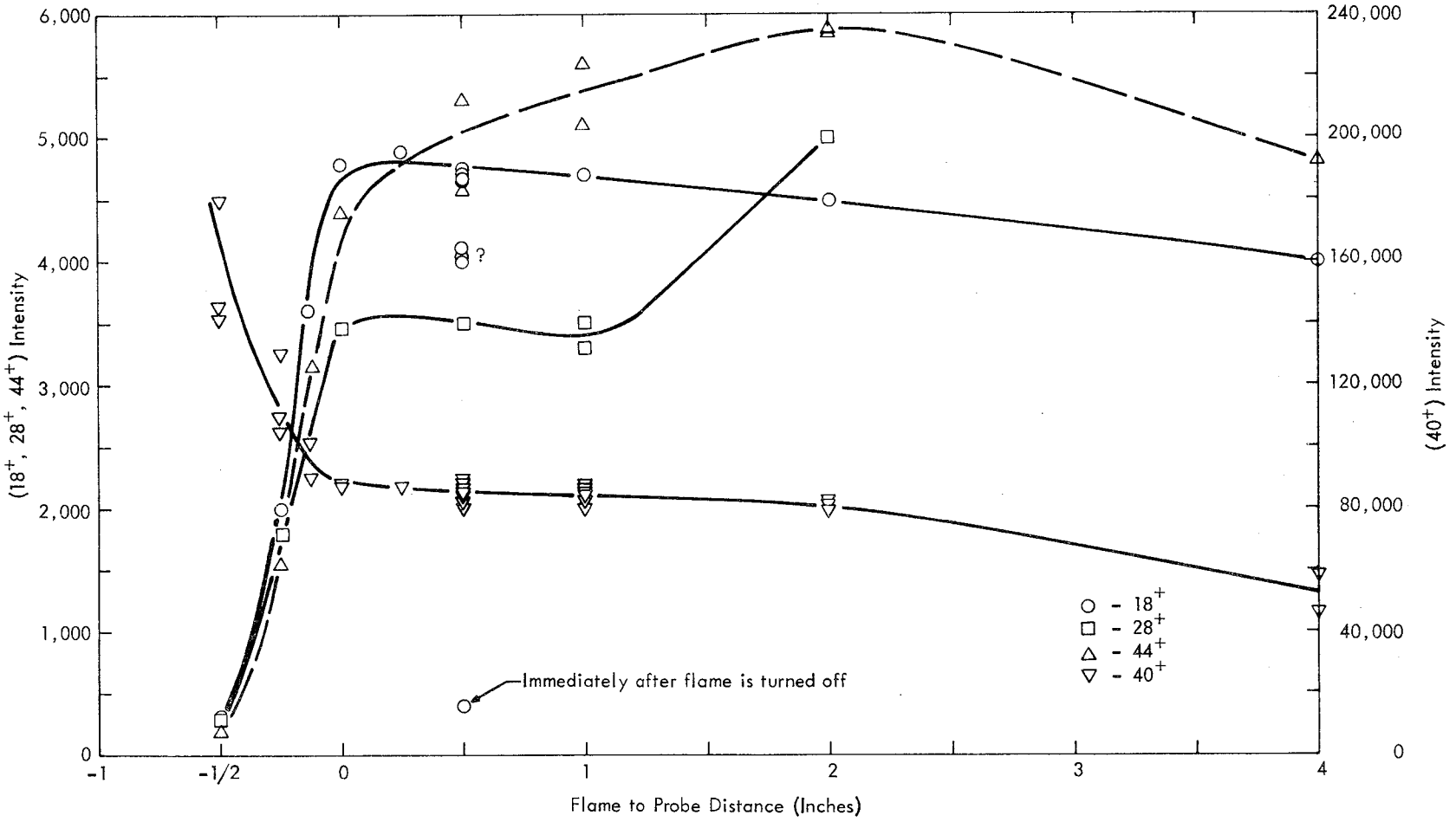

Figure 22 - Relative Changes in Species Concentrations in Gases Sampled Directly From a Lean CH_4/O/Argon Flame Using Probe System of Figure 21

TABLE 5

A COMPARISON OF EXPERIMENTAL VERSUS THEORETICAL SPECIES RATIOS IN THE BURNT-GAS REGION OF A RICH METHANE-O_2-ARGON FLAME (1/1.6/8 FEED GAS PROPORTIONS)

Experimental data are taken from smoothed data of Figure 35 (at 1/2 in. probe distance).

	Composition - Volume %					
Species	H_2	H_2O	CO	O_2	Ar	CO_2
Experimental	< 0.12	4.1	3.0	< 0.08	(72.6)	4.3
Calculated	2.8	15.2	4.5	0.009	72.6	4.6
Experimental, corrected[a/]	< 8.4	10.8	5.0	< 0.14	(72.6)	3.2

a/ A first power of molecular weight mass separation correction is applied and cross sections for H_2, H_2O, CO and CO_2 relative to argon are taken from Kiser.[55/]

The three approaches each have their advantages as well. Use of argon allows one to check for entrainment of substantial amounts of surrounding air downstream of the primary reaction zone. With entrainment eliminated, one can easily follow such crucial ratios as the CO/CO_2 ratio through various regions of the flame. The second procedure has the advantage of measuring all species in a completely realistic coal-air flame. The third approach not only solves the $CO-N_2$ problem, but allows small amounts of hydrocarbons and H_2 to be detected. H_2, in small quantities, is a difficult species in free-jet sampling, due to the combined effects of large mass separation and low ionization cross section.

The plan which we chose was a combination of the second and third approaches.

D. Preliminary Diagnostic Coal-Air Flame Sampling

With a coal-air flame of about 270 $\pm$ 20 mg/liter of coal in air, gases were sampled through quartz probes to provide initial species profiles through the flame and to indicate problems.

1. Gas chromatography of samples collected from flames: Some difficulties were experienced in the initial attempts to collect bulk gas samples for GC analysis. The original plan was to insert a hypodermic needle through a septum in the wall of Stage 1/2 and extract gas samples into 250-ml glass or steel bulbs at the same time as molecular-beam, mass-spectrometer measurements were being made. It turned out that rapid plugging of the hypodermic needle (ID = 0.030 in.) or of a length of capillary (ID = 0.040 in.) occurred with the coal flame, preventing filling of 250-ml bulbs in a reasonable time (minutes). Also, with Stage 1/2 sampling, the bulbs filled only to a pressure of about 1/10 atmosphere which resulted in susceptibility to leaks and lowered sensitivity in the GC analysis. The solution adopted was to extract the GC samples directly from the 1-atmosphere, coal-air flame by inserting a drawn-quartz probe into the flame from above. This probe is identical in shape to the one used in molecular beam sampling and is the same one used to collect particles for proximate analysis. Both probes are operated in sonic flow during most of the sampling, so that the region of extraction from the flame should be similar for all samples, with the GC samples representing a position somewhat downstream relative to the mass spectrometer samples.

It was observed, during sample collection, that the flame was visibly disturbed by the high extraction rate of the 30 mil diameter sonic orifice. The pressure drop across the orifice was varied until no visible disturbance of burnt gas stream lines was apparent. This required a pressure drop of 2 cm Hg (20 torr) or less. Such a sampling condition is incompatible with the present direct molecular beam sampling requirements,

and would complicate collection of gases for GC analysis. For this program we decided to accept the sonic-flow, nonisokinetic sampling. A measure of the extent of flame disturbance was obtained by probing through the reaction zone of a well-known flame system such as a 1-atmosphere CH_4-air flame, with results presented in a later section.

In two preliminary runs without the central hole in the honeycomb GC, mass spectrometric and particulate samples were taken from the rich coal-air flames. The GC system readily permits analysis of N_2, CO, CO_2, O2 + Ar, H_2, and CH_4, but the sampling and storage system makes H_2O analysis impossible. The GC results were calibrated with known gases so that actual partial pressures are shown. Results are plotted in Figures 23 and 24 for the two separate experiments.

2. Mass spectrometry of flames: With the two-stage expansion, molecular beam sampling system shown in Figure 21, direct mass spectrometric analysis of the 270 mg/liter coal-air flame was carried out. The direct sampling mass spectrometric system, using the low-sensitivity Bendix TOF mass spectrometric as a detector, allowed measurement of H_2O, N_2 + CO, Ar, CO_2, and O_2. With the present system, small quantities of CH_4 or H_2 were difficult to detect, the former being difficult because of interference at 16^+ from fragments, and the latter due to background, mass separation and ionization cross-section effects. The mass spectrometer results were plotted as ratios to 28^+ (mainly N_2) with no corrections added for mass separation or mass spectrometer sensitivities. Results are plotted in Figures 25 and 26.

These preliminary results showed that direct sampling of coal-air flames was feasible and indicated the changes that were desirable before final, quantitative probing was attempted.

3. Pollutant species in flames: A brief search was made for the presence of major pollutant species in the rich coal-air flames discussed above. Sampling at a position 3 cm above the burner, well past the initial bright reaction zone, a $30^+/28^+$ ratio of about 2×10^{-3} was measured with the flame on and $0 \pm 2 \times 10^{-4}$ with the flame off. The 28^+ signal is mainly due to N_2 so that with an approximate N_2 percentage of 60, the NO in this flame is about 1,200 ppm.

A search for the species H_2S, SO_2 and SO was made by monitoring $34^+/28^+$, $64^+/28^+$ and $48^+/28^+$, respectively, with the coal-air flame on and off. With the flame off a $34^+/28^+$ ratio of about 1×10^{-3} was observed, attributed to $O^{16}O^{18}$. With the flame ignited, both $32^+/28^+$ and $34^+/28^+$ fell to $0 \pm 1 \times 10^{-4}$. A $64^+/28^+$ ratio of about 1×10^{-3} was measured for the coal-air flame giving an uncorrected SO_2 concentration of about 0.06%. Likewise, a $48^+/28^+$ ratio of about 5×10^{-4} was observed which, if no fragment contribution to 48^+ occurred from SO_2, would indicate an uncorrected SO concentration of about 0.03%.

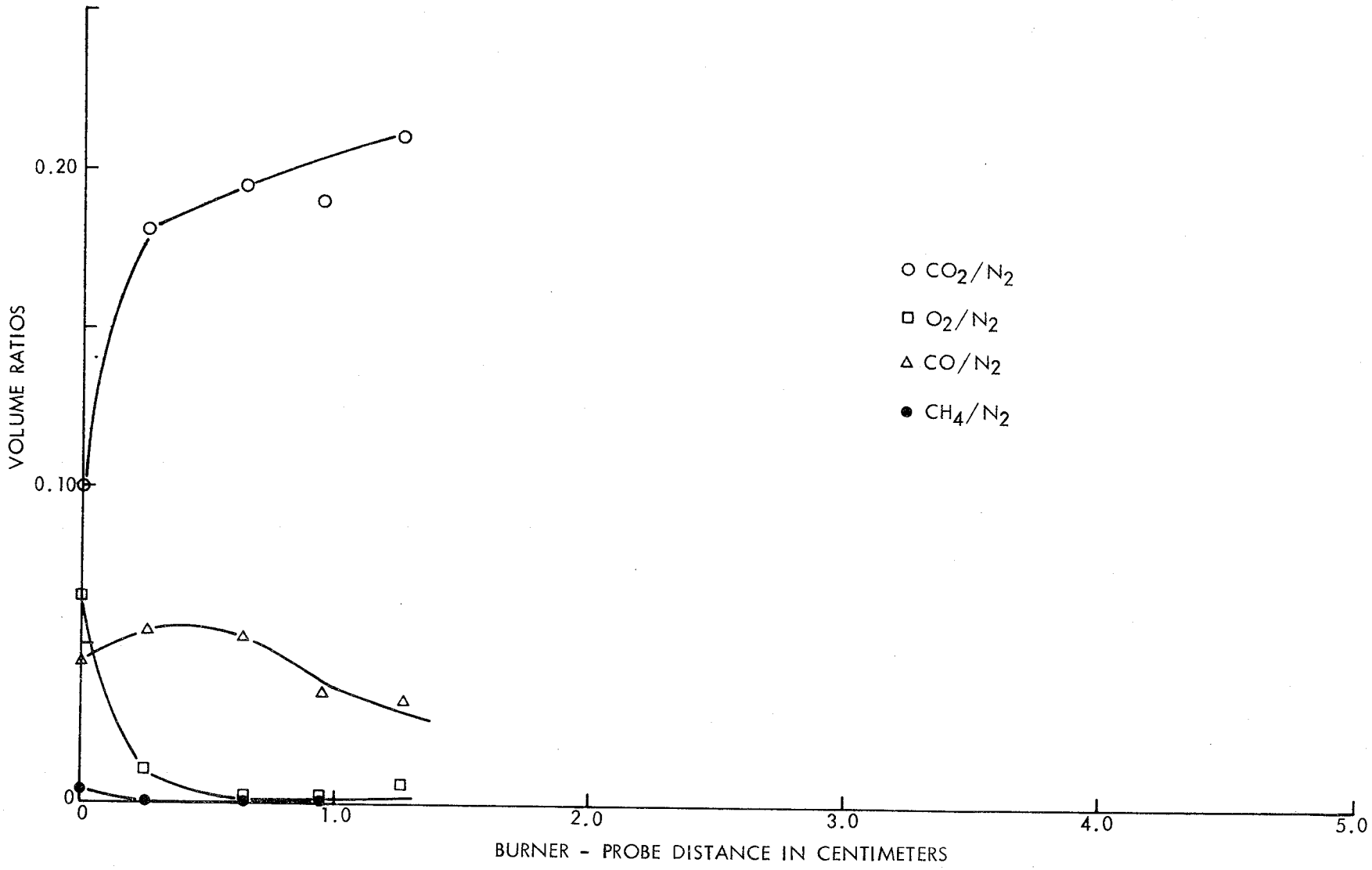

Figure 23 - Variation of CO_2, O_2, CO, and CH_4 with Position in a Rich (≈ 270 mg/liter), Coal Dust-Air Flame as Measured by Gas Chromatography of Gases Sampled Through a 30-mil Diameter Quartz Probe. (H_2 was not analyzed in this series of samples.)

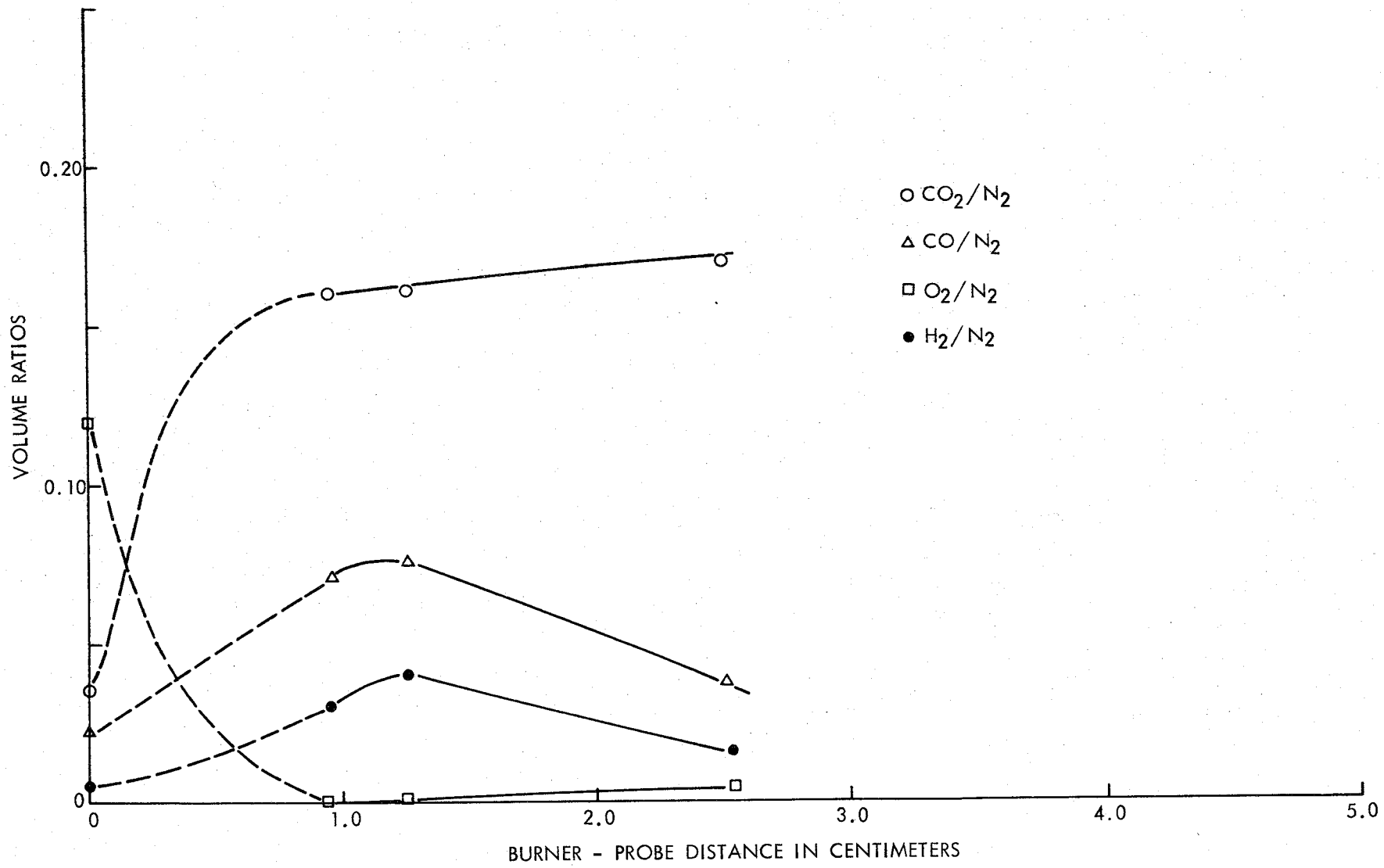

Figure 24 - Variation of CO_2, O_2, CO and H_2 with Position in a Rich (~ 270 mg/liter), Coal Dust-Air Flame as Measured by Gas Chromatography of Gases Sampled Through a 30-mil Diameter Quartz Probe. (CH_4 was not detected in this series of samples.)

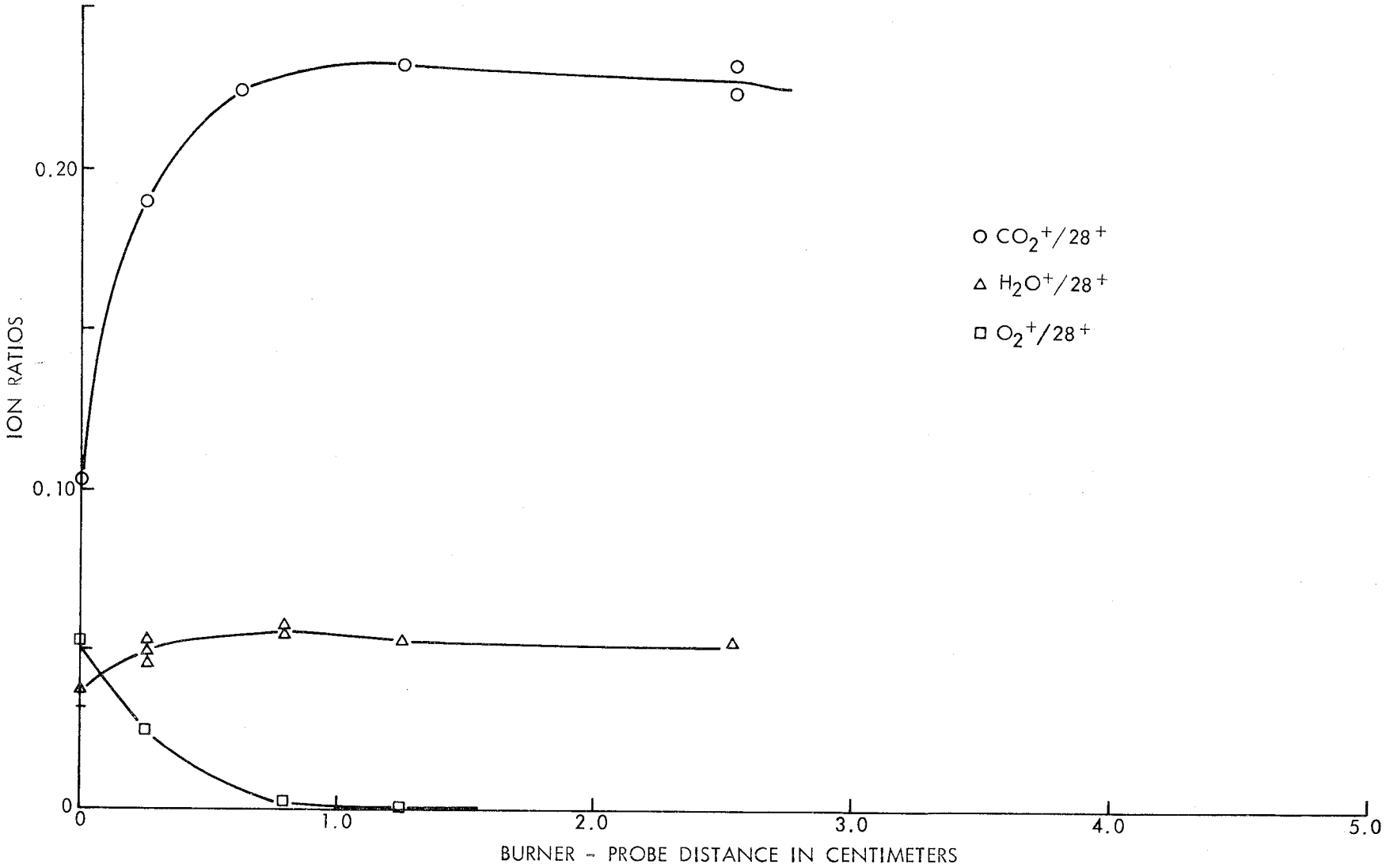

Figure 25 - Variation of CO_2, O_2, and H_2O (relative to 28^+) with Position in a Rich (270 mg/liter), Coal Dust-Air Flame, as Measured by Direct Mass Spectrometric Probing with a 30-mil Diameter Quartz Probe Under Two-Stage Expansion Conditions. Ionizing electron energy was 50 eV.

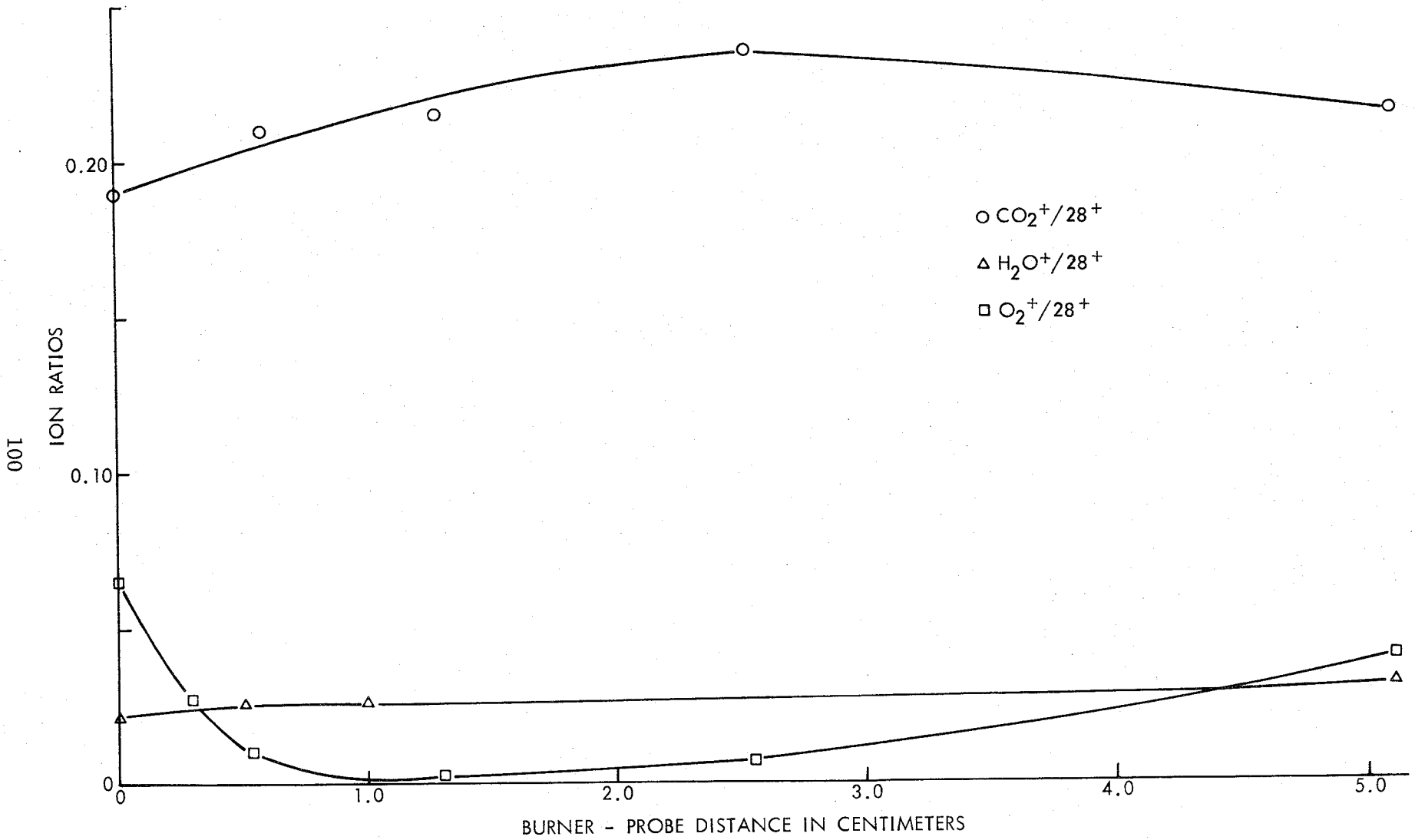

Figure 26 - A Second Sampling Experiment Under the Same Conditions as for Figure 25

These values of pollutant concentrations showed the potential of the direct molecular beam sampling, coal-air flame arrangement for detailed studies of pollutant formation and destruction. Some pollutant species profiles are shown in a later section.

4. Coal-O_2-Ar flames: An attempt was made to burn coal dust in a synthetic air in which the N_2 was replaced by Argon. Such a flame, if it could be adjusted to simulate a coal-air flame, would make direct CO measurements possible by mass spectrometry and would be valuable in tracing NO production from bound nitrogen in the coal. With direct substitution of Ar for N_2 it was found that a much brighter, faster burning flame resulted. In fact, even with extra argon added, the coal-"air" flame flashed back erratically through the burner matrix. No calculations were made to deduce the Ar-O_2 ratio necessary to give the same final flame temperature as a coal-air flame.

In spite of the very erratic behavior of this flame, resulting in frequent flashback, an attempt to measure NO in the burnt-gas region was made. Such a measurement would indicate an upper limit for NO production from fuel-N_2 in the coal and would demonstrate the utility of the coal-"air" flame sampling system arrangement to study this problem in detail. The Bendix was used to follow the ion peaks 40^+ and 30^+ simultaneously. The flame was not stable for much more than 30 sec at a time, but each time the gases were ignited the 30^+ signal rose markedly, while the 40^+ signal declined. (The Stage 1/2 beam conditions were optimized for cold gas rather than hot flame gases.) From a series of lightings of the flame, a $30^+/40^+$ ion ratio of about 2×10^{-3} was estimated. The ratio $28^+/40^+$ was also monitored to get an approximate upper limit for CO in this flame. (The flame was too unstable to check for entrainment of surrounding air.) An average $28^+/40^+$ ratio of 8×10^{-2} was obtained. The argon concentration in the flame was about 61% so that the upper limits of NO and CO, ignoring corrections for mass spectrometer sensitivities, were about 1,200 ppm and 5%, respectively.

E. Additional Changes in Coal-Air Flame Sampling, Burner, and Detection System

Prior to the final, calibrated series of flame species probe measurements, improvements and changes were made based on the preliminary results reported above.

1. Quadrupole mass spectrometer addition: Earlier results have shown the Bendix TOF to possess inadequate sensitivity to carry out either sampling of stable species from the sticky region of coal-air flames or potassium-containing species from CH_4-air flames. Therefore, the Institute purchased a high-sensitivity, quadrupole mass spectrometer, suited for

molecular beam detection, from the Extranuclear Company.[51] This device was received, installed and tested during the third year of the program. A schematic of the new sampling quadrupole arrangement is shown in Figure 27. The assembly shown mounts directly over the Bendix Ion Source Tee.

The Extranuclear quadrupole operated satisfactorily, with a gain in ion current, for the same molecular beam, of about 300 compared to the Bendix TOF. Two problems have been encountered, both of which could be mitigated and did not limit the present program of coal studies. First, with the ion source of the quadrupole mounted close to the Bendix TOF ion source, the electron beam focusing magnets of the TOF seriously disrupted the operation of the quadrupole, reducing ion intensity unacceptably. Removing the Bendix magnets decreased the 28^+ peak in the TOF by a factor of 20; but since the Bendix was used for strong peaks, if at all, this was a workable solution.

Second, in the presence of a modulated beam of argon (and possibly also of helium) a general phase-locked, modulated signal exists over the entire spectrum. This "AC noise" depends on ion source and multiplier parameters just as does the Ar^+ beam signal and could seriously interfere with weak signal detection. Fortunately this AC noise is proportional to Ar strength in the modulated beam. For an air beam, containing about 1% Ar, the between-peak AC noise signal represents about 1 ppm of the 28^+ signal from N_2. For the coal studies this should present no problems, while for the K- and P-containing species work, CH_4-N_2-O_2 flames can be used, if necessary, rather than CH_4-air, with no great inconvenience or cost.

In an attempt to verify the proper performance of the quadrupole, the ion yield was compared with a theoretical neutral beam intensity at the ion source, based on ideal free-jet expansion and scatter-free collimation. This calculation indicated a lower limit for neutrals ionization efficiency of about 1 part in 4,000.

2. Self-cleaning orifice: The new high-sensitivity Extra-nuclear quadrupole mass spectrometer has a sensitivity at least two orders of magnitude greater than the Bendix. We thus decided to repeat direct, single-stage, free-jet expansion sampling tests with coal-air flames. For this purpose a 90-degree spun-copper conical orifice, 1/2 in. high, with a 0.010 in. diameter hole drilled in the apex, was used. With an optimized orifice-skimmer distance of 1/2 in., this 10 mil orifice produced intense beams from either air or a Bunsen burner flame. Unfortunately, the small orifice plugged within tens of seconds in the char burning region and in about a second in the sticky, early reaction zone. Since present instrumentation available for project use was not suitable for mass spectral scans of 1 sec or less, we returned to the previously tested, two-stage expansion sampling mode.

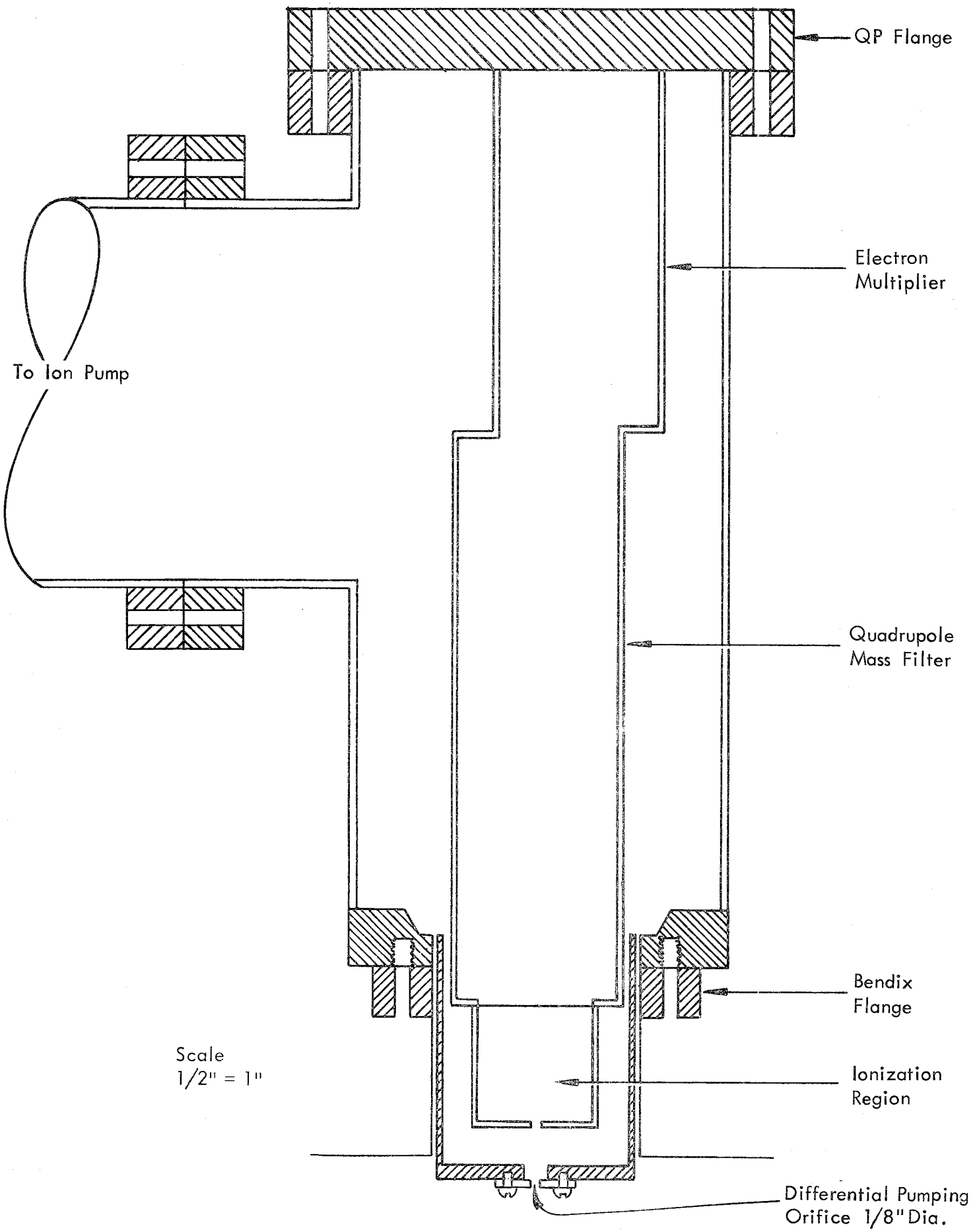

Figure 27 - Scale Schematic of Extranuclear Quadrupole and Housing as it Mounts on the Top of the Bendix TOF Ion Source Housing

The time response of the two-stage expansion sampling system was tested by observing the rate of rise of the 44^+ (CO_2^+) signal when a CH_4-air mixture issuing from a Bunsen burner was suddenly ignited. Recording the output from the PAR phase locked amplifier by means of an analog-to-digital convertor and a multichannel analyzer, it was established that the CO_2 signal reached 90% of its steady state value in 0.1 sec. The time response of the PAR or electrometer amplifiers may be limiting so that the true time response of the sampler could be even faster.

Following some coal-air flame sampling tests discussed in the next section, we designed, constructed and tested a partially self-cleaning sampling orifice. Plugging experience with the 30 mil, conical, quartz orifice-probe indicated two problems. A light, fluffy, soot-like material collects on the exterior surfaces of the conical probe. This material can easily be brushed off with a small wire while the coal-air flame is burning and sampling is taking place. The more serious problem is that of plugging of the interior of the conical orifice tip. The plugging material is not fused or coherent and can be broken loose by poking with a small stiff wire from outside. This operation is not usually possible with the flame burning, however, and shutting down the flame is time consuming and leads to more variation in flame properties within a series of flame-species profile measurements. Eventually, one of the downstream skimmers may plug, and fine char and coal material coats interior parts in Stage 1/2 and eventually falls into the sampling cone apex, but the sampling duration is first limited by primary orifice plugging.

Our approach to a self-unplugging orifice is shown in Figure 28. A water-cooled, spun-copper, 90 degree, 1/2-in. high, conical orifice is used in place of the drawn-quartz orifice, for ease of fabrication and ruggedness. The only version tested so far uses a 15-mil wire in a 30-mil drilled hole at the apex of the cone. The 6 volt DC solenoid produces a 1/16 in. linear motion of the cleaner-wire such that when extended, the wire is just flush with the exterior apex of the cone. In initial tests, this device has maintained an open orifice for from 20 to 30 min of continuous probing, including the very sticky regions of the flame. With such an orifice-cleaner it appears possible to obtain a complete set of flame species profiles without extinguishing the flame, though exterior material must still be occasionally brushed off the cone from outside. No mechanical device to do this has been constructed, since it can easily be done manually as part of the flame-probe distance adjustment process.

The Stage 1/2 pressure and the resulting modulated beam both respond noticeably to the periodic operations of the unplugging device. Figure 29 shows a record of the AC beam signal with the unplugger device operating on a cycle of 3.5 sec open and a 0.2 sec closed pulse. The time constant of the PAR was set at minimum for this run. At about a 1-sec time constant, the closed-pulses are smoothed out almost completely.

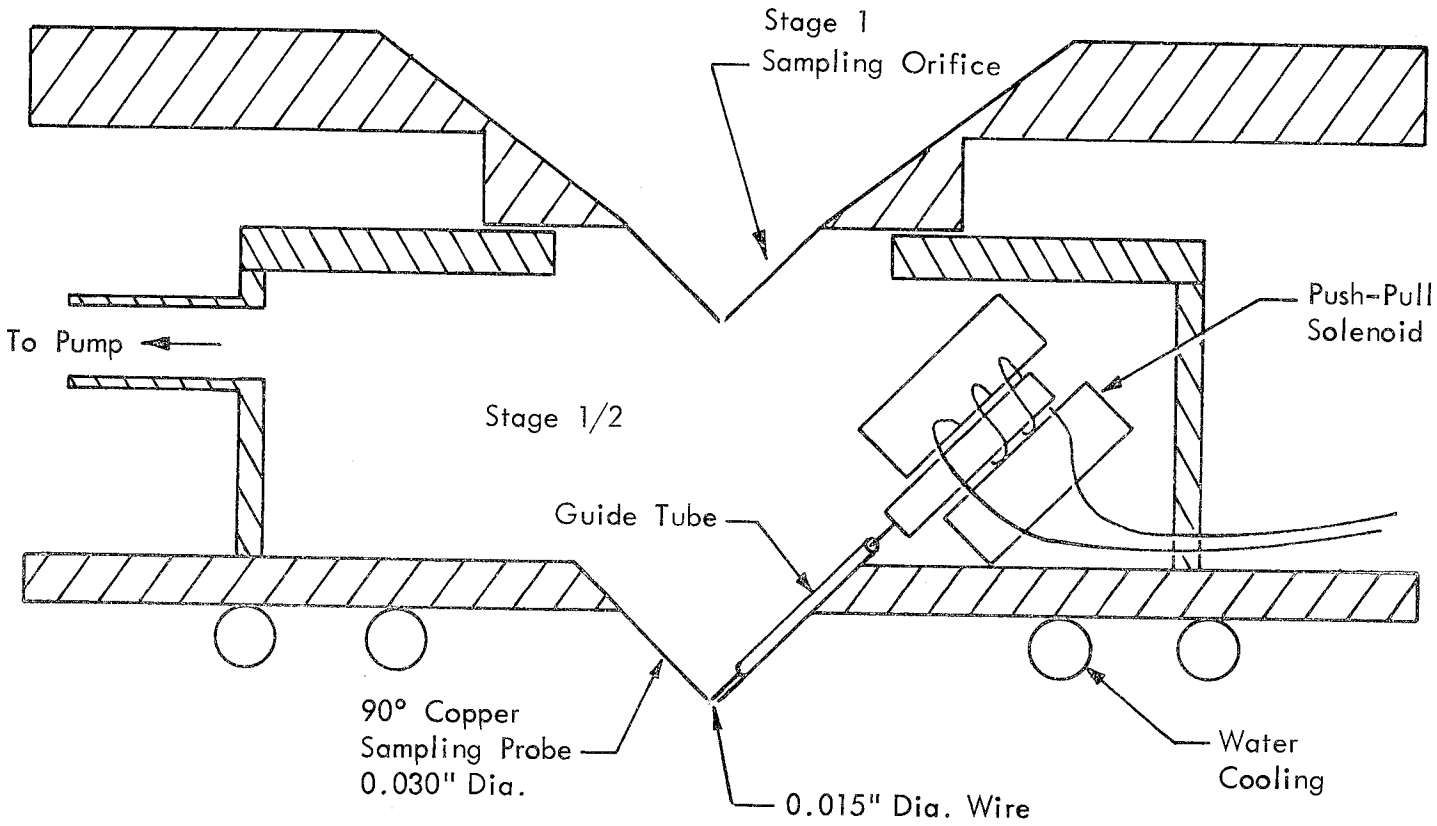

Figure 28 - Schematic of Mechanical Device Used to Keep the 30-mil Copper Orifice Unplugged During Sampling of Coal-Air Flames

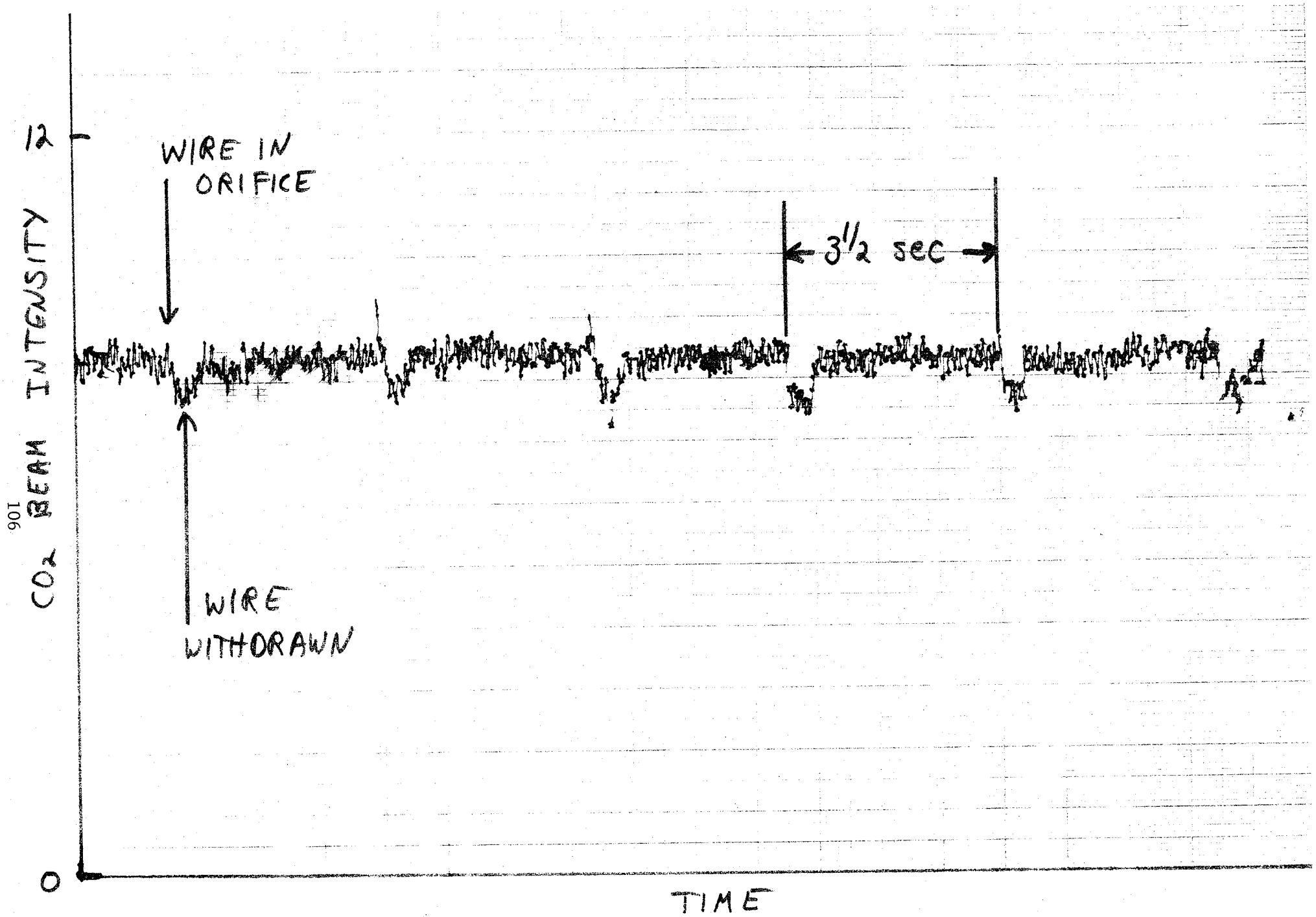

Figure 29 - Strip Chart Record of Phase-Locked 28^+ Signal from an Air Beam Sampled Through the Self-Cleaning Orifice Arrangement Shown in Figure 28

Tests reported below indicate that similar coal-air flame profiles are obtained with either the quartz probe or copper probe. The final series of measurements used the automatic unplugger, with 30 mil copper-cone orifices. There is a good possibility that orifices as small as 10 mils could be kept open with similar devices, thus permitting direct, free-jet sampling of coal-air flames.

3. Fast AC scans: The original two-stage sampling system, using a 30-mil quartz orifice, a 20-mil copper orifice-skimmer and a 10-mil skimmer was used to probe coal-air flames by operating the quadrupole in a moderately fast AC scan. An AC scan refers to monitoring the output of the PAR lock-in amplifier which records only the direct modulated beam, chopped at 100 cycles/sec.

Within the time-response limitations of the 100 cycle/sec chopping, the PAR phase-locked amplifier and the rather slow 10 kilocycle analog-to-digital converter, a 10-sec scan over the mass range 11 amu to about 46 amu was chosen. The digitized scan data were collected in a multi-channel analyzer (MCA) using one-fourth of the storage (256 channels) for each scan. Four successive scans, at four sampling positions in the flame, could be taken over the course of about 2 min. The scan data could be printed out or converted back to analog data and graphed. Figures 30 through 33 show the actual NCA printout for slightly rich and rich coal-air flames. Figure 34 is a plot of the raw, unnormalized ion intensity data versus distance above the burner. The burner grid did not have a central hole during these exploratory experiments and thus sampling did not extend to nearly unburned gases, as was achieved in data shown in the later sections.

Two problems occurred with this fast AC scan setup. First, the dynamic range was not sufficient, due to the slow analog-to-digital converter frequency, to follow both strong peaks like 28^+ and weak peaks like Ar^+. Second, weak peaks were rather noisy and more than one scan would need to be averaged to obtain precision data. The fast-scan approach has been proven, in laser-plume monitoring studies in our laboratory, for strong peaks at scanning times as short as 20 msec.[52] For the present purposes, however, it appears that we could obtain superior data by simultaneously following two ion peaks, one on the Bendix TOF and one on the Extranuclear quadrupole, as a function of probe position in the flame. In fact, considering the inevitable variability in local coal-air concentrations, due to imperfect mixing, it will probably be better to achieve at least several seconds of averaging in recording a given peak.

4. Detection-background problems for hydrocarbon intermediates: One of the major project goals was the determination of the nature and extent of devolatilization and pyrolysis products mixing with air prior to ignition and oxygen consumption. With the raised central cone in the coal-air flame, we are able to probe into substantially unburned gases, though still not into the completely cooled incoming gases.

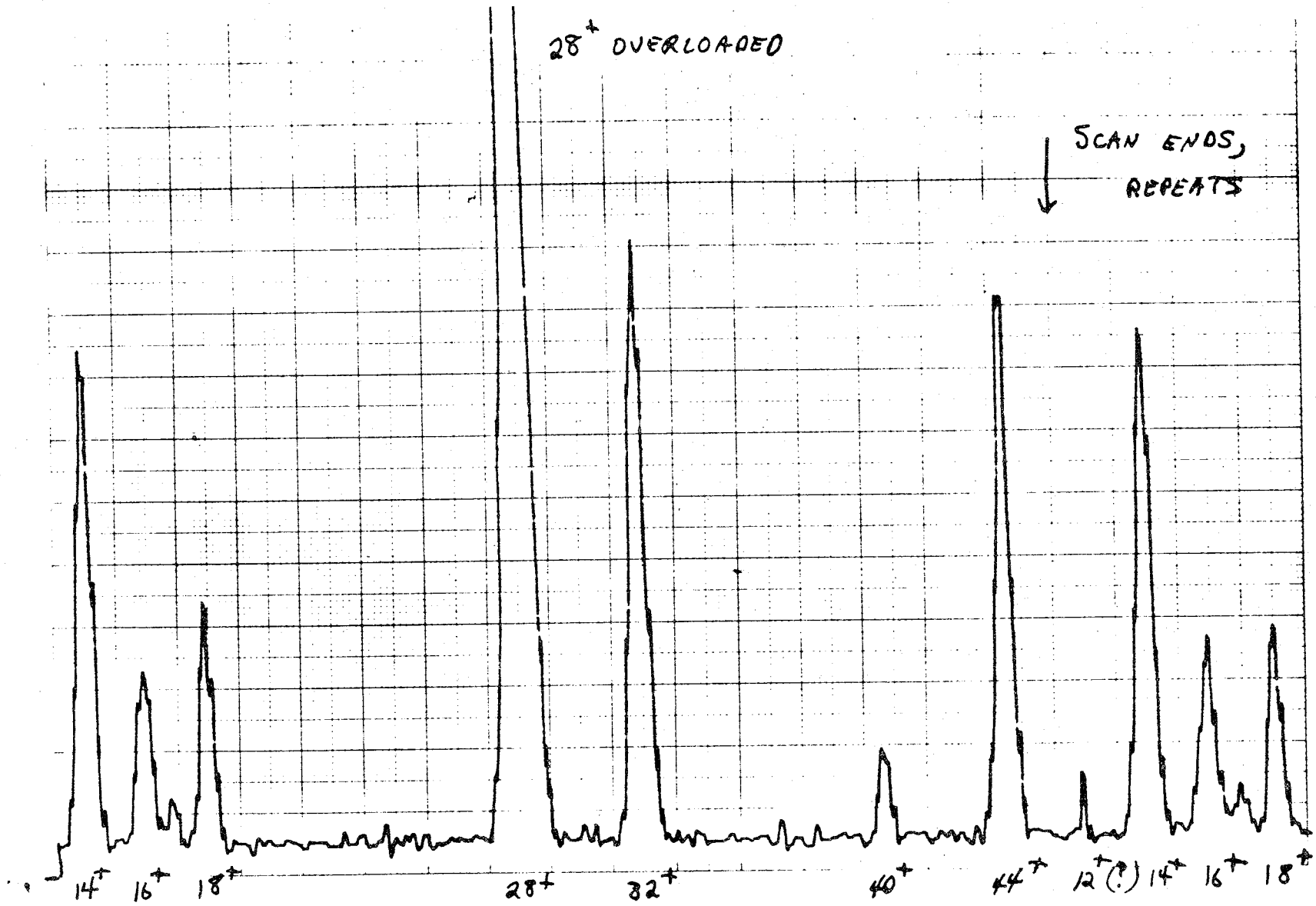

Figure 30 - Fast AC Scan of Major Species in a 197 mg/liter Coal-Air Flame on a 6.3-cm Burner with No Raised Central Cone. Total scan period shown is 10 sec. Sampling position at burner matrix surface. Quartz 30-mil probe used.

Figure 31 - Same Condition as Figure 30 but Probe at 1/4 in. Above Matrix

Figure 32 - Same Condition as Figure 30 but Probe at 1/2 in. Above Matrix

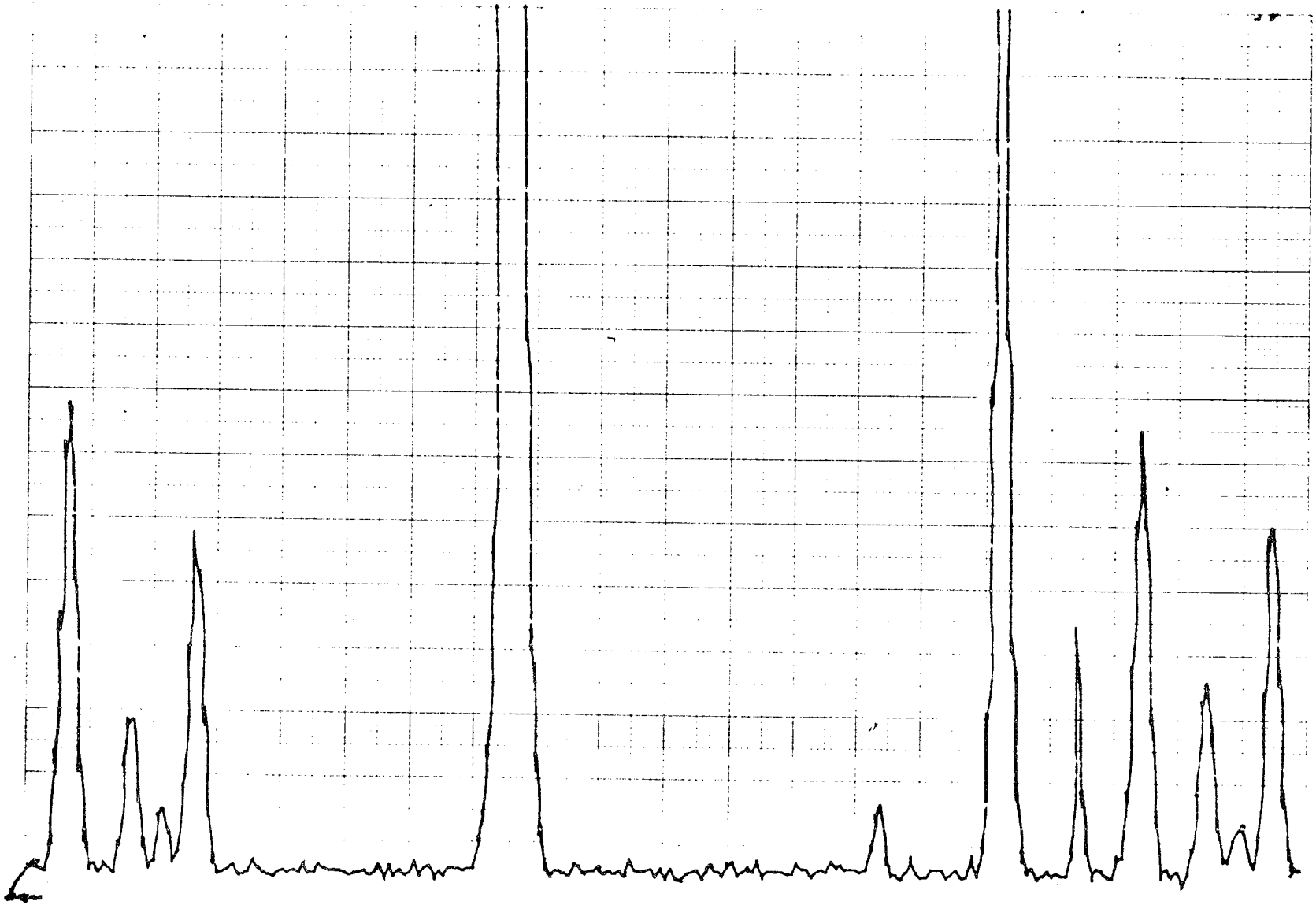

Figure 33 - Same Condition as Figure 30 but Probe at 1 in. Above Matrix

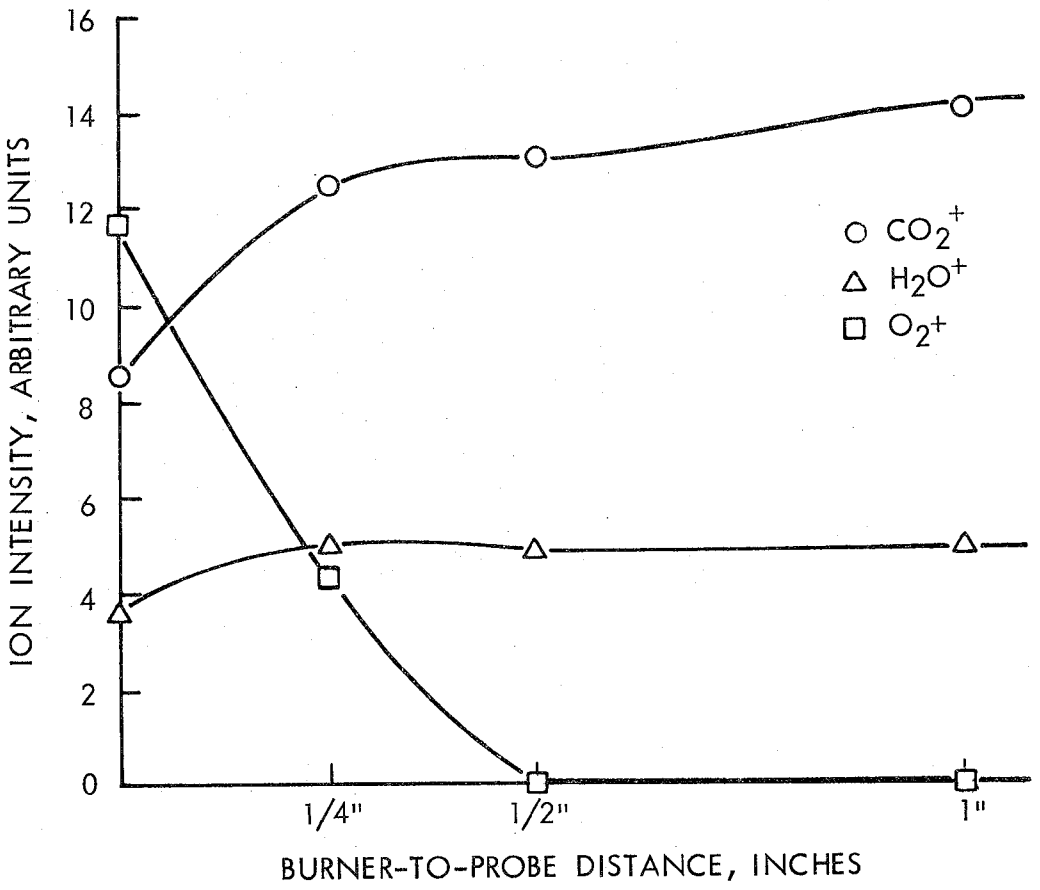

Figure 34 - Uncorrected Raw Ion Intensity Data From Figures 30 to 33 for 197 mg/liter Flame

It is possible that a larger central hole would permit a stable, larger, raised central cone but it was decided to proceed for the rest of present program with the small, approximately 5-mm diameter, central opening previously described.

The literature on coal pyrolysis seldom involves data from pyrolysis in an oxidizing atmosphere at the rate of heating typical of pulverized coal combustion. Nevertheless, under vacuum and inert gases, the major species seem to be H_2, CO, C_2H_2, CH_4, HCN and higher hydrocarbons to a lesser extent. Evidence has been given of a burst of H_2 evolution just prior to ignition in actual coal combustion.[28] Consequently, we made an initial search for detectable amounts of these species in the early stages of burning in our coal-air flames. The species CO could not be followed mass spectrometrically due to the N_2 interference. Acetylene was monitored at the parent peak 26^+ and HCN at 27^+. Methane was followed at 15^+ due to the oxygen interference at 16^+. Hydrogen was measured at 2^+ but the sensitivity was limited because the background gases in the ion-pumped quadrupole mass spectrometer ion-source region appear to be mainly H_2 and CO. This fact, coupled with the low ionization cross section of H_2 and the suspected molecular-beam mass separation discrimination effect, made it difficult to detect H_2 at much less than the 5% level. Direct calibration with a cold 10% H_2, 90% air mixture gave a $2^+/28^+$ ratio of 7.3×10^{-3}. All data were taken at 50 ev ionizing electron energy.

Figure 35 shows $2^+/28^+$ data taken in a number of different scans through a 226 mg/liter coal-air flame. Also shown is an oxygen (32^+) profile indicating the main combustion region. The scatter is bad for the H^2 data but it appears that the H^2 may actually increase as the burning proceeds. This is verified in GC results presented later. From the calibration, hydrogen levels of about 10% are indicated, but this is highly uncertain due to temperature dependent mass separation effects that may be present. There is no indication of an initial burst of H_2, at least as far into the unburned gases as we probe in this experiment. It is possible that the H_2 observed is a coal gasification product under the oxygen-deficient conditions of burning early in this rich flame.

Figure 36 shows data obtained by monitoring 15^+, 26^+ and 27^+ in a slightly richer coal-air flame. A single oxygen value, monitored at 0 cm probe distance indicated that probing extended nearly into the unburned gas region. Surprisingly, the neutrals responsible for 15^+, 26^+ and 27^+ all rise between 0 and 1 cm distance above the burner grid. Again no evidence of extensive early pyrolysis to unburned hydrocarbons is apparent.

In view of the low concentration of hydrocarbons at the earliest sampling position in the flame and the difficulties in mass spectrometric H_2 measurements, it was decided to make subsequent measurements by collecting gas samples for gas chromatography. Hydrogen, CO and hydrocarbons were determined, with CO_2 and O_2 also measured for cross comparison purposes with the mass spectrometer results.

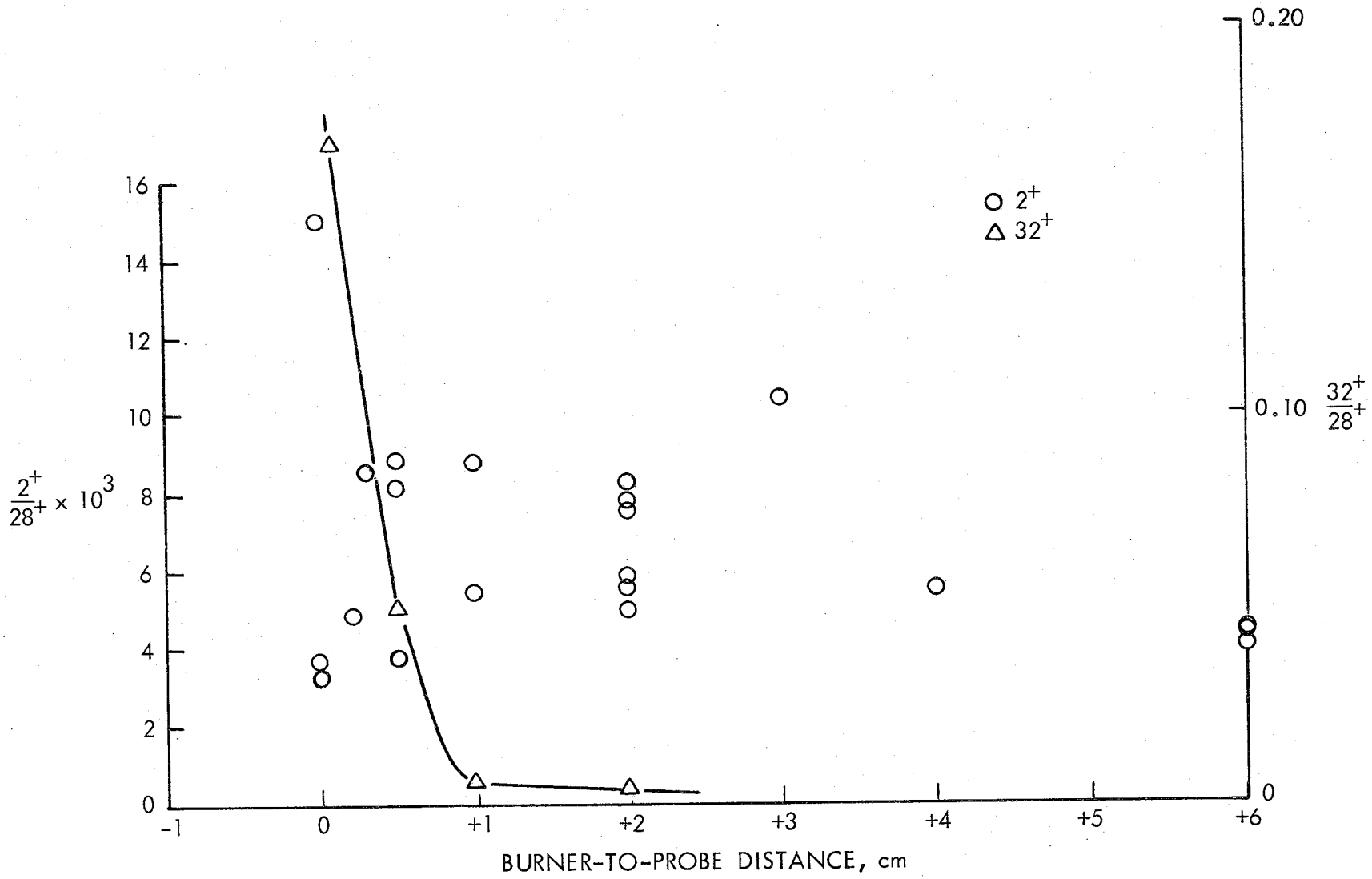

Figure 35 - A Search for H_2 in a Rich Coal-Air Flame (226 mg/liter). A 30 mil quartz probe was used.

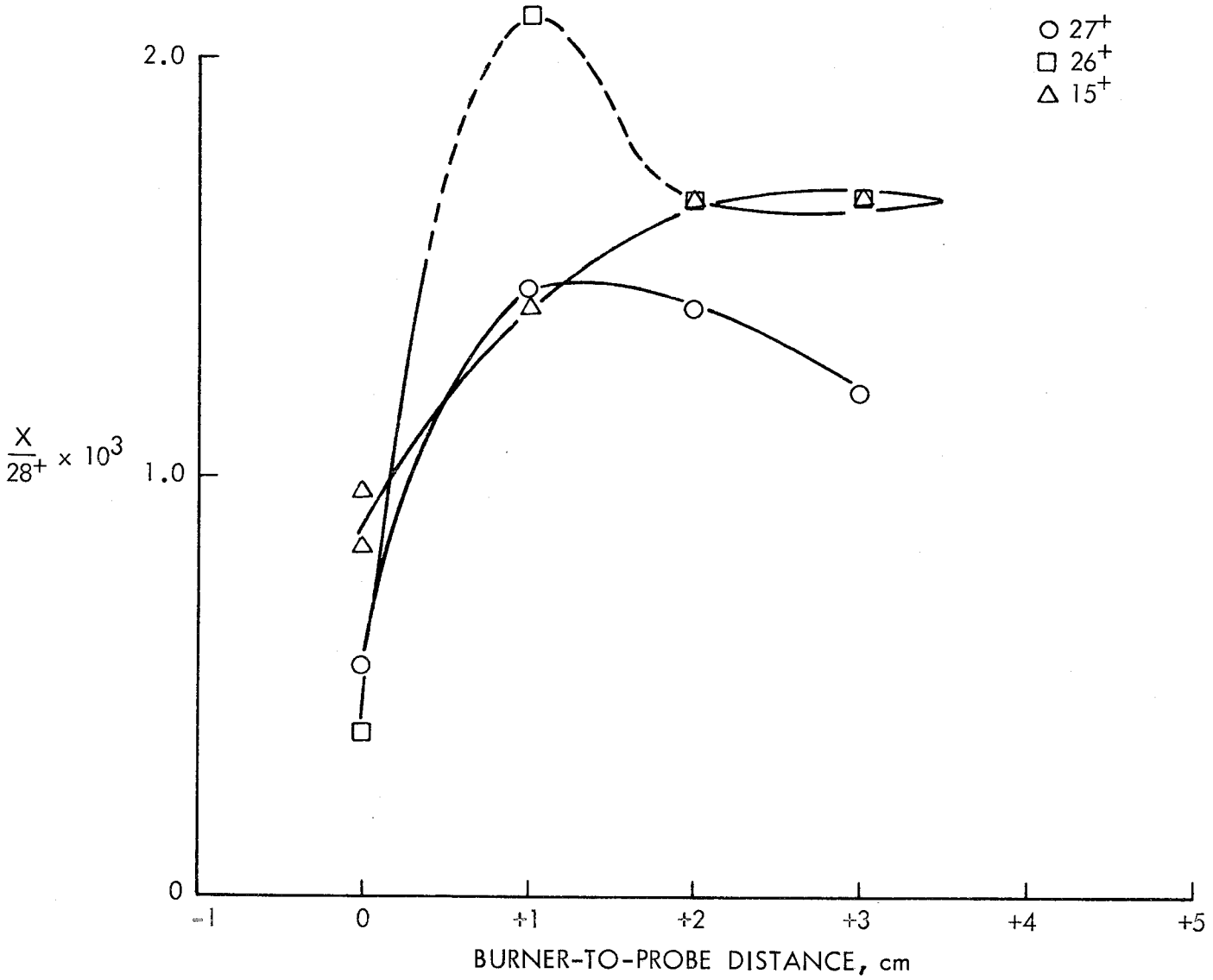

Figure 36 - A Search for Hydrocarbon Pyrolysis Products Early in the Burning of a Rich Coal-Air Flame (251 mg/liter)

APPENDIX F

QUANTITATIVE RESULTS OF DIRECT PROBING OF COAL-AIR FLAMES FOR GASES

Following the apparatus and analytical technique development and tests described above, we carried out two series of sytematic probings of coal-air flames. These tests, unless otherwise noted, involved the 6.3-cm burner with an enlarged hole in the central region of the honeycomb and 10 to 20 μ Pittsburgh seam coal of low ash content.

A. Gaseous Profiles Without Quadrupole Sensitivity Calibration

The first series of final runs surveyed behavior in coal-air flames, without an attempt to quantitatively determine relative species concentrations. Relative changes in species composition through the flames should be quantitatively significant, however. The series was designed to test the capabilities of the quadrupole sampling system and to help finalize a burner configuration and range of coal-air flames for the final series of runs described below.

1. Stable combustion products: The sampling situations are summarized in Table 6, which contains references to the appropriate figures showing raw, uncorrected data. All data were taken with the two-stage expansion system employing either a 30-mil quartz or copper orifice, a 20-mil copper orifice-skimmer and a 10-mil skimmer. Mass spectral data involved 50 ev ionizing electrons. The ion 28^+ was determined on the Bendix TOF, all other peaks on the Extranuclear quadrupole by occasional comparison of 28^+ signals between the TOF and quadrupole. Neither mass spectrometer had been calibrated for sensitivity to H_2O, CO_2 or O_2 relative to N_2.

The data shown in Figures 37 through 42 indicate the narrowness of the reaction zone and the success in approaching the unburned gas composition with the raised central-cone burner configuration. Based on these survey results, which it should again be emphasized do not involve calibrated species ratios and which cannot be used in mass balance considerations, the final series of runs were chosen as described below. In all data shown, a 2-min grid warm-up period was allowed before species ratios were measured. A profile taken by moving the probe toward the grid and then out, showed no evidence of hysteresis effects caused by flame attachment to the probes. In all cases, however, the large pumping speed of the 30 mil sonic orifice was seen to visibly draw in flame gases from a region in advance of the probe, as would be expected from such extremely nonisokinetic sampling.

2. Pollutant species profiles: Once a coal-air flame was established and coupled with the quadrupole mass spectrometer sampling system, it was a simple matter to observe the behavior of minor speices in the flame--particularly with the extended operating times before plugging made possible by the self-cleaning orifice arrangement.

TABLE 6

BURNER AND FLAME CONDITIONS UNDER WHICH SPECIES RATIO PROFILES WERE OBTAINED ON 6.3-CM DIAMETER BURNERS

Coal/Air Composition	Burner Grid	Sampling Orifice	5 mm dia. Central Hole	Approximate Maximum Central Grid Temperature	Data Shown in Figures	Coal
165	Uncooled Nickel alloy	copper	yes	700°C	Figure 37	10-20 μ Pittsburgh Seam. Normal ash content.
177	Uncooled Nickel alloy	quartz	yes	700°C	Figure 38	10-20 μ Pittsburgh Seam. High ash content.
212	Uncooled Nickel alloy	quartz	yes	700°C	Figure 39	10-20 μ Pittsburgh Seam. High ash content.
304	Uncooled Nickel alloy	copper	yes	700°C	Figure 40	10-20 μ Pittsburgh Seam. High ash content.
215	Uncooled copper-plated Nickel alloy	quartz	no	300°C	Figure 41	10-20 μ Pittsburgh Seam. High ash content.
243	Uncooled copper-plated Nickel alloy	quartz	yes	300°C	Figure 42	10-20 μ Pittsburgh Seam. High ash content.

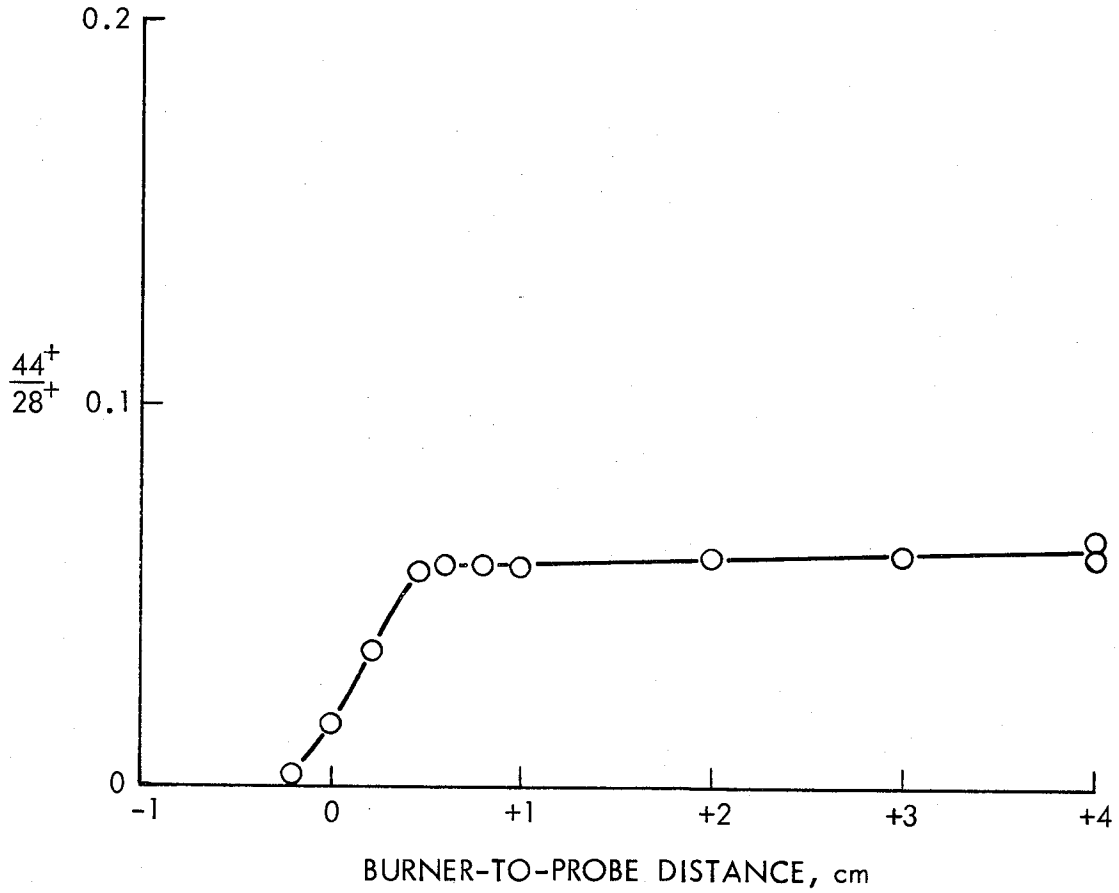

Figure 37 - CO_2 Profile in a 165 mg/liter Coal-Air Flame

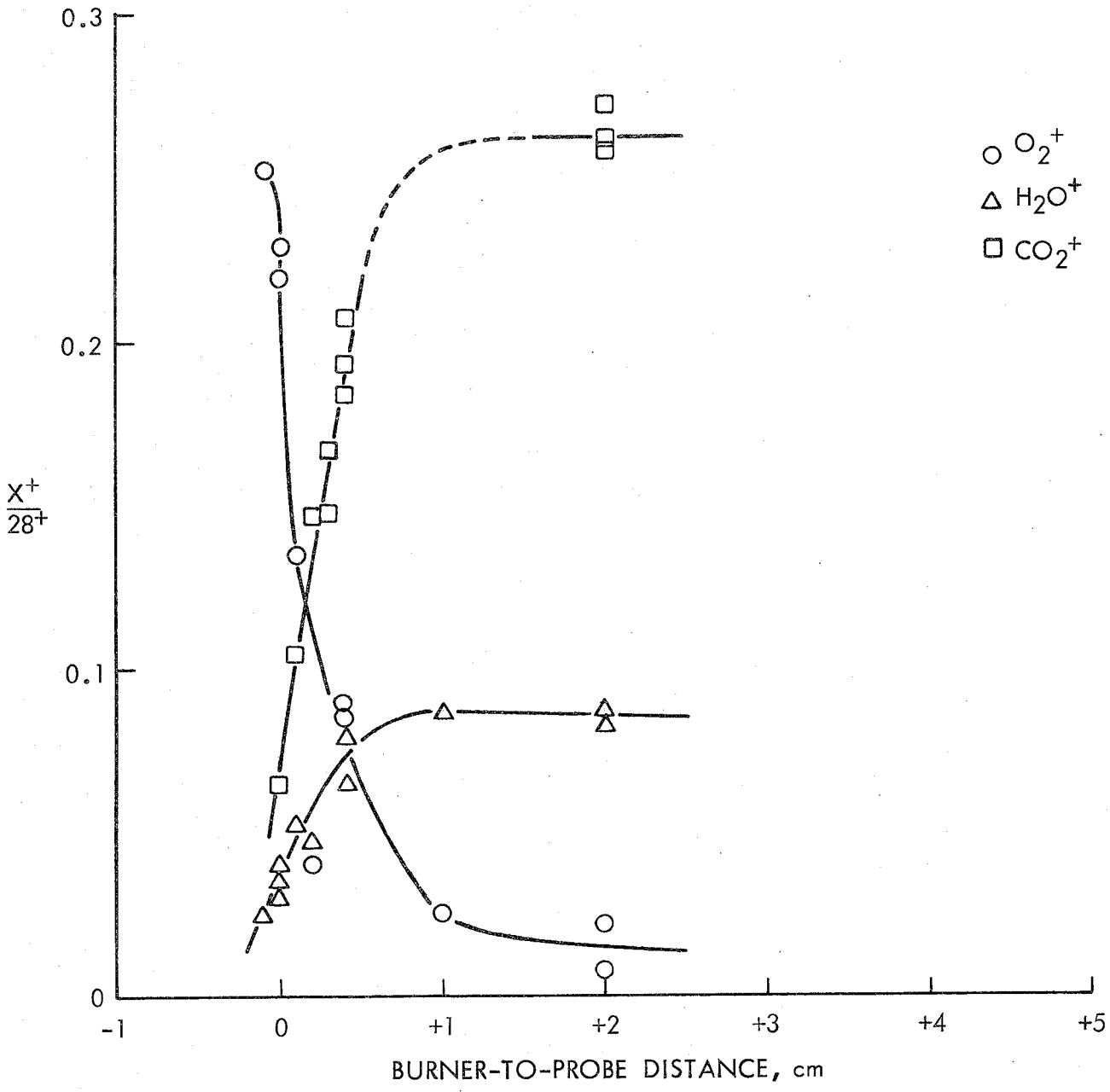

Figure 38 - Major Species Profiles in a 177 mg/liter Coal-Air Flame. (A scale error is suspected in the high relative value of CO_2 shown in the raw ion intensities for this run.)

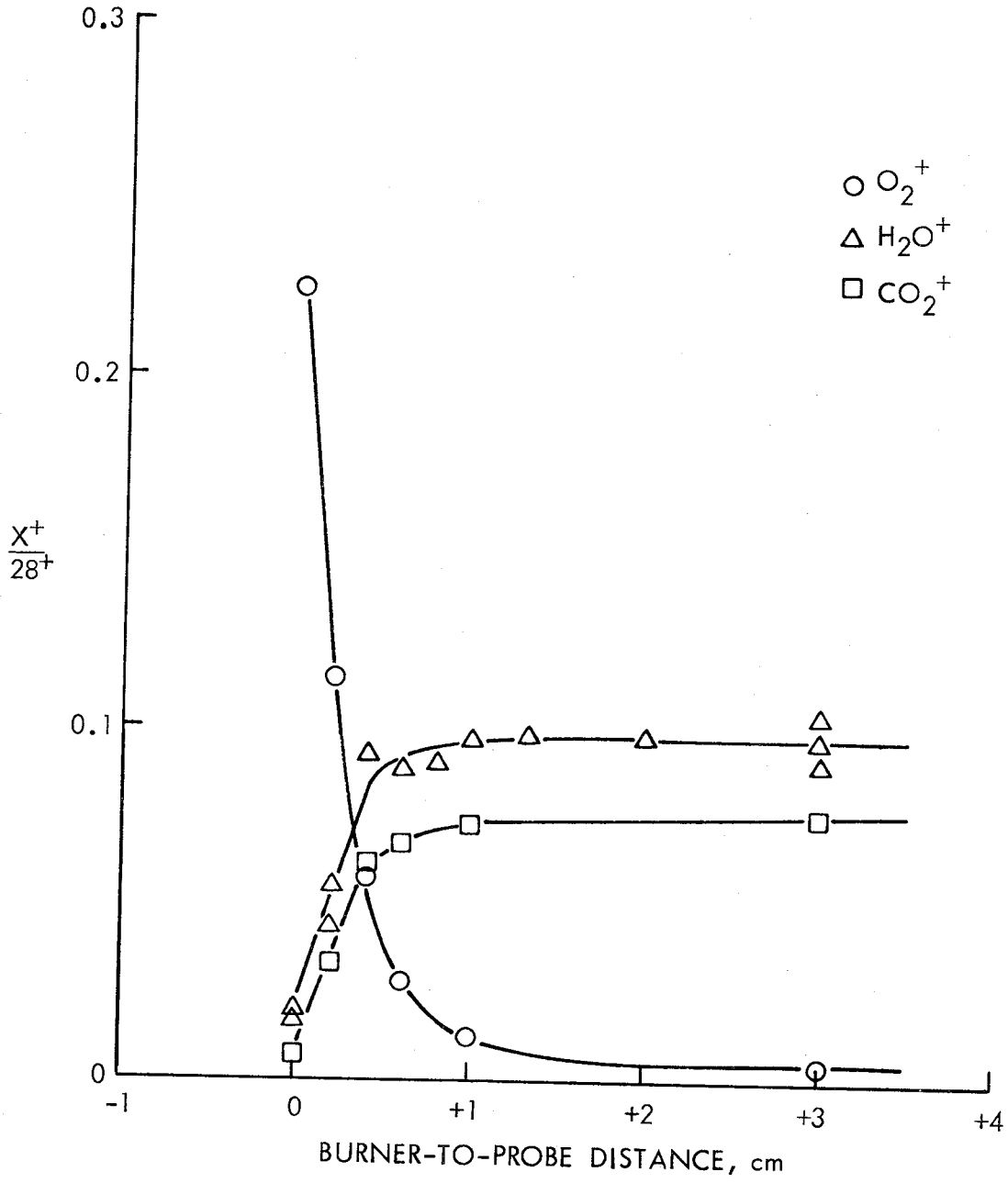

Figure 39 - Major Species Profiles in a 212 mg/liter Coal-Air Flame

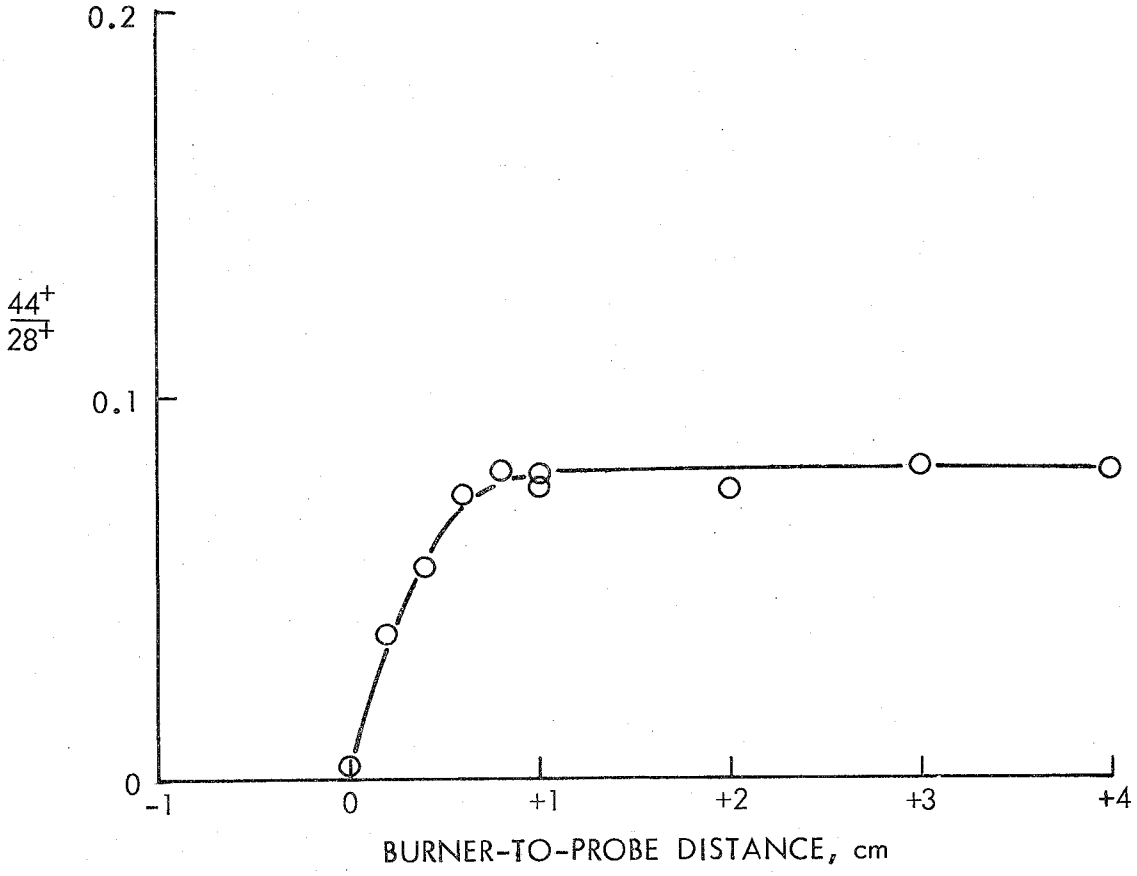

Figure 40 - CO_2 Profiles in a 304 mg/liter Coal-Air Flame

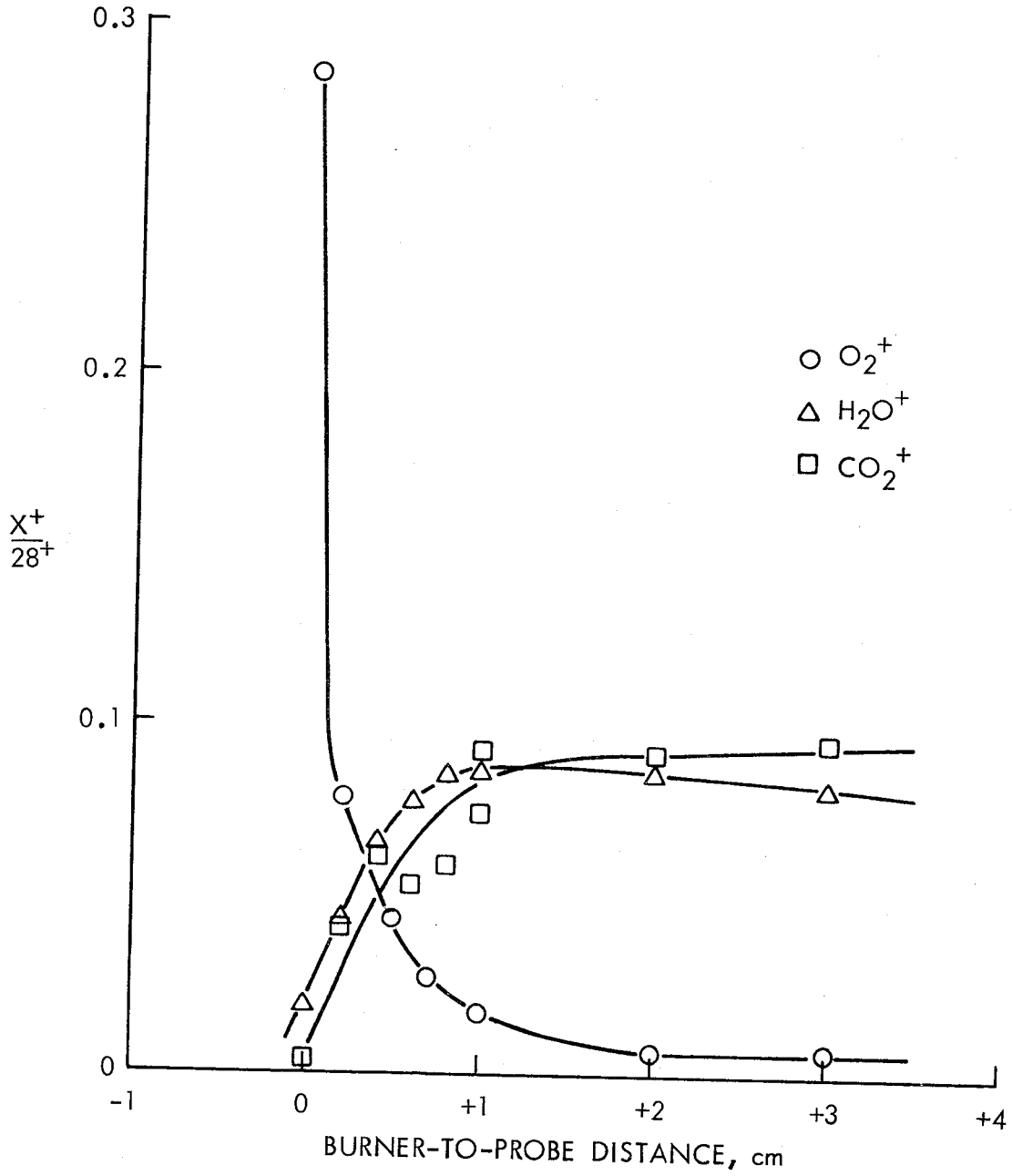

Figure 41 - Major Species Profiles in a 215 mg/liter Coal-Air Flame

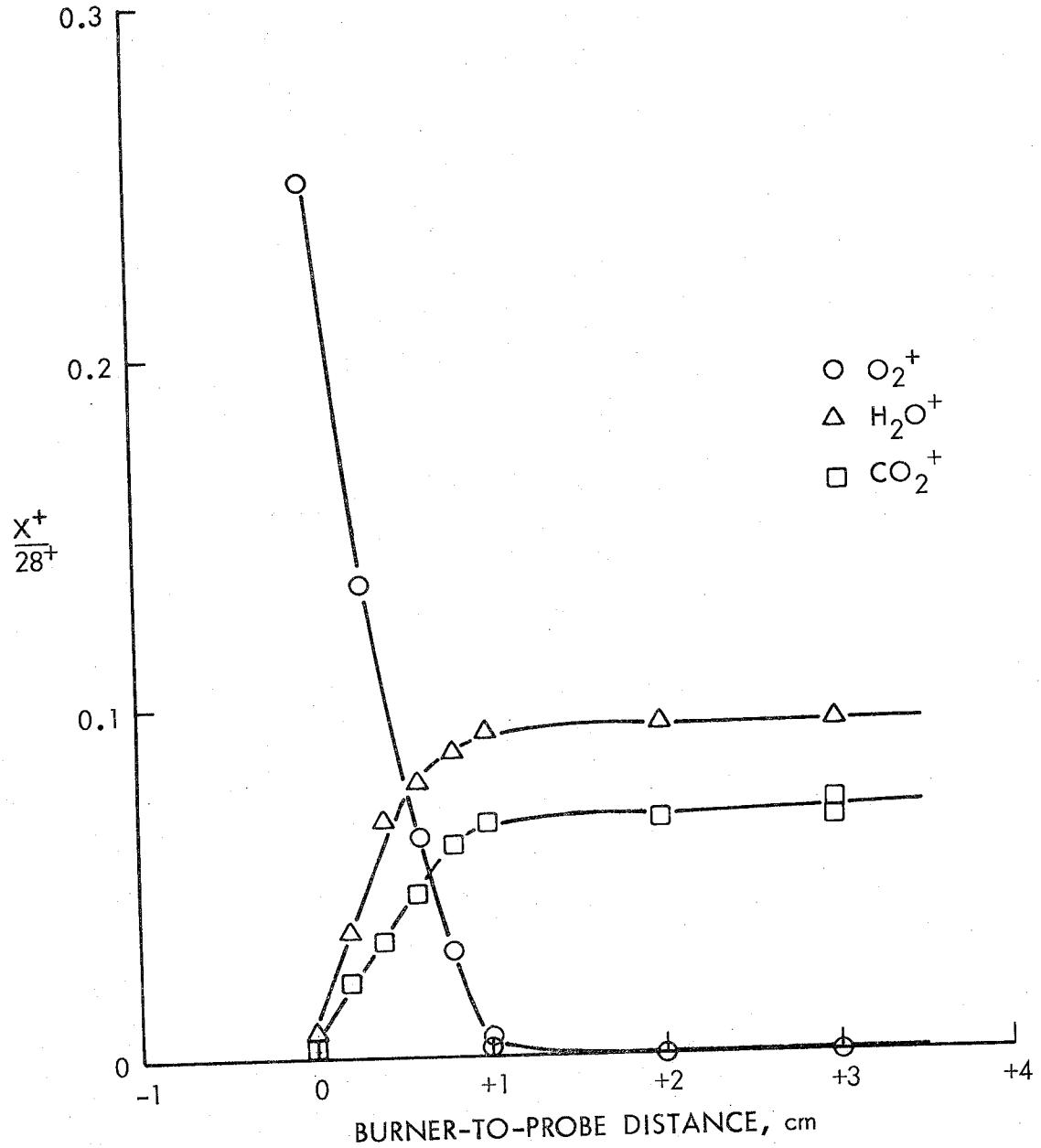

Figure 42 - Major Species Profiles in a 243 mg/liter Coal-Air Flame

A number of ions suspected of arising from pollutant species or precursors, were briefly measured in connection with some of the runs in Table 6. Data are shown in Figures 43 to 46. Ions followed, and their presumed neutral precursors, are shown in Table 7. Extensive tests have not been carried out to be absolutely certain of these assignments of modulated beam signals, but the potential for studying detailed pollutant formation and destruction kinetics is apparent.

B. Final, Quantitative Series of Coal-Air Flame Profile Measurements

Based on the preliminary results, we arrived at a final series of coal-air flame experiments to complete the study. The flames chosen involved 10 to 20 μ coal in rich and lean flames, on cooled and uncooled burners and on 6.3- and 12.6-cm diameter burners. A rich, 10 to 20 μ coal, 6.3-cm diameter flame was sampled with and without the addition of dry powder and gaseous inhibitors. Each of the flames described was sampled mass spectrometrically and for several flames solids were collected for proximate and scanning electron microscope analysis, gas samples collected for gas chromatographic analysis and thermocouple temperatures measured in the flame gases.

1. Gaseous species profiles: During this final series of flame sampling experiments, an attempt was made to calibrate the quadrupole mass spectrometer for H_2O, O_2, and CO_2 relative to N_2 by the use of the burnt gas region of lean, CH_4-air flames. We likewise measured species profiles through a given CH_4-air flame using several sonic-orifice sampling configurations to assess qualitatively the probe-flame interference with the 30 mil orifice. A series of mass spectrometer and gas chromatograph analyses were made on several coal-air flames, with the chromatography being used to measure pyrolysis products and CO. These results are presented below.

a. Effect of probe configuration on flame reaction zone species profiles: One of the lean CH_4-air flames used to calibrate the quadrupole was probed with several orifice and expansion configurations to determine first-order effects on species profiles. A 0.6 equivalence ratio CH_4-air flame was burned on an uncooled 1-in. diameter copper burner with a smoothing screen across the mouth. The resulting flame was slightly waffled and looked not unlike the coal-air flames on the honeycomb burner.

Profiles taken with orifice configurations are shown in Figures 47 through 50. Distance is measured from the burner screen. All orifices are water-cooled spun-metal, 90-degree cones, with the orifice drilled in the apex. The cones are soldered to the massive, flat, water-cooled holding plates used in the coal studies and against which the flames impinge.

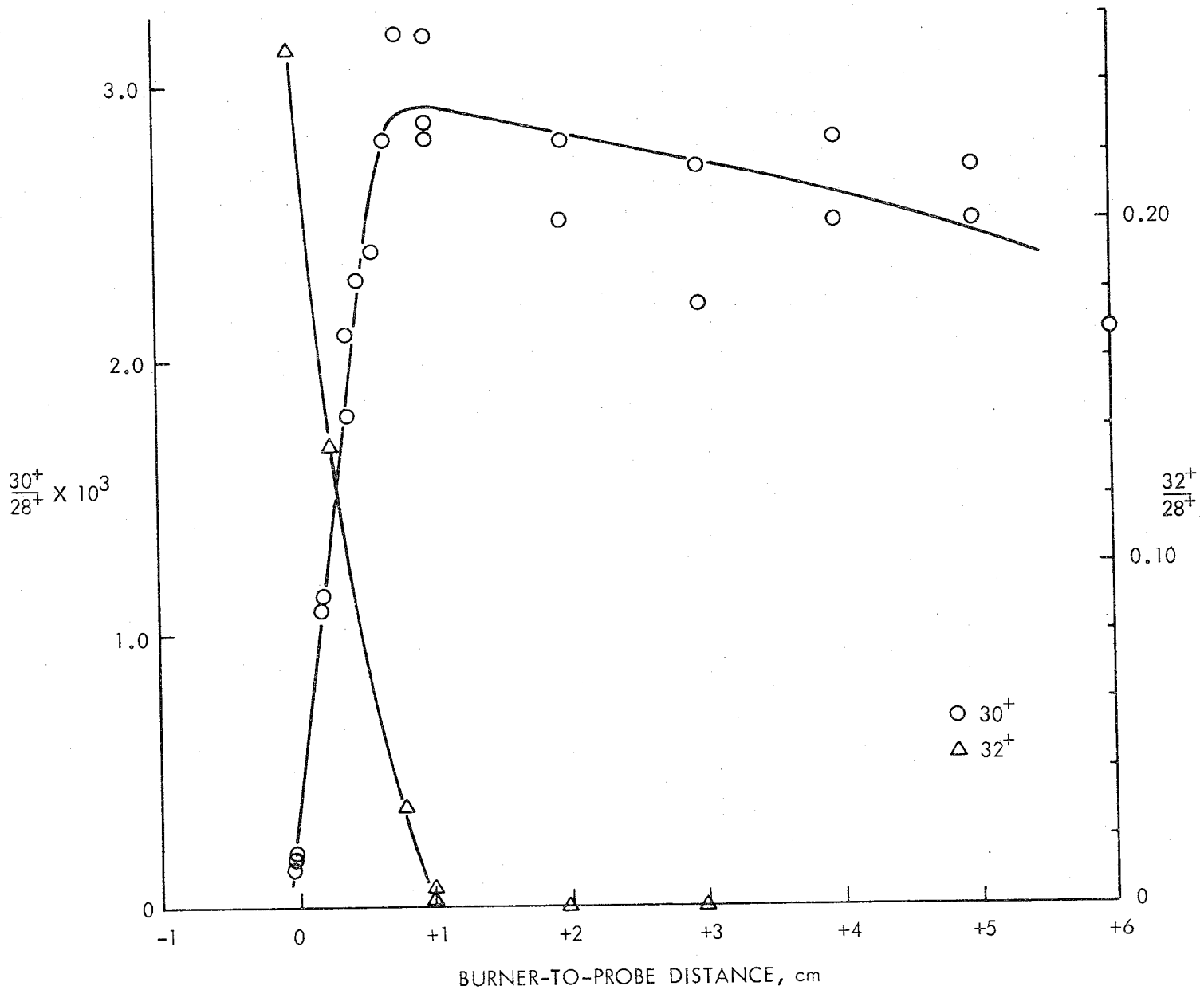

Figure 43 - Profile of NO Through a 243 mg/liter Coal-Air Flame. (See Figure 42 for stable species profiles.)

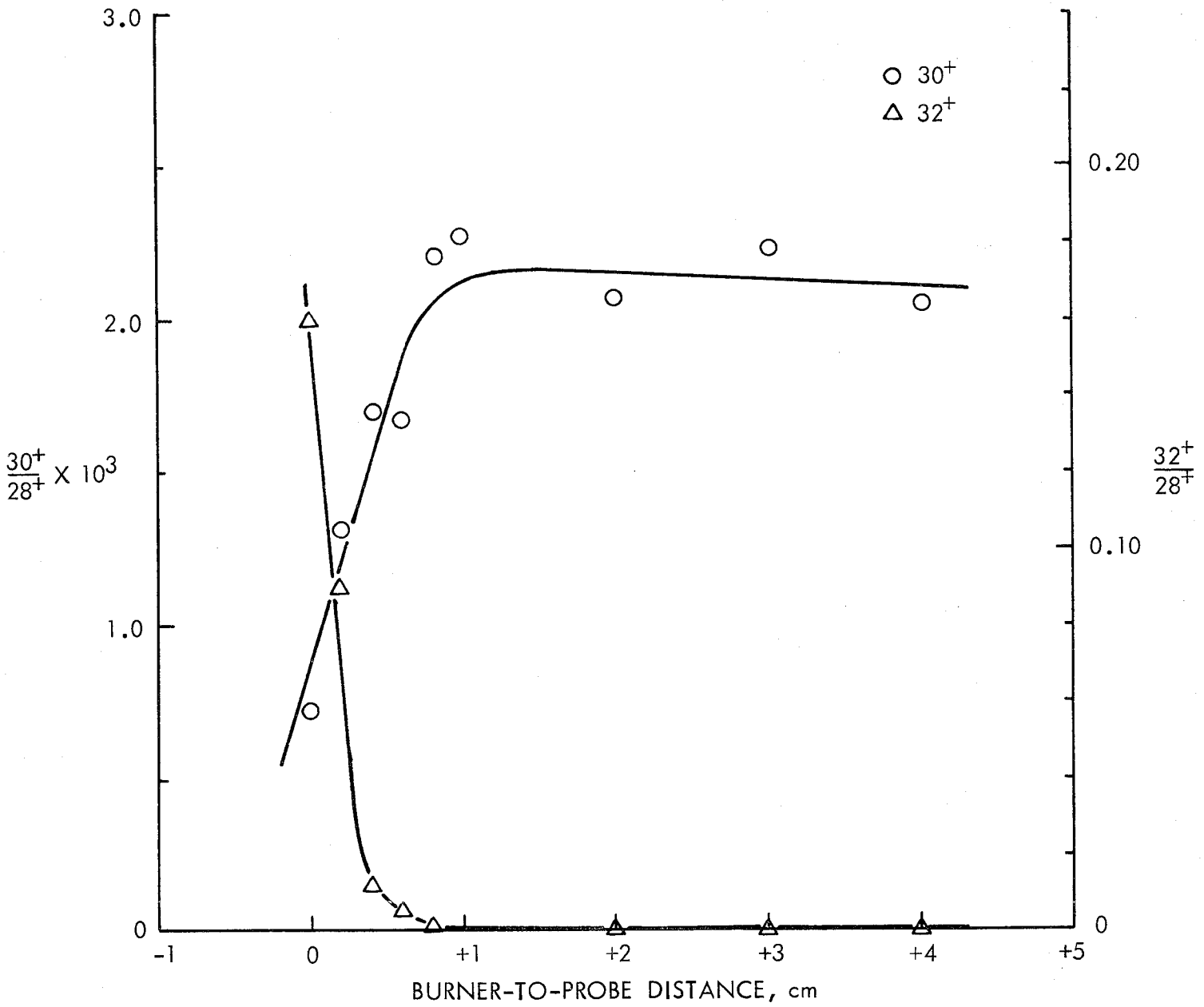

Figure 44 - Profile of NO and O_2 Through a 208 mg/liter Coal-Air Flame

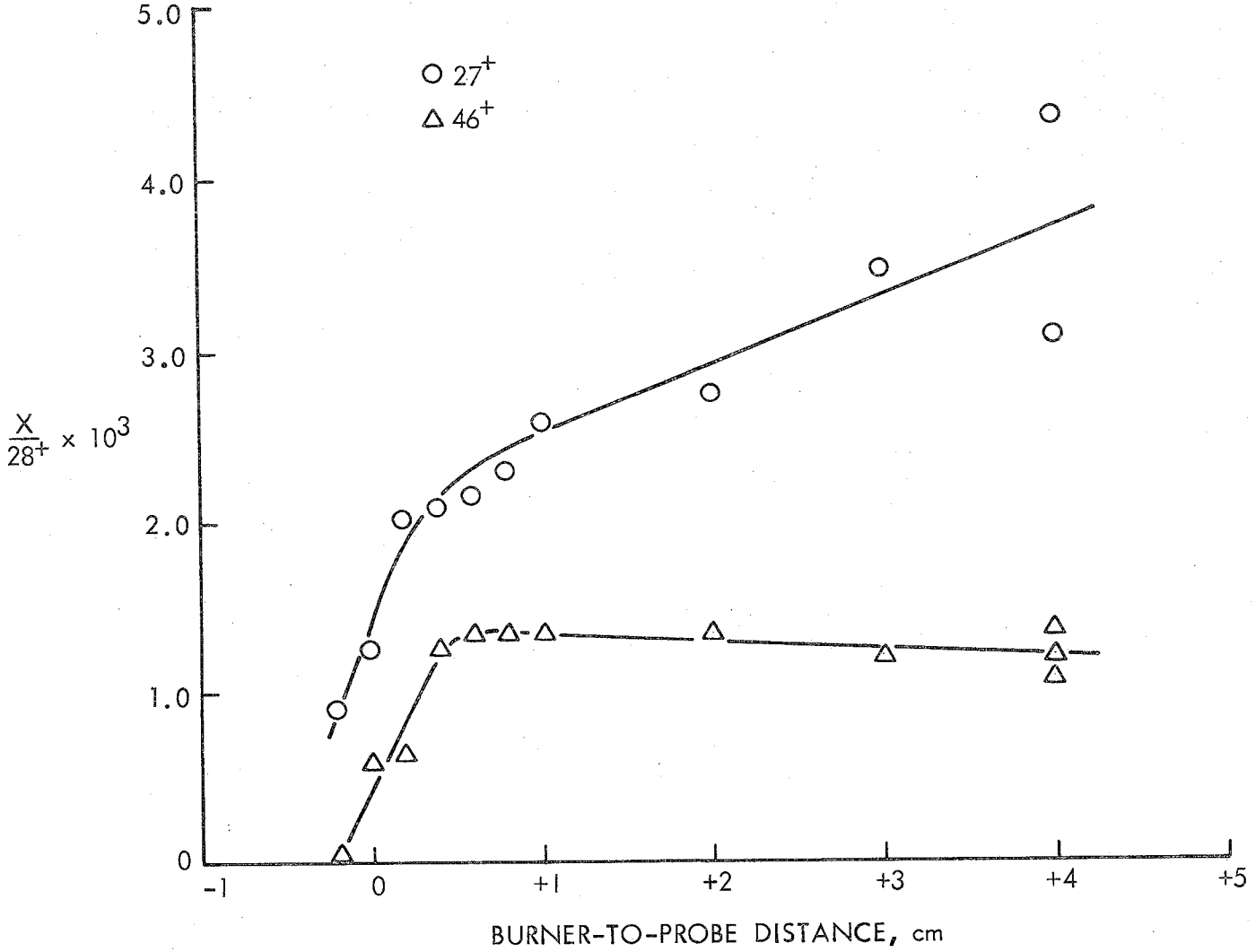

Figure 45 - Profile of 27^+ and 46^+ Through a 165 mg/liter Coal-Air Flame. (See Figure 47 for the CO_2 profile in this flame.)

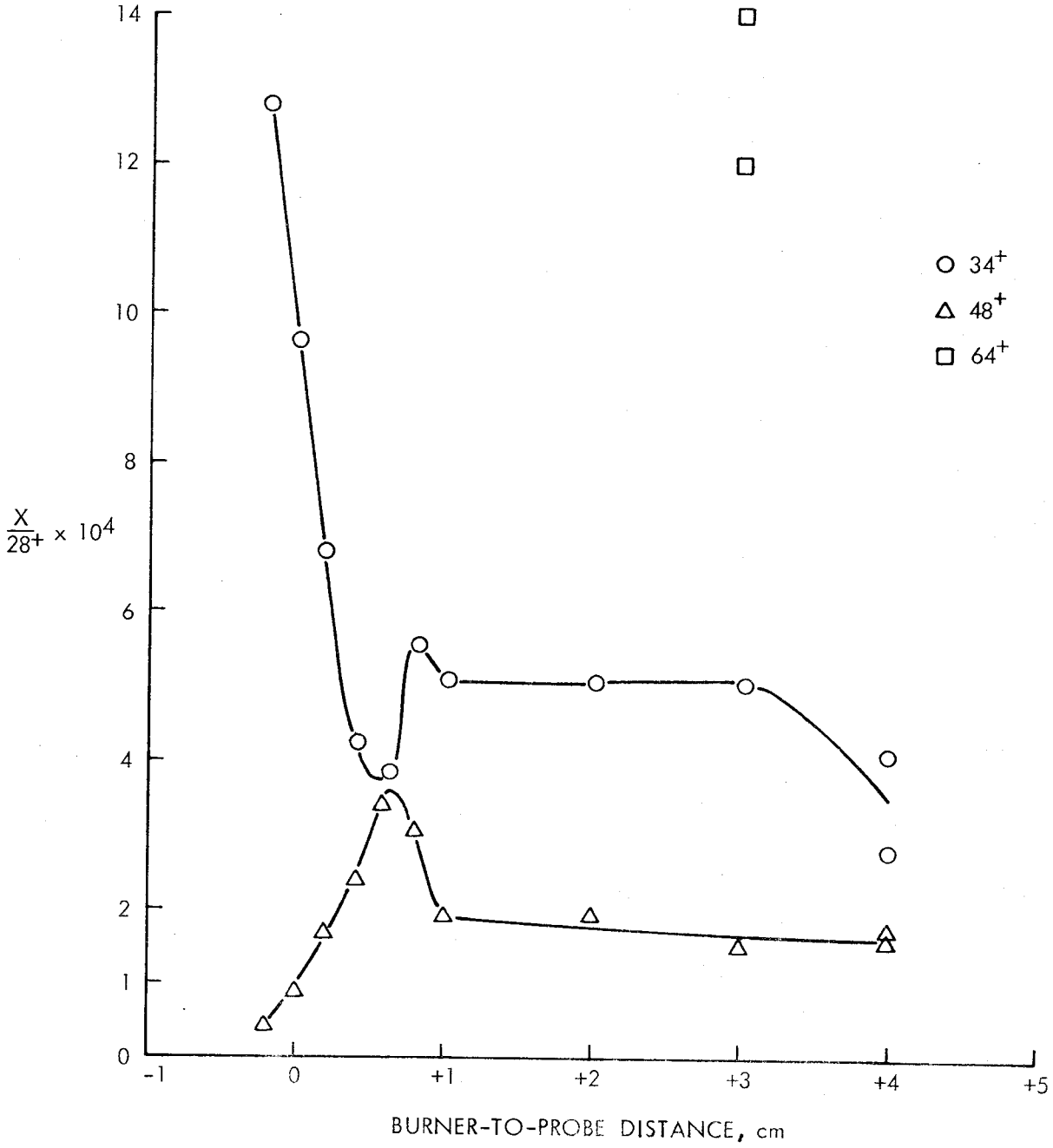

Figure 46 - Profiles of Sulfur Species in a 165 mg/liter Coal-Air Flame. The 34^+ peak is dominated by a O_2 isotope contribution early in the flame.

TABLE 7

POSITIVE IONS, AND PRESUMED PRECURSORS, FOR POLLUTANT SPECIES MEASURED IN COAL-AIR FLAMES

Positive Ion Observed	Presumed Precursor	Data Given In
26	C_2H_2, CN or HCN	Figure 49
27	HCN	Figures 49, 60
30	NO	Figures 58, 59
46	NO_2	Figure 60
34	H_2S	Figure 61
48	SO	Figure 61
64	SO_2	Figure 61

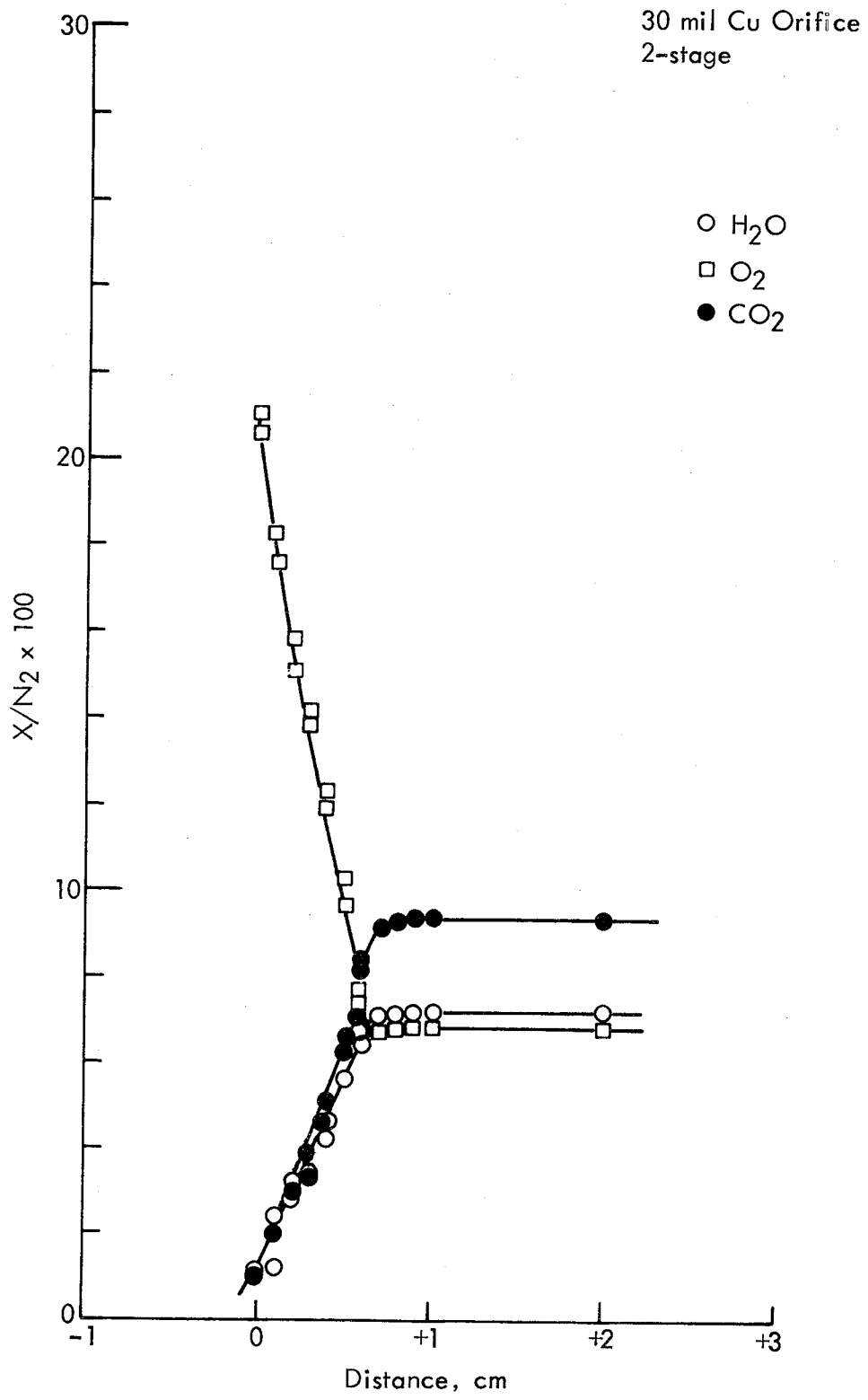

Figure 47 - Mass Spectrometer Profiles Through a Flat, 0.6 Equivalence Ratio CH_4-Air Flame. This sampling configuration was identical to that used with the coal-air flames.

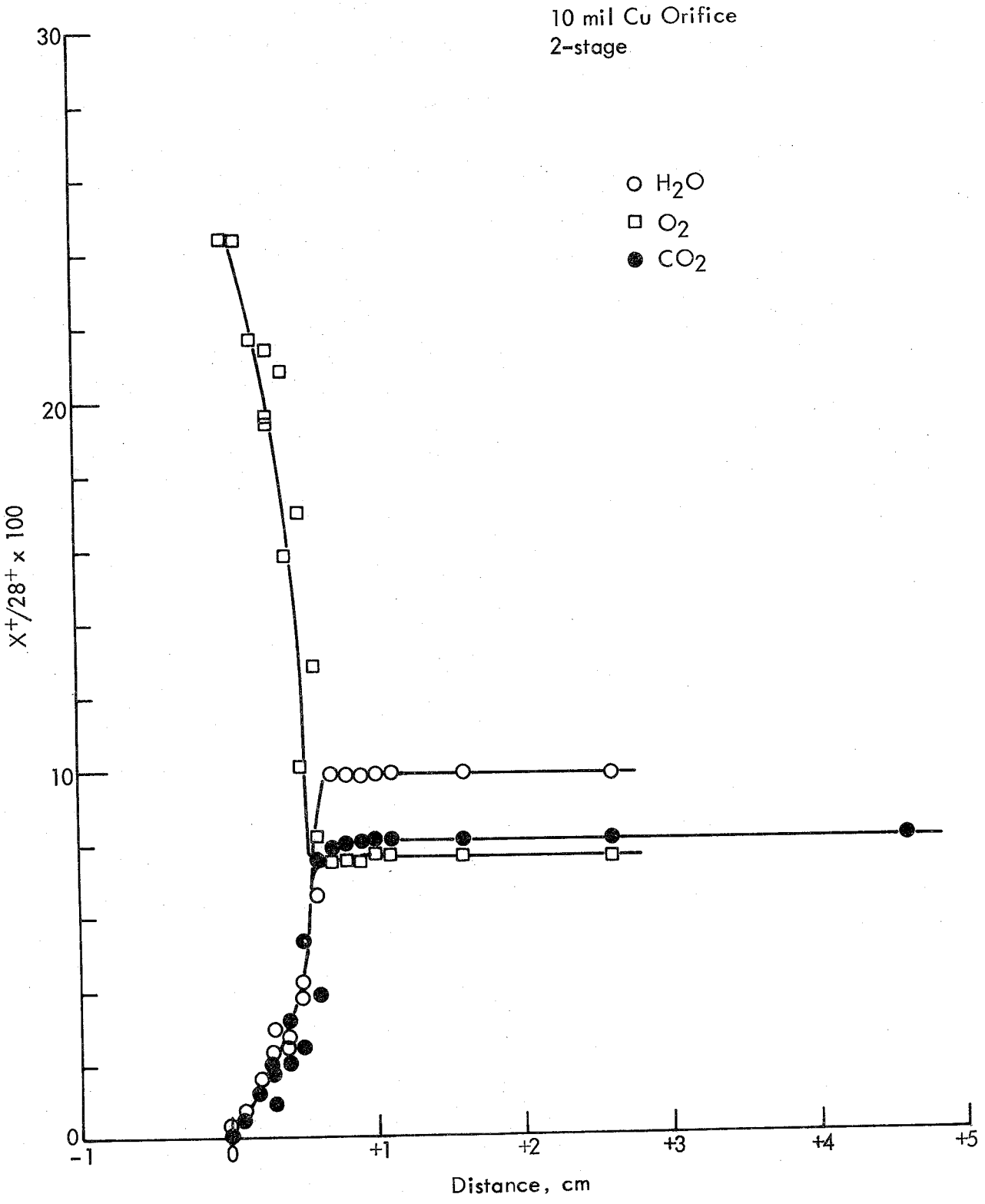

Figure 48 - Mass Spectrometer Profiles Through the Flame of Figure 47 but With a 10-mil, Two-Stage Orifice Expansion

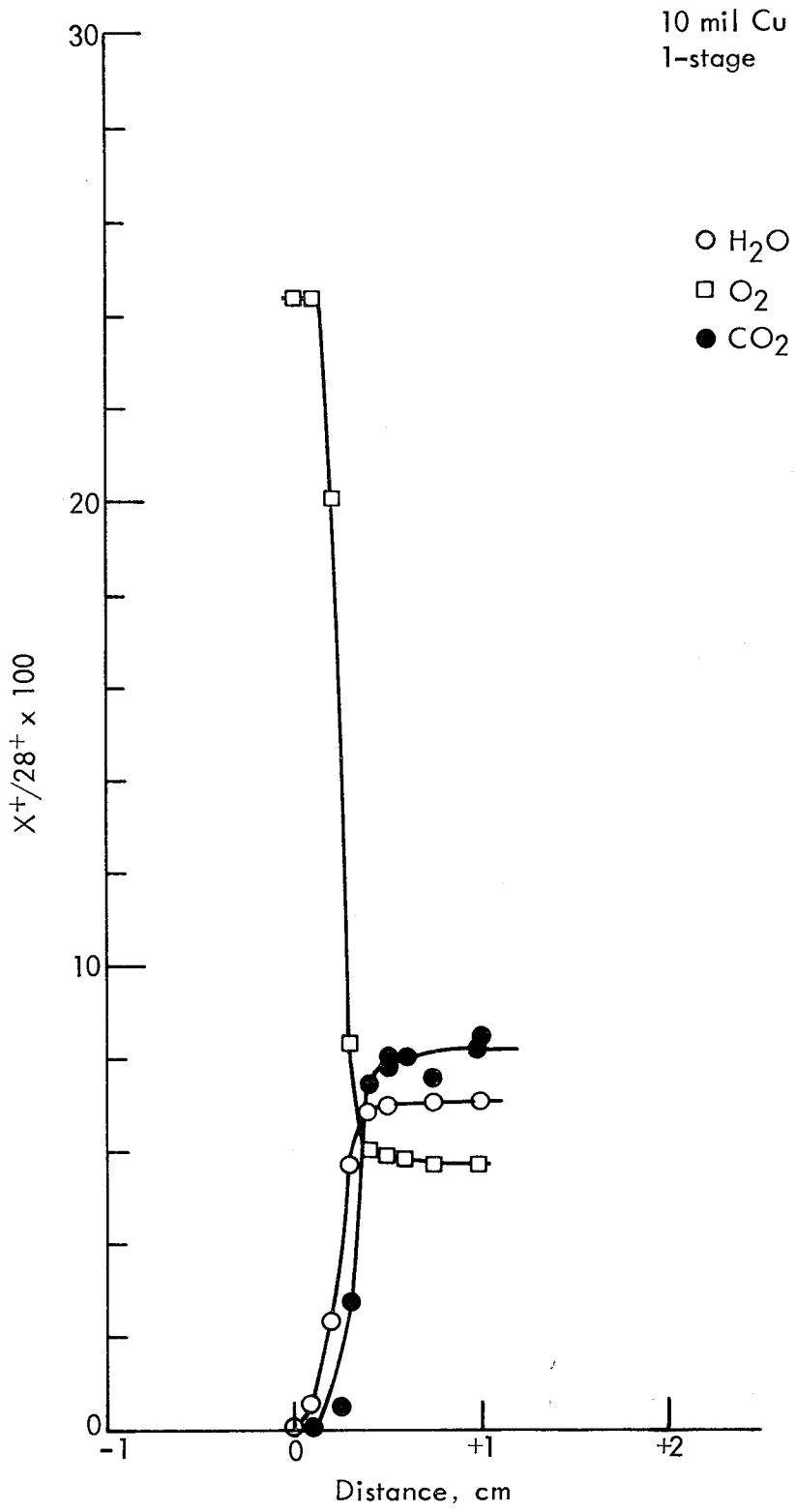

Figure 49 - Mass Spectrometer Profiles Through the Flame of Figure 47 but With a Single-Stage, Free-Jet Expansion to Molecular Flow

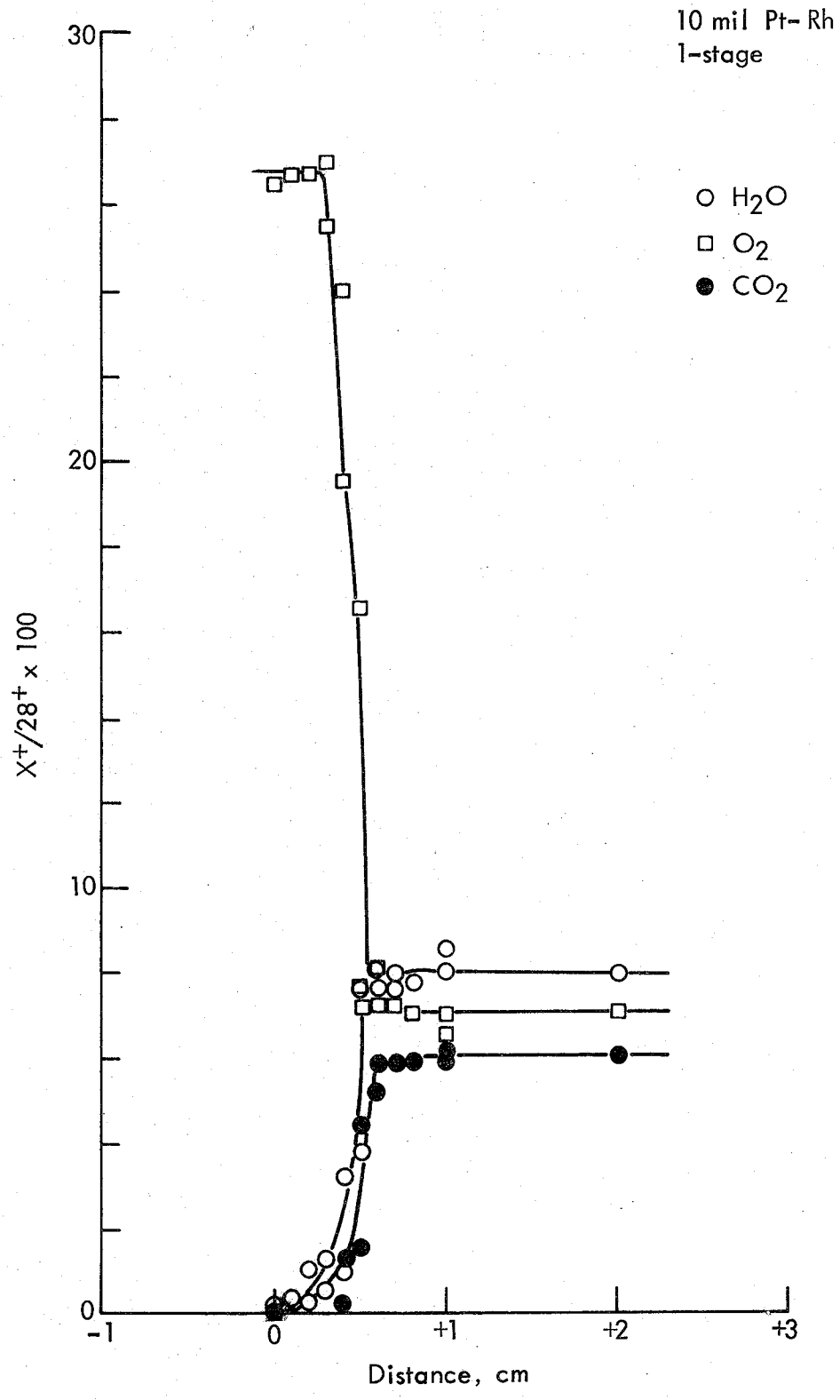

Figure 50 - Same Conditions as Figure 49 but a Pt-Rh Orifice Instead of Copper

In Figures 47 and 48 a two-stage expansion occurred before molecular flow was achieved. In Figures 49 and 50, expansion was by free-jet to molecular flow in one stage. In all cases the initial orifice involved sonic flow.

The notable facts from Figures 47 through 50 are that the 10 mil orifice results in a narrower apparent reaction zone width than the 30 mil orifice. The width of the reaction from the 30 mil, two-stage sampling is of the same order ($\sim$ 5 mm) as that observed in many of the coal-air flames. Since the true reaction zone width for the 1-atmosphere flame is considerably narrower than this, it might be argued that we are probably observing too broad an apparent reaction zone width in the coal-air flames. (The discrepancies in $O_2/H_2O/CO_2$ ratios among Figures 47 through 50 have not been explained.)

b. Calibration of the molecular beam-mass spectrometer sampling system: In order to make accurate measurements of species ratios in coal flames by mass spectrometry, it is necessary to calibrate for sampling orifice effects, mass separation in the molecular beam, relative ionization efficiencies, ion separation efficiencies, and electron multiplier efficiencies. These corrections were made in one operation on a day-to-day basis by sampling from flames of known equilibrium composition, containing the species of interest in coal flames, and having temperatures close to those in the coal flames. In Table 8 are listed the adiabatic flame temperatures and the theoretical equilibrium values of CO_2/N_2, O_2/N_2, and H_2O/N_2 for the three calibration flames used.

The burner used for the calibration flames consisted of a 1-in. diameter copper tube fitting with a screen and 5/16 in. thick honeycomb for a grid. The inside of the burner was filled with glass beads for mixing and smoothing the flow.

The calibration flames were flat but slightly waffled with reaction zones approximately 5 mm above the grid. In Figures 47 through 50 are profiles from the calibration flames, showing a large, flat, burnt-gas region. All calibration data were taken 1 cm from the flame front and were presumed to represent the equilibrium values.

The calibration procedure that was adopted was to measure daily the CO_2/N_2, O_2/N_2, and H_2O/N_2 ratios from the three flames shown in Table 8, to determine the correction factors to be applied to the coal data. Rather than repeaking the mass spectrometer settings each day for maximum sensitivity, the focusing voltages were monitored with a digital voltmeter and were set to the same values each day. All data were taken with 50 ev ionizing electrons and at a constant electron multiplier voltage.

TABLE 8

THEORETICAL EQUILIBRIUM COMPOSITIONS AND ADIABATIC GAS TEMPERATURES OF CH_4-AIR FLAMES USED FOR CALIBRATION OF MASS SPECTROMETER SAMPLING SYSTEM

Equivalence Ratio[a/]	T (°K)	CO_2/N_2	O_2/N_2	H_2O/N_2
0.5	1477	0.0663	0.132	0.133
0.6	1662	0.0796	0.105	0.159
0.7	1835	0.0929	0.0778	0.185

a/ Equivalence ratio = $\left(\frac{\text{Fuel}}{\text{Air}}\right)_{\text{Actual}} \Big/ \left(\frac{\text{Fuel}}{\text{Air}}\right)_{\text{Stoichiometric}}$

The calibration technique described above revealed that a single correction factor does not apply to all data for each ion. In Figures 51 through 53 are plotted the correction factors that were determined from data taken over the 2-month period during which the mass spectrometer sampling of coal flames was done. Each data point represents an average of values taken from the three calibrating flames. While there is considerable scatter in the data ($\pm$ 10%), there seems to be a clear trend showing that the system sensitivity to CO_2 increased with time and decreased for H_2O and O_2 during the same time.

In addition to the high temperature calibrating points, a room temperature point was provided by the occasional measurement of O_2/N_2 in air. In Figure 54, the correction factors obtained from the room temperature air values of O_2/N_2 are plotted along with the high temperature corrections. This figure suggests that the correction factor changes with temperature.

The procedure adopted to correct the coal data was to apply the high temperature corrections from the straight line in Figures 51 through 53 to all data except at and below the burner surface, where the room temperature correction of 1.1 from Figure 54 was used for O_2/N_2. Direct calibration data in the transition temperature region are not available.

c. Gas chromatography of samples collected from five coal-air flames: Using the same sampling procedures as applied earlier we collected a total of 20 gas samples from four positions for each of five flames. The emphasis was on the early ignition and pyrolysis region of the flame. The results are listed in Table 9 and presented graphically as ratios to N_2 in Figures 55 to 59. Most noteworthy seems to be the small percentages of pyrolysis products very early in the flame and the fact that CO and H_2 are far below equilibrium, but appear to be growing, following oxygen depletion.

d. Direct mass spectrometry of coal-dust air flames: A number of on-line, direct, mass spectrometric analyses were made with coal-air flames on 6.3- and 12.6-cm diameter burners. These included the nominally same five flames for which gas chromatographic results were presented in the last section. The species profiles are presented in Figures 60 through 77. The observed ion ratios have been converted to volume ratios to N_2 using the quadrupole-flame calibration results discussed earlier. In these initial presentations no correction has been made to the 29^+ signal, used to monitor N_2, for contributions from $C^{13}O^+$ either from CO or CO_2.

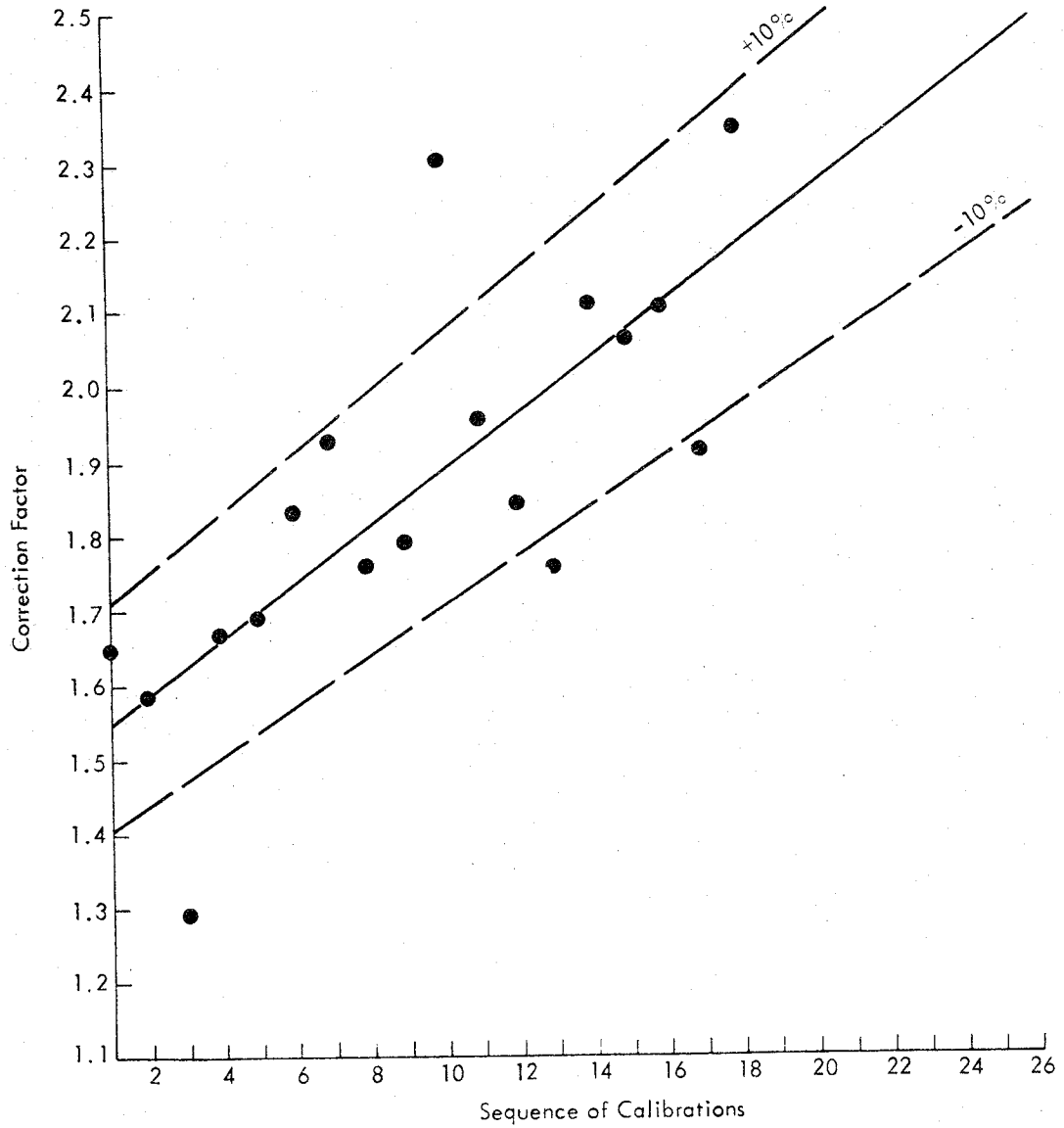

Figure 51 - Correction Factors for H_2O/N_2 Data Taken by Mass Spectrometer During the 2-Month Period of Coal Flame Sampling. Each point represents an average of values obtained from the three CH_4-air calibrating flames.

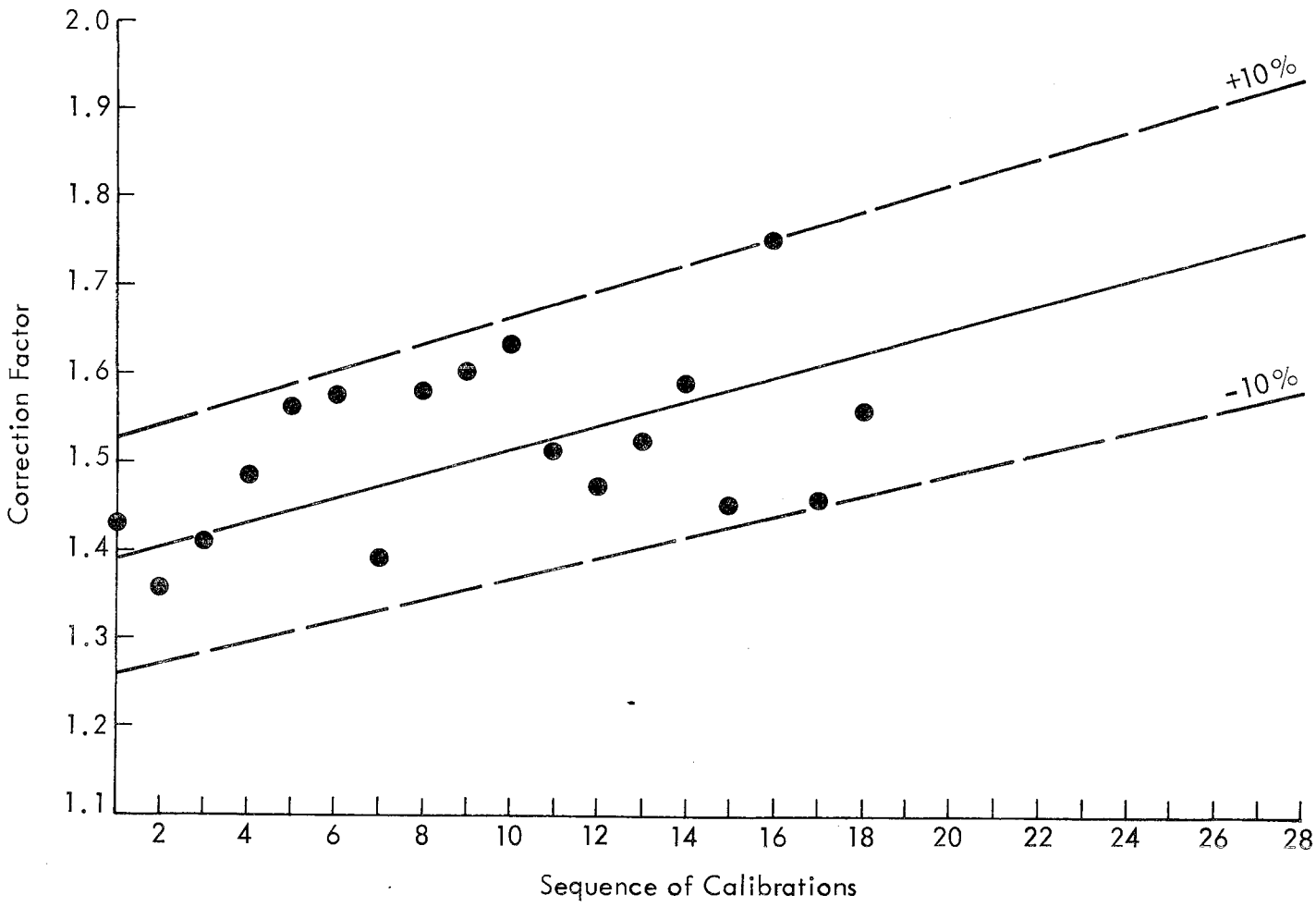

Figure 52 - Correction Factors for O_2/N_2 Data Taken by Mass Spectrometer During the 2-Month Period of Coal Flame Sampling. Each point represents an average of values obtained from the three CH_4-air calibrating flames.

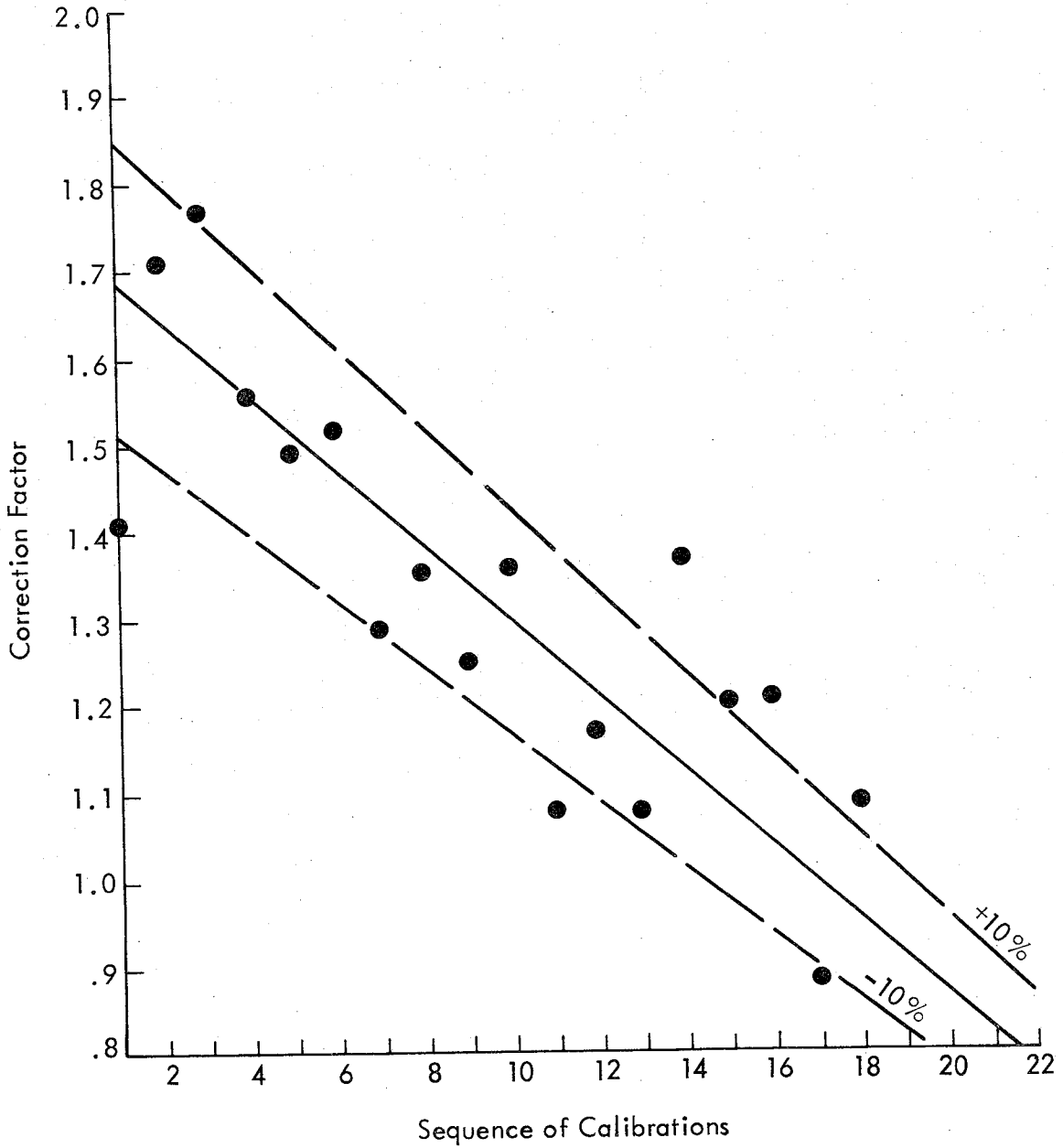

Figure 53 - Correction Factors for CO_2/N_2 Data Taken by Mass Spectrometer During the 2-Month Period of Coal Flame Sampling. Each point represents an average of values obtained from the three CH_4-air calibrating flames.

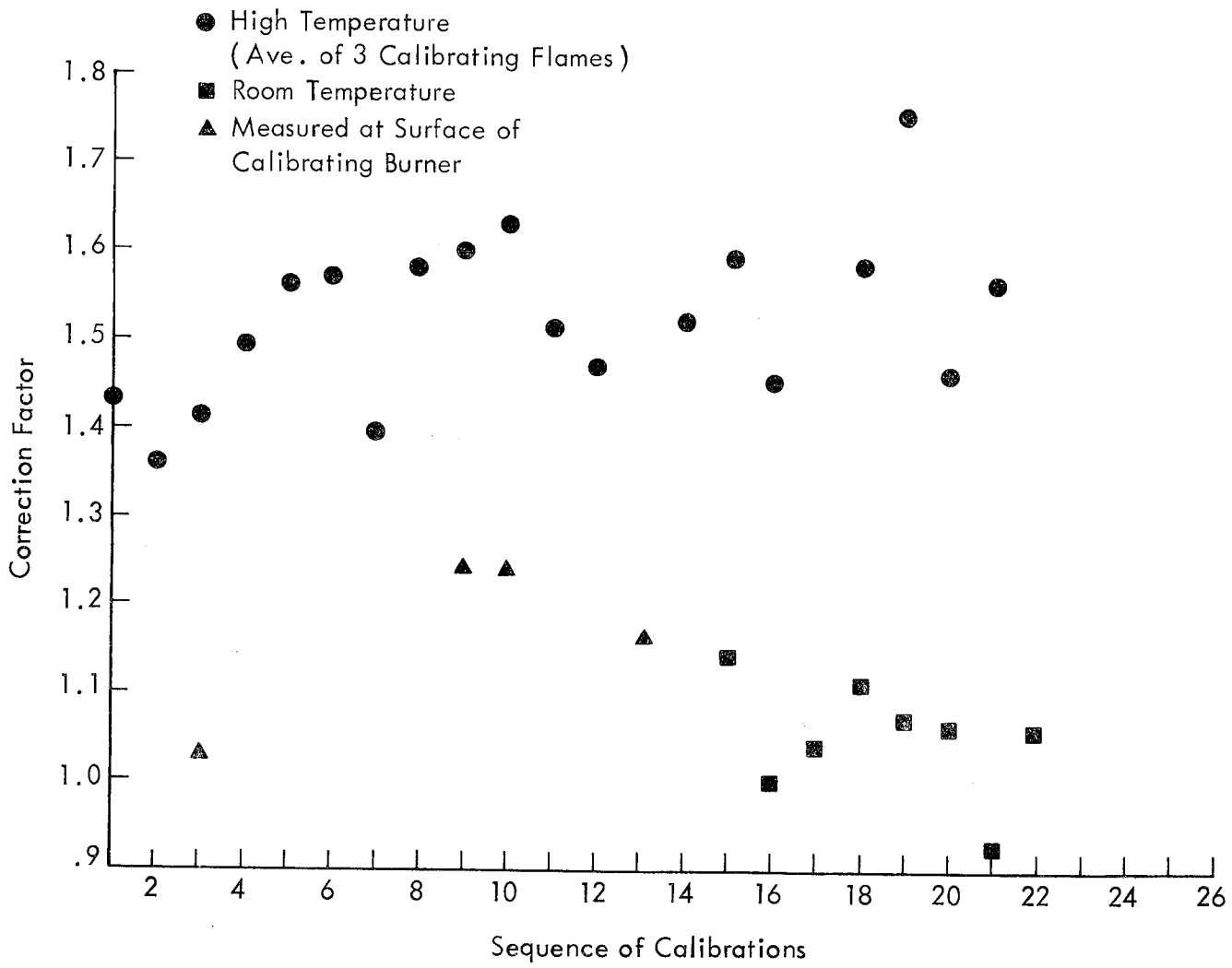

Figure 54 - Correction Factors for O_2/N_2 Data Taken by Mass Spectrometer at Room Temperature and at High Temperature

TABLE 9

GAS CHROMATOGRAPHIC ANALYSIS OF GASES COLLECTED FROM SEVERAL COAL-AIR FLAMES

Distance, cm	Sample No.	O_2	N_2	CO	CO_2	H_2	C_2's	CH_4	Total Volume %	Flame Conditions
0	1	1.11	80.2	4.55	15.7	0.72	0.092	0.114	102.49	Medium,
1/4	2	1.71	77.2	3.37	15.9	0.51	0.003	0.004	98.70	unsieved
1/2	3	8.13	80.0	1.84	8.26	0.18	0.036	0.042	98.49	coal,
1	4	13.2	78.2	0.12	0.17	0.01	0.001	0.001	91.55	215 mg/ℓ
0	5	12.2	78.4	0.15	1.55	0.01	0.003	0.002	92.32	Lean,
1/4	6	7.47	79.6	1.94	9.04	0.16	0.043	0.028	98.28	10 to 20 μ,
1/2	7	1.97	70.7	3.19	14.9	0.34	0.032	0.020	91.15	143 mg/ℓ
1	8	2.52	78.9	0.16	19.4	0.06	0.001	< 0.001	100.90	
0	9	13.2	78.0	0.19	0.21	0.56	0.007	0.007	92.17	Medium,
1/4	10	3.05	78.8	4.18	14.2	0.49	0.092	0.091	100.90	10 to 20 μ,
1/2	11	3.48	80.2	5.20	12.4	0.02	0.147	0.095	101.54	233 mg/ℓ
1	12	1.39	74.9	5.39	14.3	0.66	0.116	0.112	96.87	
0	13	12.2	74.6	0.23	0.16	0.01	0.002	0.006	87.21	Rich,
1/4	14	8.08	77.7	3.31	7.10	0.25	0.071	0.099	96.61	10 to 20 μ,
1/2	15	1.50	76.8	4.71	15.4	0.67	0.128	0.150	99.34	263 mg/ℓ
1	16	9.46	77.0	2.01	4.78	< 0.01	0.051	0.035	93.35	
0	17	11.9	74.6	0.23	1.29	0.02	0.005	0.005	88.05	Rich,
1/4	18	9.89	76.8	1.49	5.10	0.07	0.039	0.033	93.42	10 to 20 μ,
1/2	19	3.28	75.2	5.01	12.4	0.78	0.209	0.189	97.07	263 mg/ℓ
1	20	1.79	73.0	7.77	10.1	1.16	0.304	0.372	94.50	Purple-K added, 6 mg/ℓ

Note: Concentrations given in volume percent. O_2 values include approximately a 1/2% contribution from Argon.

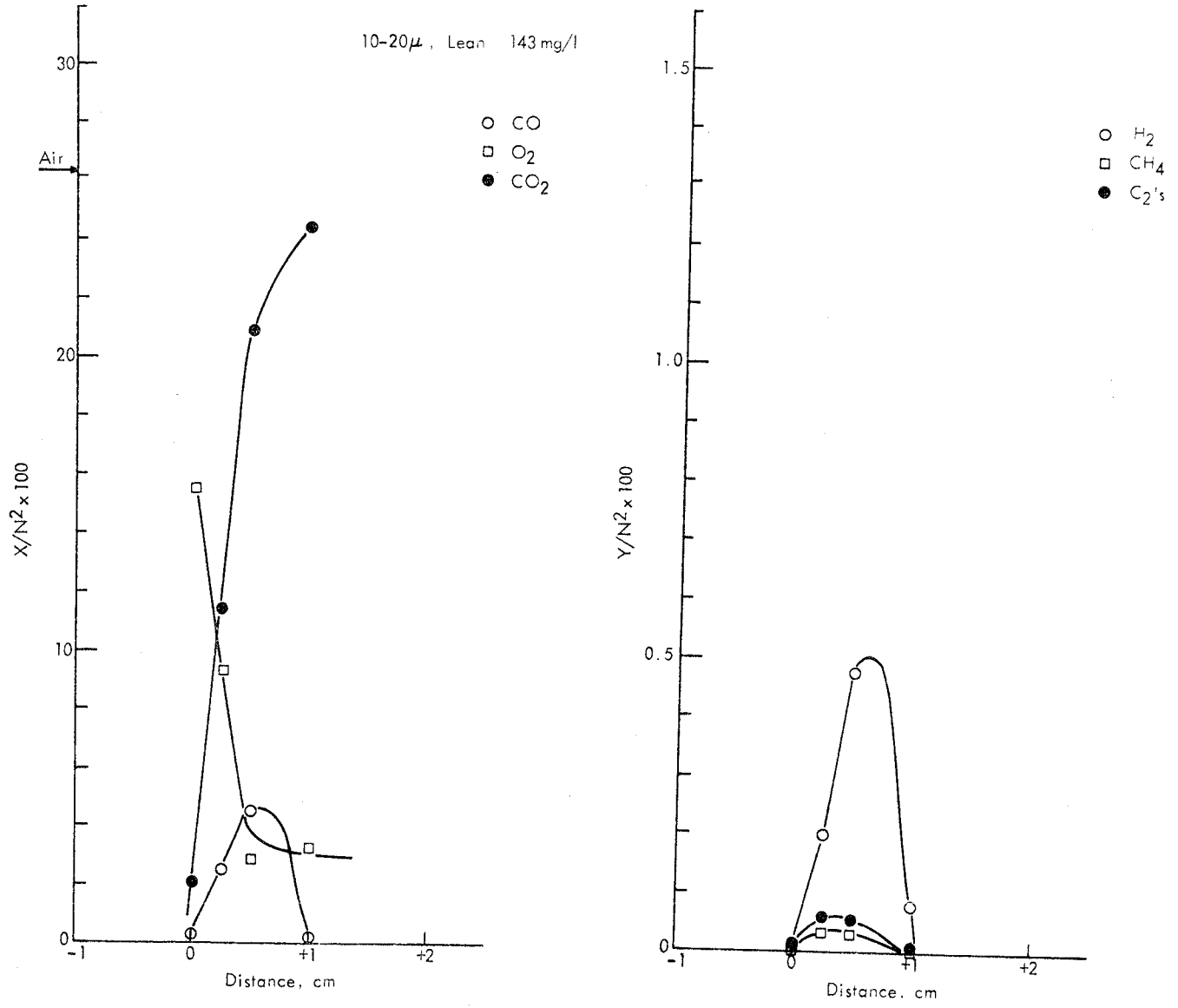

Figure 55 - Results of Gas Chromatographic Analysis of Samples Collected From a Relatively Lean, 10 to 20 μ, Coal-Air Flame

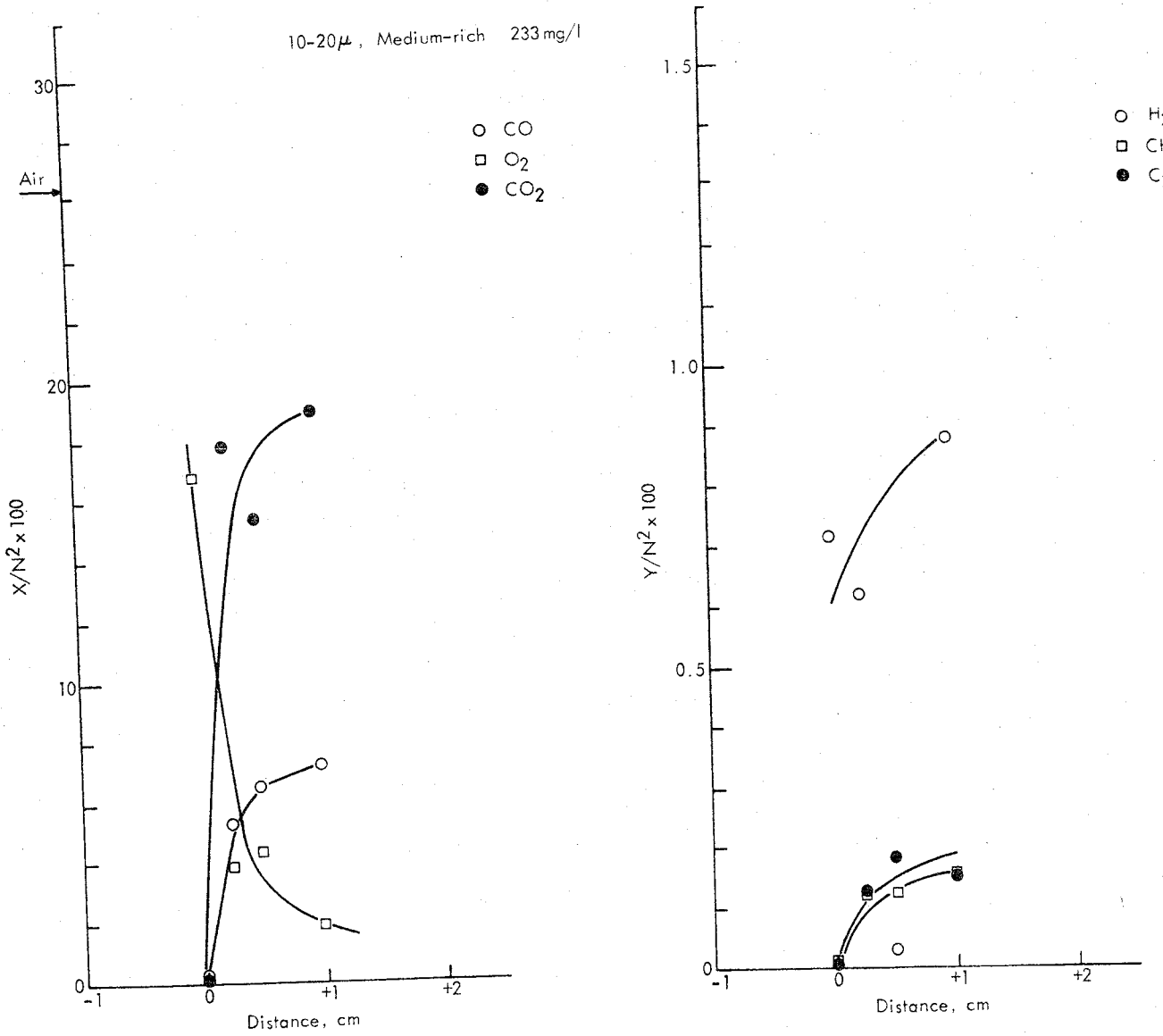

Figure 56 - Results of Gas Chromatographic Analysis of Samples Collected From a Medium, 10 to 20 μ, Coal-Air Flame

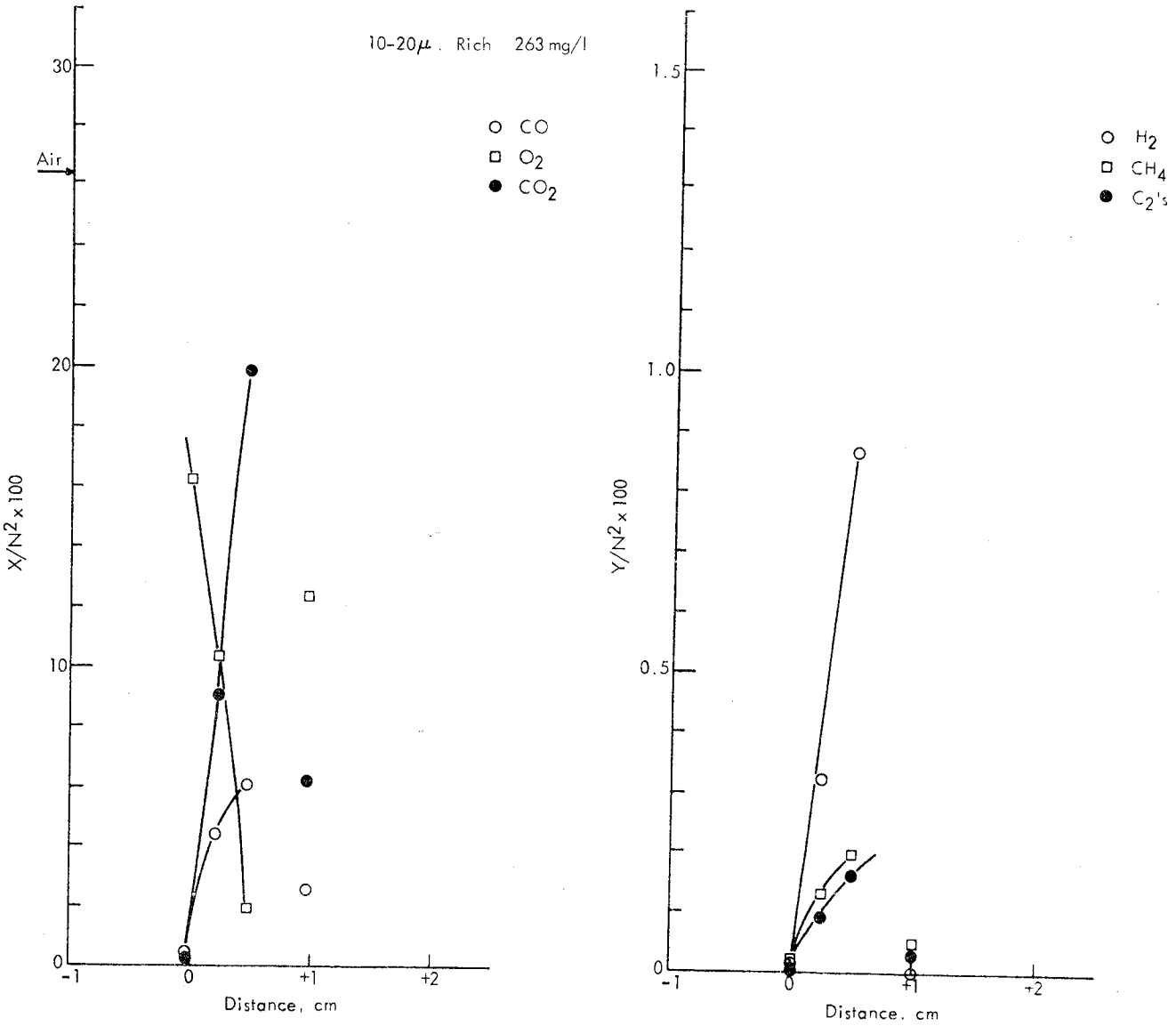

Figure 57 - Results of Gas Chromatographic Analysis of Samples Collected From a Rich, 10 to 20 μ, Coal-Air Flame

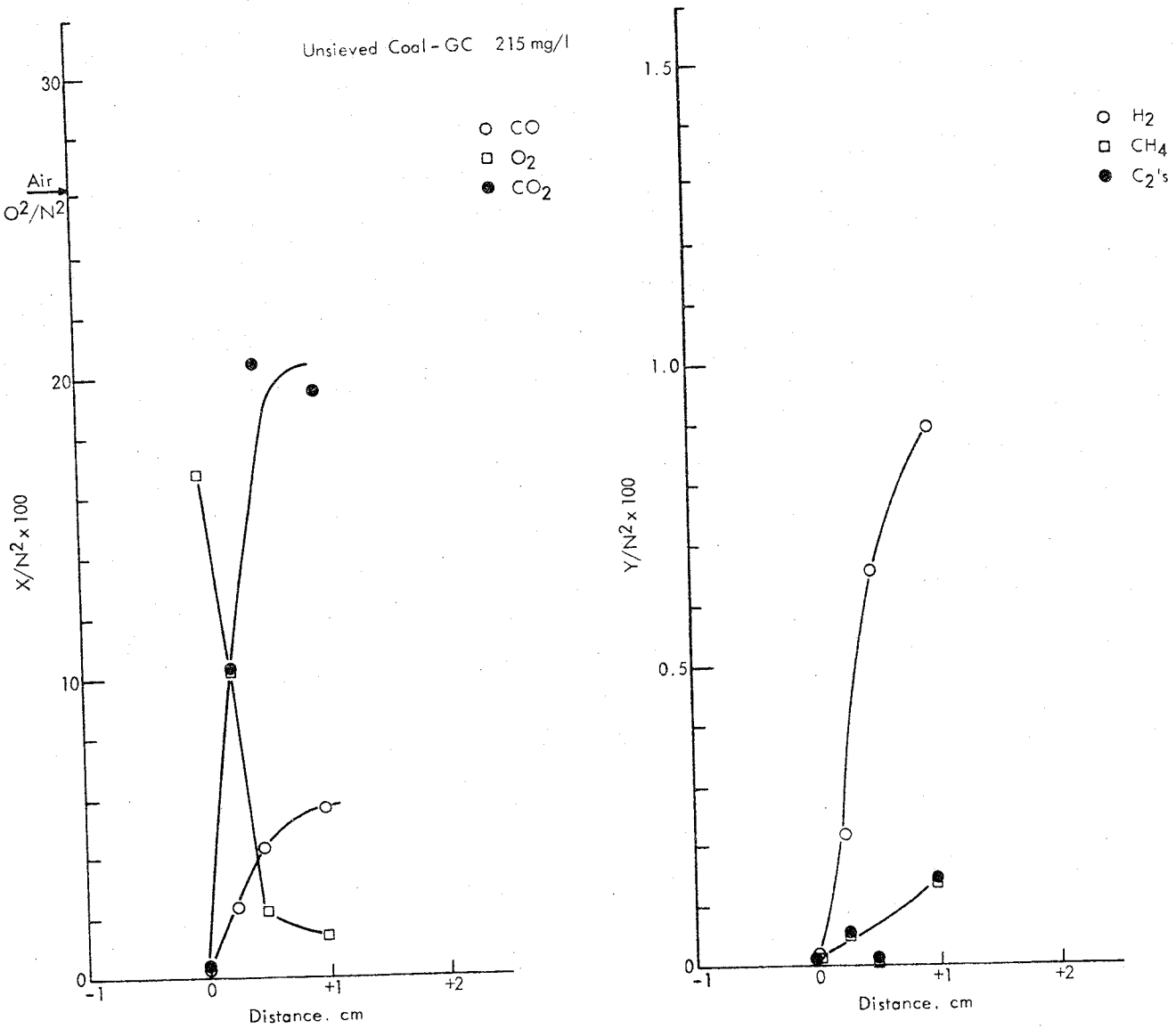

Figure 58 - Results of Gas Chromatographic Analysis of Samples Collected From a Medium, Unsieved, Coal-Air Flame

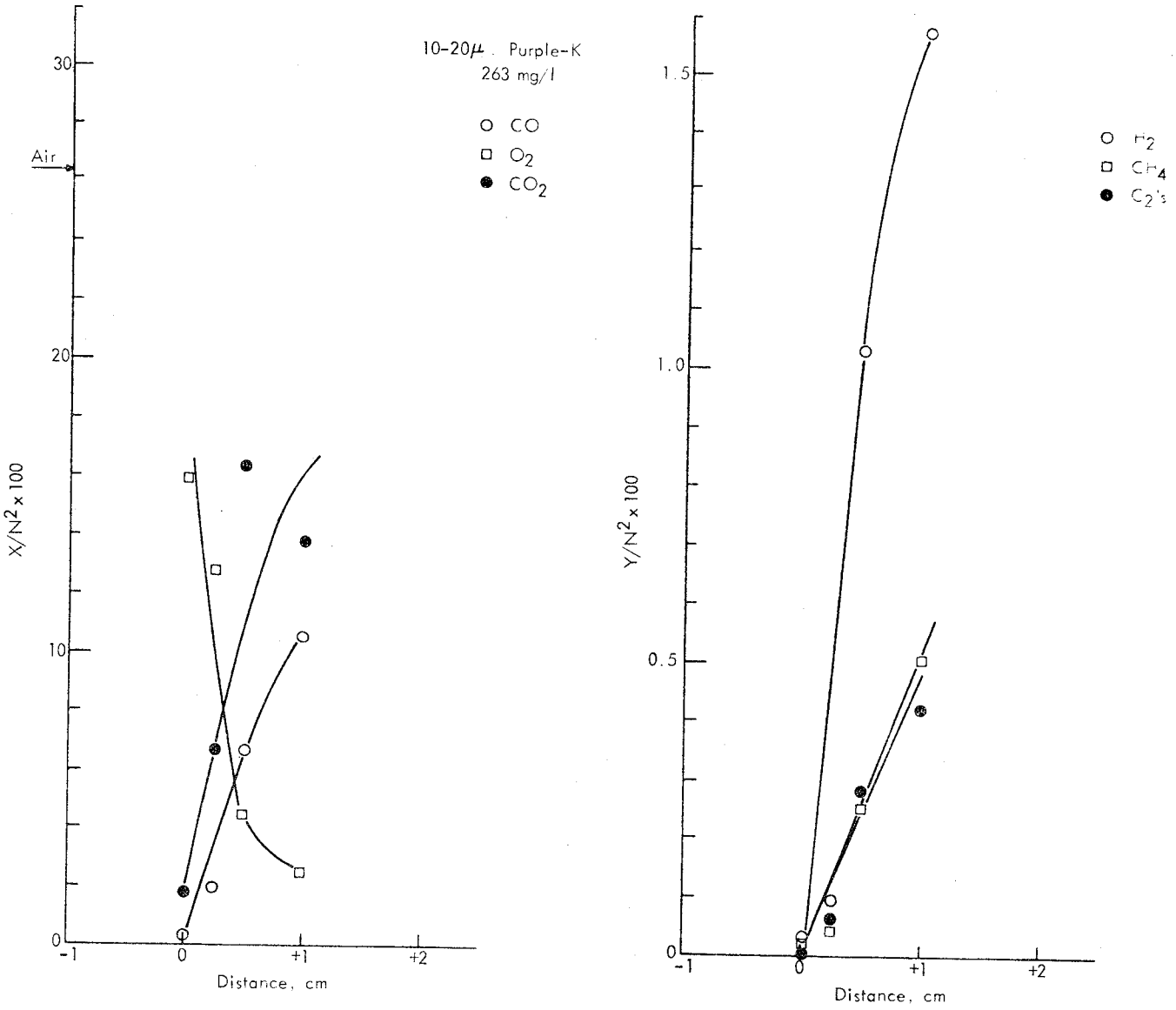

Figure 59 - Results of Gas Chromatographic Analysis of Samples Collected From a Rich, 10 to 20 μ, Coal-Air Flame to Which Purple-K Dry-Powder Inhibitor Had Been Added

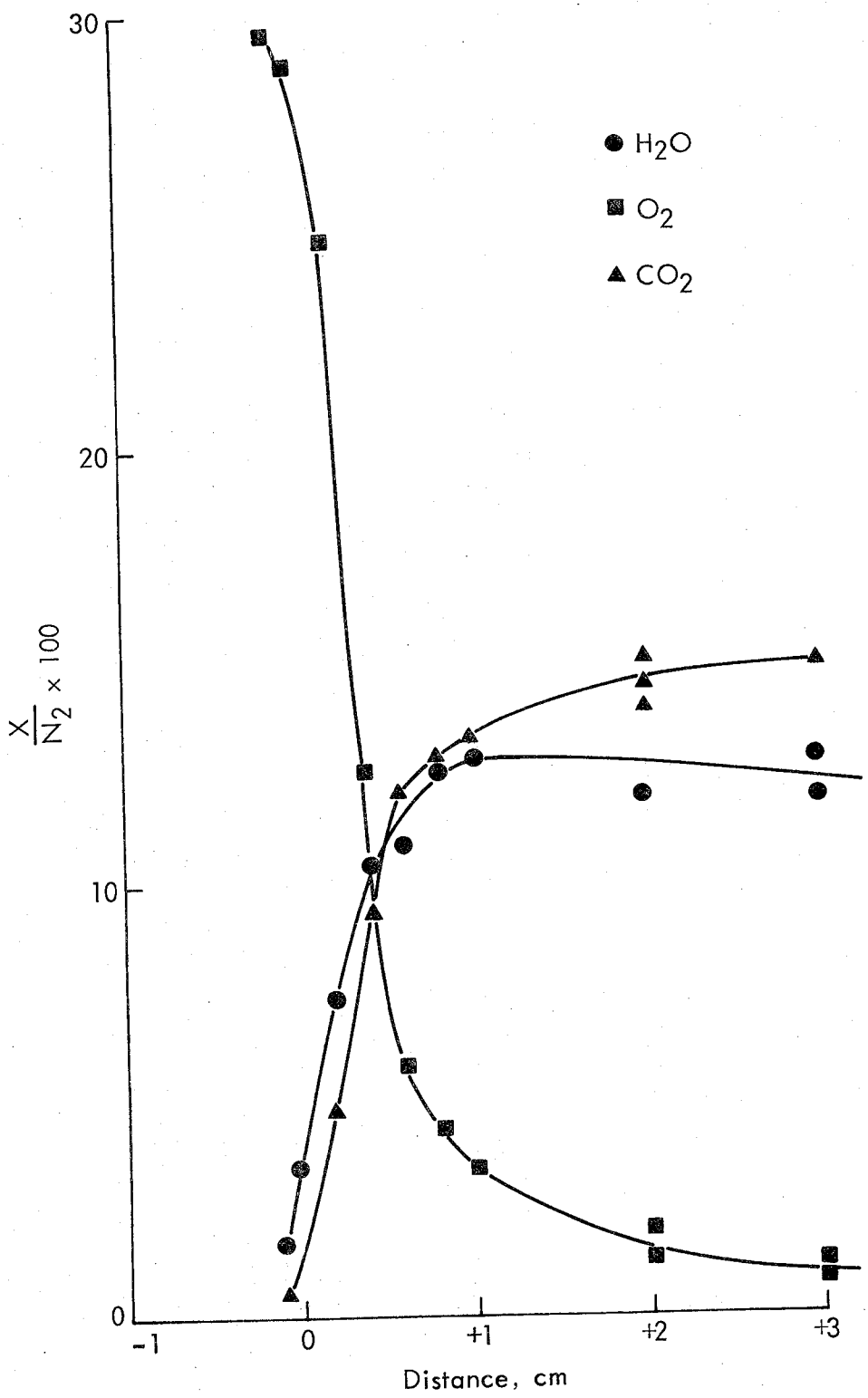

Figure 60 - Calibrated Mass Spectrometer Profiles Through a 10 to 20 μ Coal-Air Flame on a 6.3-cm Diameter Burner. 146 mg/liter.

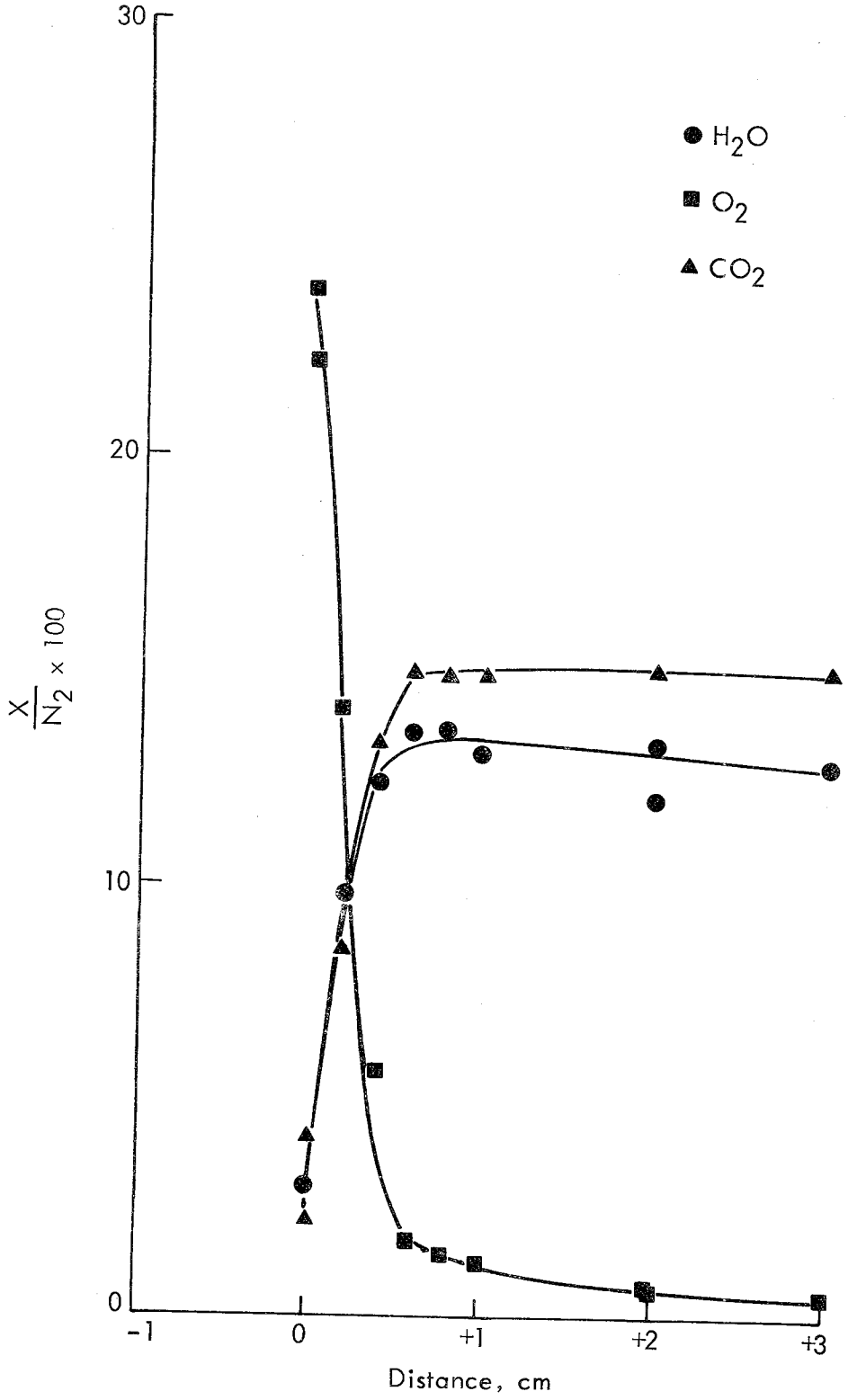

Figure 61 - Calibrated Mass Spectrometer Profiles Through a 10 to 20 μ Coal-Air Flame on a 6.3-cm Diameter Burner. 191 mg/liter.

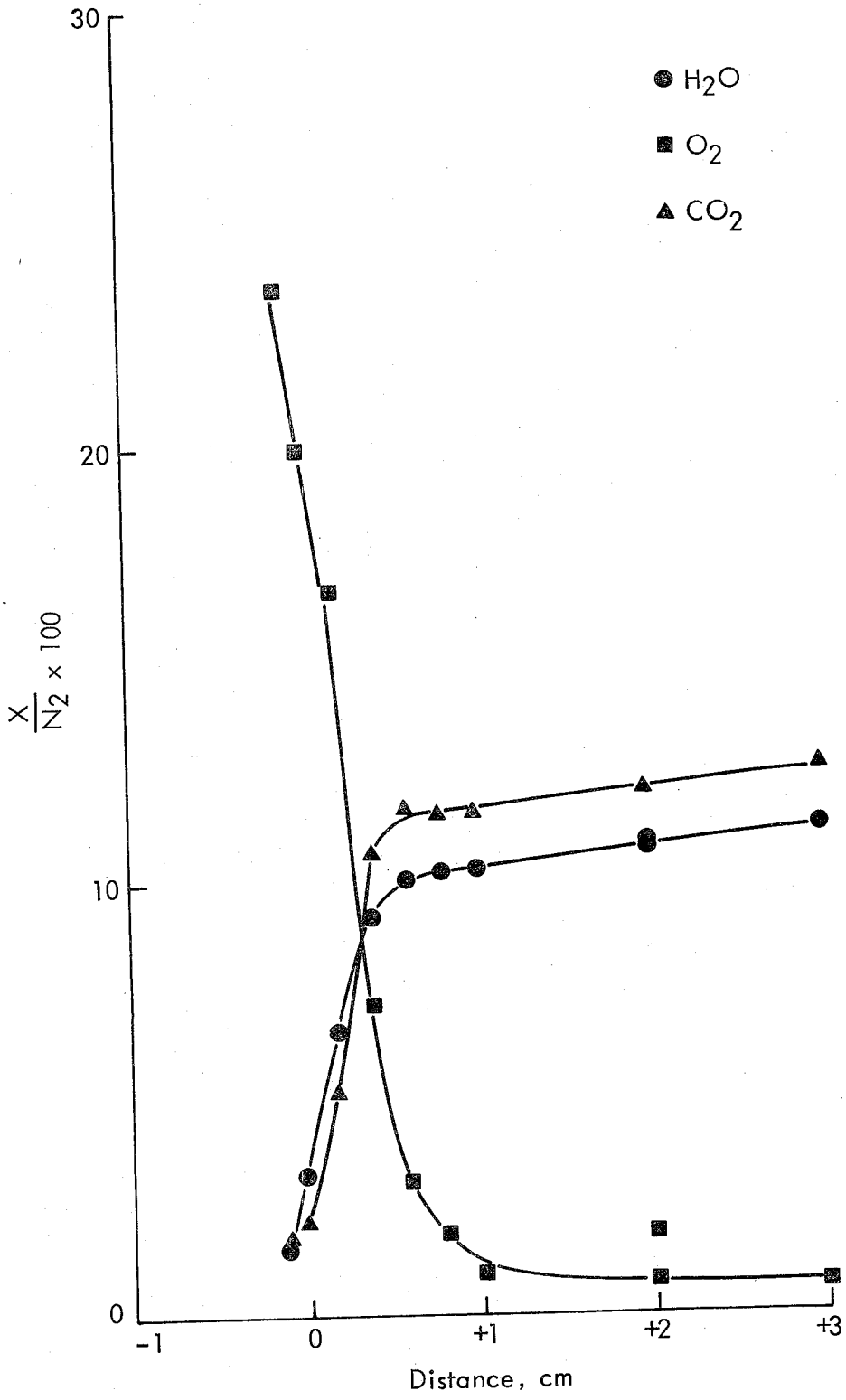

Figure 62 - Calibrated Mass Spectrometer Profiles Through a 10 to 20 μ Coal-Air Flame on a 6.3-cm Diameter Burner. Coal varied from 277 mg/liter to 214 mg/liter.

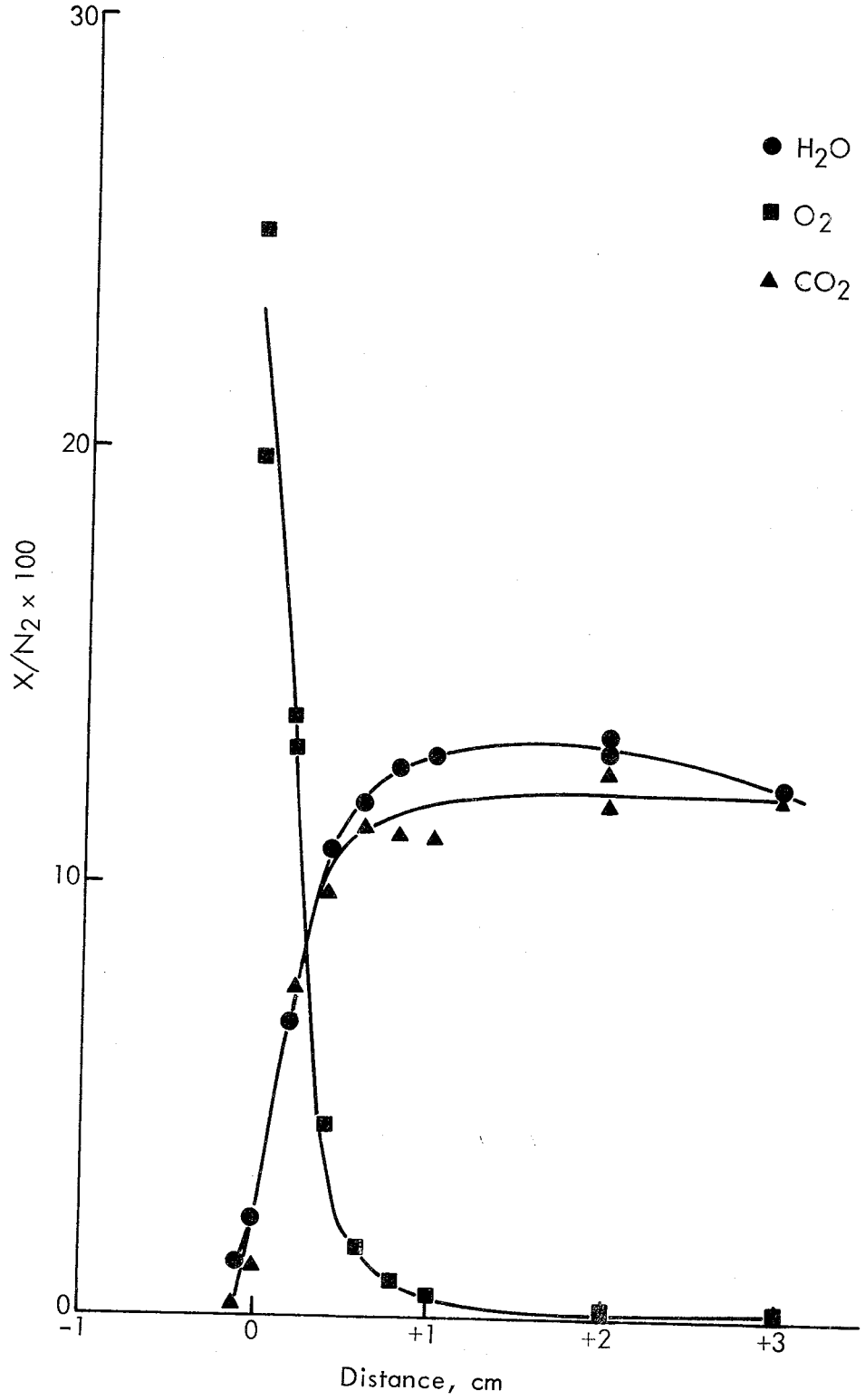

Figure 63 - Calibrated Mass Spectrometer Profiles Through a 10 to 20 μ Coal-Air Flame on a 6.3-cm Diameter Burner With a Copper-Plated Honeycomb Grid. 206 mg/liter.

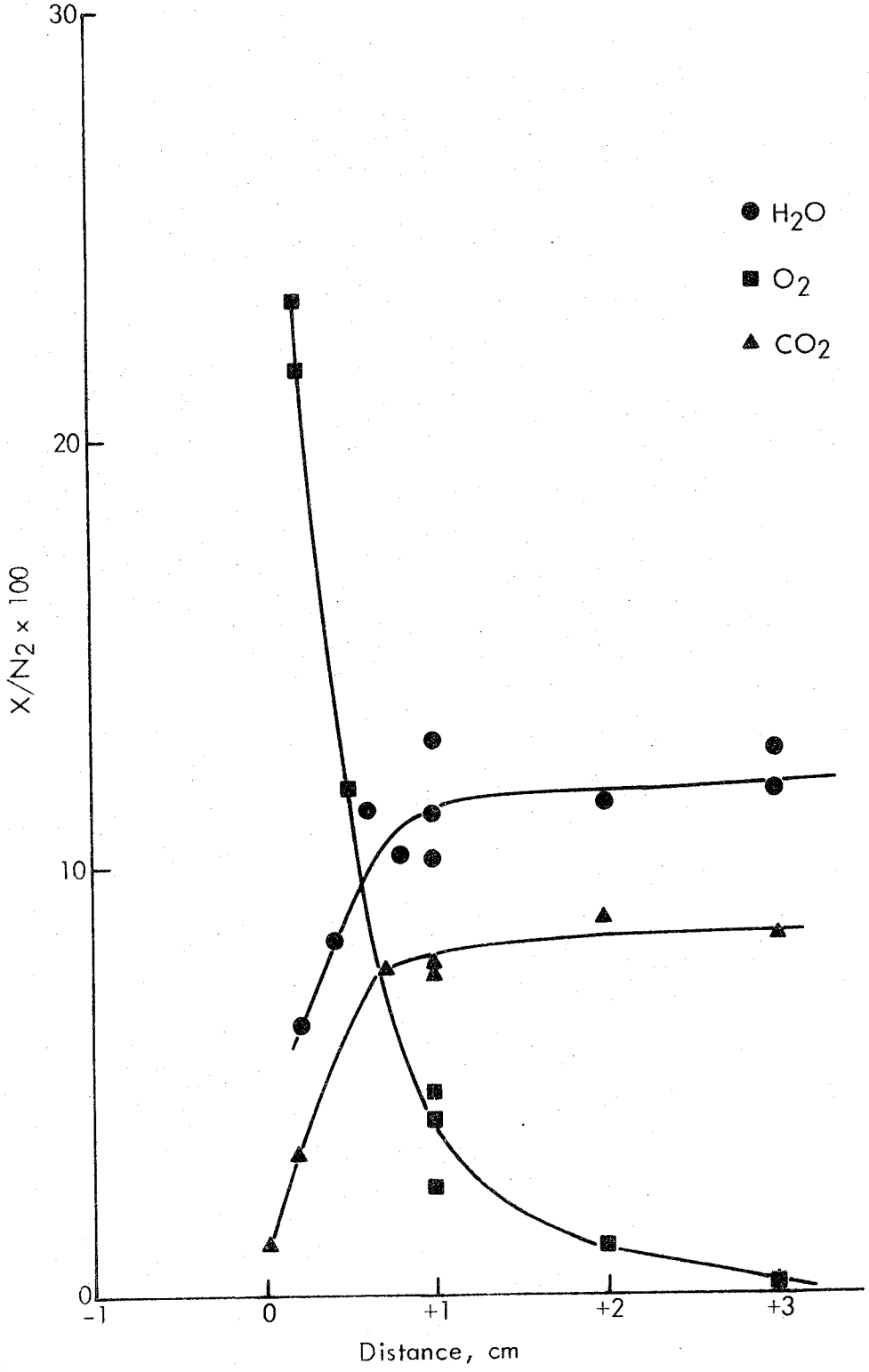

Figure 64 - Calibrated Mass Spectrometer Profiles Through a 10 to 20 μ Coal-Air Flame on a 12.6-cm Diameter Burner. The 12.6-cm Flame was less uniform and stable than 6.3-cm flames and was greatly perturbed by the probe at small distances. 154 mg/liter.

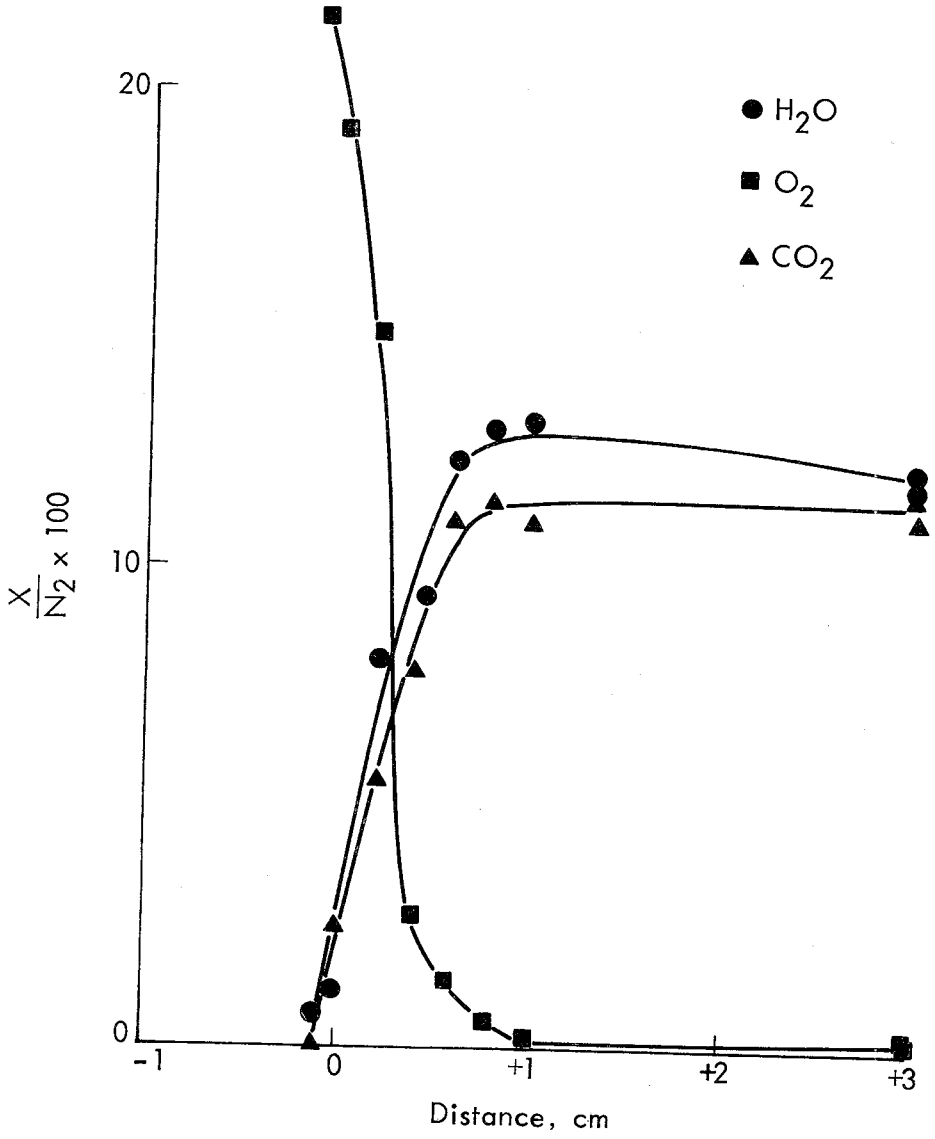

Figure 65 - Calibrated Mass Spectrometer Profiles Through an Unsieved Coal-Air Flame on a 6.3-cm Diameter Burner. 181 mg/liter.

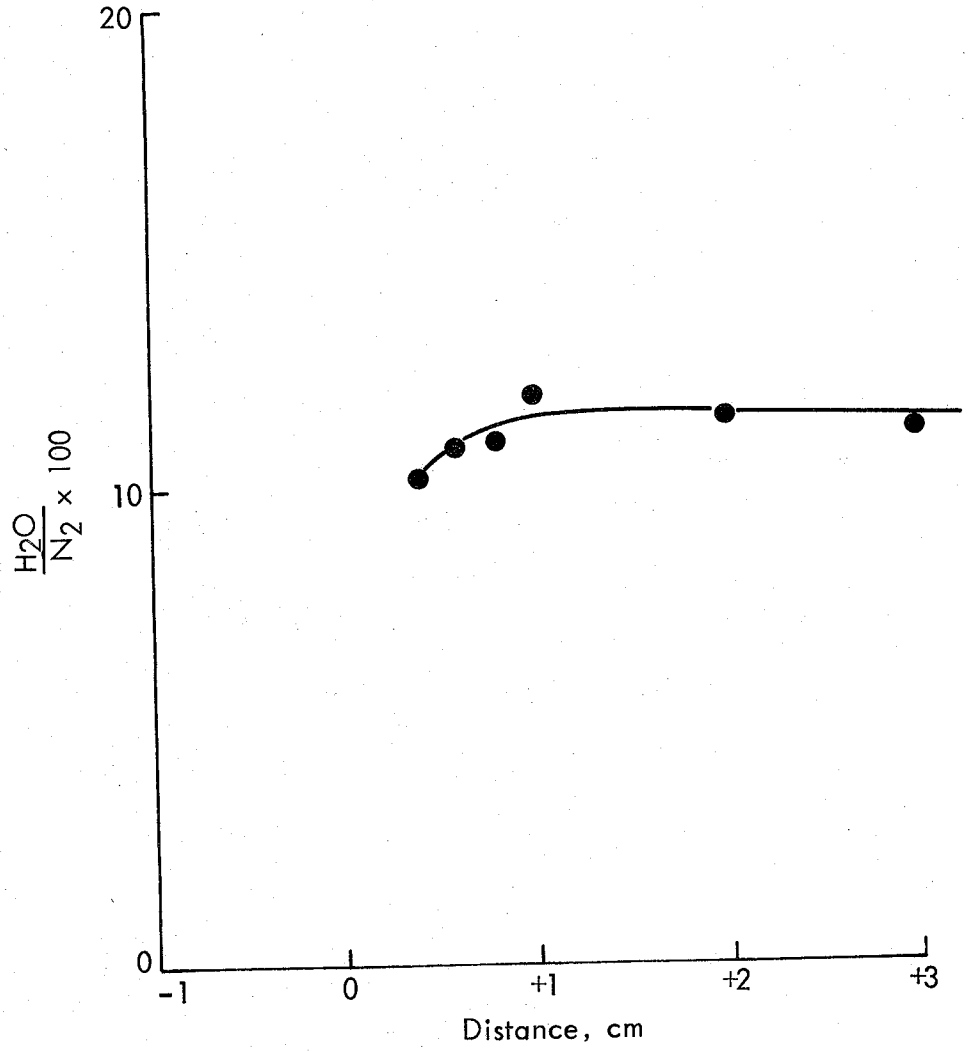

Figure 66 - Calibrated H_2O Profile Through a 10 to 20 μ Coal-Air Flame on a 6.3-cm Diameter Burner. 207 mg/liter.

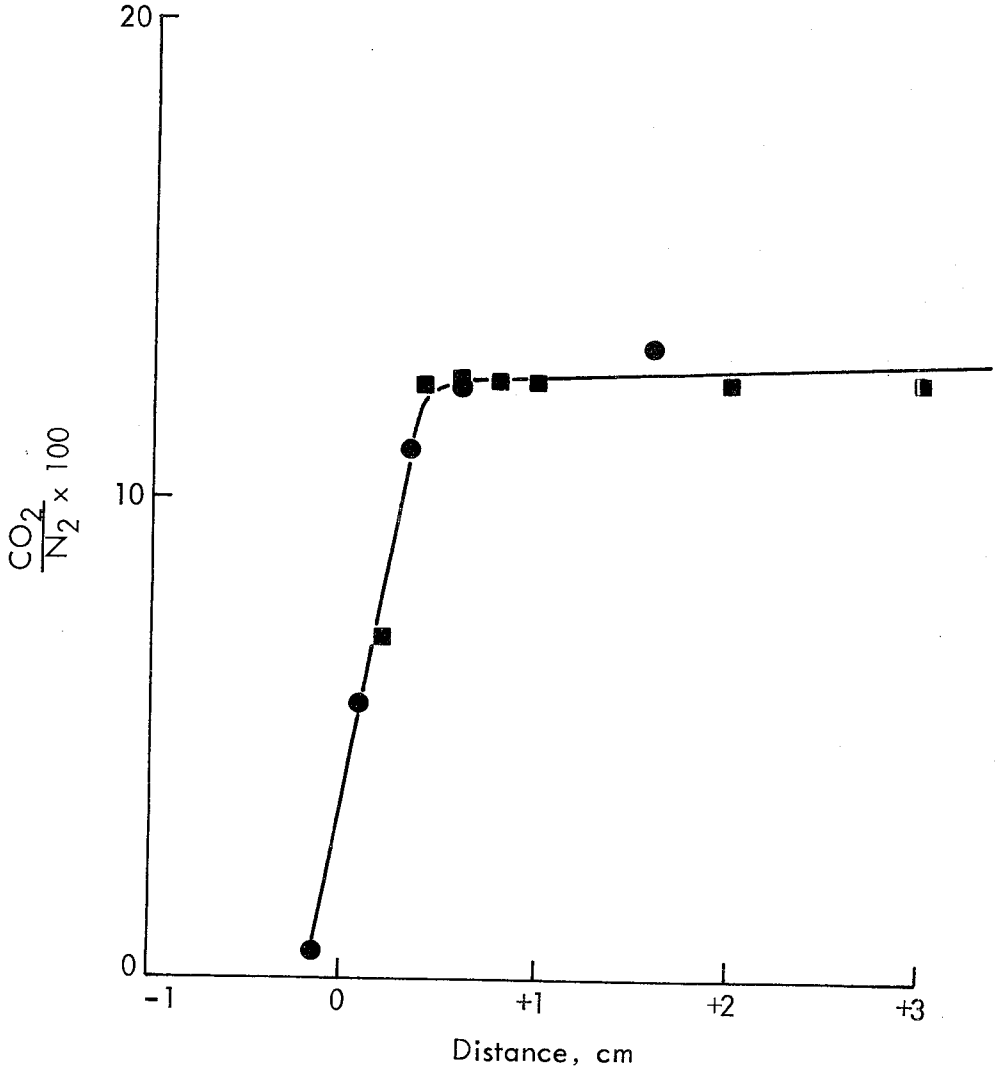

Figure 67 - Calibrated CO_2 Profile Through a 10 to 20 μ Coal-Air Flame on a 6.3-cm Diameter Burner. 161 mg/liter.

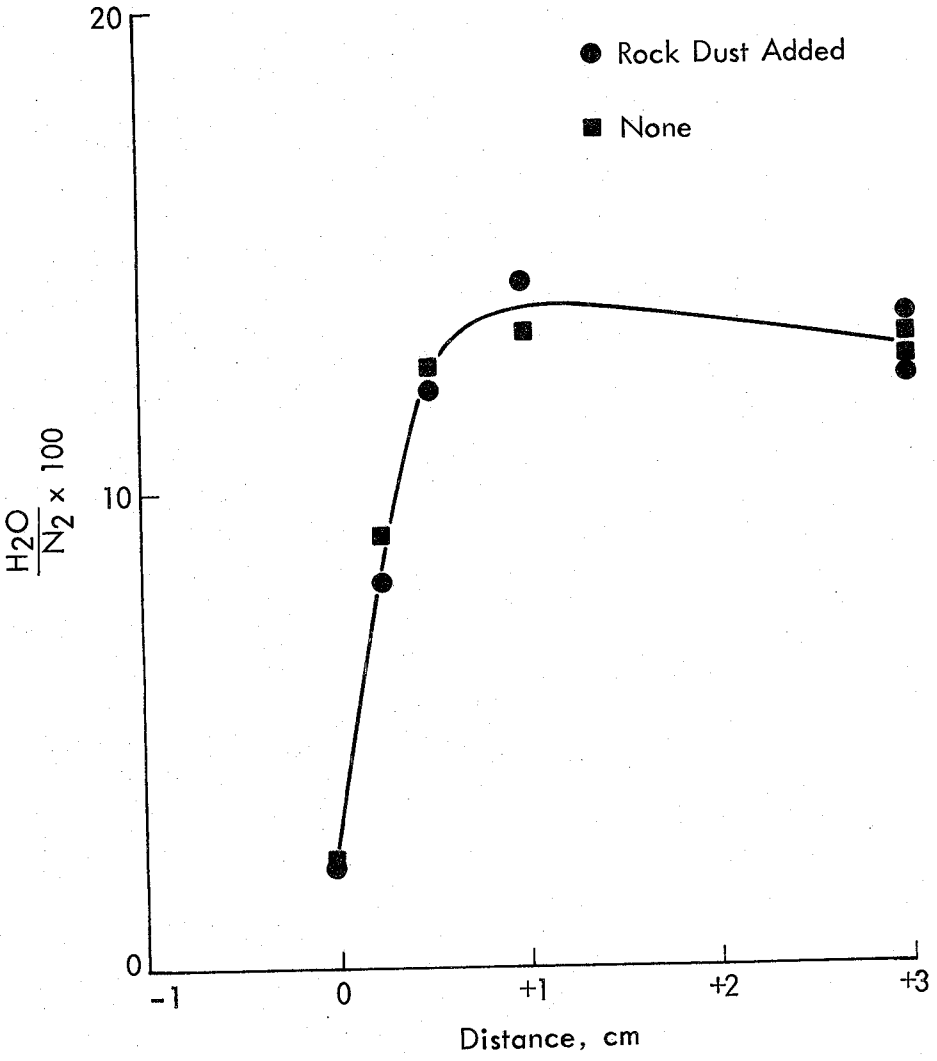

Figure 68 - Effect of Rock Dust on Mass Spectrometer H_2O Profiles Through a 10 to 20 μ Coal-Air Flame. Coal at 182 mg/liter. Rock dust at 32 mg/liter.

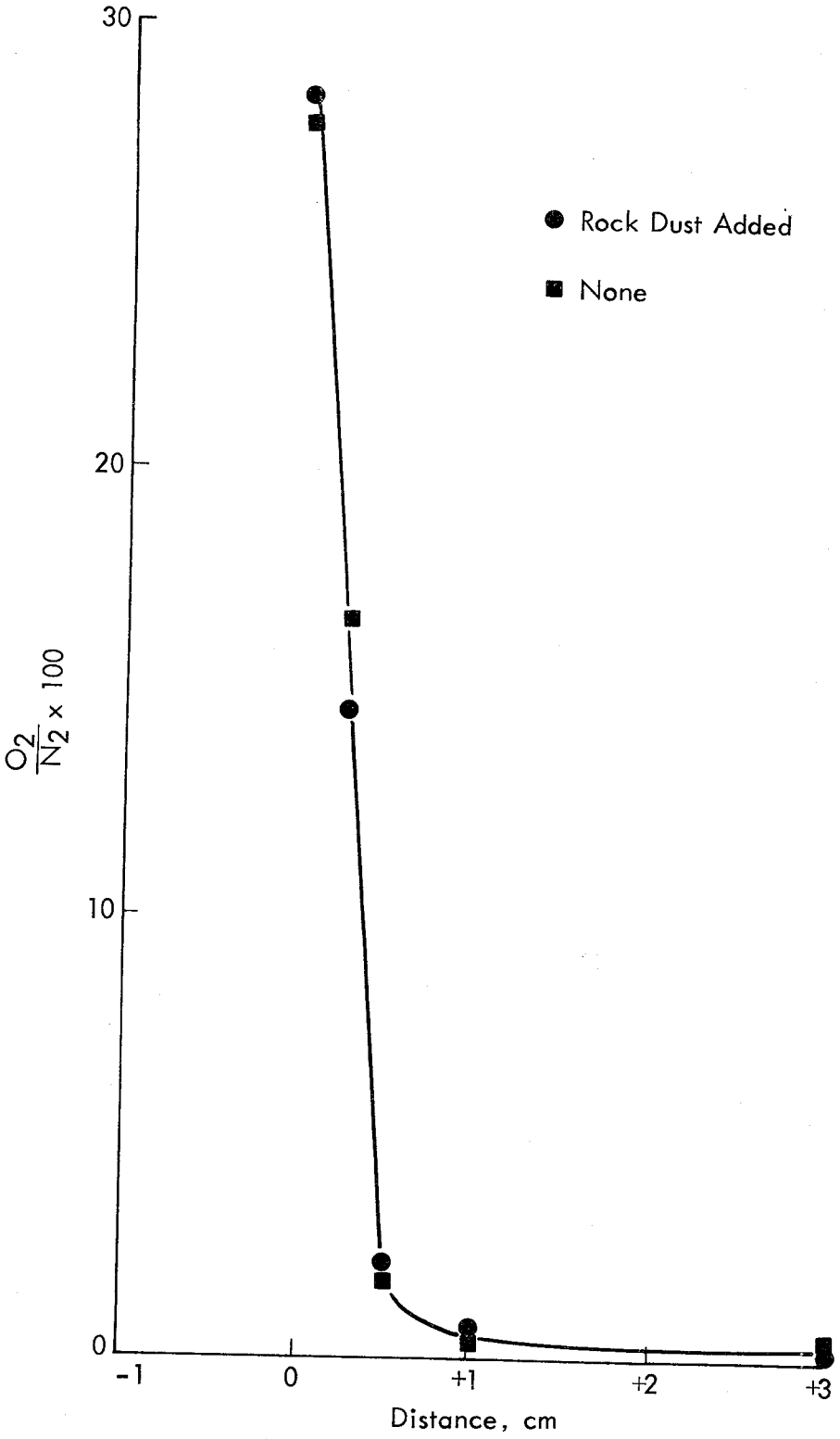

Figure 69 - O_2 Profile in Flame of Figure 68

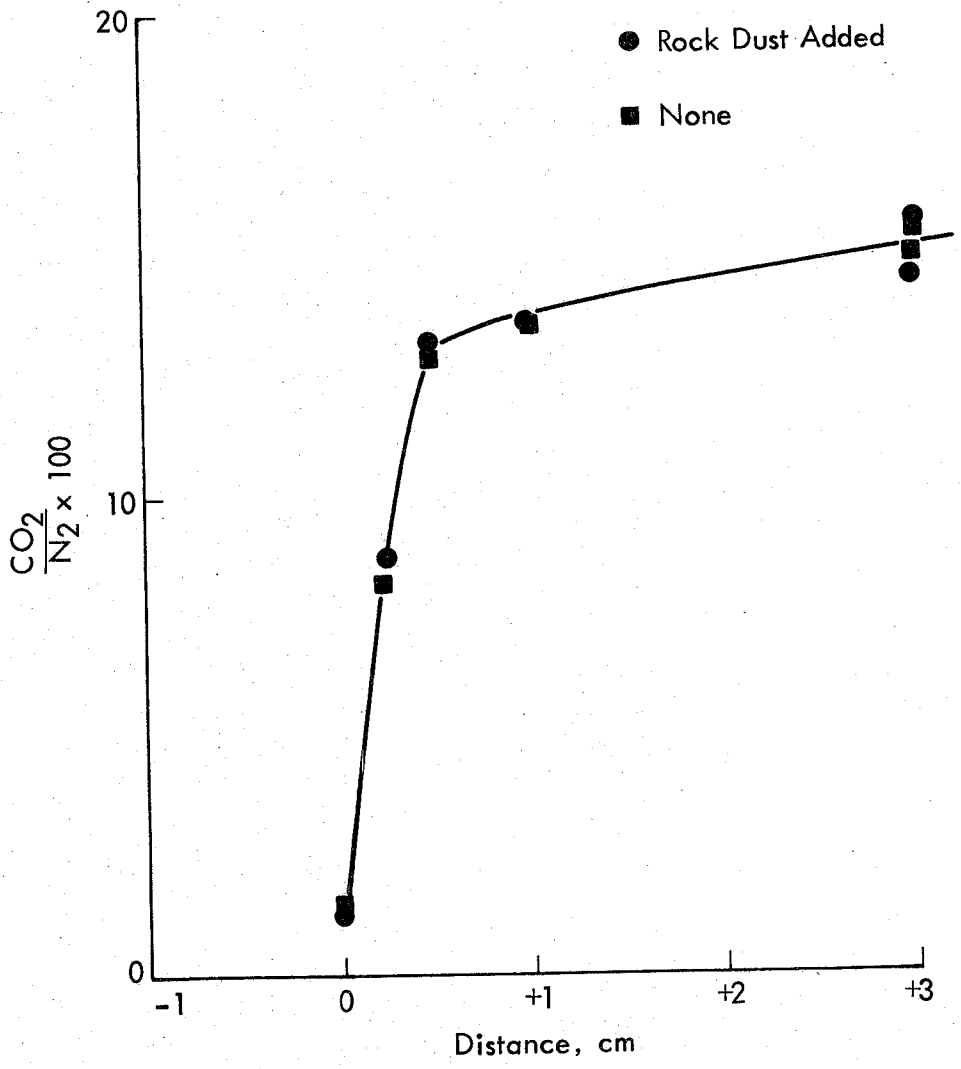

Figure 70 - CO_2 Profile in Flame of Figure 68

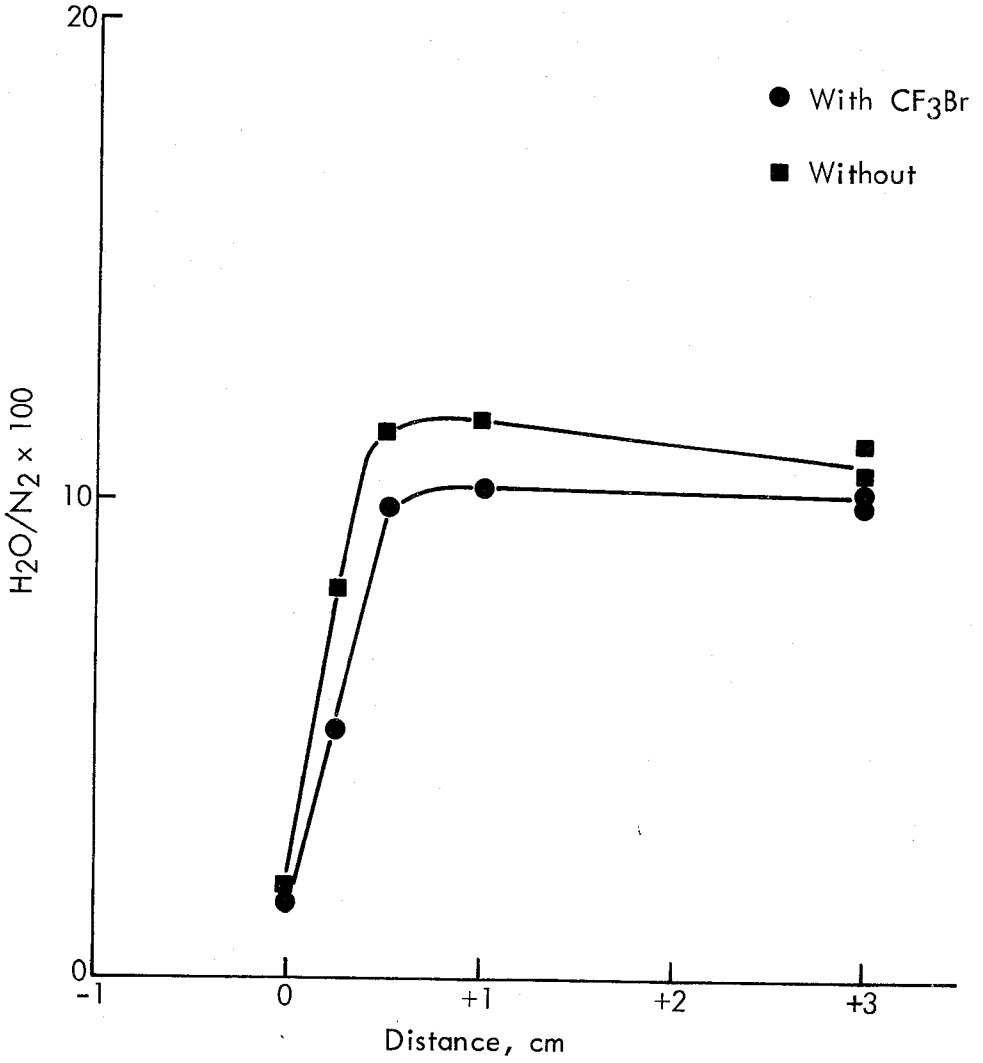

Figure 71 - Effect of CF_3Br on Mass Spectrometric H_2O Profiles Through a 10 to 20 μ Coal-Air Flame. Coal at 203 mg/liter. CF_3Br at 26.4 mg/liter.

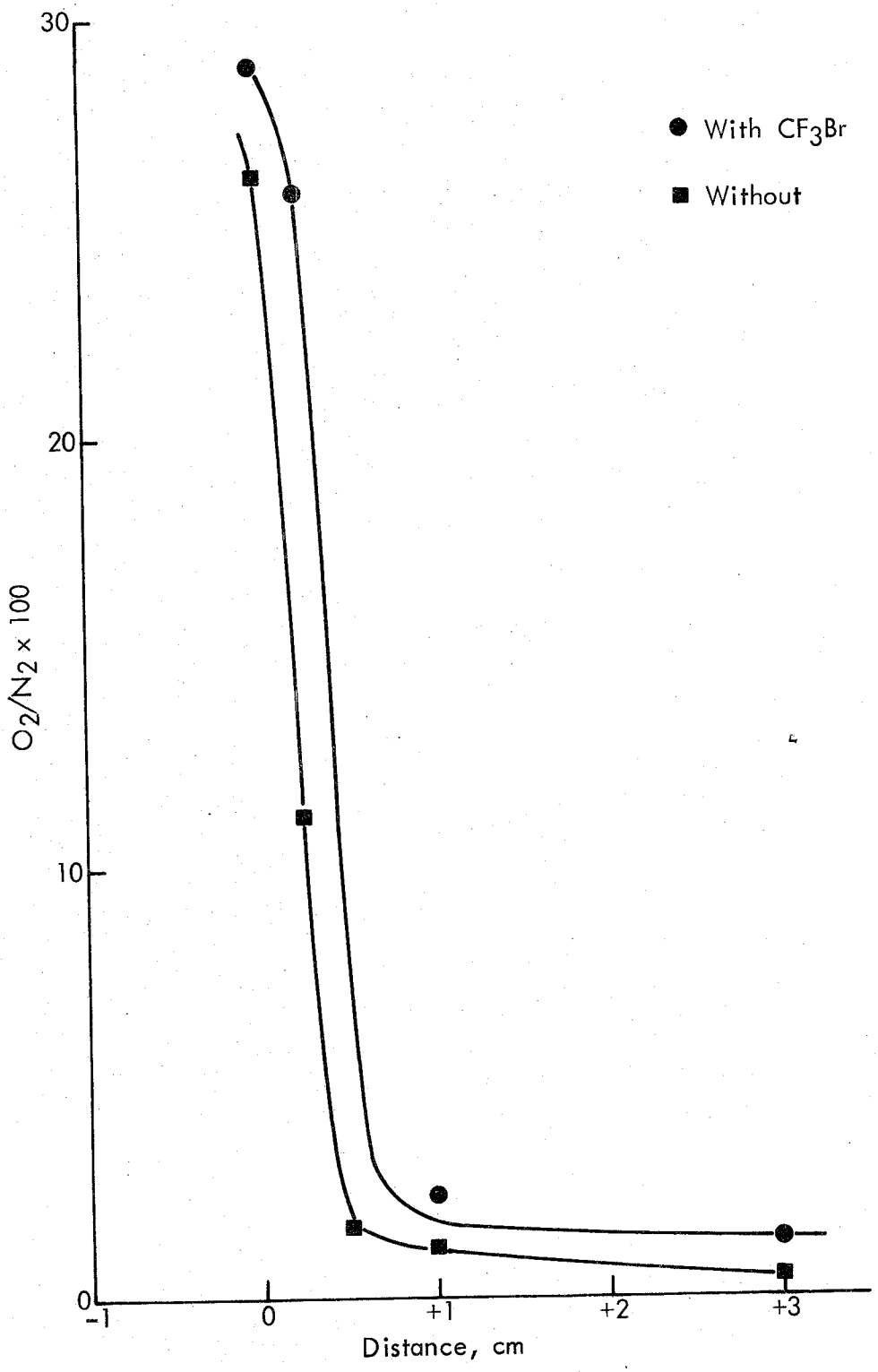

Figure 72 - O_2 Profiles Through Flame of Figure 71

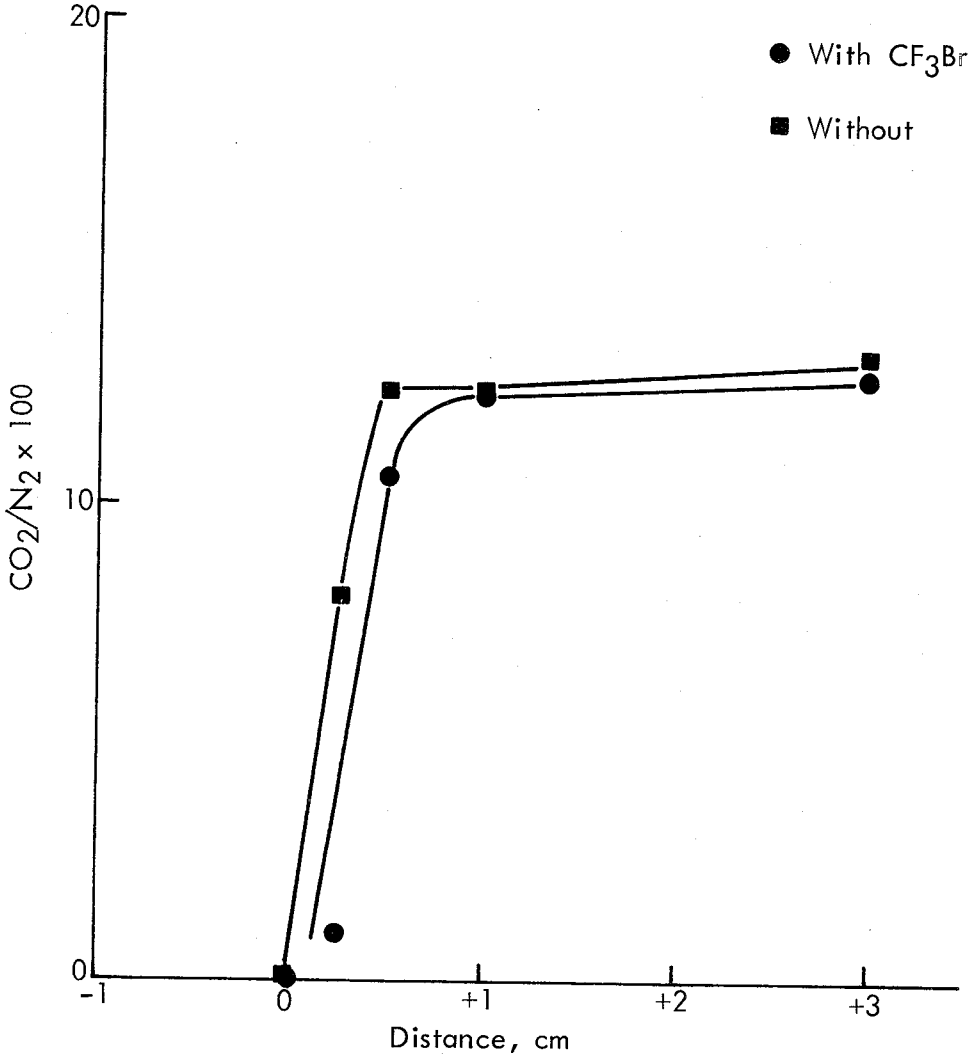

Figure 73 - CO_2 Profiles Through Flame of Figure 71

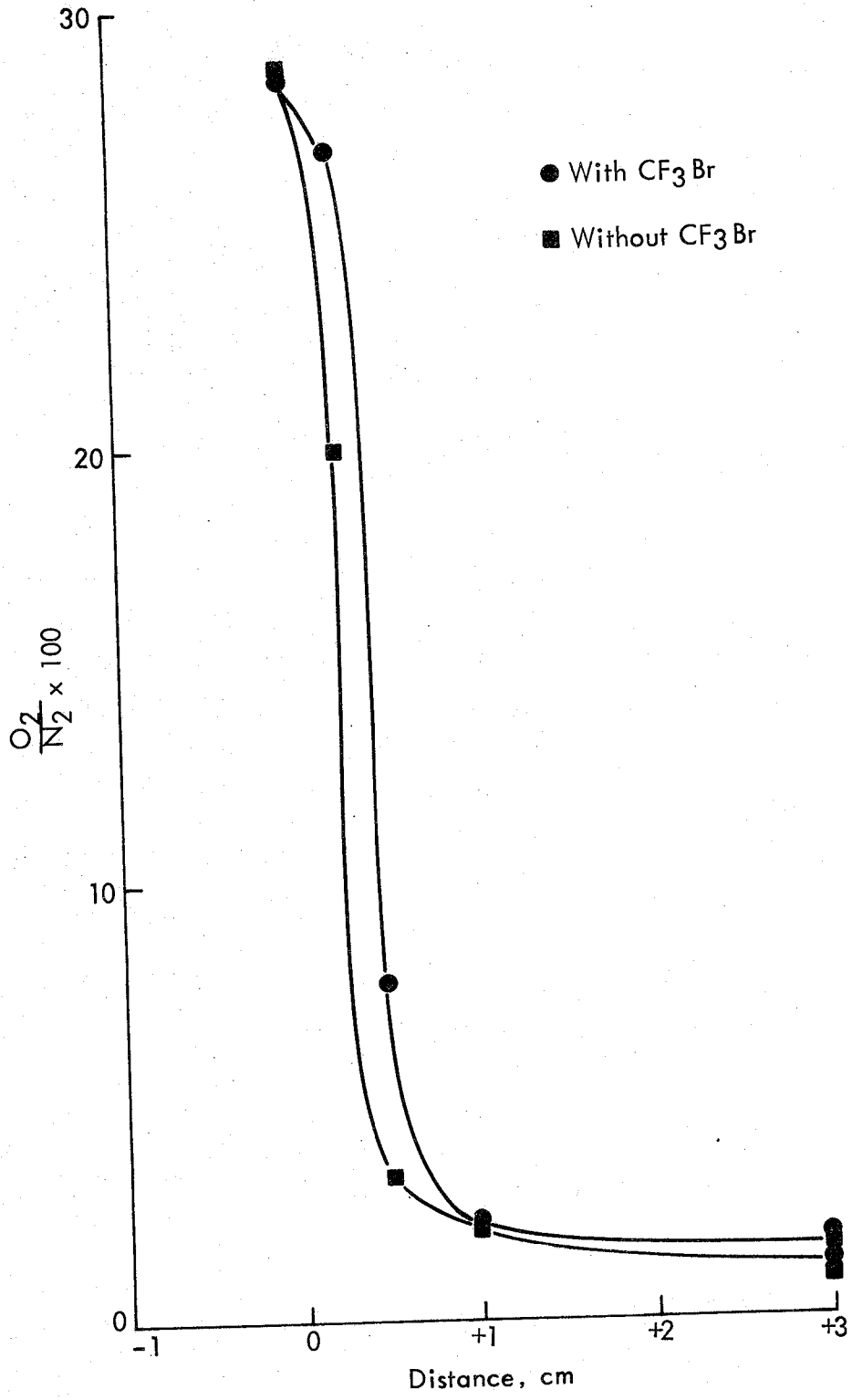

Figure 74 - Effect on CF_3Br on Mass Spectrometer O_2 Profile in a 10 to 20 μ Coal-Air Flame. Coal at 147 mg/liter. CF_3Br at 9.3 mg/liter.

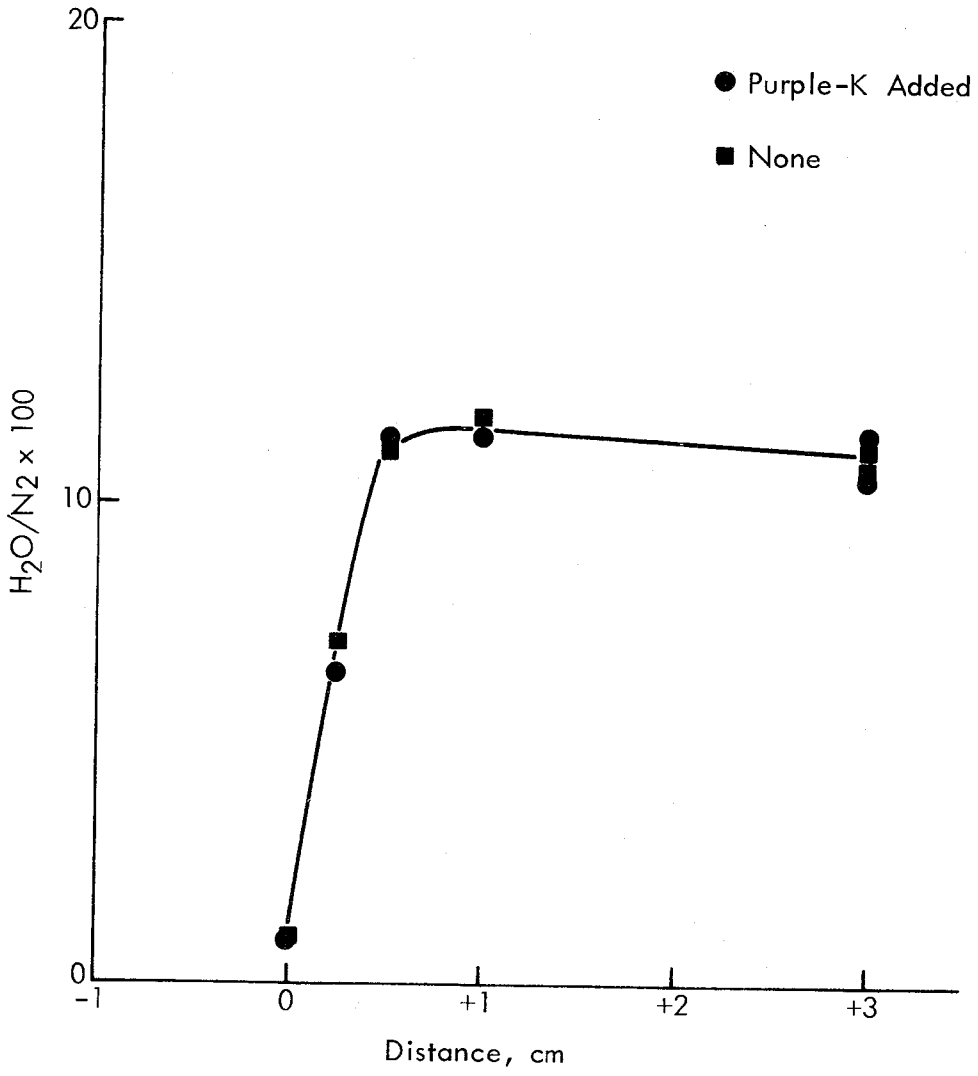

Figure 75 - Effect of Purple-K on Mass Spectrometer H_2O Profiles in a 10 to 20 μ Coal-Air Flame. Coal at 182 mg/liter. Purple-K at 2.4 mg/liter.

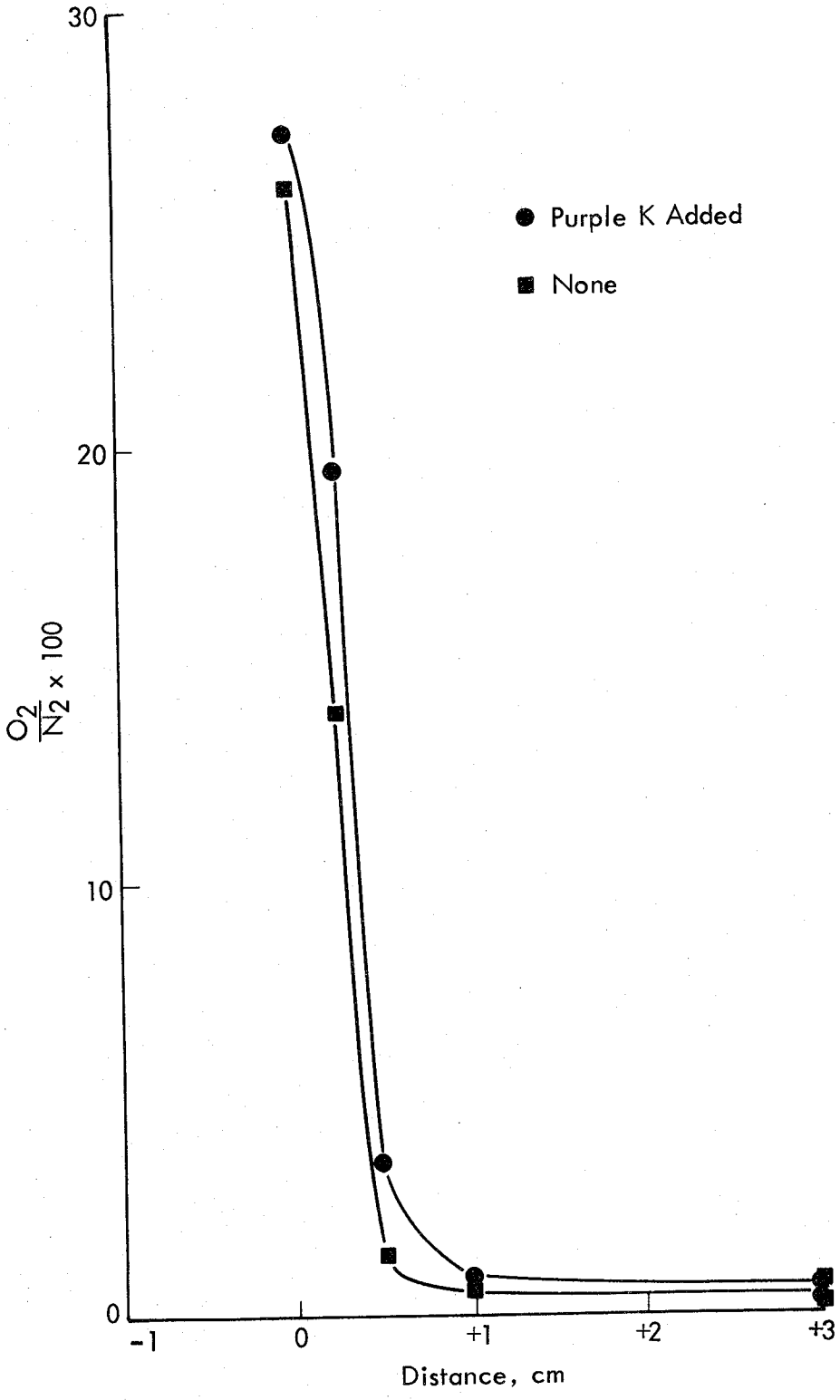

Figure 76 - O_2 Profiles in Flame of Figure 75

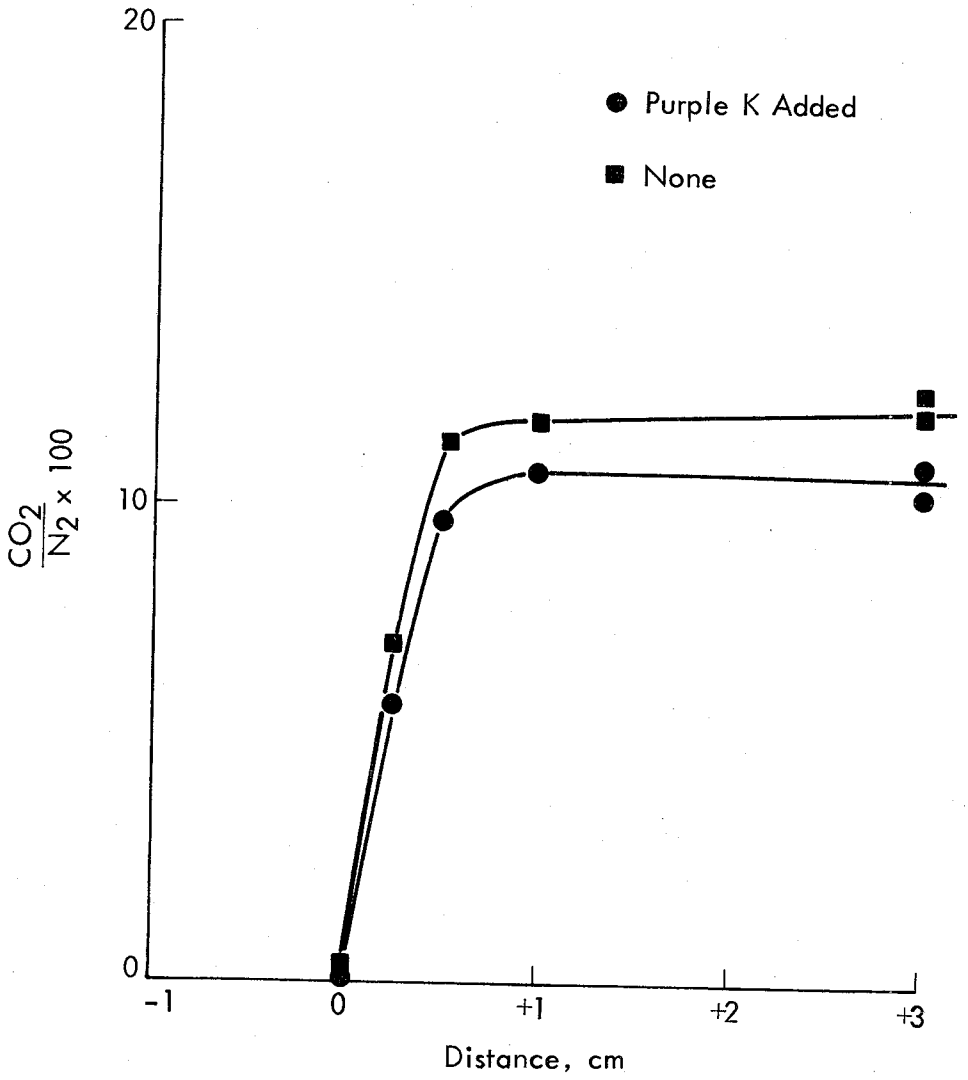

Figure 77 - CO_2 Profiles in Flame of Figure 75

APPENDIX G

DIRECT PROBING OF COAL-AIR FLAMES FOR PARTICULATES

Because the flat-flame burners we have developed provide a stable, laminar flow of coal dust-air into a stationary primary reaction zone, it appeared worthwhile to probe, with high spatial resolution (small probe diameters), through the flame to collect particulates as well as gaseous species. Small quartz probes, similar in shape to those used in mass spectrometric sampling, were used to extract and collect, on fritted disks, sufficient quantities of coal dust to permit proximate analysis (about 50 mg for duplicate analyses). Sampled coal and char particulates were also collected by impact on coated microscope slides for subsequent microscopic examination.

A. Solids Sampling for Proximate Analysis

With the standard 6.3-cm diameter burner, the honeycomb grid without central hole and a rich coal-air flame (270 mg/liter $\pm$ 10%), samples of particulates have been extracted through the conical quartz probe discussed above. Collections were made on a fritted disk, and the particles were then transferred to glass bottles for shipment. The samples, containing typically 0.3 g, were subjected to a standard proximate analysis at the Pittsburgh Mining and Safety Research Center, through the courtesy of Mr. Joseph Grumer.

Collection of enough particulates from the region of the bright reaction zone (position labeled 0 cm above burner in Table 10 were troublesome in that rapid plugging of the orifice occurred and several cleanings had to be made to get one sample of sufficient size for proximate analysis. Table 10 is taken from the Bureau of Mines analytical reports, with the last two columns added to show normalization of fixed carbon and volatile matter to percent ash in the original coal. The values in the last two columns are plotted in Figures 78 and 79.

B. Solids Sampling for Microscopic Analysis

Using the same quartz probe for sampling as for the collections for proximate analysis and gas chromatography, particles were collected by placing a Dow Corning 200 fluid coated microscope slide just downstream of the orifice. Photomicrographs for positions in the flame of 2 mm, 2 cm, and 4 cm, respectively, were obtained. From these photographs it appeared that the percentages of large particles had increased with passage through the flame. Features visible to the eye using the microscope were not clear in these figures due to a depth-of-field problem. More information on changes in coal char and ash morphology with passage through the flame can be obtained through scanning electron microscopy of similarly collected particles, and this technique was used in later series. For SEM analysis, collection was an aluminum impregnated Scotch Tape mounted on 1/2 in. diameter aluminum stubs for easy mounting in the scanning electron microscope.

TABLE 10

PROXIMATE ANALYSIS OF COAL-DUST SAMPLED FROM A RICH (~ 270 MG/LITER) COAL DUST-AIR FLAME, THROUGH A 30-MIL DIAMETER QUARTZ PROBE

Sampling Distance Above Burner Matrix (cm)	% Ash	% Volatile Matter (VM)	% Fixed Carbon (FC)	% Original Remaining: $\frac{\%\ \text{Volatile Matter}}{\%\ \text{Ash}} \div \frac{\%\ \text{Volatile Matter}_o}{\%\ \text{Ash}_o} \times 100$	% Original Remaining: $\frac{\%\ \text{Fixed Carbon}}{\%\ \text{Ash}} \div \frac{\%\ \text{Fixed Carbon}_o}{\%\ \text{Ash}_o} \times 100$
No Flame	12.0	34.0	54.0	100	100
0	16.5	18.1	65.4	38.6	88.0
0.6	22.6	3.1	74.3	4.8	73.0
1.2	27.5	4.7	67.8	6.0	54.6
2.5	25.2	9.5	65.3	13.2	57.6
No Flame	11.2	34.4	54.4	100	100
0	14.9	22.2	62.9	48.5	87.0
0.6	20.2	7.2	72.6	11.6	74.0
1.2	22.1	4.2	73.7	6.2	68.7
2.5	18.1	5.9	76.0	10.6	86.5

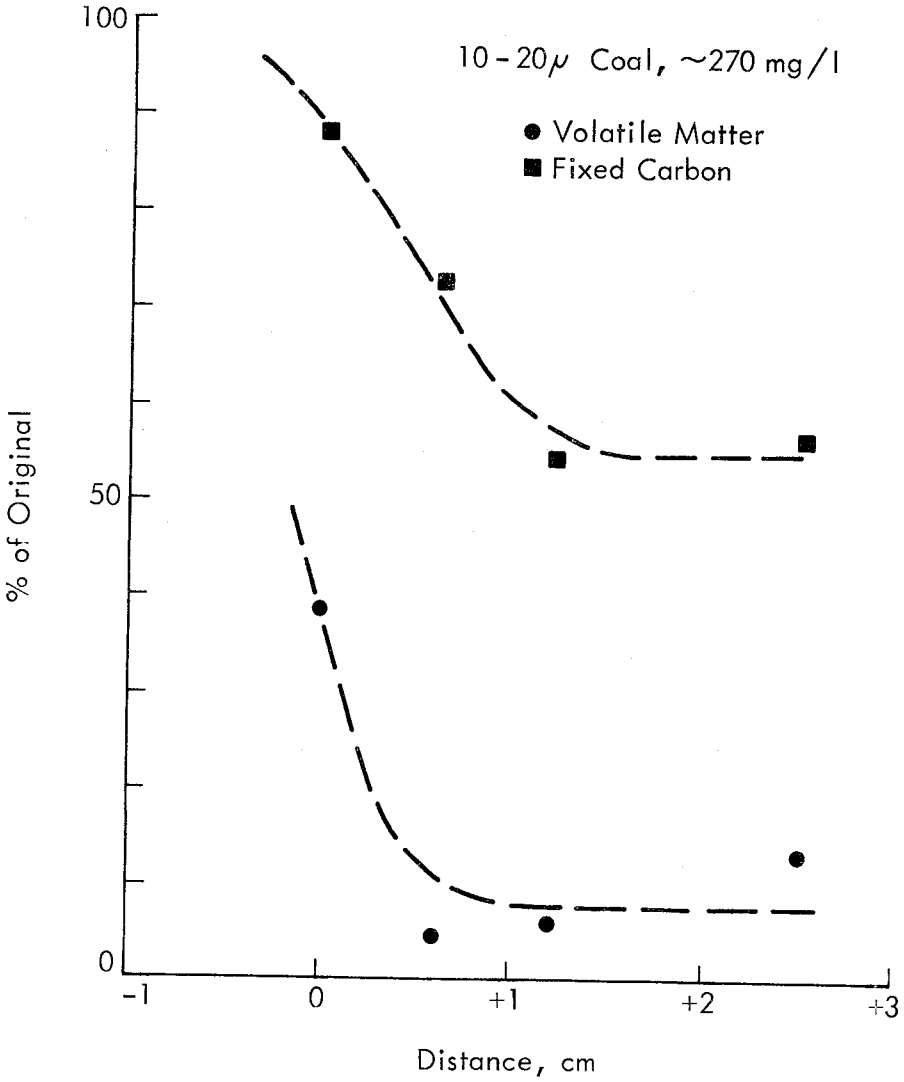

Figure 78 - Variation of Volatile Matter and Fixed-Carbon, Relative to Ash Content, with Position in a Rich, Coal Dust-Air Flame. (Data from the last two columns of Table 10.)

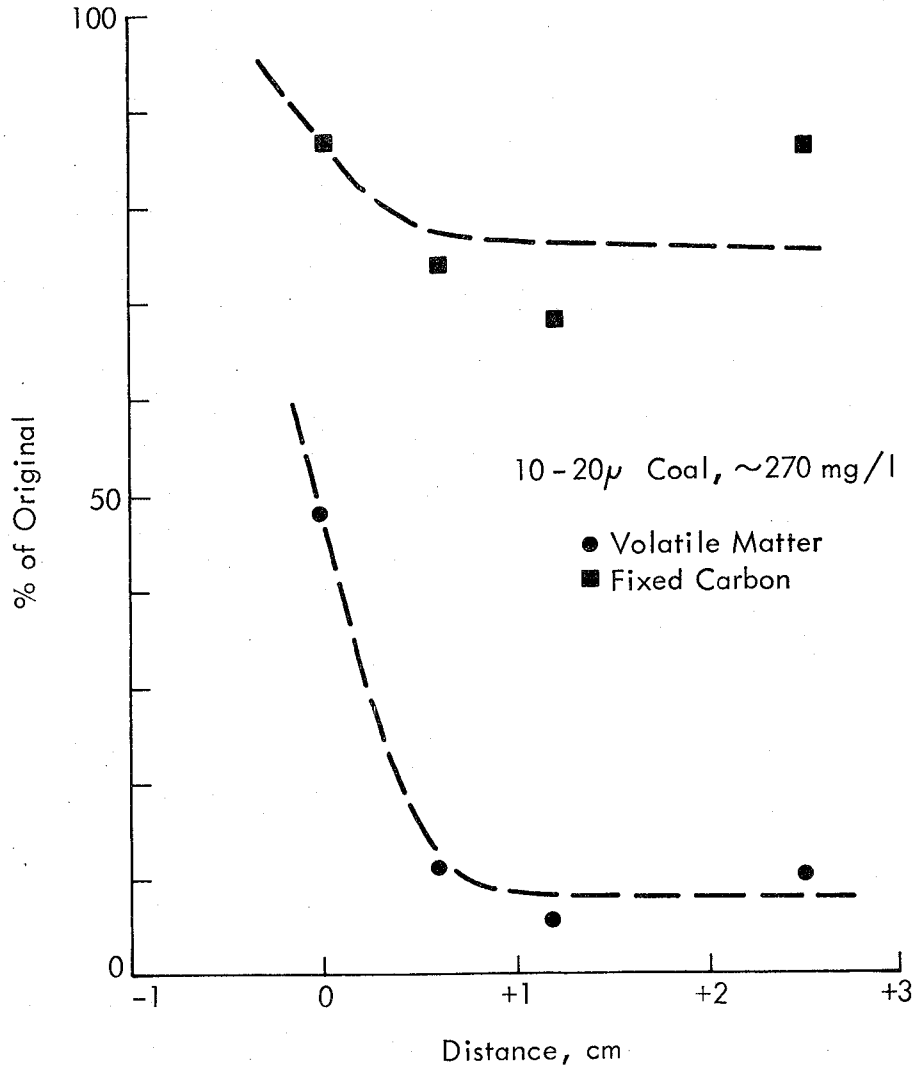

Figure 79 - Variation of Volatile Matter and Fixed-Carbon, Relative to Ash Content, with Position in a Rich, Coal Dust-Air Flame. (Data from the last two columns of Table 10.)

Coal and char particle profiles: Particles in bulk, and on scanning electron microscope tabs, were collected from the same four positions and five flames as with the GC and mass spectrometer experiments included in Appendix F. The sampling procedures used have been described above. The bulk samples for proximate analysis were collected at a pressure drop across the orifice of about 0.6 atmosphere. Mr. Grumer arranged for the micro-proximate analyses of the samples at the Bruceton Laboratory. The SEM samples were collected on aluminum impregnated Scotch Tape with a pressure drop across the orifice of only 1 in. water. While this appoximated isokinetic sampling and thus did not give the disproportionate representation of fines that sonic-orifice sampling conditions would, it may have resulted in the collection of only big particles, since proper impaction conditions for fines were not achieved at the collection stubs. Since the emphasis in this series was on the early ignition and pyrolysis regime, the SEM results are expected to be representative of early changes in the large, primary coal particles.

The proximate analysis results are tabulated in Table 11 and graphically displayed in Figures 80 to 85. The results are presented as percent of remaining volatile matter and fixed carbon, using the ash as a tracer.[13]

Typical examples of particles photographed by scanning electron microscopy are shown in Figure 86. These photos are from an earlier series of runs in which collections were made well beyond the initial reaction zone. The features observed are quite representative of the many SEM samples photographed under the five conditions corresponding to the mass spectrometer, GC and proximate analysis series. Preliminary perusal of the many new SEM photos revealed no new features, nor any readily apparent changes with flame richness, starting coal size or addition of Purple-K at the 7 mg/liter level.

TABLE 11

PROXIMATE ANALYSES OF COAL AND CHAR SAMPLES EXTRACTED FROM THE EARLY REACTION ZONE OF PULVERIZED COAL-AIR FLAMES

Sampling Distance, cm	Sample No.	Coal (mg/liter)	% Moisture	% Ash	% Volatiles	% Fixed Carbon	% Remaining: $\frac{\%\ VM}{\%\ Ash} \div \frac{\%\ VM\ o}{\%\ Ash\ o} \times 100$	% Remaining: $\frac{\%\ FC}{\%\ Ash} \div \frac{\%\ FC\ o}{\%\ Ash\ o} \times 100$	Remarks
1	1	213	3.8	20.8	6.6	68.8	5.89	41.5	Unsieved coal
1/2	2	213	3.6	8.5	4.6	83.3	10.0	123	
1/4	3	213	3.6	9.3	13.2	73.9	26.3	99.8	
0	4	213	2.0	8.4	28.0	61.6	61.8	92.2	
0	5	141	2.2	-	28.0	-	~ 61.8	-	10 to 20 μ coal
1/4	6	141	2.4	8.7	24.2	64.7	51.6	93.4	
1/2	7	141	4.8	8.1	8.4	78.7	19.2	122	
1	8	141	5.1	21.1	7.6	66.2	6.69	39.3	
0	9	231	1.5	13.2	32.9	52.4	46.2	49.9	10 to 20 μ coal
1/4	10	231	2.8	17.4	19.4	60.4	20.7	43.7	
1/2	11	231	3.6	11.0	9.5	75.9	16.0	86.7	
1	12	231	3.7	19.0	6.9	70.4	6.75	46.6	
0	13	260	1.5	8.9	35.3	54.3	73.7	76.7	10 to 20 μ coal
1/4	14	260	3.2	15.1	20.6	61.1	25.3	50.8	
1/2	15	260	4.5	12.1	7.1	76.3	10.9	79.2	
1	16	260	4.3	8.5	4.4	82.8	9.60	122.4	
0	17	199	1.6	13.4	31.0	54.0	43.0	50.6	Purple-K added at 6 mg/liter, 10 to 20 μ coal
1/4	18	263	2.8	11.3	21.8	64.1	35.8	71.2	
1/2	19	263	2.6	13.3	14.4	69.7	20.1	65.9	
1	20	263	2.9	13.8	12.0	71.3	16.1	64.8	
0	17A	199	1.6	10.6	32.6	55.2	57.0	65.4	Materials scraped from samples wall after each of Runs 17 to 20
1/4	18A	263	2.5	13.5	25.3	58.7	34.7	54.6	
1/2	19A	263	3.2	15.4	13.0	68.4	15.6	55.7	
1	20A	263	5.3	17.2	8.8	68.7	9.49	50.3	
	21	-	1.0	6.9	37.2	54.9	100.00	100.00	Raw coal

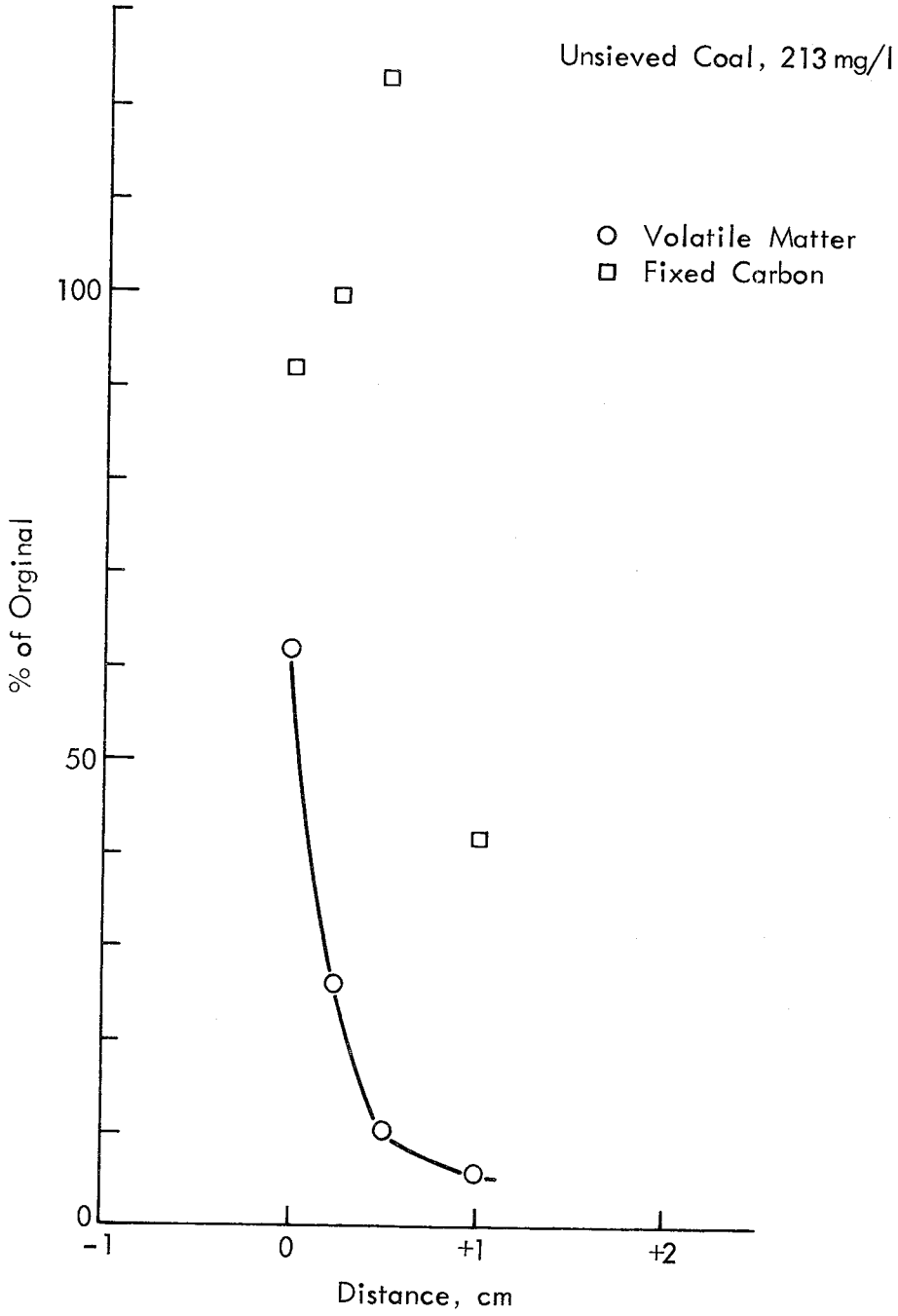

Figure 80 - Proximate Analysis Results for Particulates Sampled From the Early Region of an Unsieved Coal-Air Flame. 213 mg/liter.

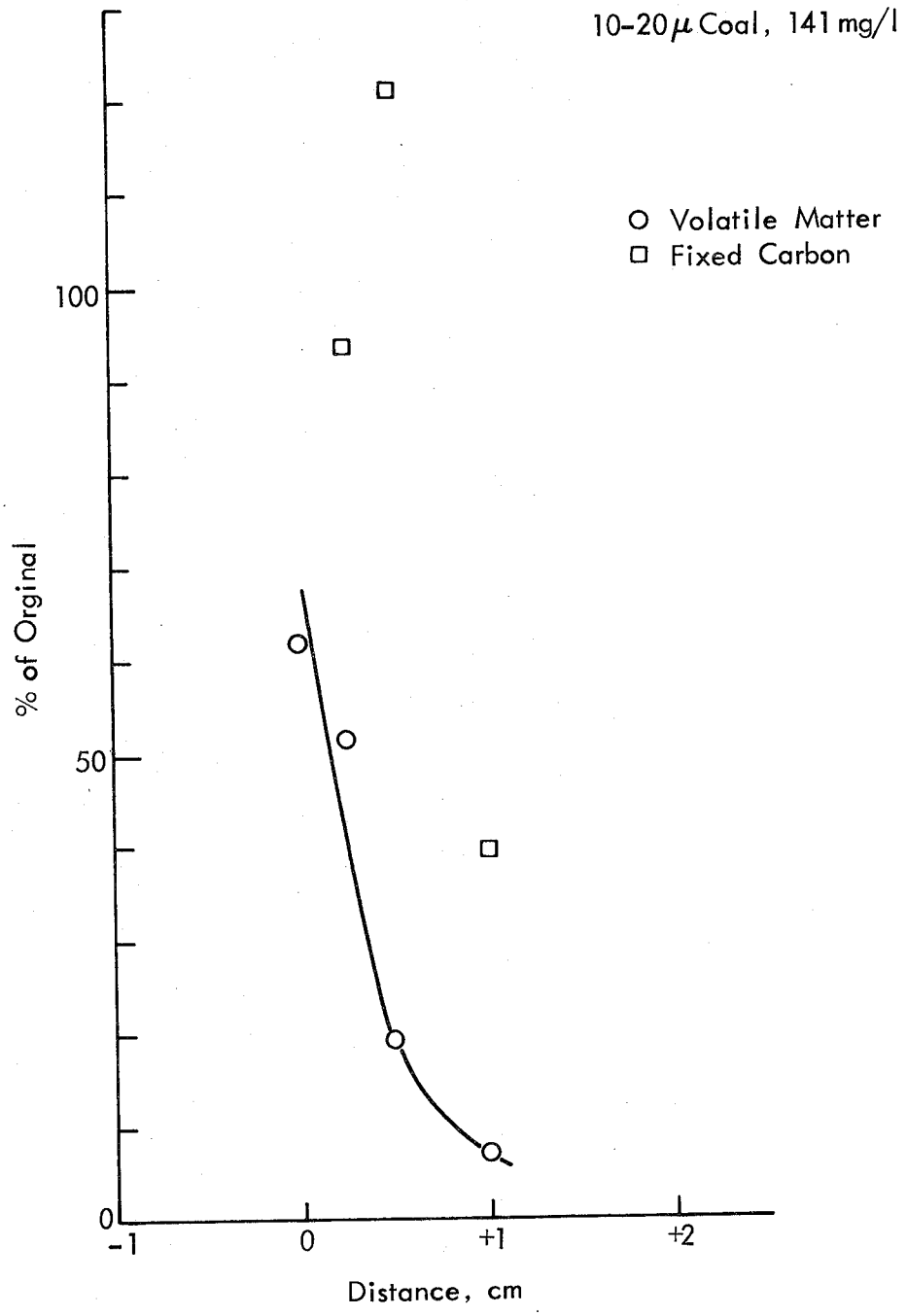

Figure 81 - Proximate Analysis Results for Particulates Sampled From the Early Region of a 10 to 20 μ Coal-Air Flame. 141 mg/liter.

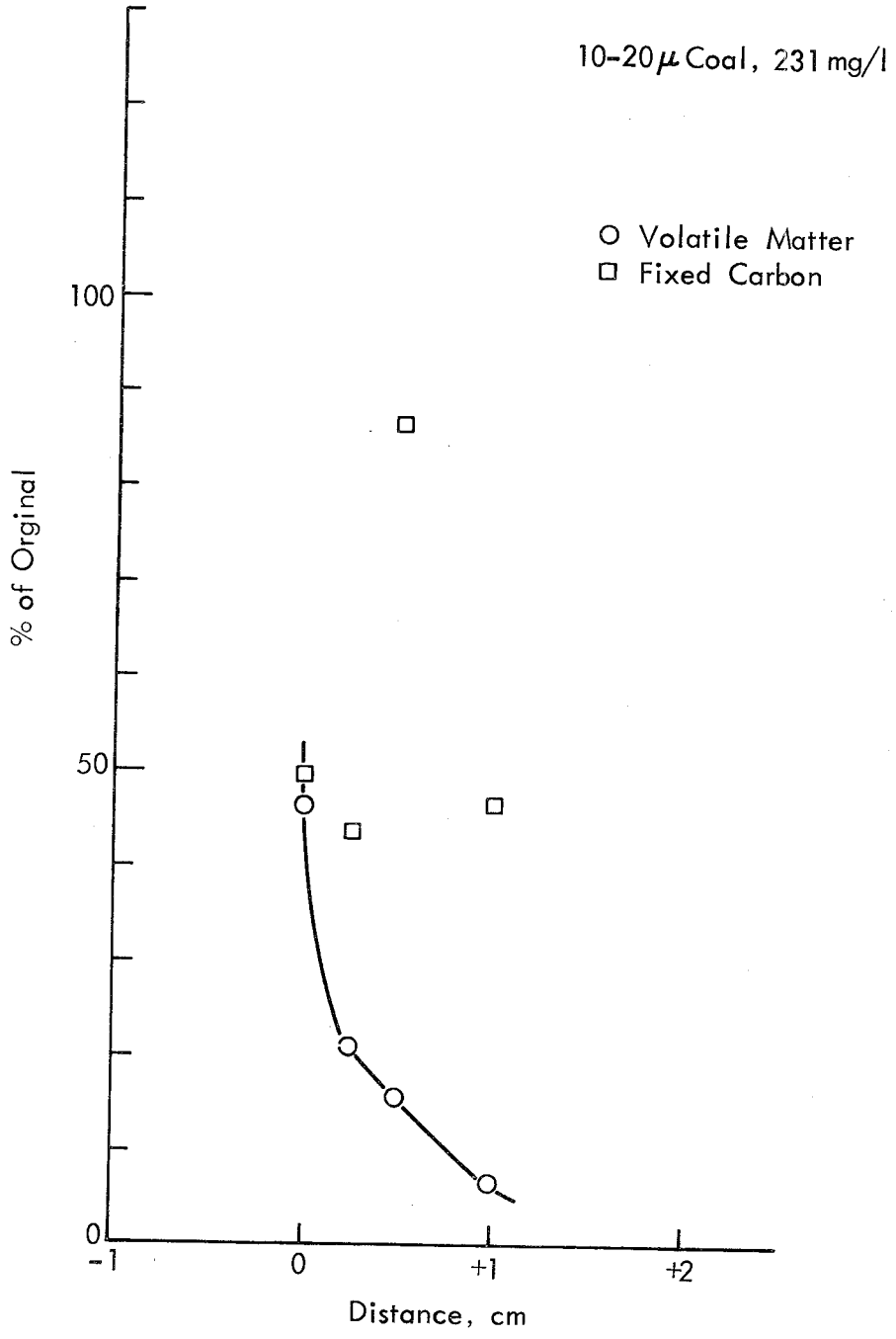

Figure 82 - Proximate Analysis Results Particulates Sampled From the Early Region of a 10 to 20 μ Coal-Air Flame. 231 mg/liter.

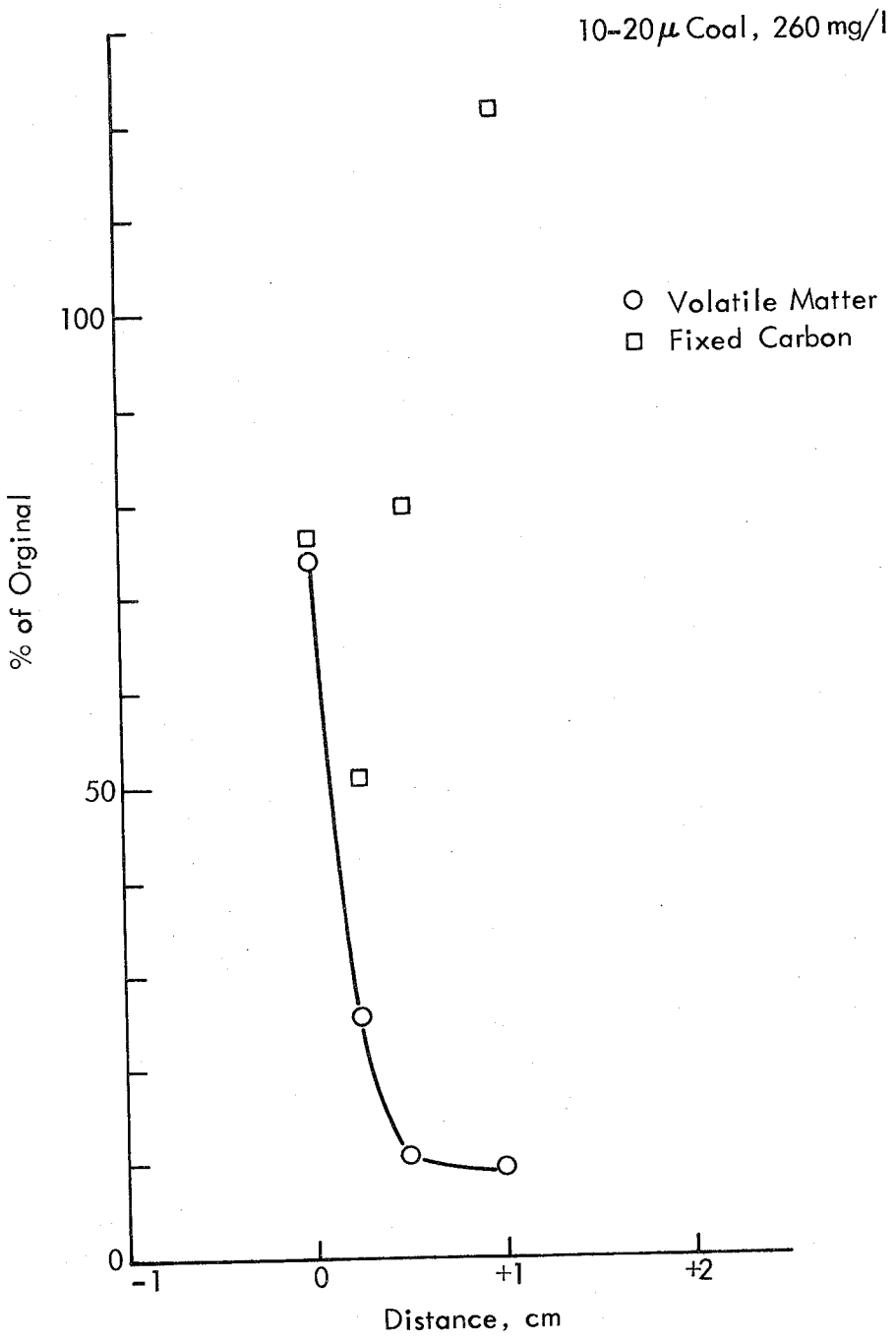

Figure 83 - Proximate Analysis Results for Particulates Sampled From the Early Region of a 10 to 20 μ Coal-Air Flame. 260 mg/liter.

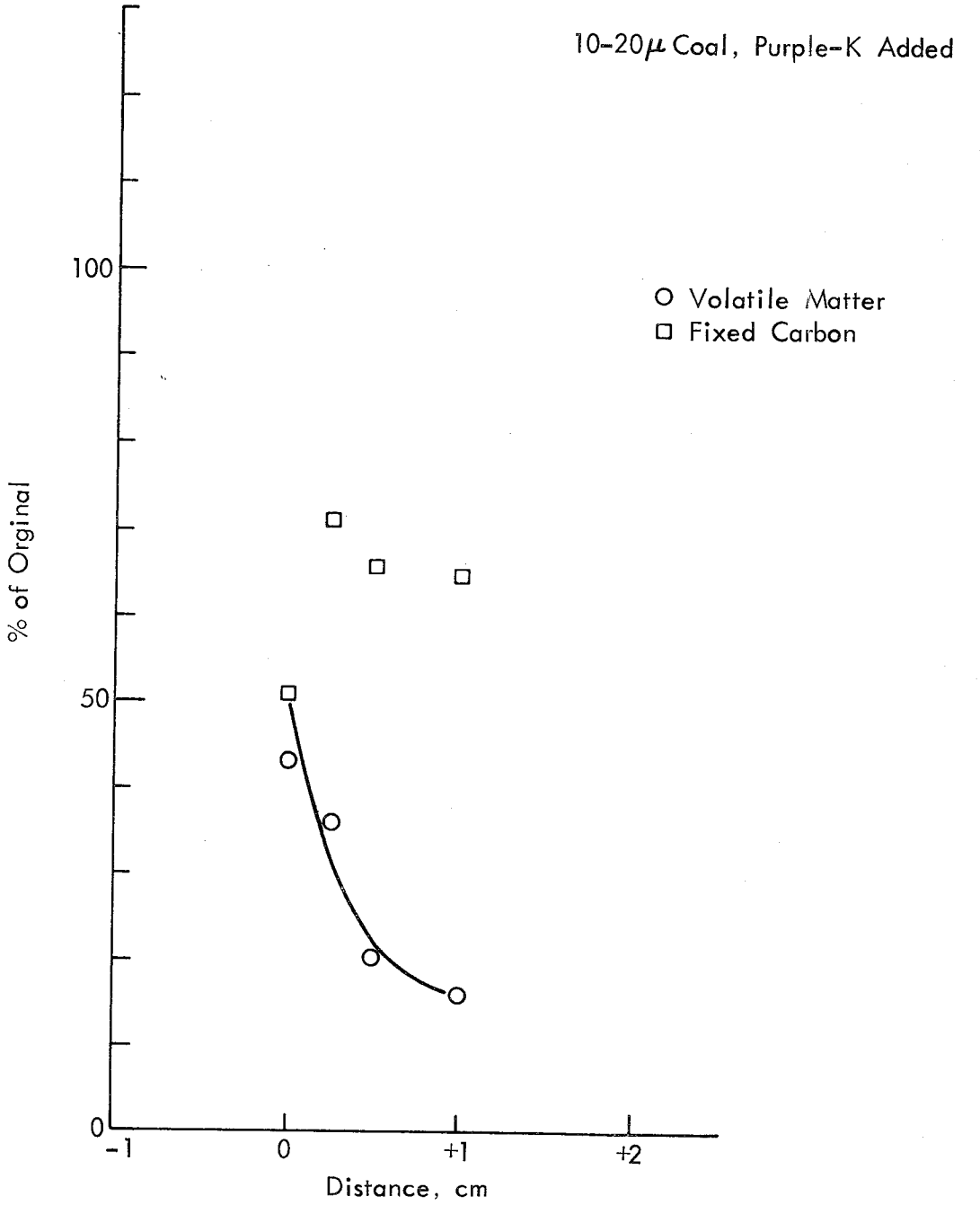

Figure 84 - Proximate Analysis Results for Particulates Sampled From the Early Region of a 10 to 20 μ Coal-Air Flame to Which Purple-K Had Been Added. Coal was 199 mg/liter at 0 cm and 263 mg/liter otherwise. Purple-K was 6 mg/liter.

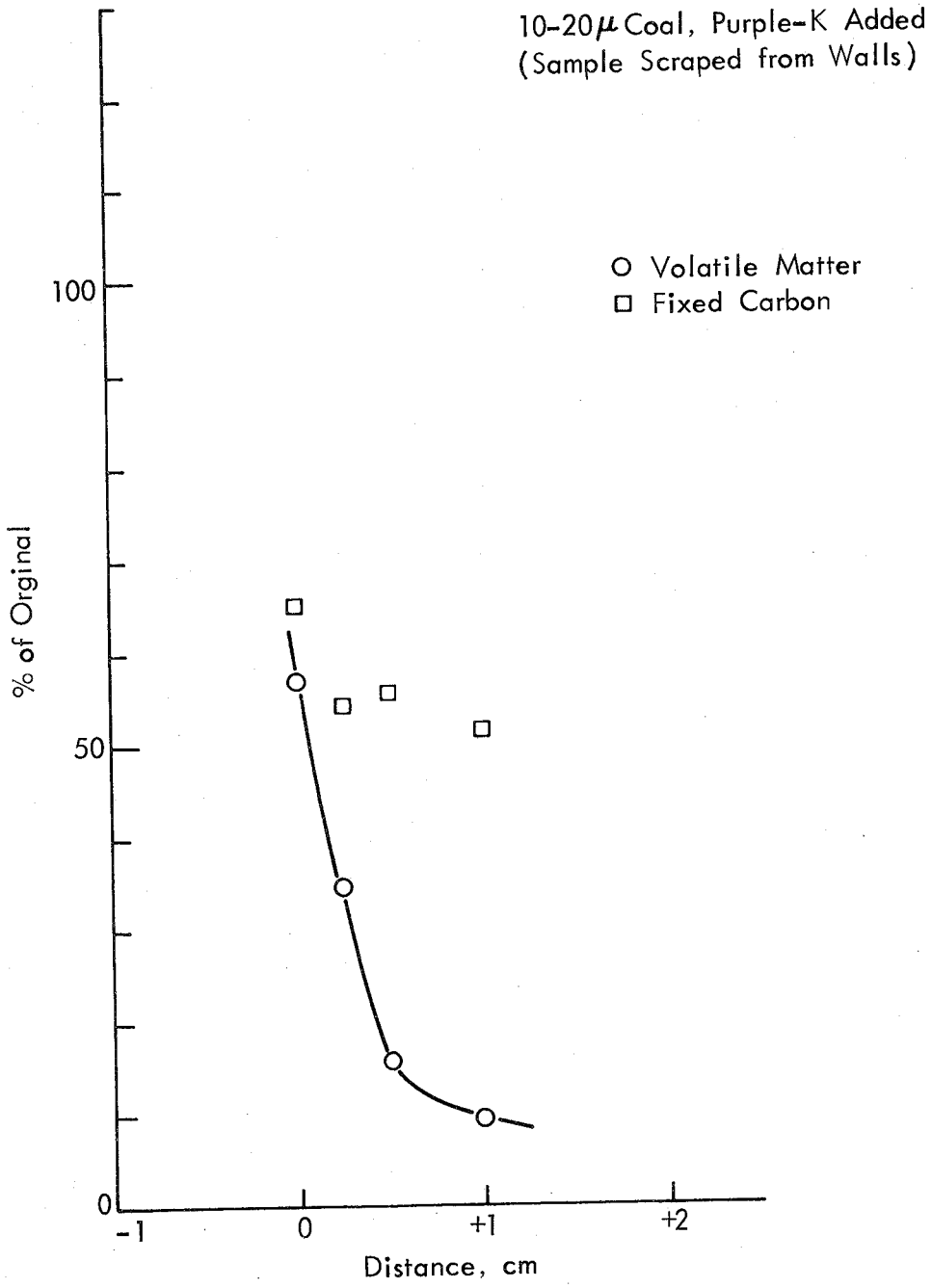

Figure 85 - Same Conditions as Figure 84. Samples scraped from the walls of probe after each collection of Figure 84.

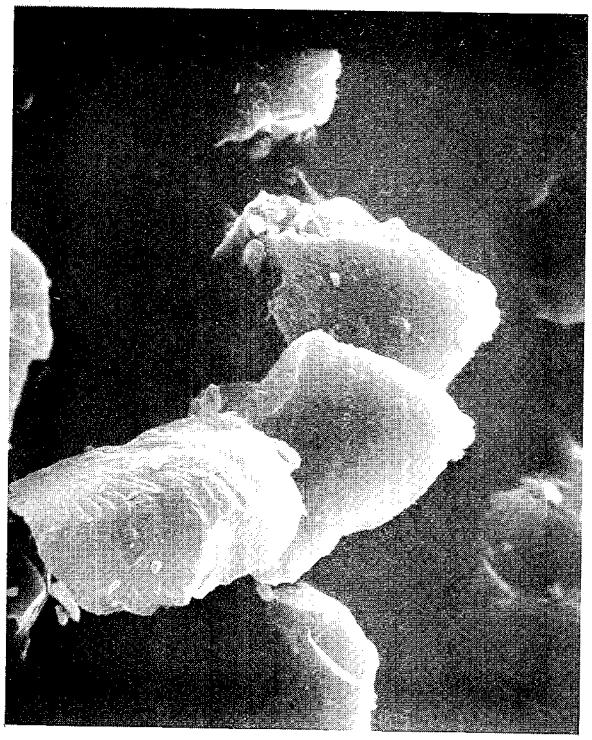

RAW COAL

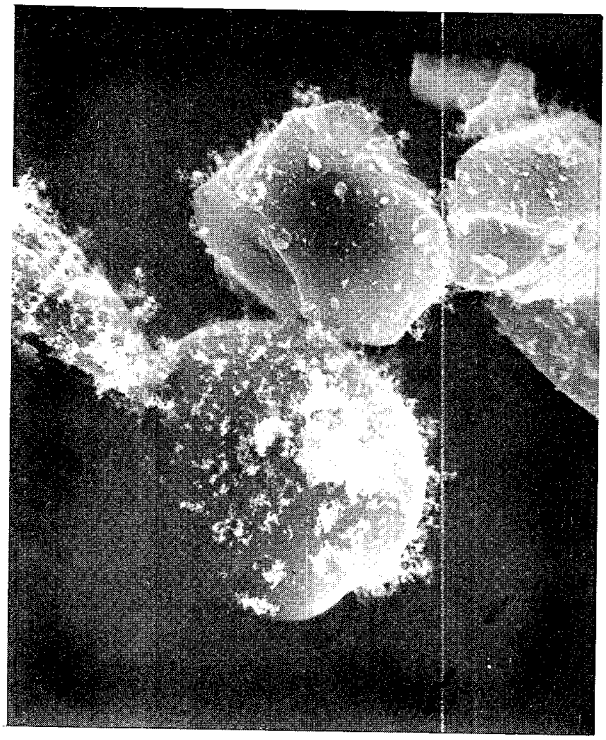

0 cm

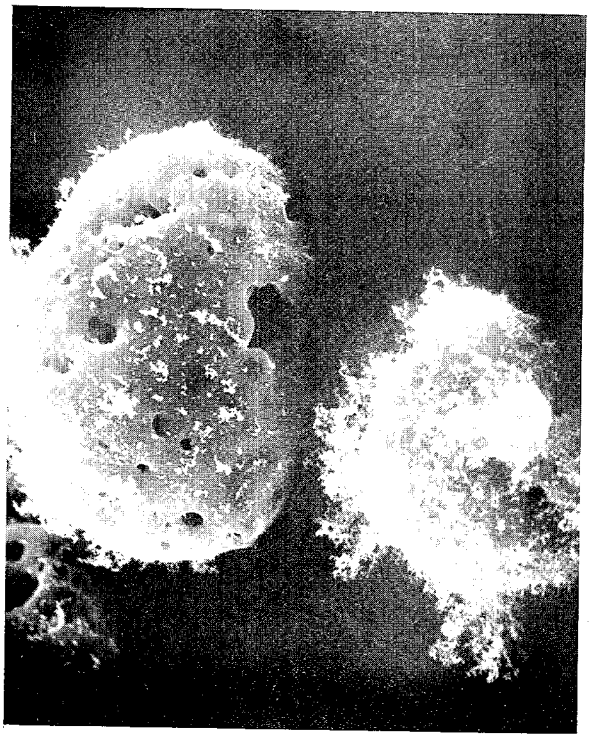

0.5 cm

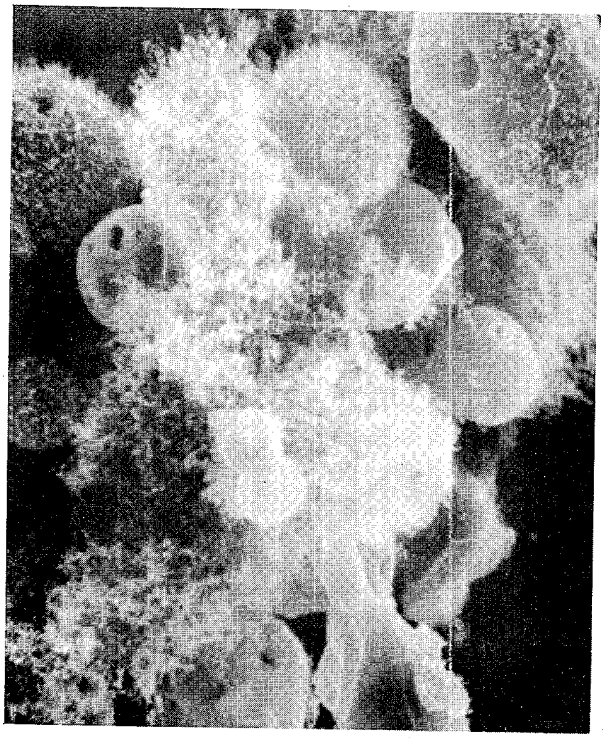

4.0 cm

10μ

Figure 86 - Scanning Electron Microscope Photographs of Typical Particles Sampled from a 10 to 20 μ Coal-Air Flame. Coal concentration was 176 mg/liter.

APPENDIX H

THERMOCOUPLE MEASUREMENTS OF FLAME-GAS TEMPERATURE PROFILES

In connection with the final coordinated series of coal-air flame sampling experiments, more extensive thermocouple traverses were made. In all cases the 6.3-cm burner honeycomb had a central, enlarged hole, effectively raising the flame several millimeters above the grid.

To achieve rapid response and to minimize radiation corrections, very small diameter thermocouple wire was used. For most of the probes, a commercially available 1 mil Pt-Pt·Rh thermocouple,[53] with a bead of about 3 to 4 mils, was used. Because it had been previously observed that a glassy coating quickly builds up on beads exposed to the coal flame, we took pains to insert the thermocouple rapidly into the burned-gas region of the coal-air flame on each initial use of a new thermocouple. The initial 1 to 8 sec were recorded on a storage oscilloscope, with simultaneous but longer term recording of thermocouple voltage on a fast strip chart recorder.

The rise time of the thermocouple was very rapid and probably limited by the mechanics of swinging the thermocouple into the flame at the chosen distance above the burner. Also, rapid, almost oscillatory variations in flame temperature could be seen on both the scope and the strip chart. These fluctuations are probably due to imperfect mixing and flow of coal-air through the burner and could correspond to the visual observation of bright areas sweeping across the burner face with even the best of our flat, stabilized flames.

The thermocouple temperature data for flames burning on the 6.3-cm burner are shown in Figures 87 through 98. The main features to be noted are the consistently higher readings during the first few seconds of thermocouple exposure, the rather high temperatures at the grid surface, the steep temperature rise near the visibly bright reaction zone and the tendency for apparent temperatures to fall as large quantities of char and soot collected on the thermocouple.

Figure 99 shows the attempt to measure temperatures through a conical flame whose center was clearly lifted from the burner grid. This flame was less stable than the flat, well-anchored, 6.3-cm burner flames and hence the temperature profile may have been broadened. It does appear, however, that in the absence of a hot grid or screen, there is still major preheating of the incoming coal-air mixture, presumably by radiation.

Considering the fact that uniform coal-air mixtures seem to burn well on small-tube burners as lifted conical flames, one can explain the observed grid temperature-flame interactions as follows. With a water-cooled grid or honeycomb, too much heat is extracted from the incoming gases to allow normal burning. Allowing the grid to heat up allows the incoming coal-air mixture to radiatively heat up in the normal fashion, resulting in a more nearly adiabatic flame.

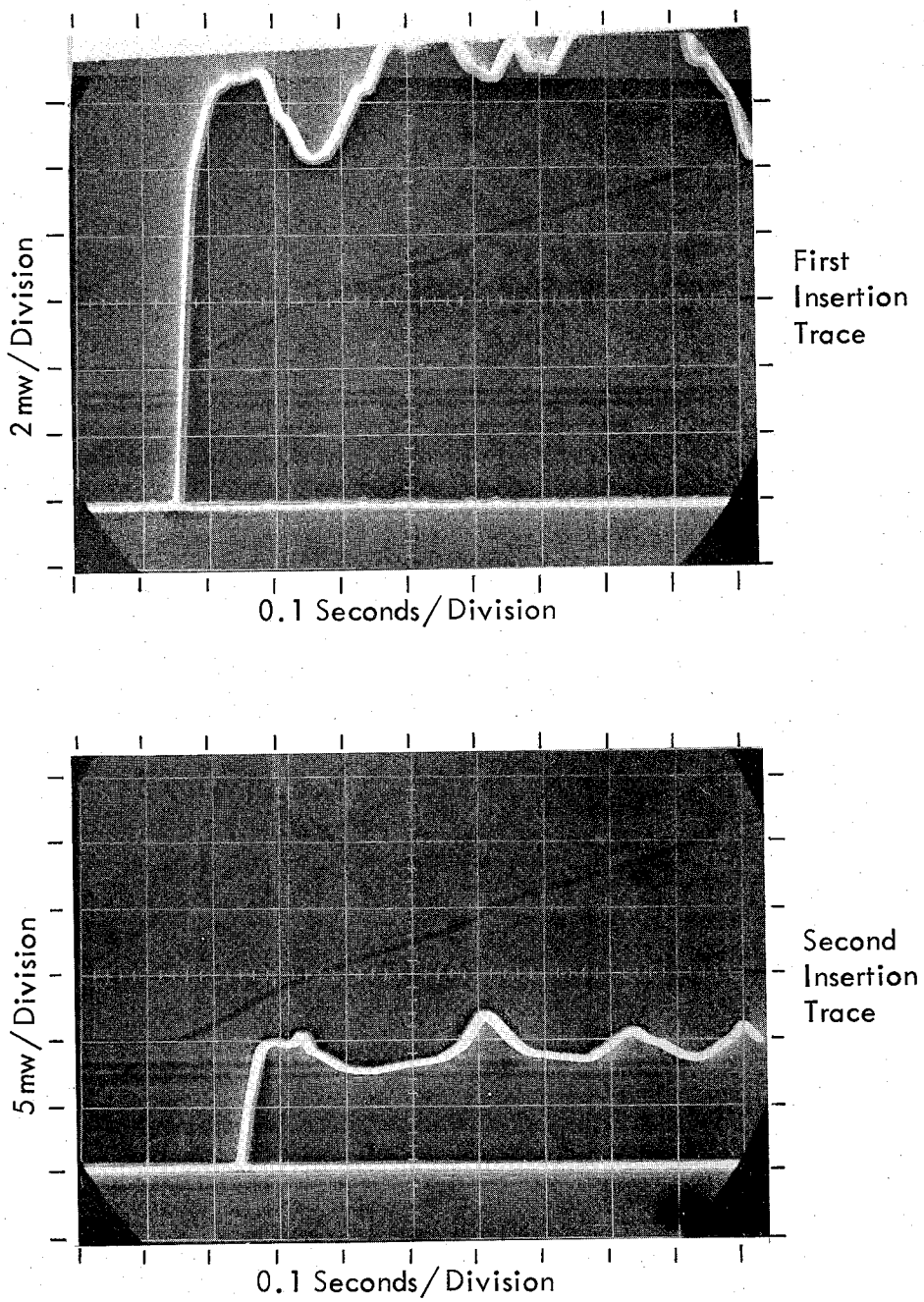

Figure 87 - Initial Thermocouple Response to Insertion in an Unsieved Coal-Air Flame at About 220 mg/liter. New 1 mil Pt-Pt·Rh thermocouple inserted at 1 cm above burner grid. These traces preceded the strip chart recorded data in Figure 88.

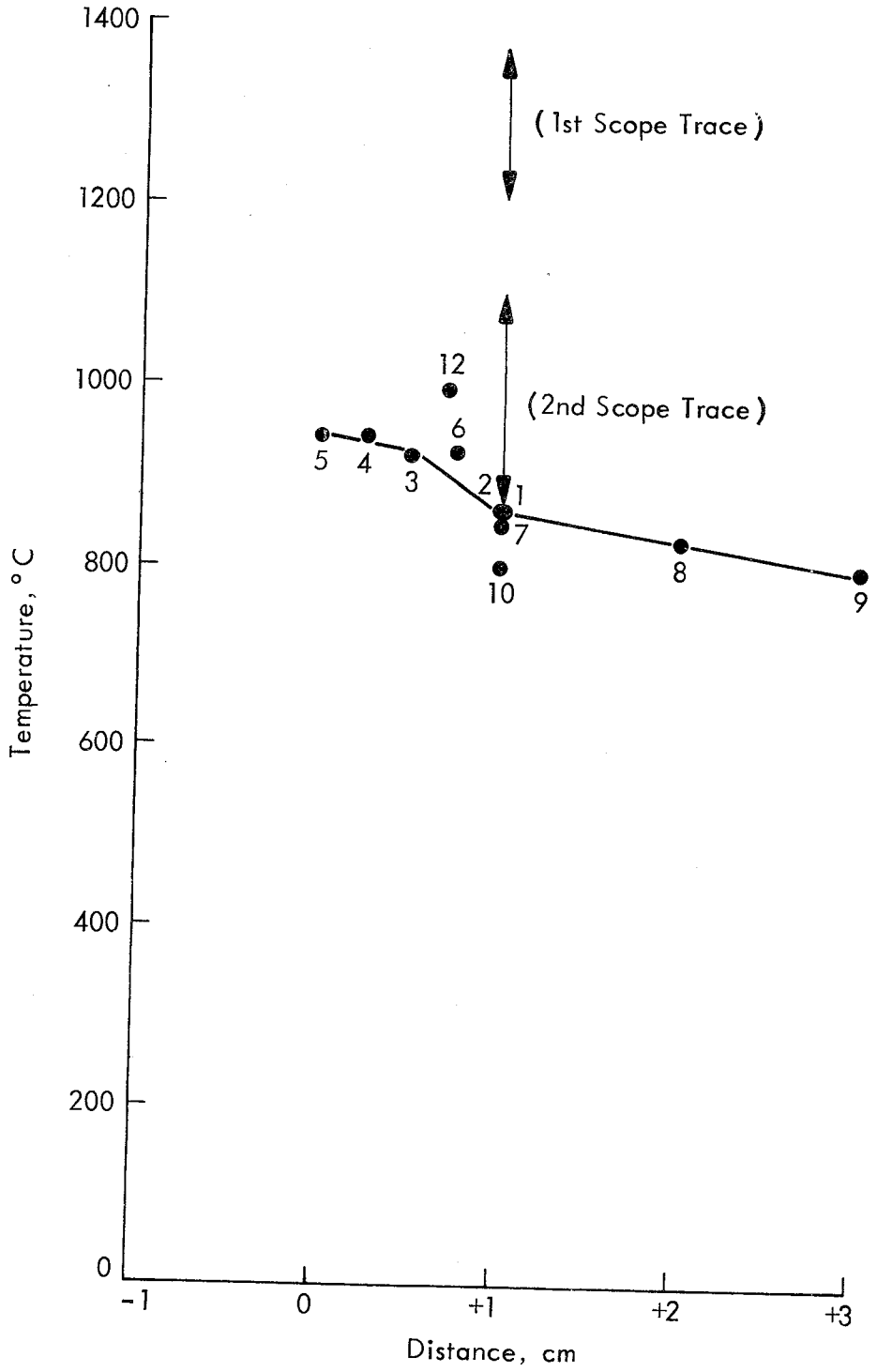

Figure 88 - Strip Chart Data for Flame of Figure 87. Numbers give sequence of measurements. All temperatures are uncorrected. Coal concentration varied from 266 mg/liter to 224 during this sequence.

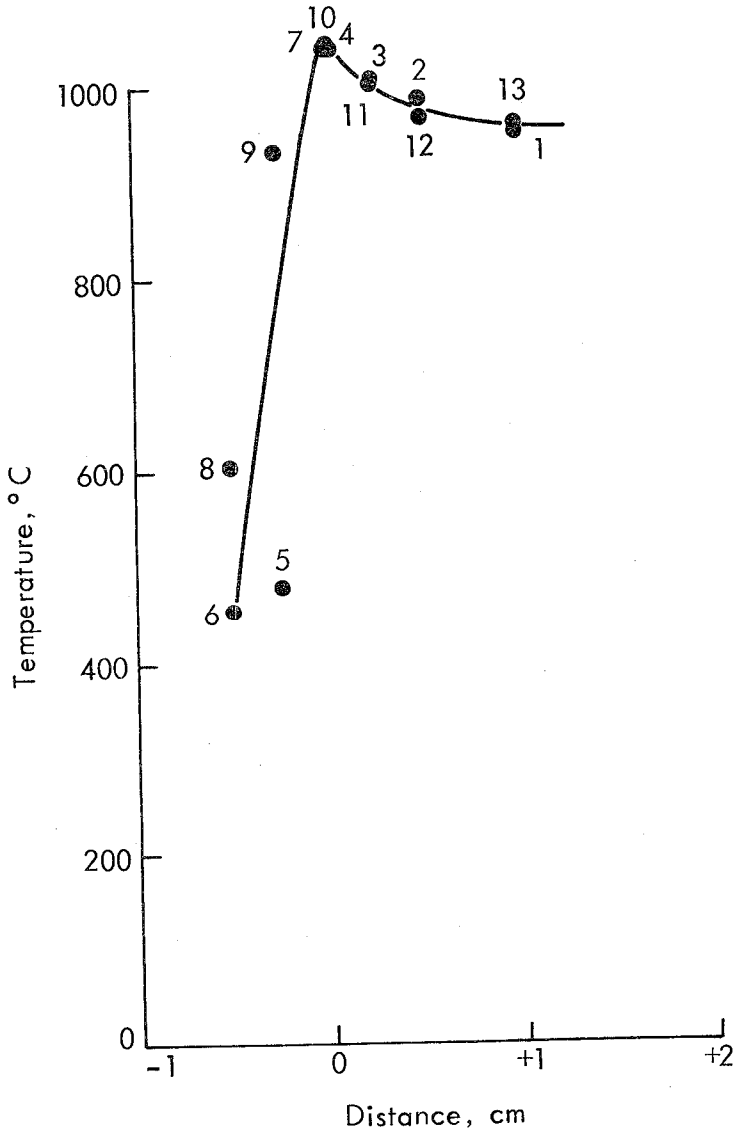

Figure 89 - Same Flame as for Figures 87 and 88. Second traverse. Thermocouple was cleaned and bent to permit it to penetrate into central hole in honeycomb grid. Coal concentration varied from 224 to 206 µg/liter.

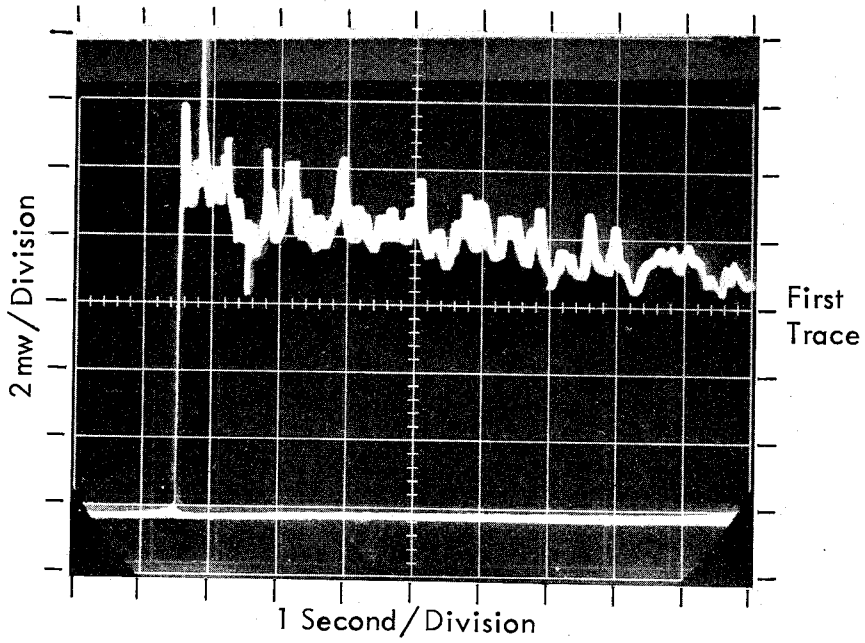

Figure 90 - Initial Thermocouple Response. New thermocouple 10 to 20 μ coal at 220 mg/liter. Data precedes strip chart record shown in Figure 91.

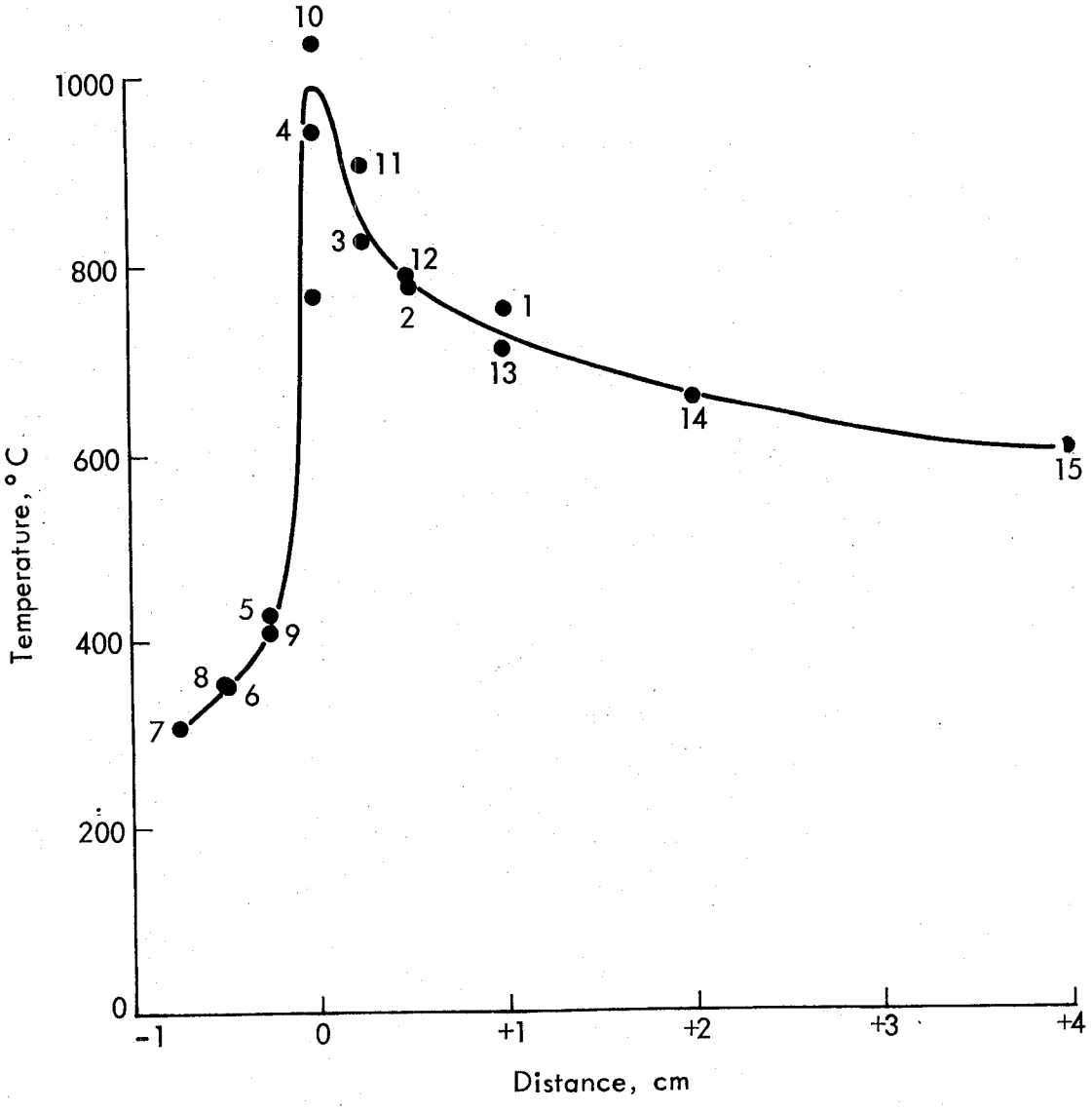

Figure 91 - Strip Chart Data for Flame of Figure 90. Coal concentration varied from 220 to 189 mg/liter.

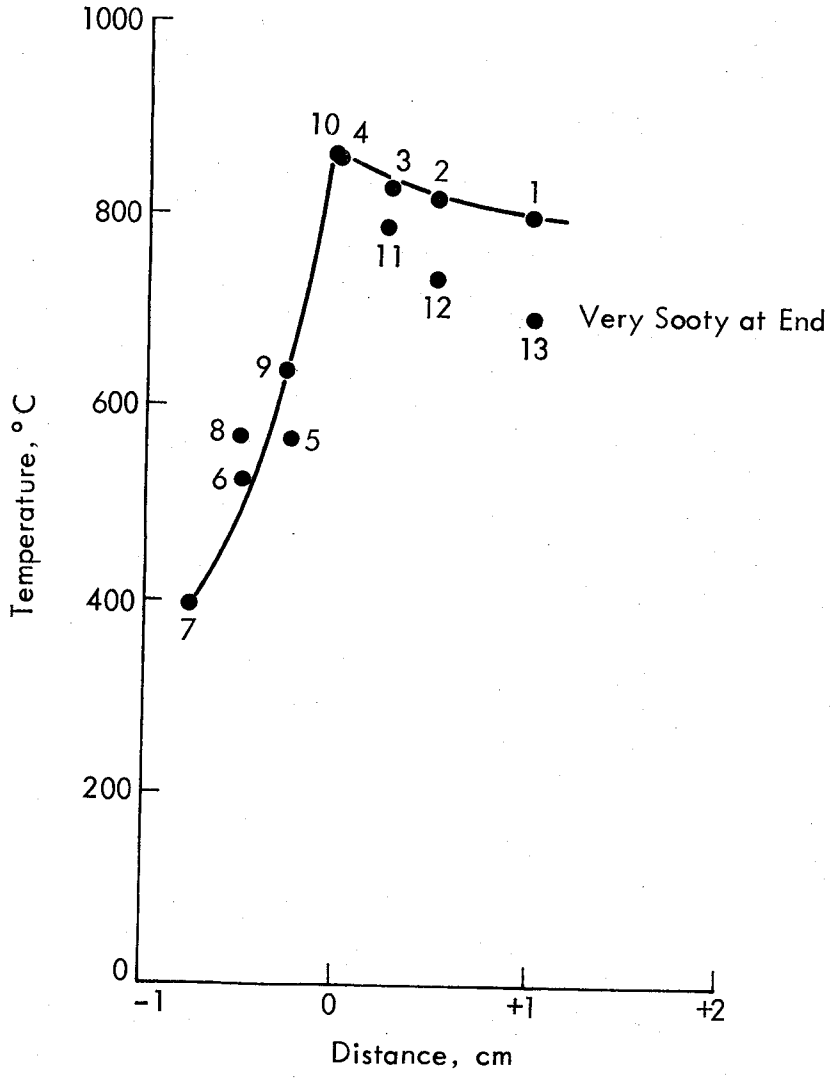

Figure 92 - Same Flame as for Figures 90 and 91. Coal concentration varied from 189 to 139 mg/liter. Second traverse after cleaning thermocouple.

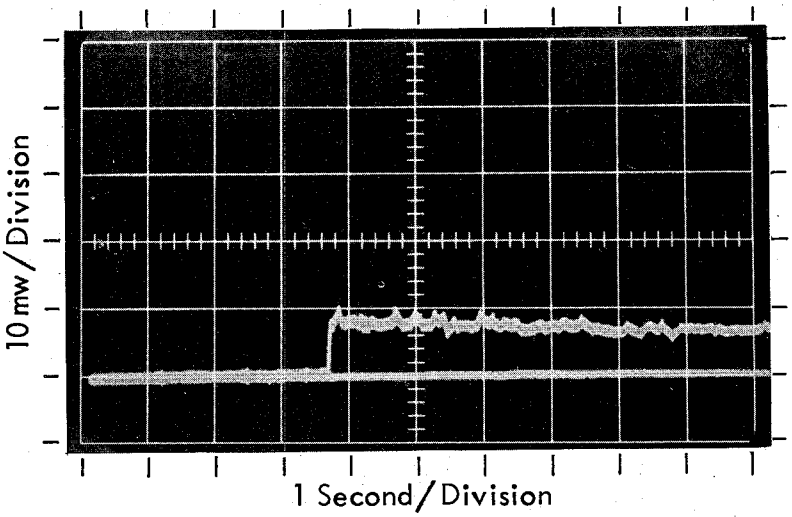

Figure 93 - Initial Thermocouple Response. New thermocouple 10 to 20 μ coal at 272 mg/liter. Data precedes strip chart records in Figure 94.

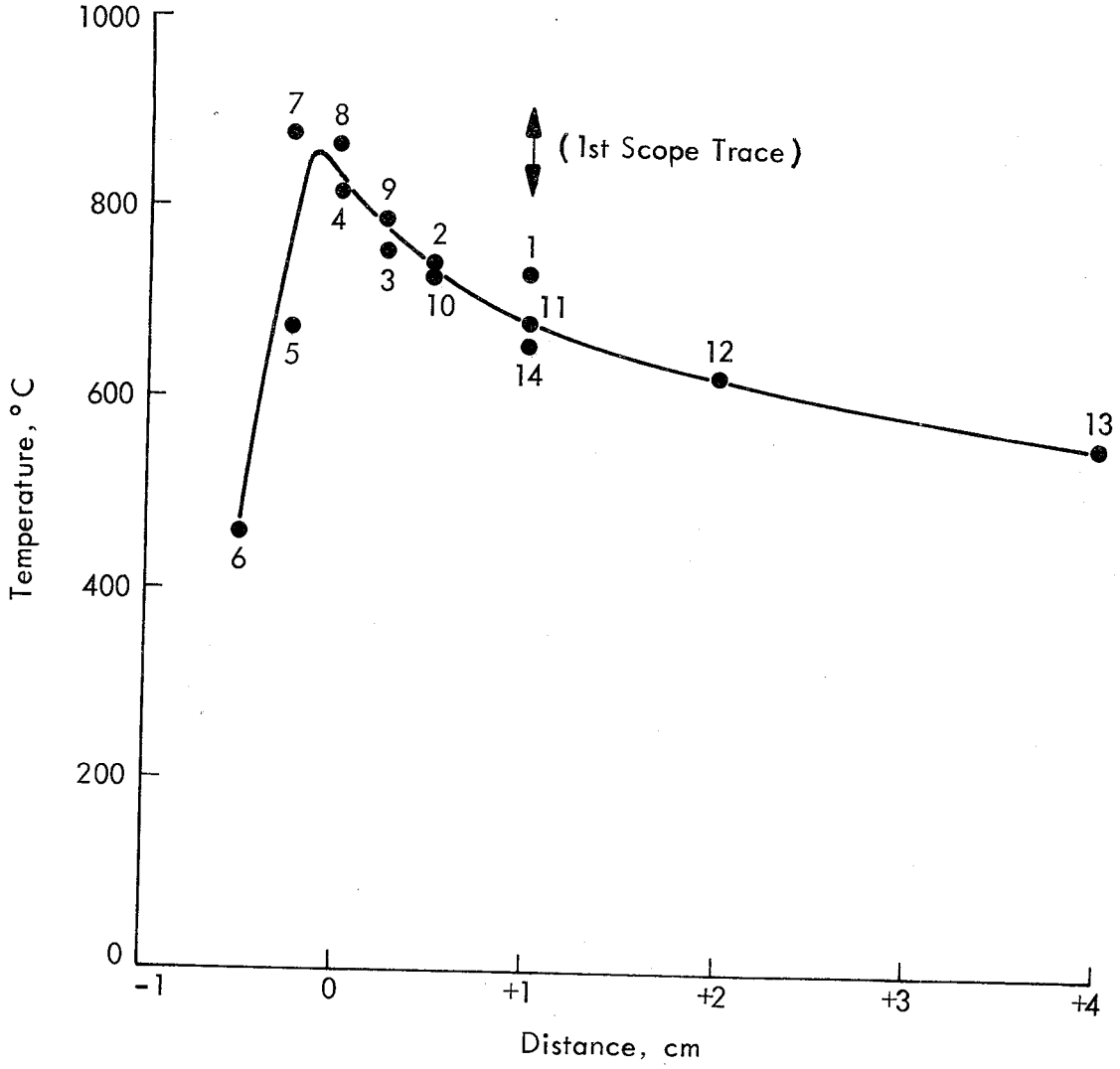

Figure 94 - Strip Chart Data for Flame of Figure 93. Coal concentration varied from 272 to 206 mg/liter.

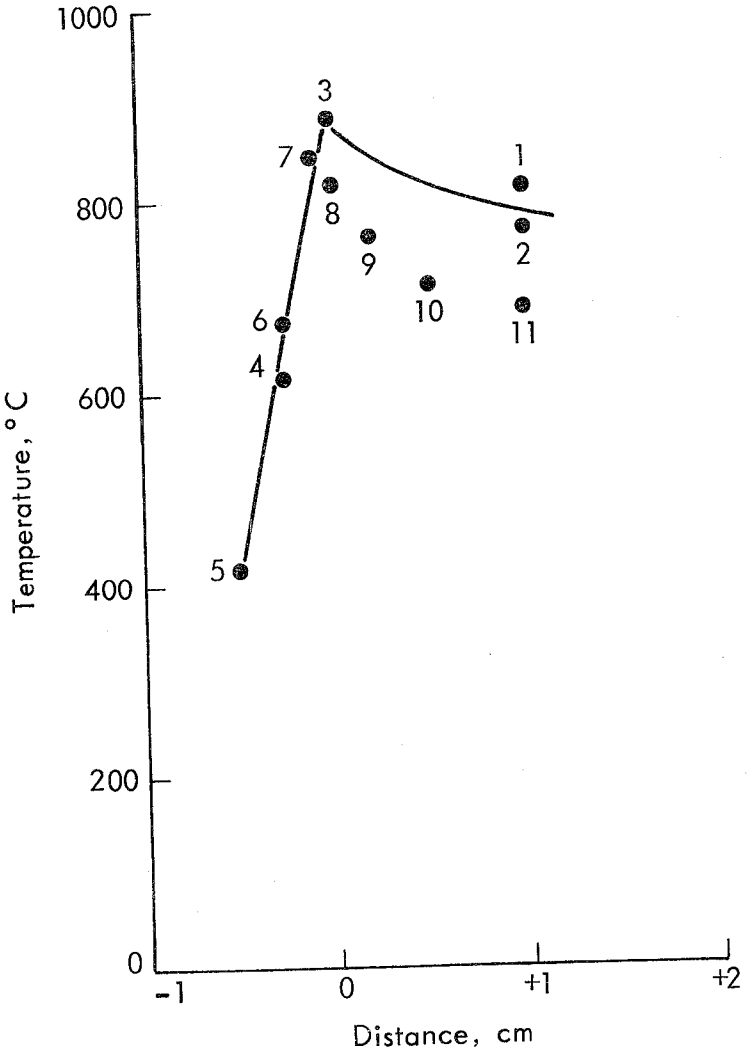

Figure 95 - Same Flame as for Figures 93 and 94. Second traverse after cleaning thermocouple. Coal concentration varied from 272 to 206 mg/liter.

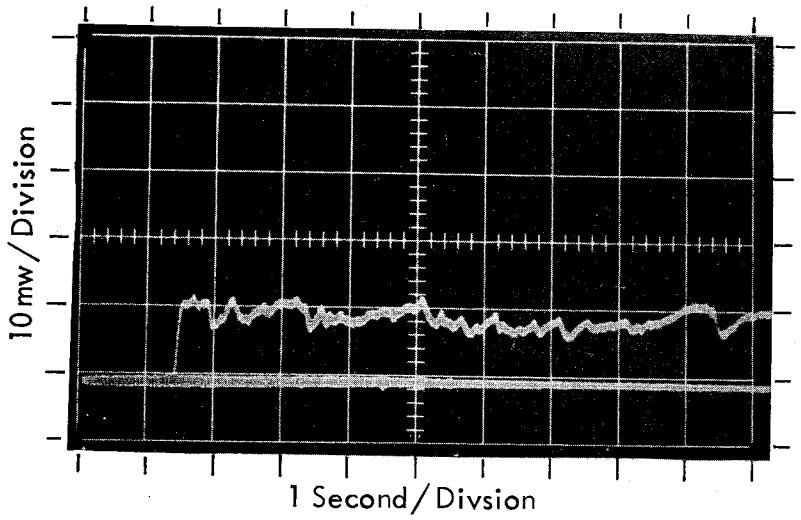

Figure 96 - Initial Thermocouple Response. Used thermocouple 10 to 20 μ coal at 201 mg/liter. Data precede strip chart record of Figure 97.

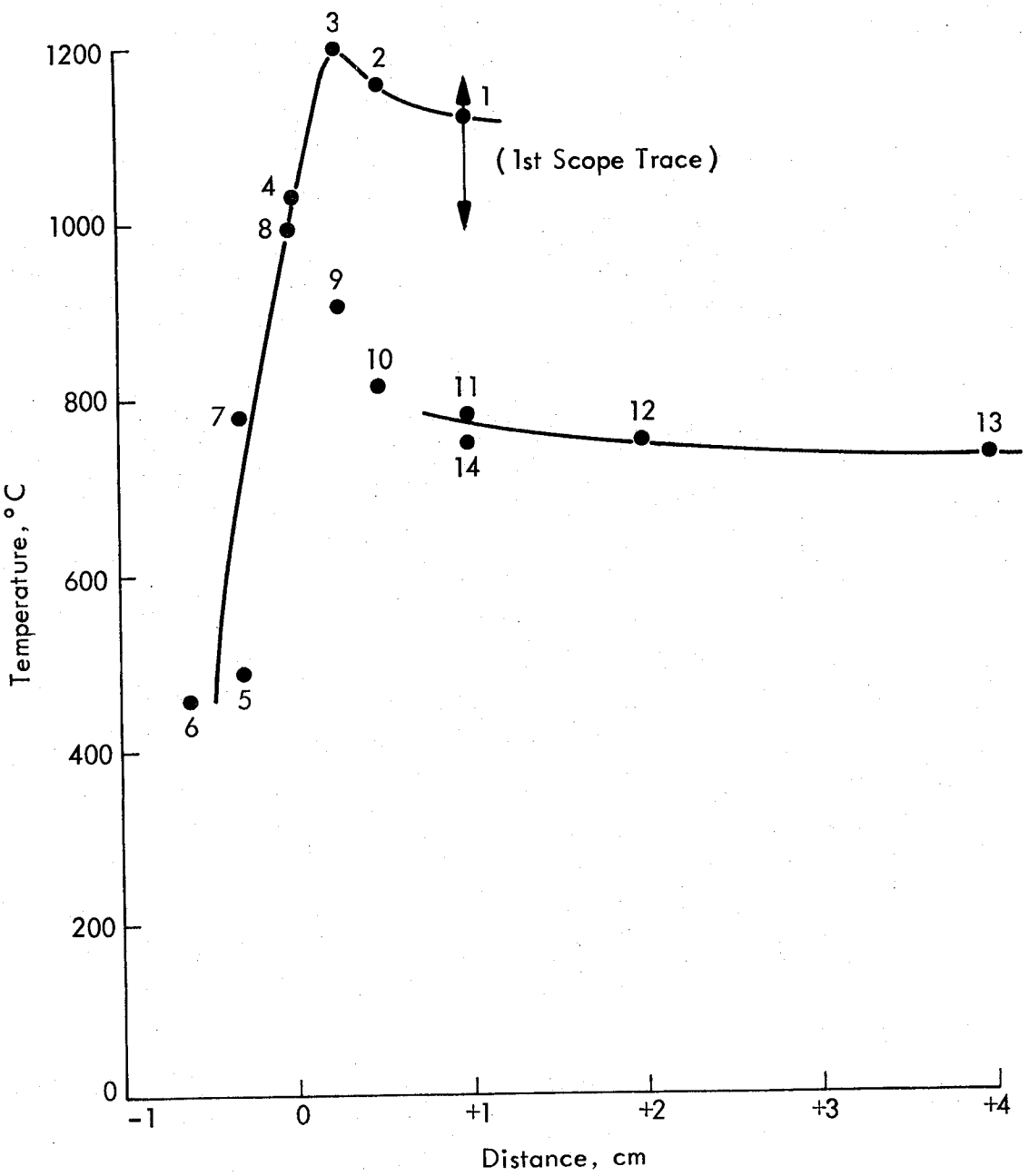

Figure 97 - Strip Chart Data for Flame of Figure 96. Coal concentration varied from 201 to 119 mg/liter.

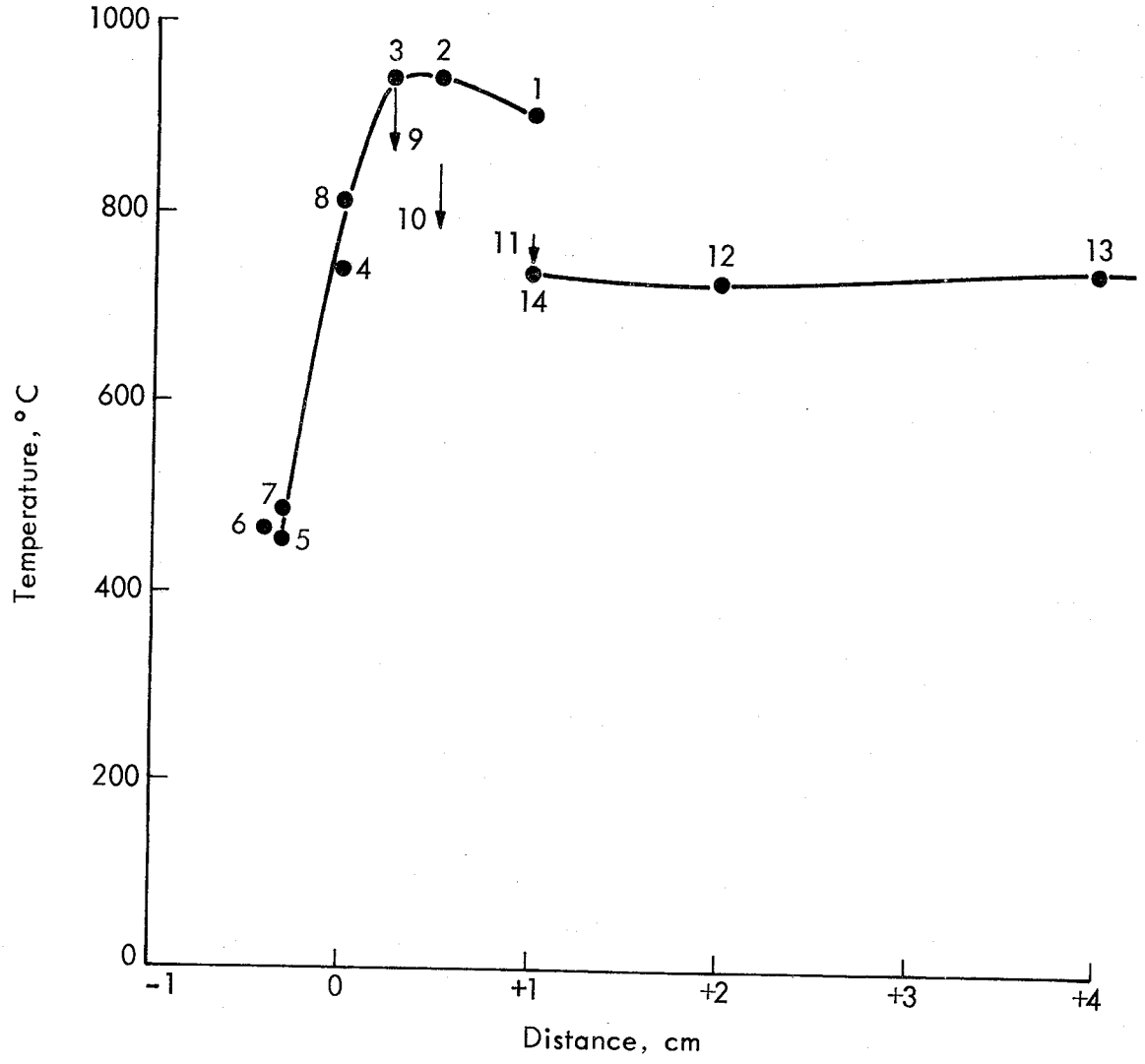

Figure 98 - Same Flame as for Figures 96 and 97. Second traverse after cleaning thermocouple. Coal concentration varied from 119 to 190 mg/liter.

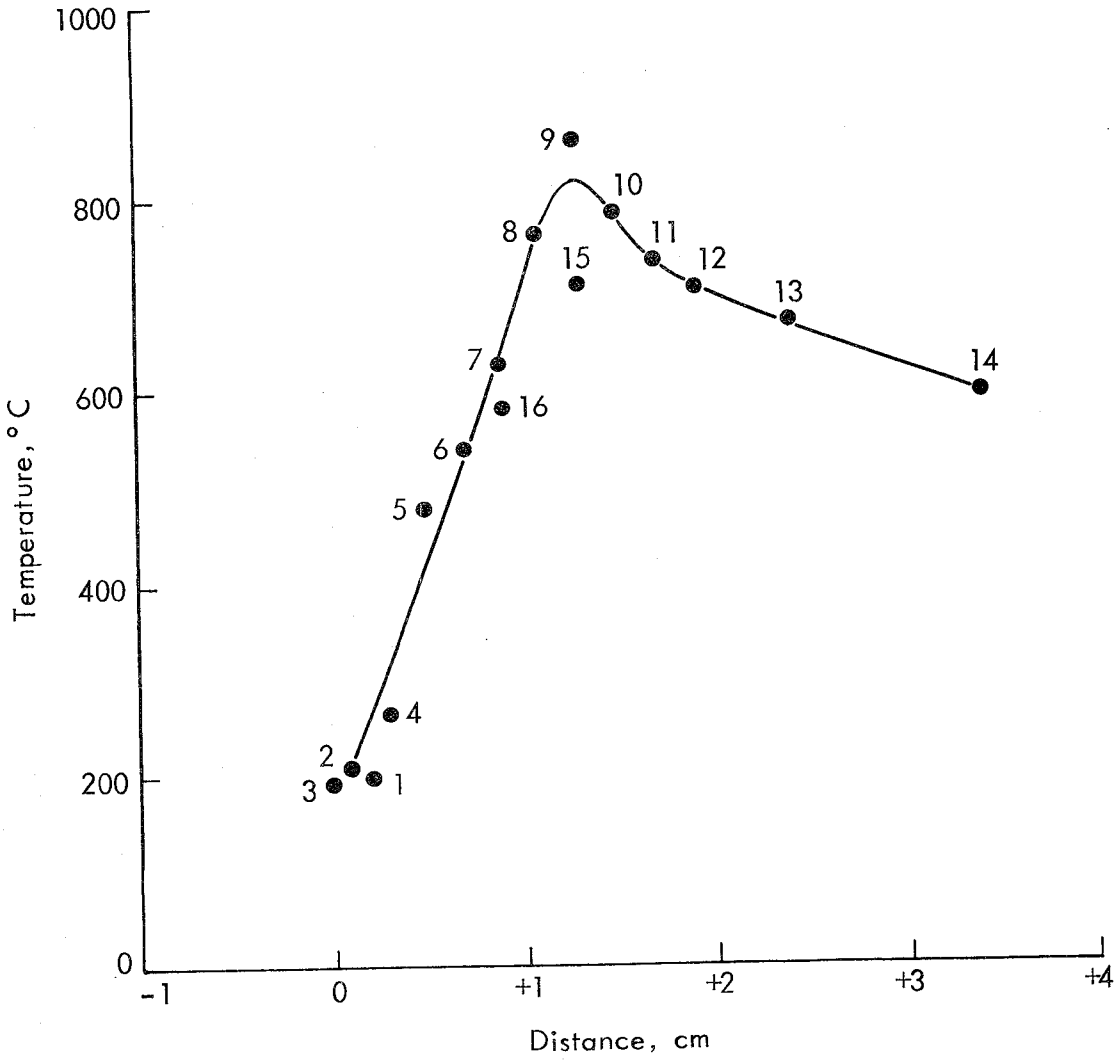

Figure 99 - Temperature Profile Through an Unsteady Conical Flame Burning on an Upright, 3-cm Diameter Metal Burner With Screen Wire Grid. Used thermocouple. Air flow was 6.0 liters/min. Coal concentration, 253 mg/liter. The bright reaction zone was estimated visually to center at 1.5-cm distance.

It is possible that the difficulty Howard and Essenhigh experienced in stabilizing their enclosed flames, without extensive preheating of the refractory walls, was due to their use of a water-cooled entry grid.

Further probing of lifted, Bunsen burner-like conical flames, for gaseous and particulate species as well as for temperature, should be most rewarding.

APPENDIX I

COAL-AIR FLAME QUENCHING BEHAVIOR

I. INTRODUCTION

During an extended phase of work, exploratory experiments were performed, using equipment and techniques developed over the past 3 years, in an attempt to provide semiquantitative information about the quenching diameter for propagation of coal dust-air flames through tubes of small diameter. An understanding of the quenching behavior should be helpful in assessing the explosion hazards which may be involved in practical coal handling and mining situations as well as indicating the scale at which laboratory studies of coal explosions and flames can be studied.

In these studies, flames were successfully propagated through tubes ranging in diameter from 6.3 cm down to 1 cm. Mixtures ranging from moderate to quite rich were tested using an unsieved, and a 10- to 20-μ size fraction, of Pittsburgh seam coal.

This section describes the apparatus used for the experiments and gives a summary of the quenching observations that were made.

II. QUENCHING APPARATUS

A major problem in studying the propagation behavior of dust flames in tubes is that uniform dispersal of the coal dust is very difficult to achieve. The powder delivery and dispersal system described earlier was used for these studies. The coal feeder consisted of a fluidized bed from which dust was extracted. From there the dust was mixed with additional air as it entered the apex of a conical burner terminated by a honeycomb or wire-screen grid. Visual observation of the flame stability and uniformity provided a qualitative indication of the uniformity of the coal dust delivery system. The quenching tubes (which consisted of glass, plastic, or metal tubes of various sizes) were either hand held or clamped in place downstream of the burner grid. Both upright and inverted configurations were used.

The ignitors used for these studies ranged from a methane-air flame on a Bunsen burner, which is a fairly powerful source, to the more gentle ignition of a kitchen match. A laboratory striker-ignitor also was capable of lighting coal dust-air flames. In some cases the coal dust-air flame could be stabilized on the end of the tube and simply allowed to propagate through the tubes by reducing the air velocity, thus completely eliminating the effect of the ignitor on the propagation.

The normal procedure for producing a propagation flame was to hold the tube about 1 cm downstream of the burner until steady flow was achieved, and then to ignite at either the upstream or the downstream end of the tube.

The coal concentration was measured by collecting for 20 sec, on a weighed filter paper, all the coal from the end of the explosion tube.

Two rolls of movie film were used to record ignition, propagation and quenching under a variety of configurations. A close examination of the films by stop-action projection is helpful in examining the effect of ignition source, and gives a crude measure of flame speed and shape.

III. SUMMARY OF QUENCHING OBSERVATIONS

In this preliminary investigation of the quenching behavior of coal dust-air flames, it was obviously impossible to obtain results for a complete matrix of quenching parameters. However, several observations were made for a limited number of cases, which may help establish new limits for the quenching diameter of coal dust-air flames, and which should help in planning and designing further quenching studies.

In Table 12 are shown some of the confugurations that were tested, along with the observations that were made. The dimensions (lengths and diameters of tubes) in Table 12 are not necessarily limits, but represent the actual tubes tested. The coal concentrations are approximate and were not carefully measured after each attempt to propagate a flame. In all cases where negative results were recorded, an attempt was made to force propagation by increasing the coal concentration.

All of the tests were made with either unsieved Pittsburgh seam coal dust or with a 10- to 20-μ cut of the same coal. All of the unsieved coal tests were made with the coal-air mixture traveling in the downward direction because when flowing upward the air speed necessary to eliminate fallout in the tube was too great.

In all of the tests, the necessity for uniform coal dispersal was apparent. An improvement over the open tube was made by attaching an extension with a screen on the end as shown in Figure 2 of Table 12. This technique appeared to decrease turbulence, which develops rather quickly in the larger diameter, open tubes. A steady flame on the lower screen served as an indicator of uniform dispersal.

TABLE 12

SUMMARY OF QUENCHING OBSERVATIONS

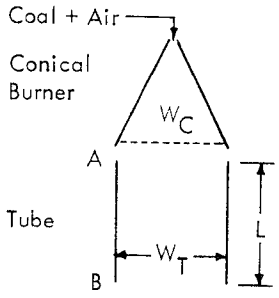

Figure 1

L (cm)	W_C (cm)	W_T (cm)	Coal	Coal Concentration (mg/ℓ)	Ignitor	Results and Observations
30	6.3	6.3	Unsieved	240	Bunsen burner	Ignition at B - Flame propagates to A Ignition at A - Flame does not propagate to B
15	6.3	6.3	Unsieved	240	Kitchen match	Flame will not propagate to A unless flow is smoothed by temporarily holding screen at B
10	3.0	3	Unsieved	Fairly rich	Kitchen match	Flame propagates from B to A causing ignition of flat flame on screen. (Probability for "successful" propagation is greater when grid is hot.)

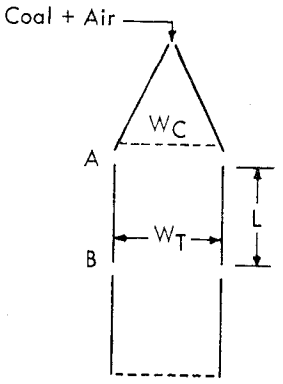

Figure 2

20	6.3	6.3	Unsieved	370	Kitchen match	Ignition at B - Flame propagates to A
30	6.3	6.3	Unsieved	370	Kitchen match	Does not propagate from B to A
30	6.3	6.3	Unsieved	370	Bunsen burner	Ignition at B - Flame propagates to A
40	6.3	6.3	Unsieved	370	Bunsen burner	Does not propagate all the way from B to A

TABLE 12 (Continued)

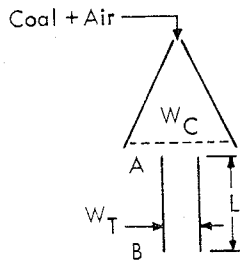

Figure 3

L (cm)	W_C (cm)	W_T (cm)	Coal	Coal Concentration (mg/ℓ)	Ignitor	Results and Observations
10	6.3	3	Unsieved	~ 300	Kitchen match	Ignition at B - Flame propagates through tube to light flat flame at A
20	6.3	3	Unsieved	~ 300	Kitchen match	Does not propagate from B to A
20	6.3	3	Unsieved	~ 300	Bunsen burner	Ignition at B - Flame propagates to A (only by trapping hot gases in end of tube)

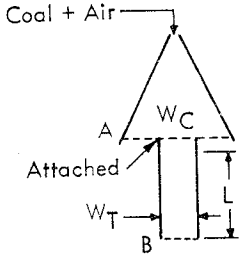

Figure 4

2.5	6.3	2	Unsieved	275	Kitchen match	Flat flame burns on lower screen (B)
2.5	6.3	1	Unsieved	275	Kitchen match	No conditions were found which would stabilize flame on lower screen (B)

TABLE 12 (Concluded)

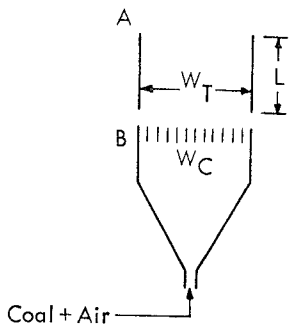

Figure 5

L (cm)	W_C (cm)	W_T (cm)	Coal	Coal Concentration (mg/ℓ)	Ignitor	Results and Observations
53	6.3	6.3	10-20 μ	298	Kitchen match	Ignition at B - Flame propagates to A
63	6.3	6.3	10-20 μ	297	Kitchen match or Bunsen burner	Ignition at B - Propagates to approximately 10 cm from A
30	3.0	3	10-20 μ	~ 300	Kitchen match	Ignition at B - Flame propagates to A (on 3 cm burner - grid is wire screen)

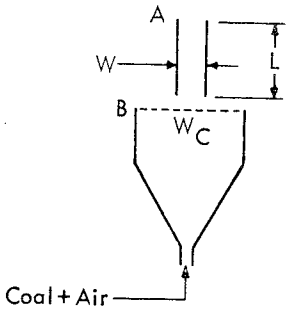

Figure 6

10	3.0	1	10-20 μ	275-360	Kitchen match	Flame stabilizes at A--then propagates to B when tube is moved to side or when coal-air is turned off
10	3.0	1	10-20 μ	275-360	Kitchen match	Ignition at B - Flame propagates to A
8	3.0	0.8	10-20 μ	275-360	Kitchen match	No conditions were found which would stabilize flame or propagate flame when I.D. of tube was 8 mm or less

In the 6.3-cm test using unsieved coal, three different kinds of tubes were used to test for the effect of the wall on flame propagation. The three tubes were stainless steel, transparent plastic, and transparent plastic covered with aluminum foil. Although there appeared to be a slight enhancement with stainless steel and with the covered plastic, further work needs to be done with well-controlled coal delivery and ignition sources to positively establish a wall effect.

The ignition source can play an important role in the observations made, particularly with the short tubes and with upward propagation of flames. When a powerful source is used it is difficult to determine the effect on upward propagating of the hot ball of gases carried up the tube by convection.

A market improvement in the propagation characteristics of 10- to 20-μ coal over that observed with unsieved coal was noted. It is not known how much of the improvement was due to better powder dispersal.

Probably the most convincing evidence that the quenching diameter for 10- to 20-μ coal dust is 1 cm or less was provided by the observation that a flame which was stabilized on the upper end of a 1-cm diameter Pyrex tube propagated downward through 10 cm of tube length when the inlet flow was stopped. It is interesting to note that the 1-cm quenching diameter measurement is in agreement with that found in experiments by Litchfield[54] in which coal dust-air mixtures are ignited by a parallel plate electrode spark discharge. It is not yet clear from our preliminary work whether the failure to propagate a flame through an 8-mm tube results from an inherent quenching diameter limitation or is due to an inadequate powder dispersal system.

APPENDIX J

DRY-POWDER INHIBITION MECHANISM STUDIES

I. INTRODUCTION

The second major objective of the experimental work was the determination of the fate of flame-inhibiting agent particles in coal dust-air flame. The initial work has been done with methane-air flames to simplify the studies. Both physical breakup and evaporation of dry powder inhibiting agents were of interest.

II. BREAKUP OF DRY POWDERS IN FLAMES (TASK II)

One of the feasible methods of determining the changes in inhibitor particles as they pass through the reaction zone of a flame involves the use of direct sampling followed by the subsequent collection and analysis of the particles. In free-jet sampling the gas-particle mixture is expanded through a small, thin orifice into a vacuum in an unconfined expansion. Since the gas-particle mixture is drawn from a region extending less than two sampling orifice diameters from the orifice, the use of gas sampling orifices having 0.005 to 0.025 cm diameter should provide adequate spatial resolution for a coal dust-air flame. Since the free-jet is divergent (and since the particle density will be low), the individual particles can be isolated and collected on a suitable target. Two potentially serious problems with such vaccum sampling are (a) the sampling is extremely nonisokinetic and (b) the impact velocities of particle are uncertain and hence bouncing and collection efficiencies can not be known a priori.

Once the particles have been isolated and collected, they can be examined by electron and optical microscopy. Scanning electron microscopy appears to be particularly suitable because of its convenience, depth of field, and ability to reveal the surface structure of particles. Scanning electron microscopy can also be used with an x-ray or auger attachment to determine the compositions of individual particles. Optical microscopy is more limited, but quite useful for large particles and for preliminary qualitative diagnostic studies.

A. Apparatus

1. Sampling system: A single-stage particle sampling system was assembled and tested. This apparatus, which is shown in Figure 100, is pumped by a 3-cfm mechanical pump. A 6-in. diffusion pump could be added without modification if lower pressures are required. Pressures are measured by NRC Alphatron and McLeod gauges. The sampling probe consisted of a 0.025-cm thick, spun, 90-degree cone of platinum-rhodium

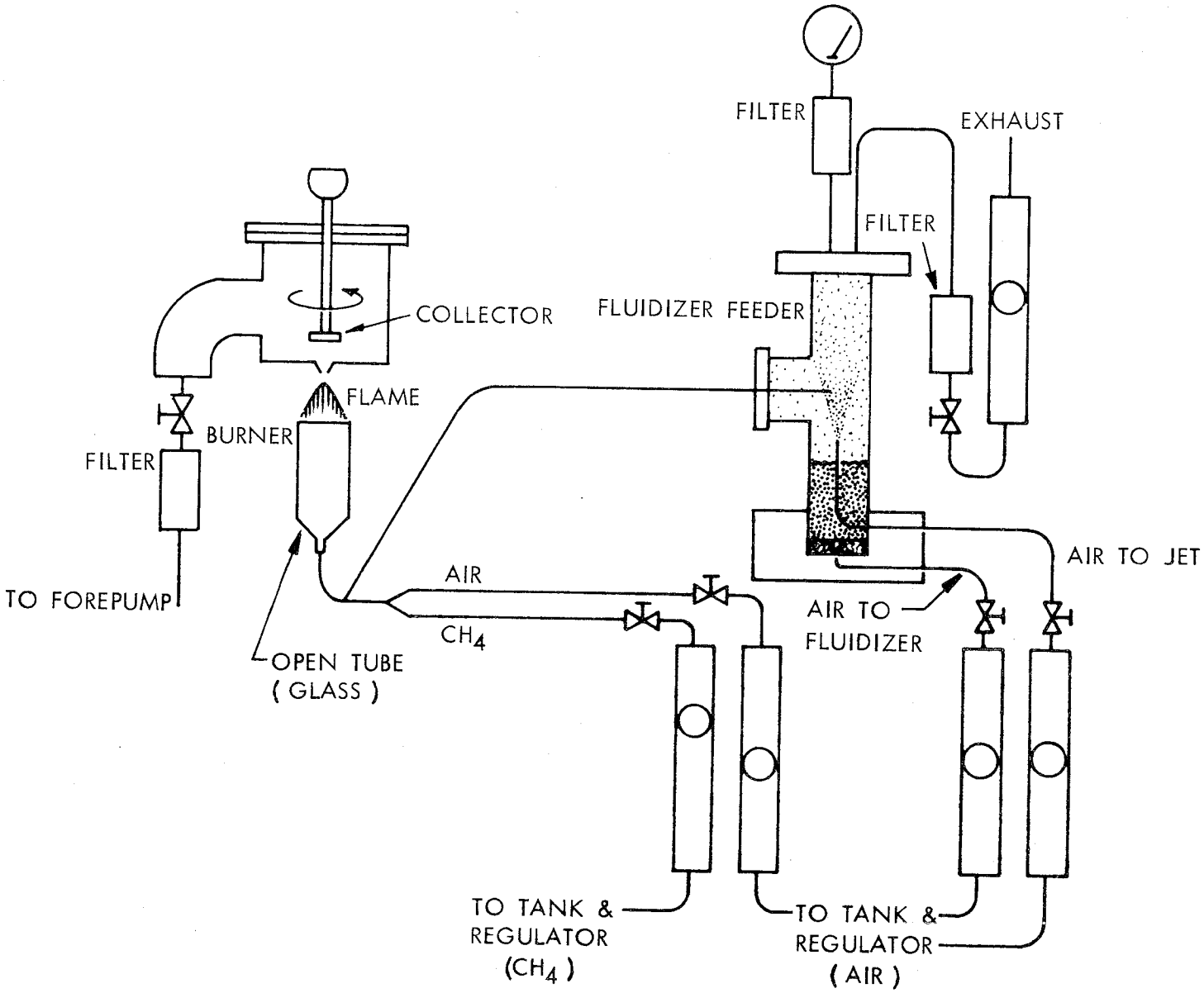

Figure 100 - A Schematic of the Gas and Powder Delivery Systems and the Burner, Flame and Sampling System used in Task II

alloy soldered to a water-cooled plate with the sampling orifice drilled in the tip of the cone. For the preliminary studies, a 0.025-cm diameter orifice was used. With this orifice, pressures of 1 to 2 torr were achieved in the sampling chamber.

The sampling system can also be used with the orifice placed on the top of the "T" shown in Figure 100 and the collecting device brought in from the bottom. Experiments were carried out in both configurations, as described below.

2. Inhibitor powder delivery system: The low-density particle feeder chosen for the introduction of fire-inhibiting particles into test flames is shown in Figure 100. This device is similar to the coal dust feeder discussed earlier and was adapted from the work of Hamor and Smith.[43] This particle feeder differs from the coal-dust feeder in that the particles are extracted from above the fluidized bed, where they have been carried by a small jet mounted in the bottom of the feeder. Unsieved Purple-K is delivered in an easily visible, laminar plume that extends 10 to 15 cm beyond the burner mouth (unignited). Fluidization of the bed was indicated by a substantial rise in powder level with fluidizer flow. A vibrator was necessary to achieve steady delivery.

The concentration of powder was chosen so that a barely visible slowing of flame speed can be detected by enlargement of the conical flame front. Under these conditions a large amount of light from the inhibitor-flame interaction is produced, and can be monitored as a measure of stability of powder delivery. To simplify interpretation of experiments the results to be reported below were obtained using size-fractionated samples of rather large (44 to 53 μ) particles.

3. Burners: The successful sampling of particles from various well-defined regions of a premixed CH_4-air flame requires a steady, laminar flow from a small burner.

The burner system chosen was simply a long Pyrex tube of 1.1 cm ID to which was fed premixed CH_4-air plus the air-transported inhibitor powder. The burner was clamped to a precision milling machine table, which was mounted on a solid stand, so that the burner-sampling orifice distance could be reproducibly varied and measured by 0.0025-cm increments. The gas and powder were introduced through flexible tubes from the fluidizer-feeder whicx was also mounted on the milling machine X-Y table.

4. Particle collectors: As the particles and hot flame gases are sampled through the orifice into a region of a few torr or less, a free-jet expansion occurs with presumed rapid quenching of gaseous reactions and without any further physical changes in the particles. A particle collector surface must be placed near enough to the orifice to collect a statistically meaningful number of particles but far enough away

to avoid thermal effects from the hot flame gases and hot orifice tip. In the studies described in this report, the collecting surface was placed about 3.2 cm away from the sampling orifice tip.

B. Particle Collection Problems

One of the major experimental problems has been to produce a sticky collector surface that is stable in vacuum, resists the heat from flame-gas sampling, provides a smooth, optically clear substrate for microscopy of collected particles, and collects a large fraction of the impinging particles.

Tests were first undertaken to find a target material which was an efficient collector of the high velocity particles and which was also suitable for microscopy. Microscope slides were tried, but were found to be inefficient collectors of 1 μ and larger carbon particles, even when coated with silicone diffusion pump oil or when cleaned by flame heating (to the annealing point). A reasonably satisfactory target material was found to be Scotch Tape, which appears to collect a large fraction of inhibitor powders. A number of problems occurred with the Scotch Tape, including a tendency to scorch and wrinkle in the sampled hot gases and difficulty in applying the tape, wrinkle free, to the substrate.

Following a suggestion by Dahneke[55] we tested the direct coating of microscope slides with Dow Corning 200 Fluid (viscosity 60,000 cs). Good streak-free coatings were obtained by spreading a 1:1 solution of the 200 Fluid in toluene directly on the glass with the aid of a "doctor's blade." Coatings of about 25 μ thickness, resulting from evaporation of the toluene, have shown good ability to collect glass beads. The behavior of this coating with hot flame gases initially appeared superior to that obtained with Scotch Tape. However, subsequent studies on another program[56] revealed that a severe wetting-meniscus problem occurs with this oil, making optical photomicrographs very hard to interpret.

C. Sampling Results with Purple-K and Monnex

In order to sample under the least ambiguous conditions and to look for gross decrepitation phenomena, the initial inhibitor sampling studies were done under the following conditions: (a) a sieved fraction (44 to 53 μ) of both Purple-K and Monnex was used; (b) the burner was inverted so that powder delivery and sampling were aided by gravity; and (c) double-backed transparent cellulose tape was used as the collection medium. Lighting control, contrast and photographic recording were achieved by using a Leitz microscope with 35 mm camera attachment.

A large number of collections and optical examinations were made with Purple-K and Monnex. (For details, see Ref. 58.) Although the sampling conditions and quality of the photographs left much to be desired in this series, it did appear that the large Monnex particles break up more completely than the Purple-K, at least when sampled from well into the burnt-gas region. This behavior is consistent with that observed by British workers.[57] The breakup or dispersal of adhering fines on large particles, even when sampled with cold gases through the orifice, was an unexpected observation and somewhat confused the interpretation of results.

In subsequent, more complete studies for the Ansul Company[56] it became apparent that the nonisokinetic sampling was dramatically favoring fine particles over large. Of even more serious concern was the observation that particles collected from the reacton zone and burnt gas region were extremely hygroscopic. Even a few seconds exposure to room air during transfer of the collected particles to the vacuum coater preceding scanning electron microscopy, often resulted in serious distortion of particle size and morphology due to water pickup and subsequent evaporation.

It appeared to be more profitable to use our specialized direct mass spectrometer sampling techniques to identify and observe the behavior of gaseous species evaporating from dry powder inhibitors as they passed through flame reaction zones; hence, particle decrepitation studies were stopped at the inconclusive state indicated above.

III. EVAPORATION OF DRY POWDERS IN FLAMES (TASK V)

A. Introduction

A significant uncertainty in the mode of action of dry powder agents inhibiting coal-air flames (and hydrocarbon flames as well) is the role and nature of gaseous species emanating from such agents. In the case of $KHCO_3$, and related alkali-metal containing agents, there has been much speculation about the relative importance of surface catalysis versus evaporation to gaseous K-containing species which destroy chain-branching radicals. Recent work by Kaskan[59] added significant new insight to this problem but as yet there have been few direct observations of K-containing gaseous species, particularly early in the reaction zone where their action would be most crucial to inhibition. Consequently a major goal of this phase of studies was to identify the species that evaporate from alkali and phosphorus-containing powders as they pass through high-temperature flame fronts.

B. Appraratus and Techniques

With an EAI quadrupole mass spectrometer mounted on top of the cross that comprises the ion-source housing for the Bendix TOF mass spectrometer, the molecular beam passing through the open Bendix ion source continues on to enter the EAI ion source in the axial configuration. In spite of the longer beam distance to the quadrupole (46 cm versus 25 cm for the TOF), the higher inherent sensitivity of the continuously ionizing quadrupole led to a large increase in signal/noise for flame species.

The Stage 1/2, quartz orifice was removed and a spun Pt-Rh conical orifice of 8 mils diameter replaced the skimmer orifice (see Figure 101). The powder feeder and burner systems used in Task II and described above were placed in the coal-flame hood so that the conical premixed CH_4-air flame impinged directly on the sampling orifice. With hot flame gases, Stage 1 pressures were low enough to permit good free-jet sampling conditions.

C. Preliminary Search for Gaseous Species

The first tests to detect K-containing species involved a Purple-K powder loading in the CH_4-air stoichiometric flame of about 11 mg/liter. Sampling occurred 1/2 in. downstream from the flame cone tip. The ion K^+ (39^+) was easily detected as a modulated beam component. At 70 ev ionizing energy a $39^+/28^+$ ratio of about 10^{-4} was observed, with the 28^+ being almost entirely N_2^+. The evidence for KOH^+ (56^+) was quite ambiguous. On several occasions, when powder was first admitted to the flame, the modulated, phase locked 56^+ signal seemed to go positive for a few seconds but then fell to near zero. In subsequent tests, mostly with a lower powder loading but in one case with powder added to the flame almost to the point of extinguishment, no 56^+ signal appeared. Likewise, in rich and lean flames only 39^+ was observed. Background noise at 56^+ was such that an upper limit for 56^+ of about a factor of 5 to 10 less than 39^+ was indicated. At lower powder additions, about 1.5 mg/liter, $39^+/28^+$ ratios of about 5×10^{-5} were seen, which, with no corrections for mass spectrometer sensitivity would indicate about 10% evaporation of the Purple-K.

Several brief tests were carried out on the species yielding 39^+. First, it was established that the 39^+ did not arise from an unburned fuel impurity such as propane, though this was a problem if technical grade CH_4 or natural gas was used. Second, the variation of 39^+ intensity with ionizing electron energy was measured. The results of this single experiment are shown in Figure 101. The scatter or systematic drift in intensity is due to the weakness of the signal and drifts due to powder delivery rate or orifice plugging. Also shown in Figure 101 is the ionization efficiency curve for 40^+ from Argon in the air. It appears that the K^+ appearance potential is several volts below that for Ar^+, but more extensive data

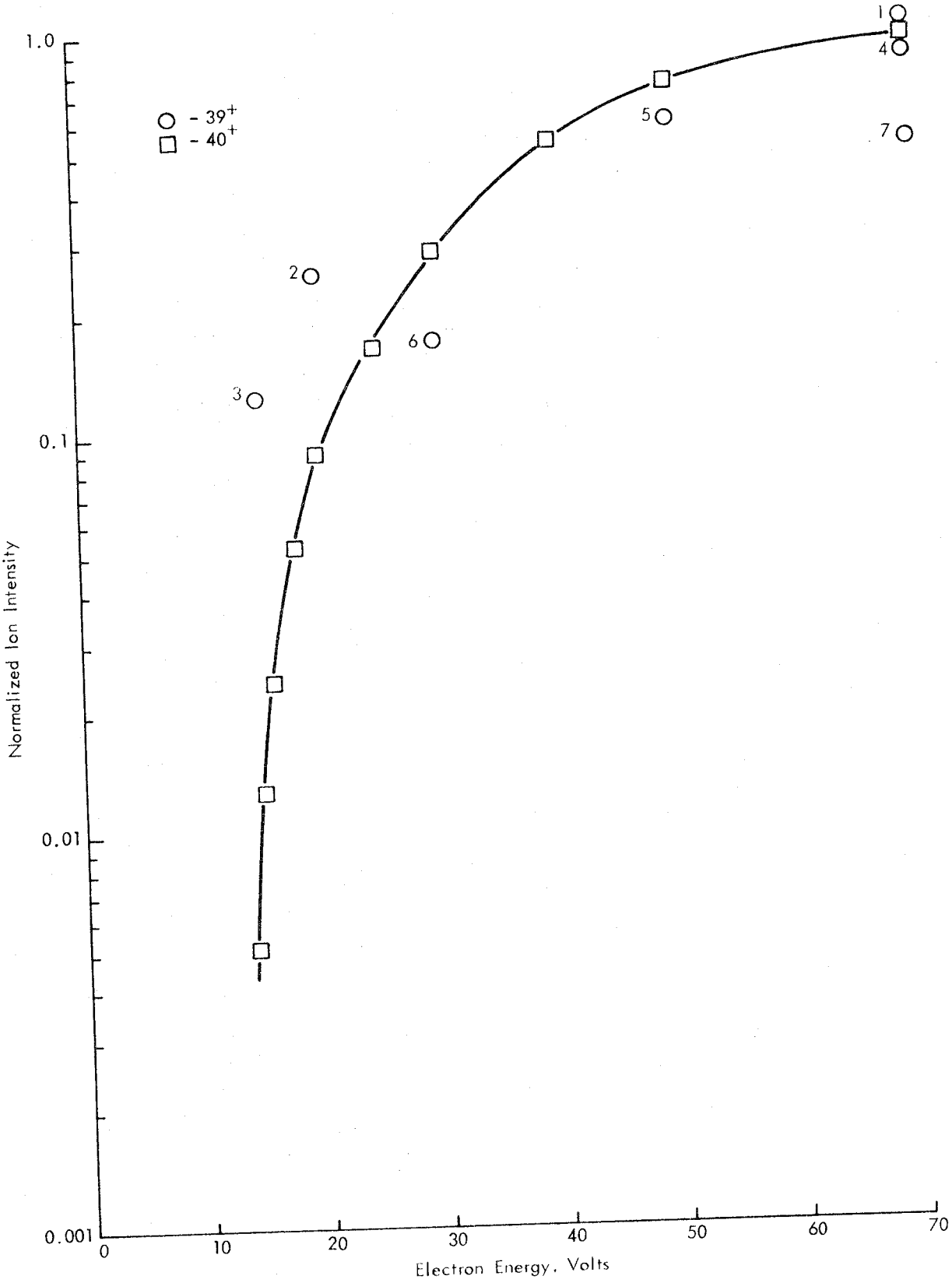

Figure 101 - Ionization Efficiency Curves for 39^+ and 40^+ from Gases Directly Sampled from a 1-Atmosphere, Stoichiometric, CH_4-Air Flame to which About 10 to 20 mg/liter of Purple-K ($KHCO_3$) had been Added. Sampling position 1/2 in. downstream of the conical tip of the flame. Power was less than 37 μ by sieving.

would be needed to determine if the K^+ comes from K(g) versus KOH(g). Third, the results of several 39 + /40$^+$ determinations made at several sampling positions in the CH_4-air flame are shown in Figure 102. The scatter in the data is quite bad and the powder delivery rate varied by a factor of two in the four separate series shown. Still it was suggestive that we were seeing the growth in K-species as the powder (less than 37 μ) passes through the flame and evaporates.

The presence of particulates in the free-jet generated molecular beam caused troublesome noise spikes all across the mass spectrum. These spikes appeared with only the quadrupole multiplier high voltages on and apparently result from ions generated when the free-jet accelerated, high-energy particles strike surfaces near the multiplier entrance.

D. Dry Powder Feeder Tests

To improve control of addition of dry powder, such as potassium bicarbonate, to coal-air flames or methane-air flames, tests of several delivery devices were carried out prior to the final evaporation-species tests. These feeders are also being used in dry powder extinguishment mechanism studies for the Ansul Company, who shared testing expenses.

Four types of feeders, or feeder operations, were compared using Purple-K in the 50-μ size range. One type of screw feeder, recently described,[60] was constructed and briefly tested, with poor results compared to the fluid-bed feeders in use. Three variations of fluidized-bed feeders were tested. One of the feeders, shown schematically in Figure 103, is easily constructed and inexpensive. It has operated quite satisfactorily in the 10- to 100-g/hr delivery range.

E. Final Series of Gaseous Species Studies

Using the new Extranuclear uadrupole mass spectrometer, we carried out a further search for species evaporating from Purple-K ($KHCO_3$) and Foray ($NH_4H_2PO_4$) powders as they passed into a CH_4-air flame. The flame chosen was a 0.9 equivalence ratio CH_4-air conical flame burning on a 1/2 in. diameter Pyrex tube. Sampling was carried out by direct, free-jet expansion through a 10-mil orifice in a water-cooled, 90-degree cone, since it is doubtful that condensible species would survive the two-stage expansion used in coal-flame sampling.

Even at powder concentrations of 10 mg/liter or less, the 10-mil orifice plugged in a matter of minutes. Further, noise spikes continued to seriously degrade signal-to-noise ratios. These spikes appear

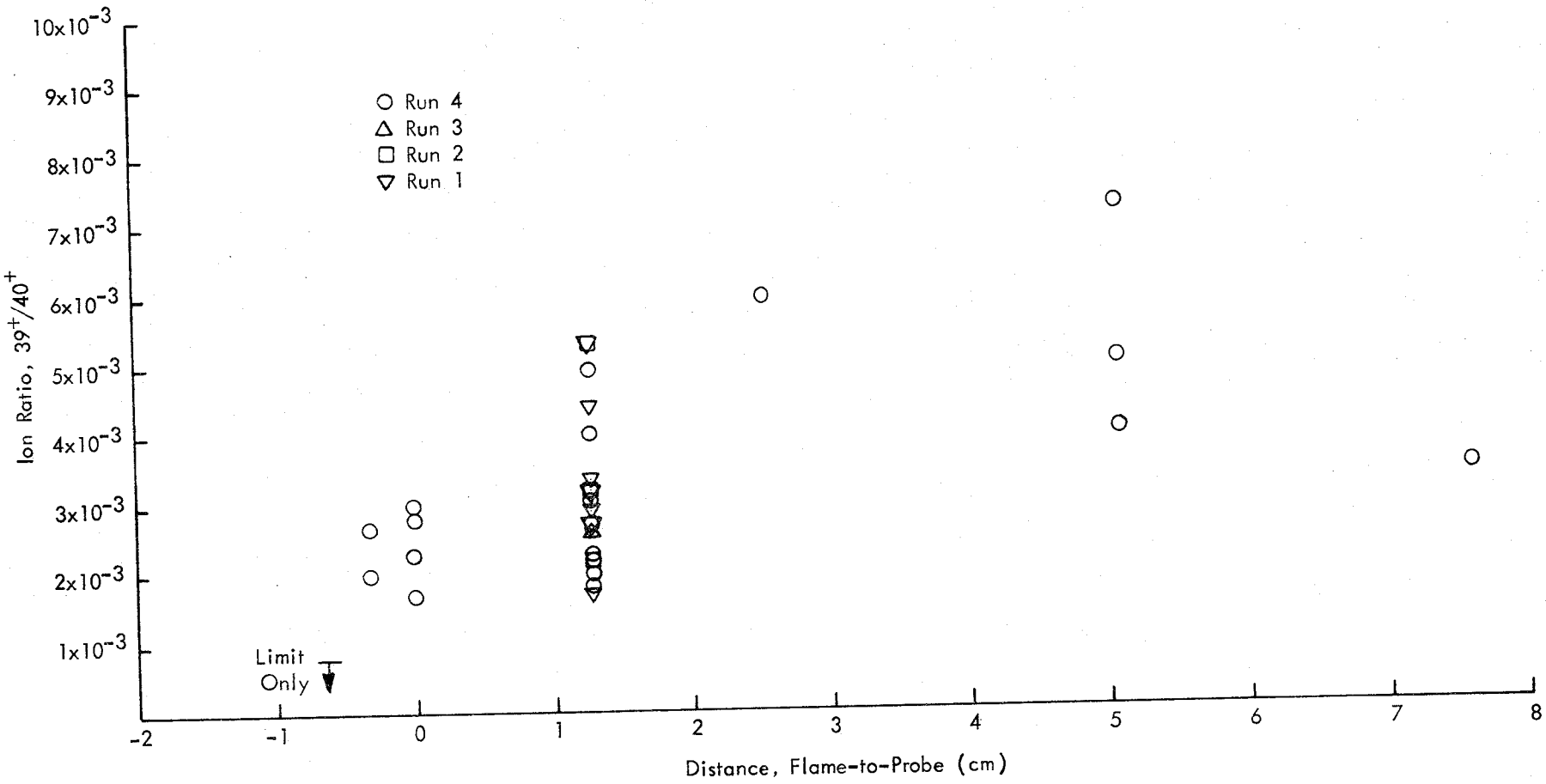

Figure 102 - Dependence of 70 ev Electron Impact Generated $39^+/40^+$ on Sampling Position in Flame. Flame and sampling conditions as in Figure 101.

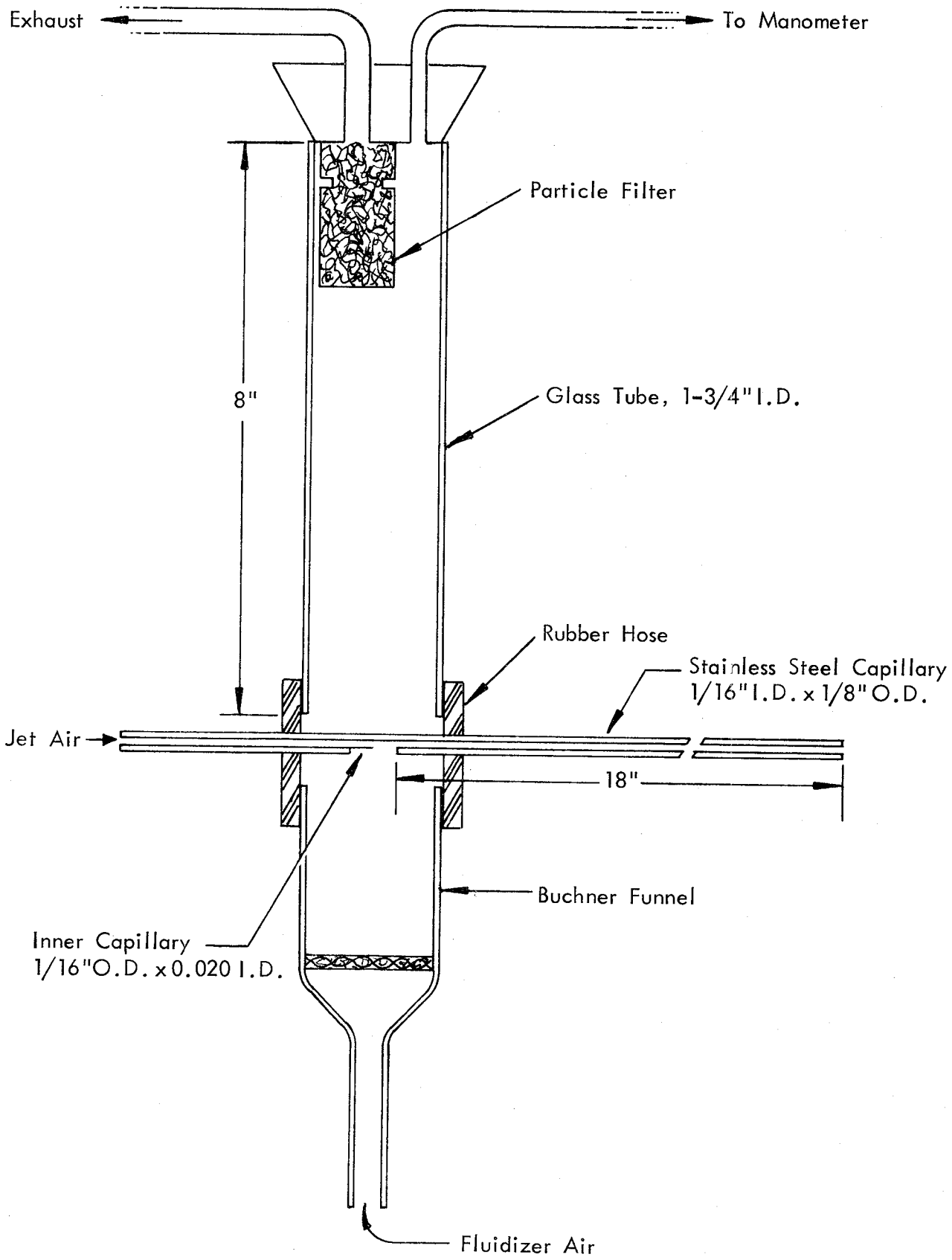

Figure 103 - Schematic of Fine Particle Feeder Suitable for Delivery in the Range 10 to 100 g/hr

to be due to the impact of the free-jet-accelerated fine particles on surfaces near the electron multiplier, even though the multiplier itself is off-axis with relation to the quadrupole and molecular beam. Similar problems have been observed, and largely mitigated, in laser-materials interaction studies using an EAI quadrupole mass spectrometer.[51] It is anticipated that our Extranuclear quadrupole system can be similarly modified in future work involving direct free-jet sampling of coal-air or seeded hydrocarbon flames.

A search was made for potassium- and phosphorus-containing species in or near the reaction zone of the slightly lean CH_4-air flame. Species definitely observed, and whose behavior is plotted below, were P^+, PO^+, K^+, and KOH^+. It has not been definitely established that these are all parent ions. Species sought for but not positively detected are listed in Tables 13 and 14.

The variation of 39^+ (K^+) and 56^+ (KOH^+) with concentration of -44 μ Purple-K added to the CH_4-air flame, is shown in Figures 104 through 106. Our estimate of the fraction of powder evaporated, at the distance of 1 cm downstream from the reaction zone chosen for these measurements, is shown in Figure 107. Species profiles through the flame are shown in Figures 108 through 111. Similar data for Foray, added as received, are shown in Figures 112 through 118.

IV. DRY-POWDER EFFECTS ON COAL-AIR FLAMES

A preliminary look was taken at the effects of adding Purple-K (< 37 μ) to the rich coal-air flame. The dry-powder feeder used in Task II was arranged to feed Purple-K into the coal feed line just before it entered the coal-dust burner. No careful calibrations of inhibitor feed rate were attempted, but the following observations were made. First, a few percent of coal was sufficient to cause lift-off and extinguishment of the coal-air flame. Second, with a percent of two of Purple-K in the coal feed, streamers of late burning particles were observed which persisted long enough to fall into the hood exhaust filter below the burner and cause ignition of collected coal dust in the filter and hood ducting below it.

In the course of measuring species profiles in inhibited coal-air flames, we observed the influence of the inhibitor on blow-off behavior. All flames were with 10- to 20-μ coal, held on the 6.3-cm diameter burner with uncooled honeycomb. The cold gas flow was 324 cc/sec, which, through the honeycomb of nominal area 31.2 cm^2, represents a cold gas velocity of very close to 10 cm/sec.

TABLE 13

UPPER LIMITS FOR KO (55^+), K_2 (78^+), AND K_2O (94^+) IN CH_4-AIR FLAME WITH PURPLE-K ADDED. Equiv. Ratio = 0.9

Purple-K Concentration (mg/ℓ)	M^+	$M^+/28^+$ (limit)	$39^+/28^+$	$M^+/39^+$ (limit)
2.3	55^+	$< 1.56 \times 10^{-5}$	3.15×10^{-4}	< 0.049
0.55	78^+	$< 4.5 \times 10^{-6}$	9.77×10^{-5}	< 0.046
0.55	94^+	$< 4.5 \times 10^{-6}$	9.77×10^{-5}	< 0.046

TABLE 14

UPPER LIMITS FOR HPO (48^+) AND P_2 (62^+) IN CH_4-AIR FLAME WITH FORAY ADDED. Equiv. Ratio = 0.9

Foray Concentration (mg/ℓ)	M^+	$M^+/28^+$ (limit)	$47^+/28^+$	$M^+/47^+$ (limit)
1.2	48^+	$< 3.9 \times 10^{-5}$	6.6×10^{-5}	< 0.58
6.0	48^+	$< 3.4 \times 10^{-5}$	5.4×10^{-4}	< 0.063
6.8	48^+	$< 1.36 \times 10^{-5}$	1.98×10^{-4}	< 0.057
12.3	48^+	$< 4.2 \times 10^{-5}$	5.9×10^{-4}	< 0.071
1.2	62^+	$< 3.0 \times 10^{-5}$	6.6×10^{-5}	< 0.45
6.0	62^+	$< 3.4 \times 10^{-5}$	5.4×10^{-4}	< 0.063
6.8	62^+	$< 4.5 \times 10^{-5}$	1.98×10^{-4}	< 0.023
12.3	62^+	$< 8.4 \times 10^{-5}$	5.9×10^{-4}	< 0.14

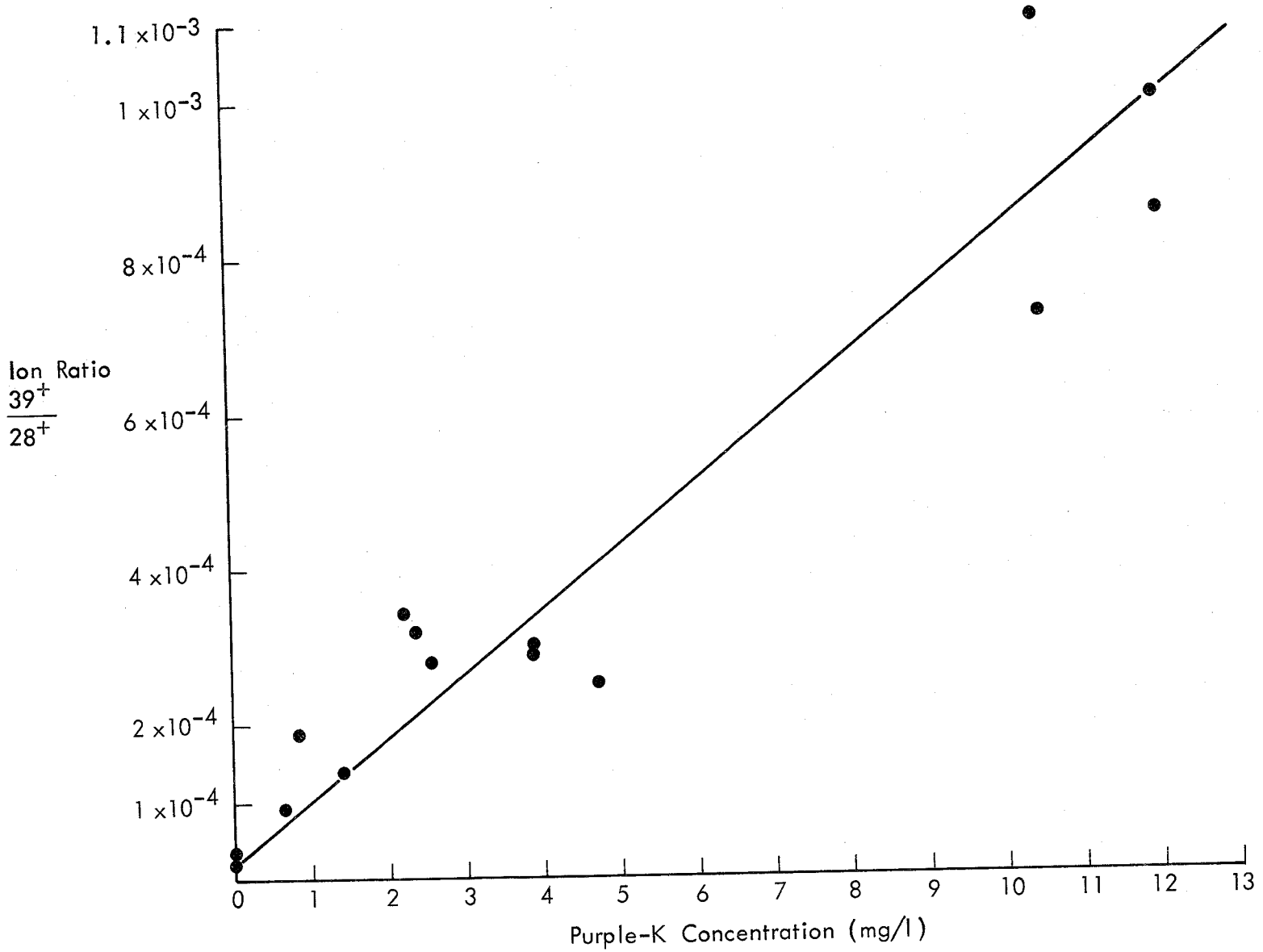

Figure 104 - Variation of the $39^+/28^+$ Ratio Observed 1 cm Downstream From a 0.9 Equivalence Ratio CH_4-Air Flame to Which Purple-K was Added

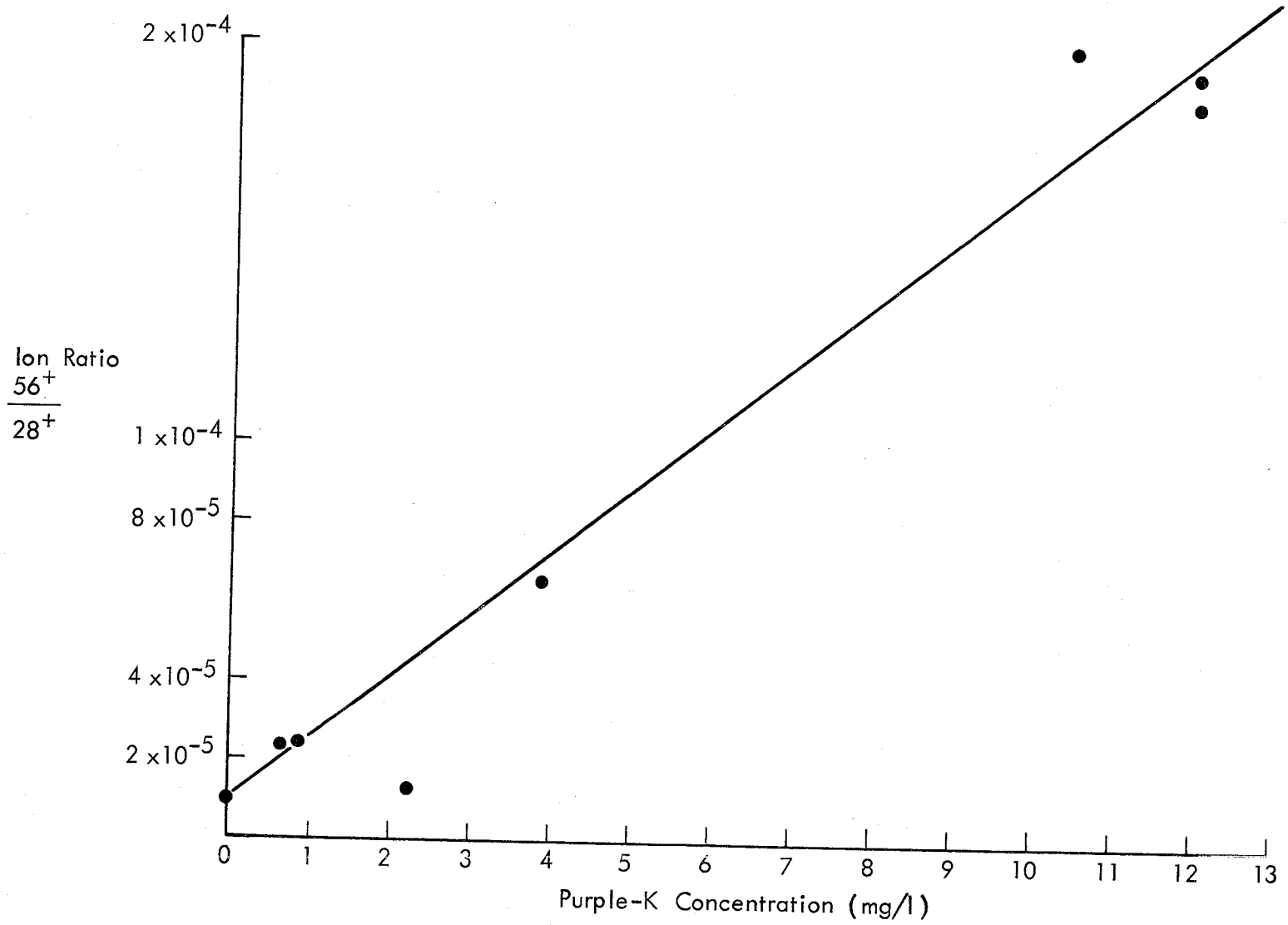

Figure 105 - $56^+/28^+$ Ratio for Flame of Figure 104

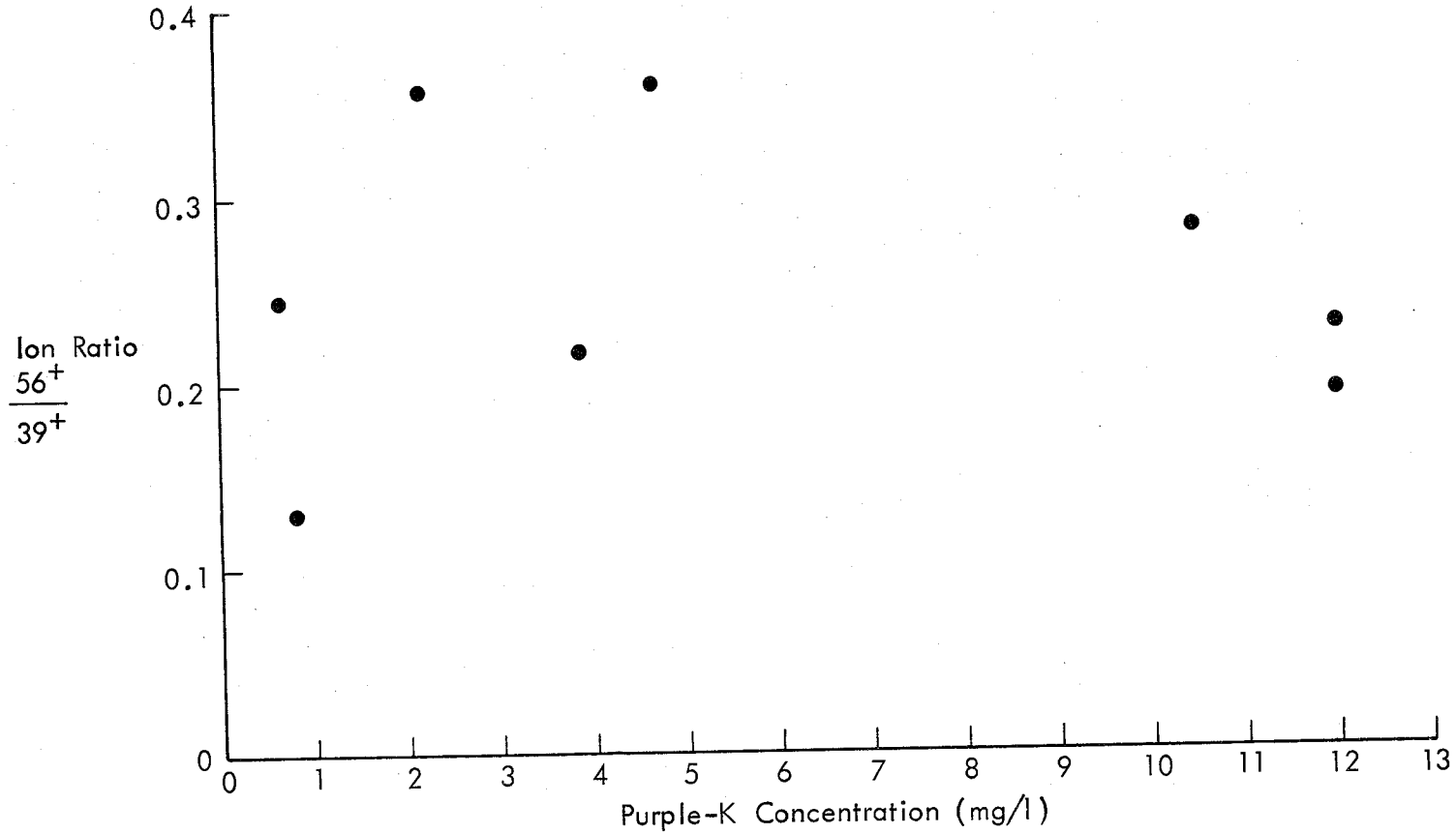

Figure 106 - $56^+/39^+$ Ratio for Flame of Figure 104

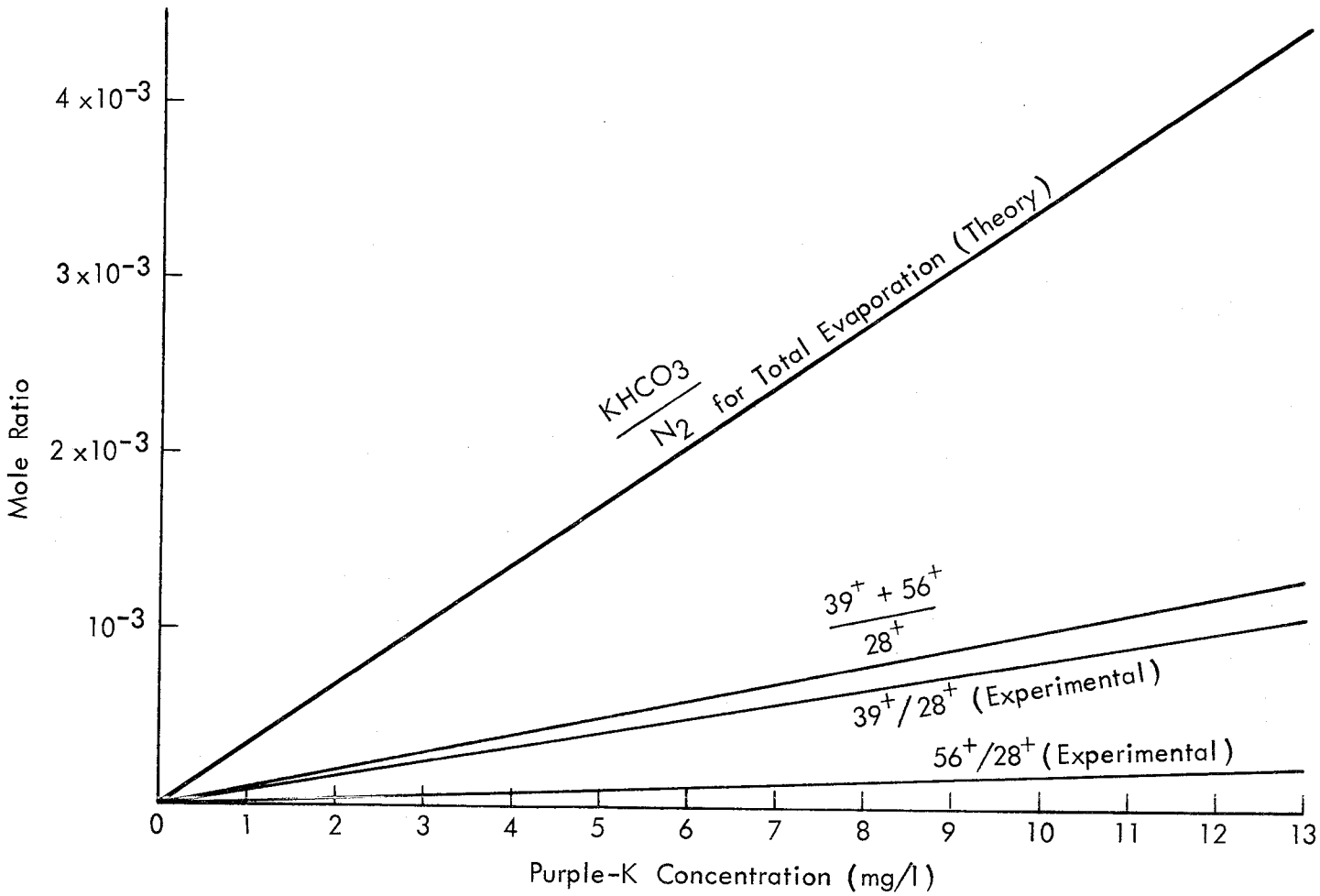

Figure 107 - Estimate of Fractional Evaporation of Purple-K 1 cm Downstream of the Flame of Figure 104

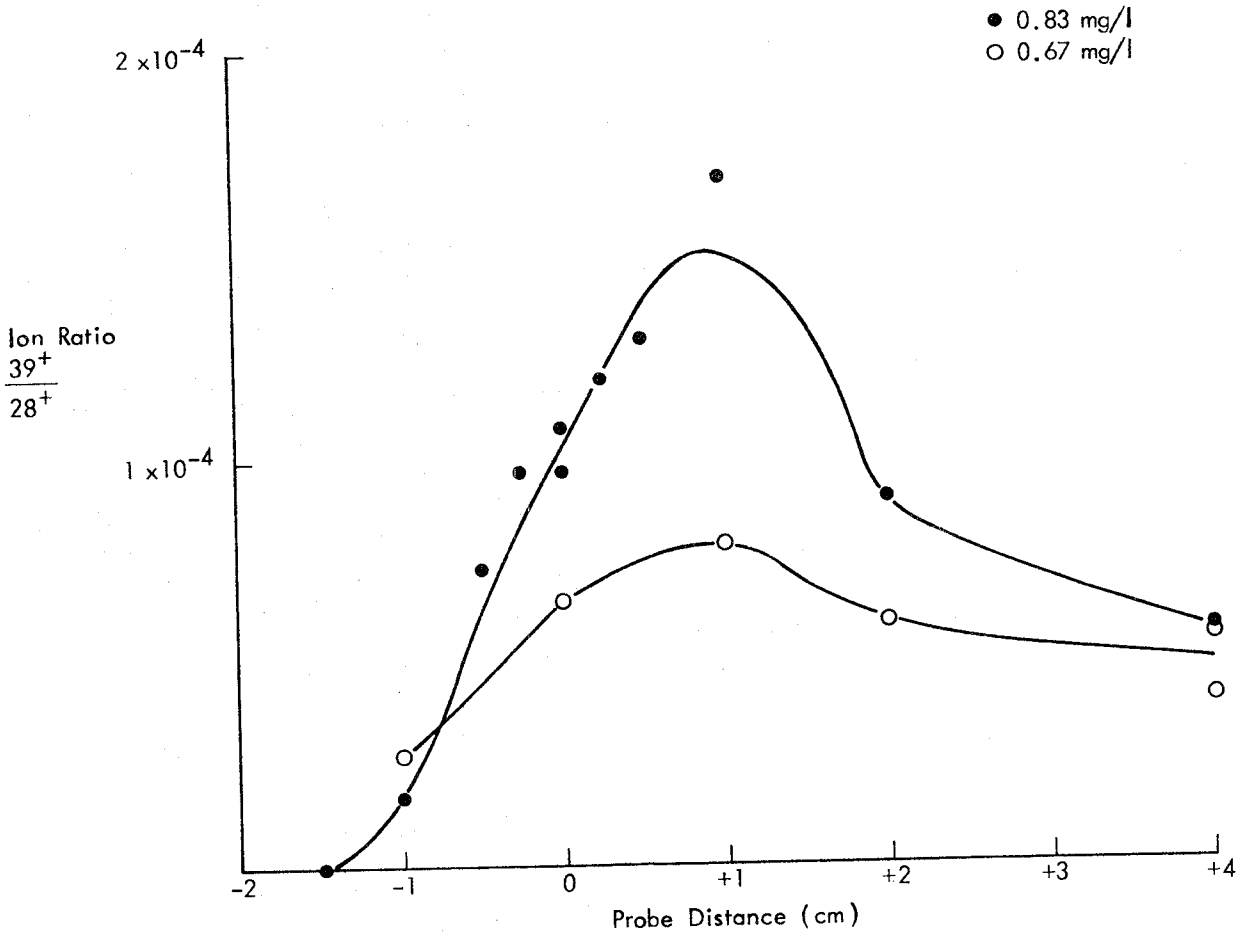

Figure 108 - Variation of $39^+/28^+$ Ratio Through a 0.9 Equivalence Ratio CH_4-Air Flame at Two Powder Loadings

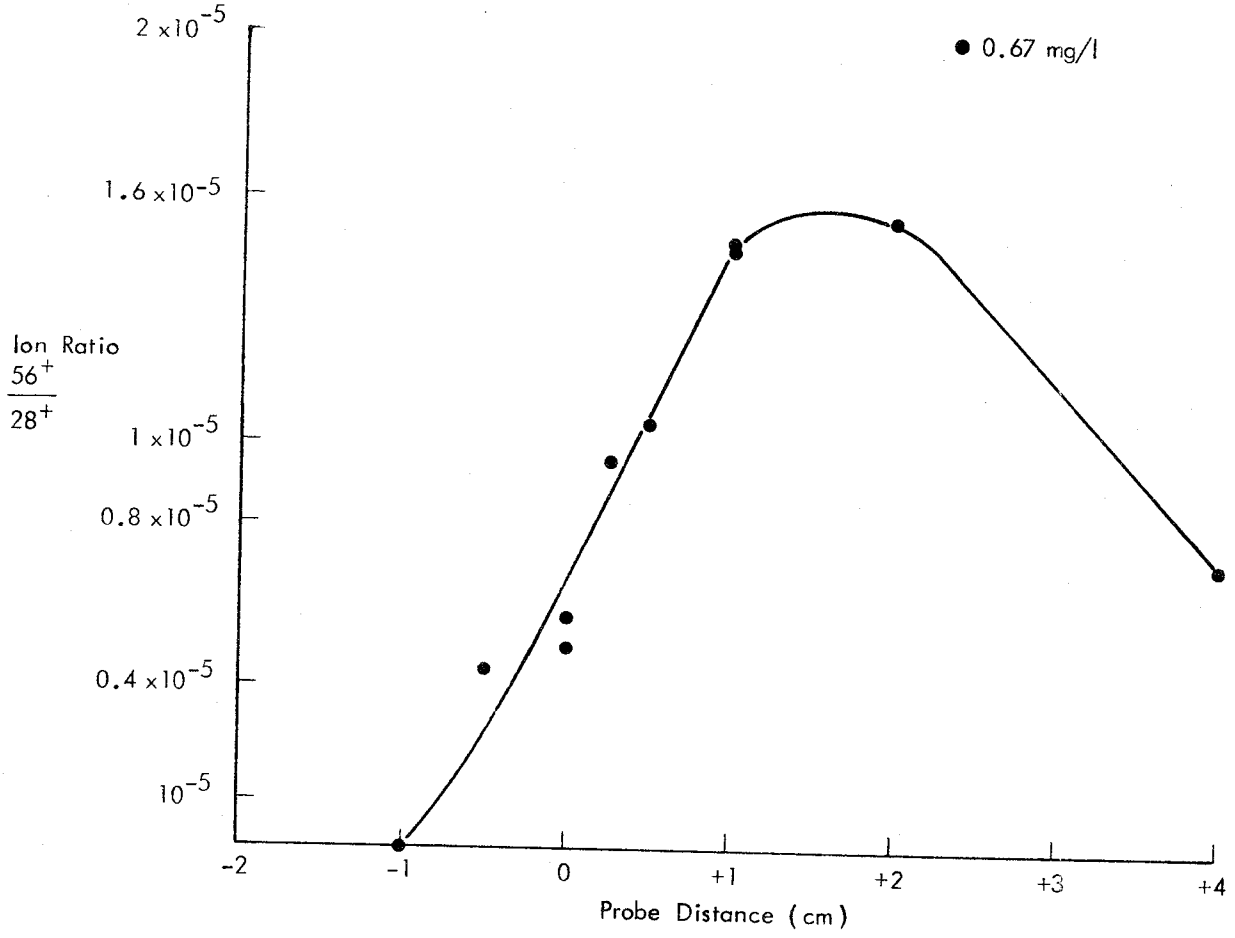

Figure 109 - Variation of $56^+/28^+$ in Flame of Figure 108

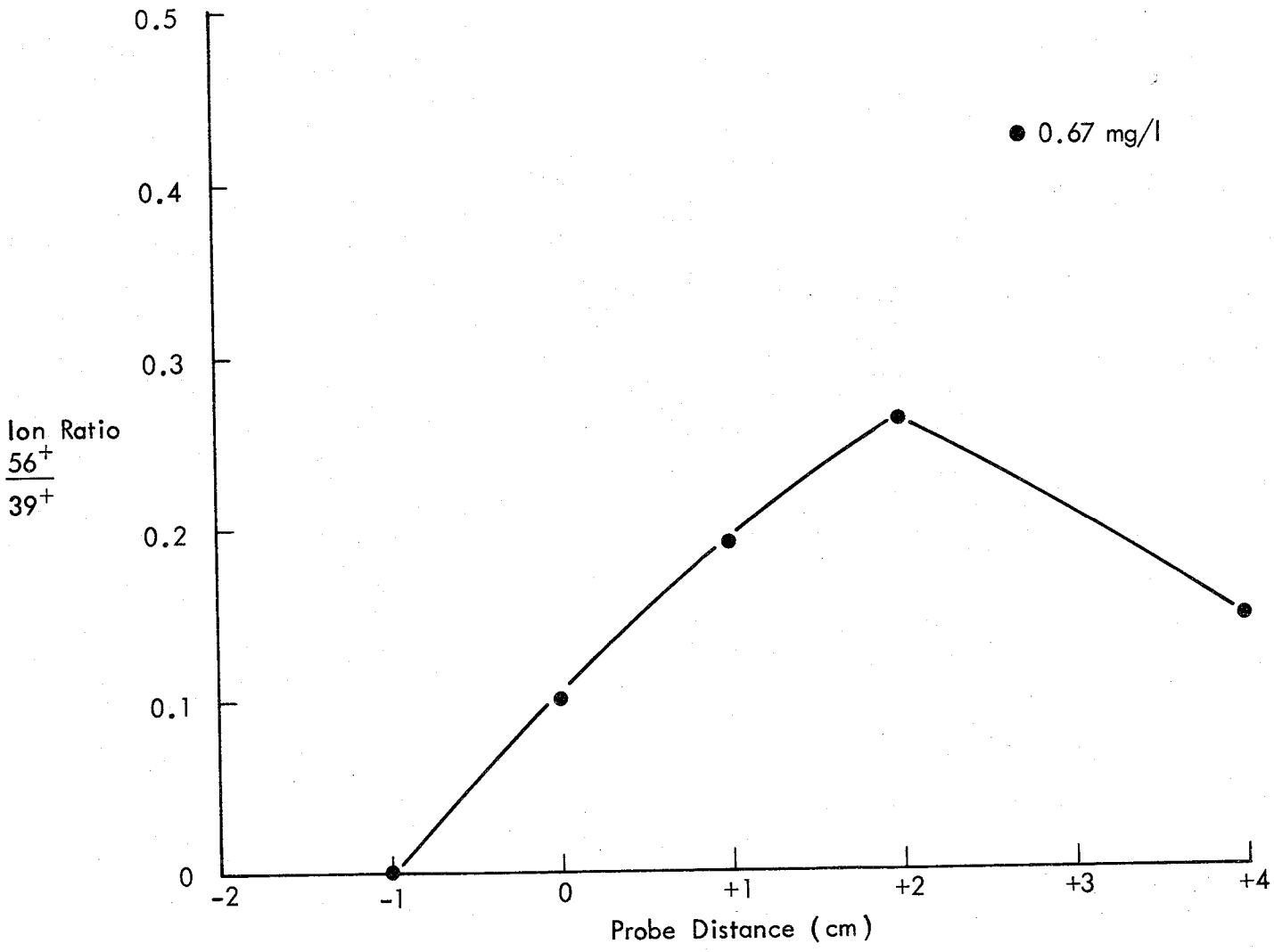

Figure 110 - Variation of $56^+/39^+$ Through Flame of Figure 108

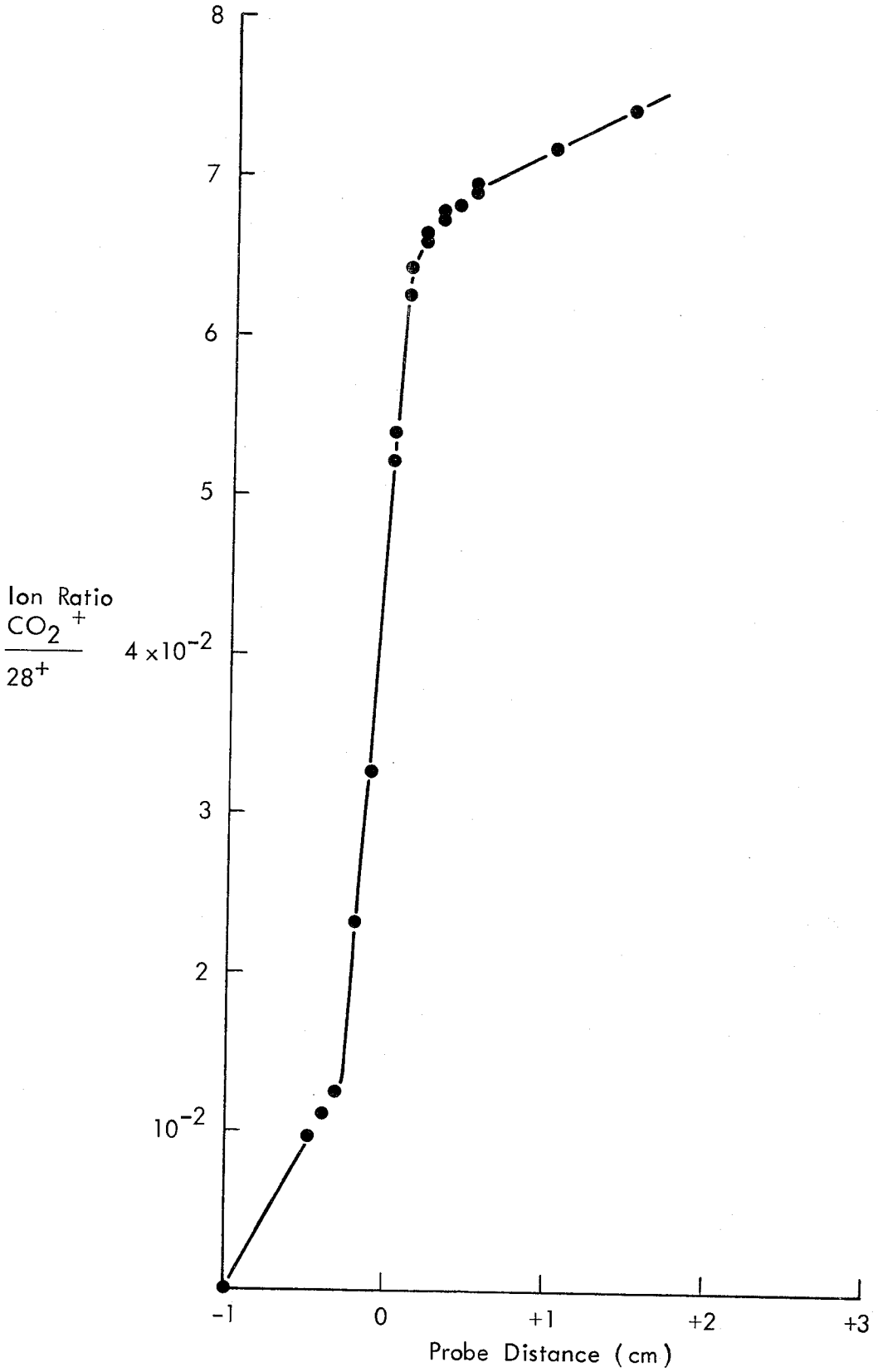

Figure 111 - Variation of $CO_2^+/28^+$ in Flame of Figure 108, Indicating Location of Reaction Zone

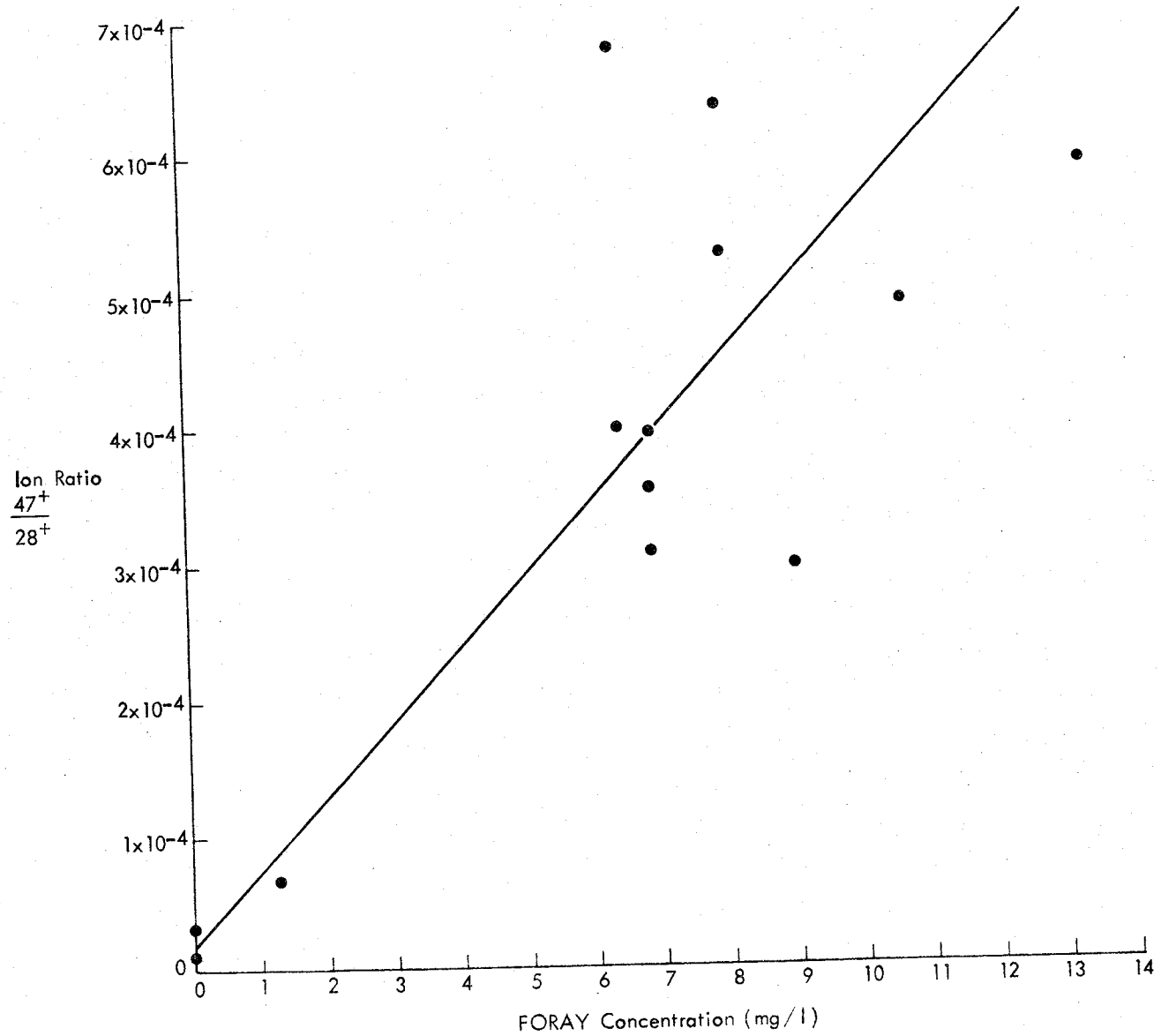

Figure 112 - Variation of $47^+/28^+$ Ratio Observed 1 cm Downstream From a 0.9 Equivalence Ratio CH_4-Air Flame to Which Foray was Added

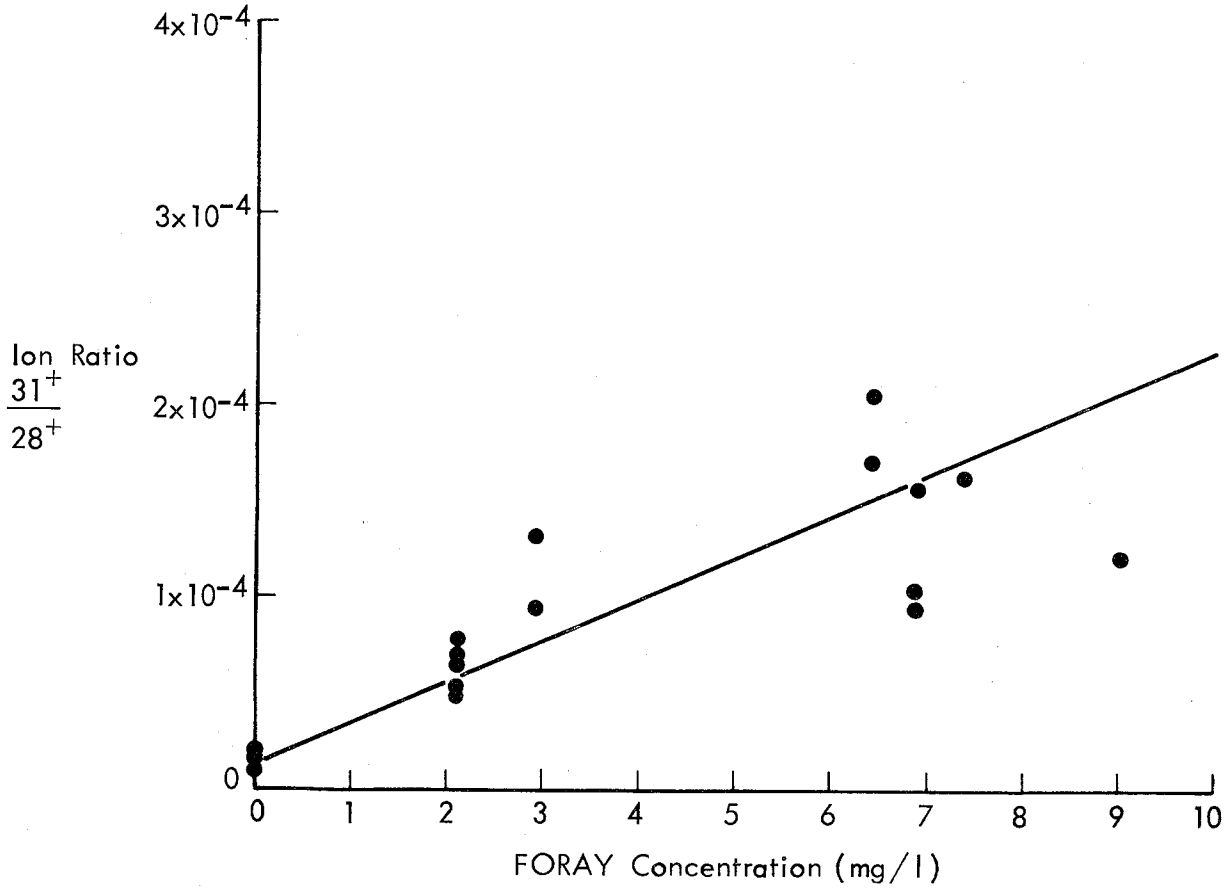

Figure 113 - Variation of $31^+/28^+$ Ratio in Flame of Figure 112

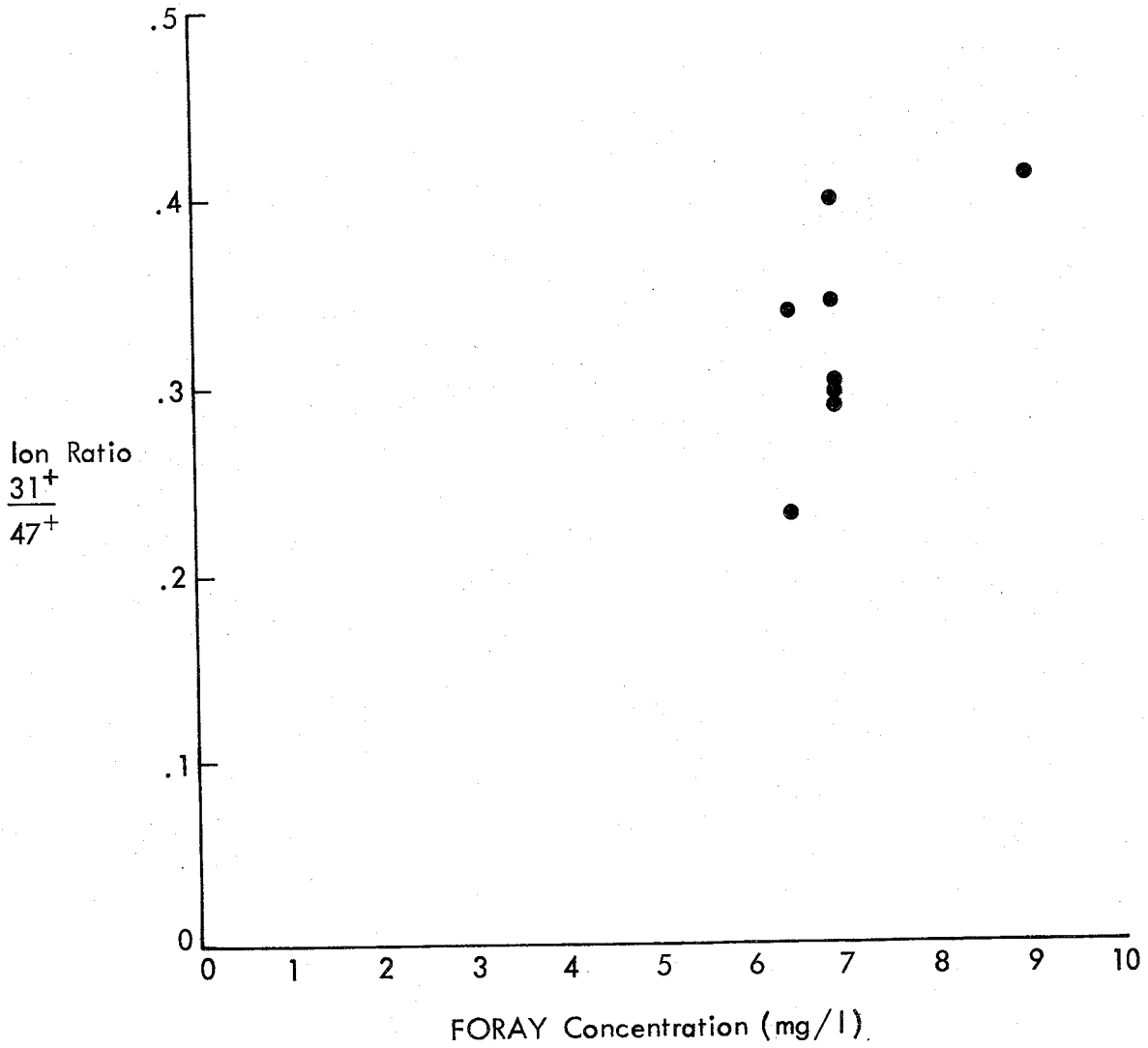

Figure 114 - Variation of $31^+/47^+$ Ratio in Flame of Figure 112

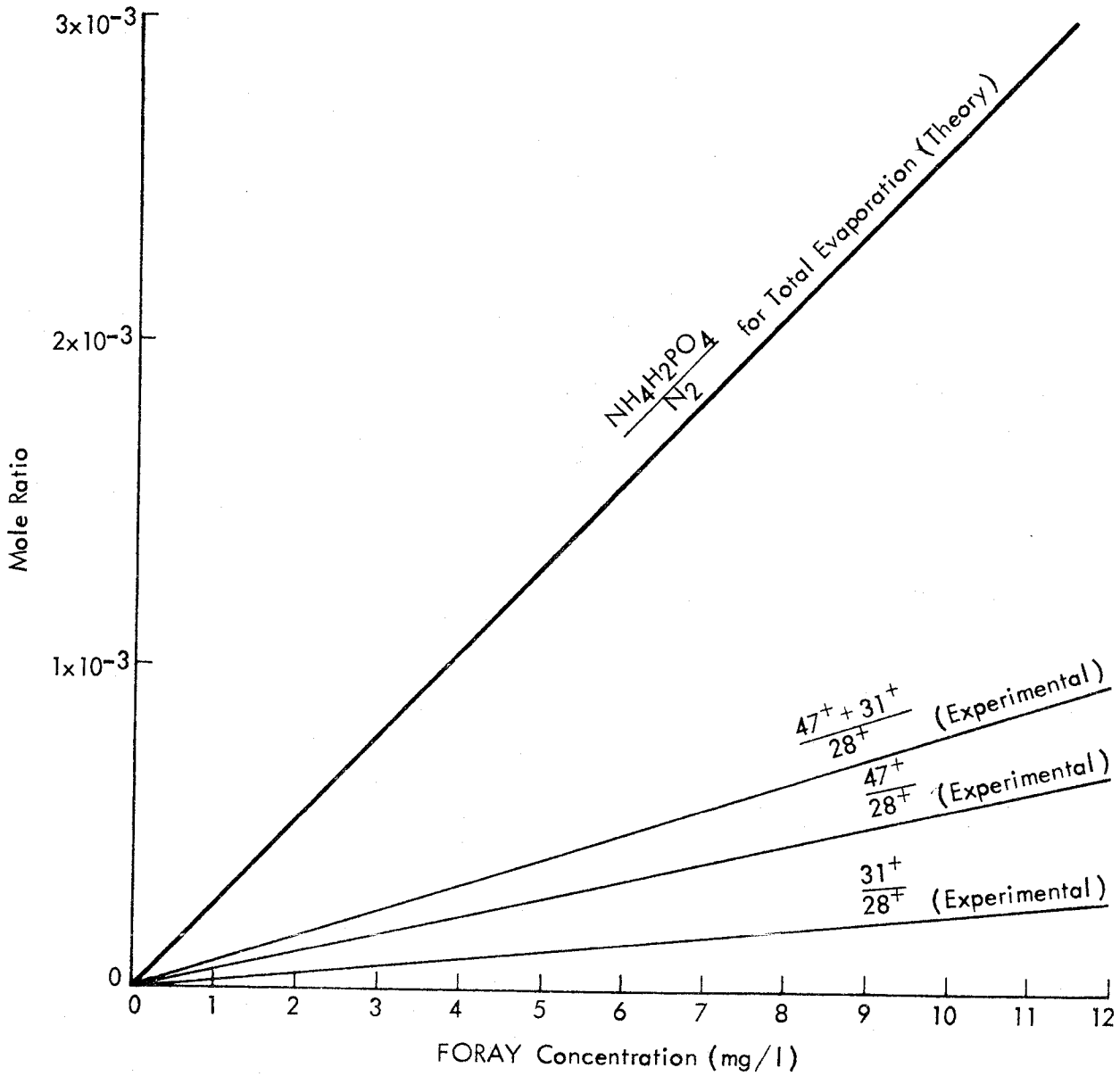

Figure 115 - Estimate of Fractional Evaporation of Foray, 1 cm Downstream of the Flame of Figure 112

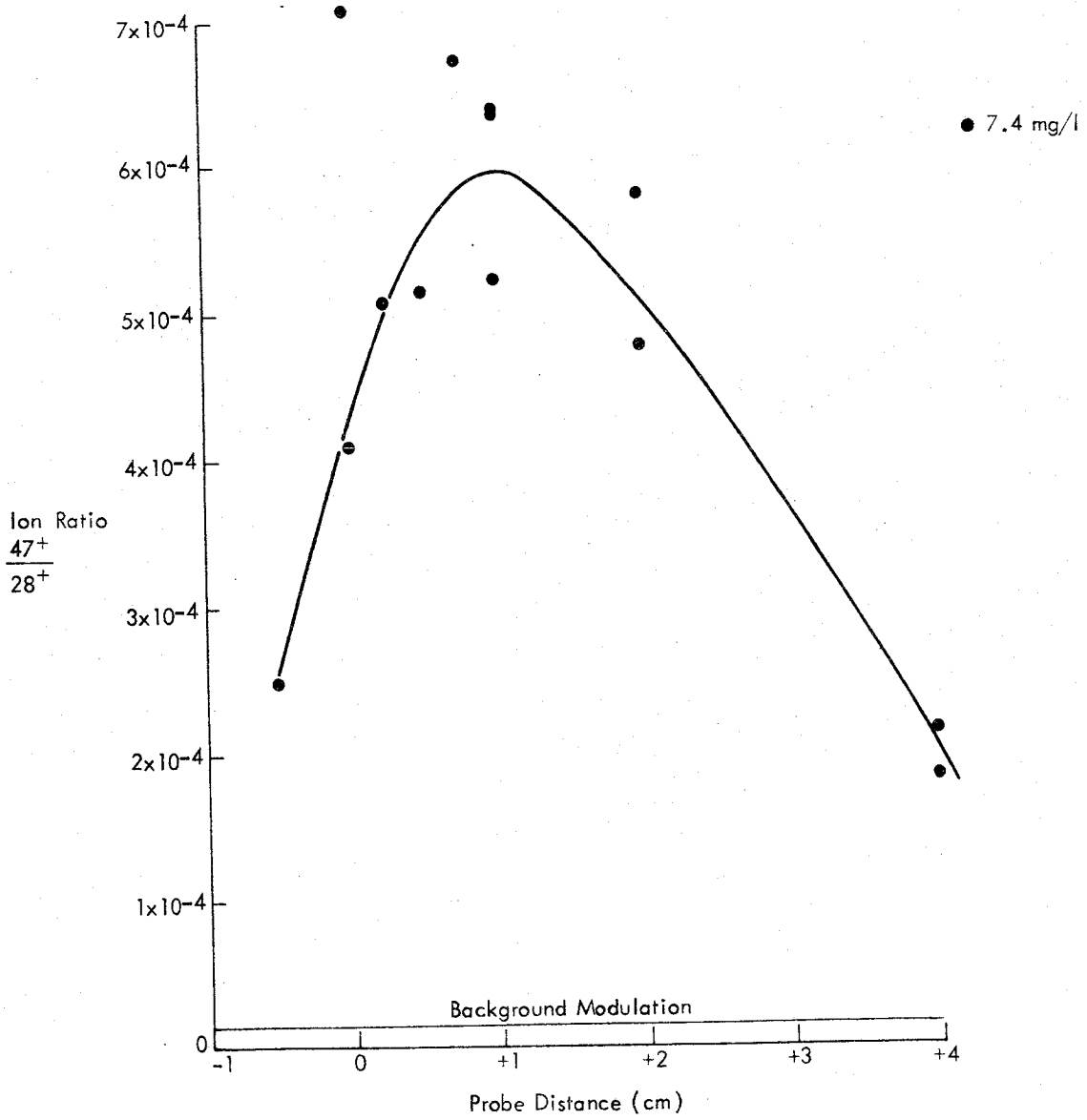

Figure 116 - Variation of the $47^+/28^+$ Ratio Through a 0.9 Equivalence Ratio CH_4-Air Flame

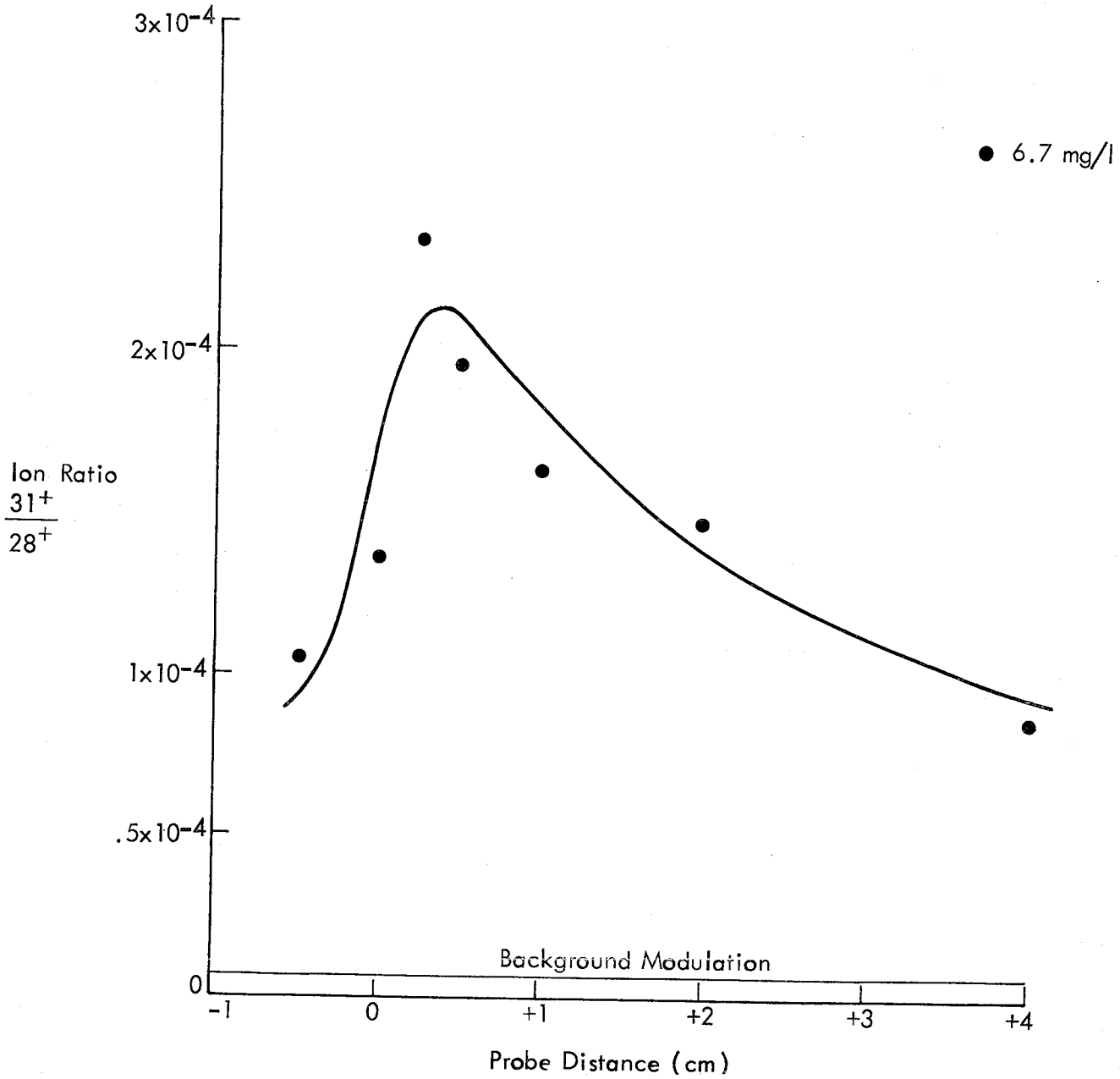

Figure 117 - Variation of $31^{+}/28^{+}$ Through the Flame of Figure 116

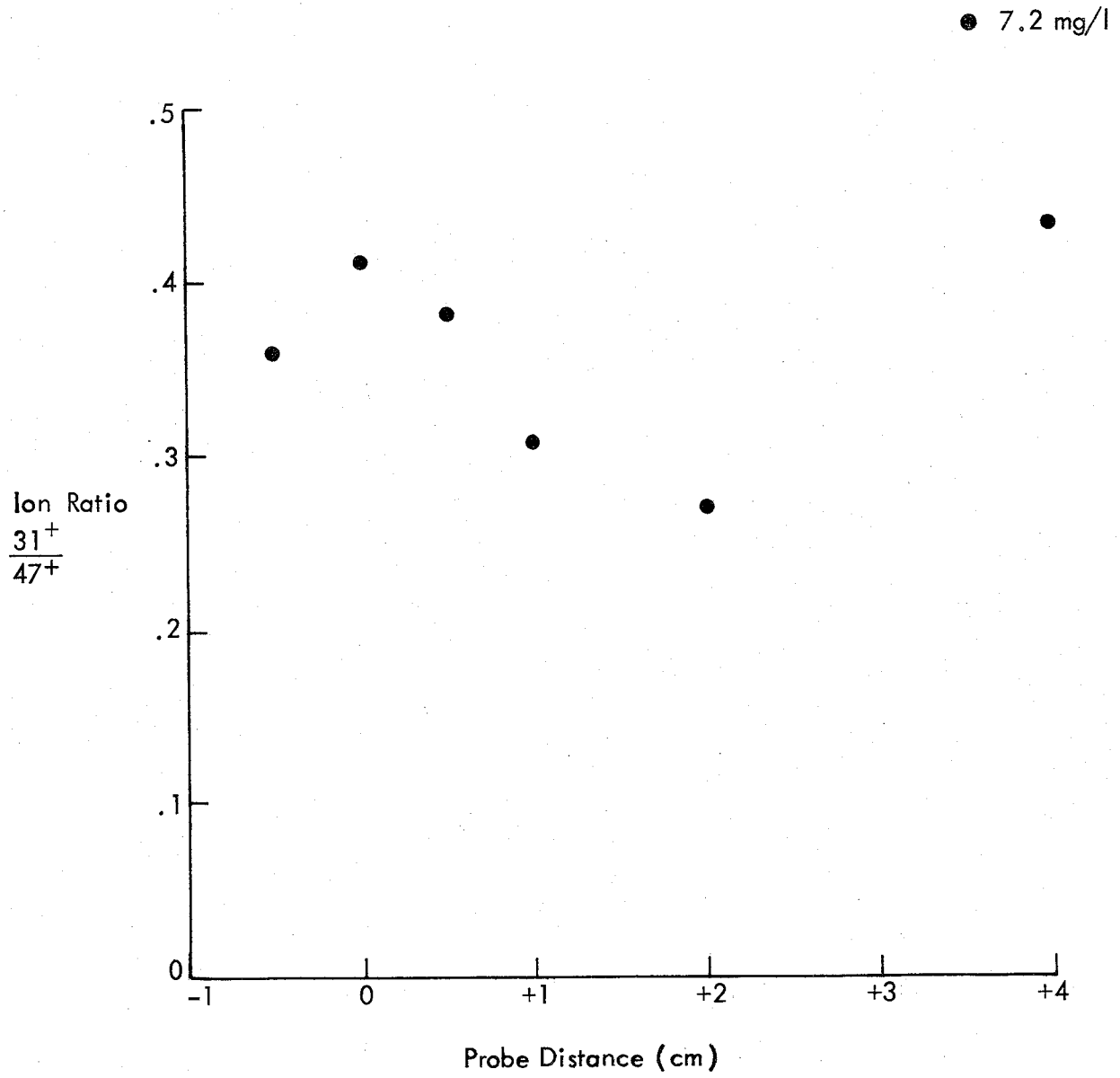

Figure 118 - Variation of $31^+/47^+$ Through the Flame of Figure 116

At a given coal concentration and with the flame attached and burning in steady state, the inhibitor was increased stepwise until the flame lifted off and extinguished in 30 sec or less. Because of difficulties in varying the powdered inhibitor, coal fluctuations and the qualitative nature of blow-off, the results were quite scattered.

Blow-off observations are summarized in Figure 119 for the three inhibitors tested. The results are qualitatively reasonable with both CF_3Br and Purple-K showing strong chemical effects, at least for these slow-moving flames.

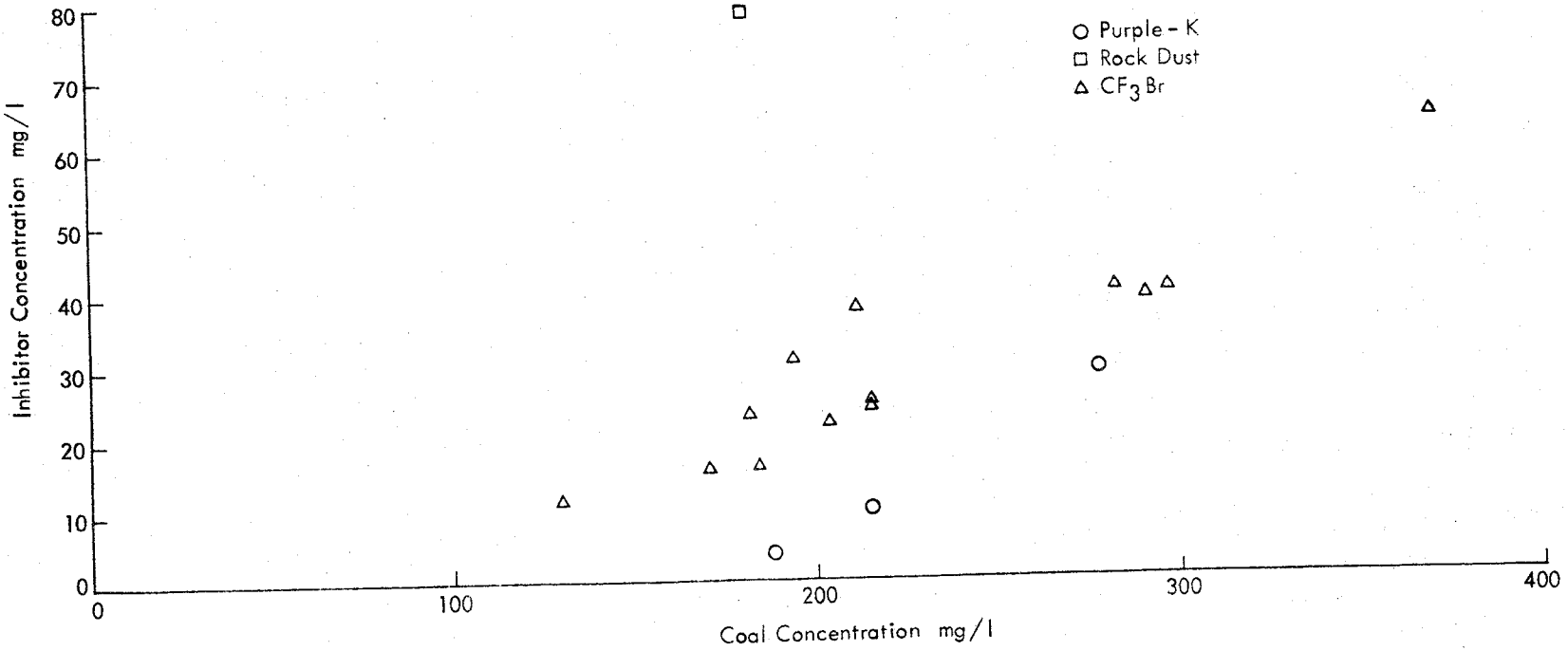

Figure 119 - Blow-Off Behavior of Coal-Air Flames Stabilized on a 6.3-cm Diameter Honeycomb Burner at a Cold Gas Velocity of 10 cm/sec. Coal was a 10 to 20 μ fractions of Pittsburgh seam.

REFERENCES

1. Newall, H. E., and F. S. Sinnatt, Fuel, 6:118 (1927).

2. Fuhrmann, E. A., and H. Koettgen, Z. Physik. Chem., A169:388 (1934).

3. Orning, A. A., Trans. Am. Soc. Mech. Engrs., 64:497 (1942).

4. Ghosh, B., and A. A. Orning, Ind. Eng. Chem., 47:117 (1955).

5. Ghosh, B., D. Basu, and N. K. Roy, Sixth Symposium (International) on Combustion, p. 595 (1956).

6. Hattori, H., ibid., p. 590 (1956).

7. Cassel, H. M., I. Liebman, and W. K. Mock, ibid., p. 602 (1956).

8. Mache, H., and A. Hebra, Sitzber. Akad. Wiss. Wien., 150:157 (1941).

9. Burgoyne, J. H., and V. D. Long, "Proceedings of the Conference on Science in the Use of Coal," The Institute of Fuel, Sheffield, England, D-16 (1958).

10. Long, V. D., J. Imperial College Chem. Eng. Sci., 13:16 (1960-1961).

11. Marshall, W. F., H. D. Palmer, and D. J. Seery, J. Inst. Fuel, 37: 342 (1964).

12. Howard, J. B., and R. H. Essenhigh, "Eleventh Symposium (International) on Combustion," The Combustion Institute, 399 (1967).

13. Howard, J. B., Ph.D. Thesis, The Pennsylvania State University, University Microfilms No. 65-14, 763 (1965).

14. Gray, D., J. G. Cogli, and R. H. Essenhigh, "Problems in Pulverized Coal and Char Combustion," Division of Fuel Chemistry (ACS) Reprints, 18(1):135 (1973).

15. Essenhigh, R. H., "Research Opportunities for Universities in Combustion of Coal," Office of Coal Research and NSF-RANN Report, "Research in Coal Technology - The Universities' Role," Proceedings of the Workshop Held at the State University of New York at Buffalo, October 21-22, 1974.

16. Shapatina, E. A., V. V. Kayluzhnyi, and Z. F. Chukhanov, Dokl. Akad. Nauk, SSSR., 72:869 (1950). Earliest work on pulverized coal (p.f.) in suspension. $T \leq 550^{\circ}C$. Times $\geq$ 500 ms. 200 μ particles.

17. Loison, R., and R. Chauvin, Chim. Ind., 91:269 (1964) 50-80 μ coal electrically heated on 50 μ mesh gauge. $1500^{\circ}C$/sec to $1050^{\circ}C$. Total yield and gas composition.

18. Hawksley, P. G. W., BCURA Mon. Bull., 31:195 (1967). Weight loss of fine coals dropped through a furnace. 20-60 μ coal heated to $1000^{\circ}C$ in 50 ms. Quenched after 100 ms.

19. Sharkey, A. G., J. C. Shultz, and R. A. Friedel, Nature, 202:988 (1964) (see Ref. 24).

20. Sharkey, A. G., J. L. Shultz, and R. A. Friedel, ACS Monograph, "Coal Science," p. 643 (1965). Compares gases evolved from flash and laser irradiated coals.

21. Karn, F. S., and A. G. Sharkey, Fuel, 47:193 (1968). Pyrolysis data on individual coal materials by laser irradiation.

22. Karn, F. S., R. A. Freidel, and A. G. Sharkey, Fuel, 48:297 (1969). More laser studies on coal. Effect of particle size, irradiated area, light flux.

23. Karn, F. S., A. G. Sharkey, A. F. Logar, and R. A. Friedel, U.S. Bureau of Mines, R.I. 7328 (1970). Detailed report of laser studies, including several coal types and data in Refs. 25-27.

24. Sharkey, A. G., A. F. Logar, and R. G. Lett, 19th ASMS Meeting, Atlanta, May 1971. Laser irradiation of coals in Bendix TOF ion source.

25. Karn, F. S., R. A. Friedel, and A. G. Sharkey, Fuel, 51:113 (1972). Ruby and CO_2 laser studies of coal. Gas and char analysis.

26. Granger, A. F., and W. R. Ladner, Fuel, 49:17 (1970). Char and gas yields from flash heating of pulverized coal.

27. Joy, W. K., W. R. Ladner, and E. Pritchard, Fuel, 49:26 (1970). Gases released in Bendix ion source by laser irradiation. Analyzed for radicals.

28. Merrill, La Vaun S., Fuel, 52:61 (1973). Ignition studies of pulverized coal in furnace. Slow heating. Large H_2 evolution at moment of ignition.

29. Howard, J. B., and R. H. Essenhigh, I&EC Process Design and Development, 6:74 (1967).

30. Kimber, G. M., and M. D. Gray, Combustion and Flame, 11:360 (1967).

31. Coates, R. L., L. D. Smoot, and M. D. Horton, Interim Report No. 1, "Exploratory Studies of Flame and Explosion Quenching," September 1973.

32. Smoot, L. D., and M. D. Hortin, Interim Report No. 2, September 1973.

33. Smoot, L. D., and M. D. Horton, Interim Report No. 3, September 1974.

34. Strehlow, R. A., L. D. Savage, S. C. Sorenson, H. Krier, and J. L. Krazinski, Interim Final Report No. 1, September 1973.

35. Ibid., Interim Report No. 2, November 1974.

36. Strehlow, R. A., L. D. Savage, and S. C. Sorenson, "Coal Dust Combusion and Suppression," AIAA Paper No. 74-1110, October 1974.

37. Krier, H., and J. L. Krazinski, "Theory of Coal Dust-Air Flame Propagation," AIAA Paper No. 74-1111, October 1974.

38. Sorenson, S. C., L. D. Savage, and R. A. Strehlow, "Flammability Limits - A New Technique," Combustion and Flame, 24:347 (1975).

39. Grumer, J., Pittsburgh Mining and Safety Research Center, U. S. Bureau of Mines, private communication.

40. Majac Company, Majac Division, the Donaldson Company, Inc.

41. Grumer, J., and A. E. Bruszak, R. I. 7552, "Inhibition of Coal Dust-Air Flames," August 1971.

42. Milne, T. A., C. L. Green, and D. K. Benson, Combustion and Flame, 15:225 (1970).

43. Hamor, R. J. and I. W. Smith, Fuel, 50:394 (1971).

44. Cartesian Diver Type Pressure Controller, range 1 mm Hg to 100 psi, Roger Gilmont Instruments, Inc.

45. Geldart, D., "The Effect of Particle Size and Size Distribution on the Behavior of Gas-Fluidized Beds," Powder Technology, 6:201 (1972).

46. Model 156, Helium-Neon Gas Laser, Spectra-Physics, Inc.

47. Model 560 Lite-Mike, Edgerton-Germeshausen and Grier, Inc.

48. Singer, J. M., A. E. Bruszak, and J. Grumer, R. I. 6761, "Equivalences of Coal Dust and Methane at Lower Quenching Limits of Flames of Their Mixture" (1966).

49. Milne, T. A., and F. T. Greene, "Mass Spectrometer Studies of Reactions in Flames II. Quantitative Sampling of Free Particles from One-Atmosphere Flames," J. Chem. Phys., 44(6):2444 (1966).

50. Kiser, R. W., Introduction to Mass Spectrometry and Its Applications, Prentice Hall, Edgewood Cliffs, New Jersey (1965).

51. The Extranuclear Company, Pittsburgh, Pennsylvania.

52. Greene, F. T., and G. Radolovich, "Molecular Beam Mass Spectrometric Studies of Laser Plumes Formed at Atmospheric Pressure," paper presented at the 23rd Annual Conference on Mass Spectrometry and Allied Topics, May 25-30, 1975, Houston, Texas.

53. Omega Engineering, Inc., Stamford, Connecticut.

54. Litchfield, E. L., U.S. Bureau of Mines, private communication (1975).

55. Dahneke, B., University of Rochester School of Medicine and Dentistry, private communication.

56. The Ansul Company, Marinette, Wisconsin.

57. Harpur, W. A., Fire Journal, p. 38, November 1960.

58. Milne, T. A., J. E. Beachey, and F. T. Greene, "Exploratory Studies of Flame and Explosion Quenching," First Annual Technical Progress Report, June 30, 1970 - June 30, 1973, U.S. Bureau of Mines Contract No. H0122127.

59. Iya, K. S., S. Wollowitz, and W. E. Kaskan, "The Mechanism of Flame Inhibition by Sodium Salts," Preprint of a paper presented at the Fifteenth International Combustion Symposium, Tokyo, August 1974.

60. Lucas, H. G., and N. S. Smith, Jr., "Multiple-Orifice Feeder for Fine Particles, R. I. 7944 (1974).